Monoclonal Antibody Aggregates:

physicochemical characteristics, stability in biological fluids and immunogenicity

Vasco Filipe

Monoclonal antibody aggregates: physicochemical characteristics, stability in biological fluids and immunogenicity
Vasco Filipe

ISBN:978-90-393-5783-5

Cover: “The Vitruvian Mouse” by Tiago Jales Tomé. An adaptation from Leonardo da Vinci’s drawing with subtle insertions of antibody “Y” shapes and aggregates thereof.

Layout: Vasco Filipe
Priniting: Off Page, Amsterdam, The Netherlands

The printing of this thesis was kindly supported by:
- The Dutch Technology Foundation STW
- Leiden/Amsterdam Center for Drug Research
- Utrecht Institute for Pharmaceutical Sciences
- NanoSight Ltd.

Monoclonal antibody aggregates:

Physicochemical characteristics, stability in biological fluids and immunogenicity

Monoklonaal antilichaam aggregaten

Fysisch-chemische eigenschappen, de stabiliteit in biologische vloeistoffen en immunogeniciteit

(met een samenvatting in het Nederlands)

Proefschrift

ter verkrijging van de graad van doctor aan de Universiteit Utrecht op gezag van de rector magnificus, prof.dr. G.J. van der Zwaan, ingevolge het besluit van het college voor promoties in het openbaar te verdedigen op vrijdag 25 mei 2012 des middags te 12.45 uur

door

Vasco Luís Seixas Filipe

geboren op 13 februari 1982 te Kiev, Sovjet-Unie

Promotor:	Prof. Dr. H. Schellekens
	Prof. Dr. W. Jiskoot
Co-promotor:	Dr. V. Brinks

This research was supported by the Dutch Technology Foundation STW, which is part of the Netherlands Organisation for Scientific Research (NWO) and partly funded by the Ministry of Economic Affairs, Agriculture and Innovation (UFA.7171)

"All religions, arts and sciences are branches of the same tree. All these aspirations are directed toward ennobling man's life, lifting it from the sphere of mere physical existence and leading the individual towards freedom."

Albert Einstein

Aos meus pais e tios

TABLE OF CONTENTS

Chapter 1

General introduction

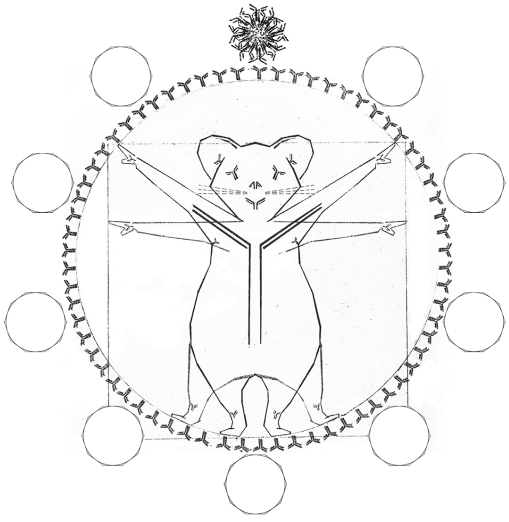

Therapeutic proteins have become invaluable in treating a wide range of serious and life-threatening diseases. However, repeated administration of these drugs to patients often induces the formation of undesirable anti-drug antibodies (ADAs), also known as immunogenicity. The formation of ADAs in patients may have serious clinical consequences, such as loss of therapeutic efficacy or even the neutralization of an equivalent endogenous protein [1]. Immunogenicity is one of the main obstacles for the development and commercialization of therapeutic proteins.

ANTIBODIES

Antibodies are glycoproteins belonging to the immunoglobulin (Ig) superfamily. These can be divided into five different classes: IgA, IgD, IgE, IgM, and IgG. The latter is the most naturally abundant class of antibodies and is most commonly used for therapeutic purposes. IgGs contain two identical heavy (50 kDa) chains and two identical light (25 kDa) chains (Fig. 1.1). Therefore, the total molecular weight is approximately 150 kDa. The IgG monomer is a "Y"-shaped molecule that consists mainly of β-sheet structures [2]. There are several *inter*chain disulfide bonds linking the two heavy chains, linking the heavy and light chains, as well as *intra*chain disulfides [3]. Each chain contains a constant and a variable region. The latter contains the sites that can specifically bind to antigens, called fragment antigen-binding (Fab) regions. More specifically, three variable loops of β-strands on each light and heavy chain are responsible for the antigen-binding specificity [4]. These loops are referred to as the complementarity determining regions (CDRs) or hypervariable regions.

IgGs are further divided into several subclasses: IgG_1, IgG_2, IgG_3, and IgG_4 (in order of relative abundance in human plasma). Each subclass contains a specific type of heavy chain and may contain one of the two light chains: lambda (λ) and kappa (κ). In mice, the average of κ to λ ratio is 20:1, whereas it is 2:1 in humans [5].

All antibodies are glycosylated, but the type and number of oligosaccharides may differ considerably, even between antibodies produced in the same cell [6]. All IgGs contain N-linked oligosaccharides on the constant region of heavy chains and approximately 15–20% also have N-linked oligosaccharides in the variable region [7]. The variable region oligosaccharides could be on either the light chain, the heavy chain, or both [8]. O-linked oligosaccharides have also been reported on the hinge region or possibly on the constant region of heavy chains [9, 10].

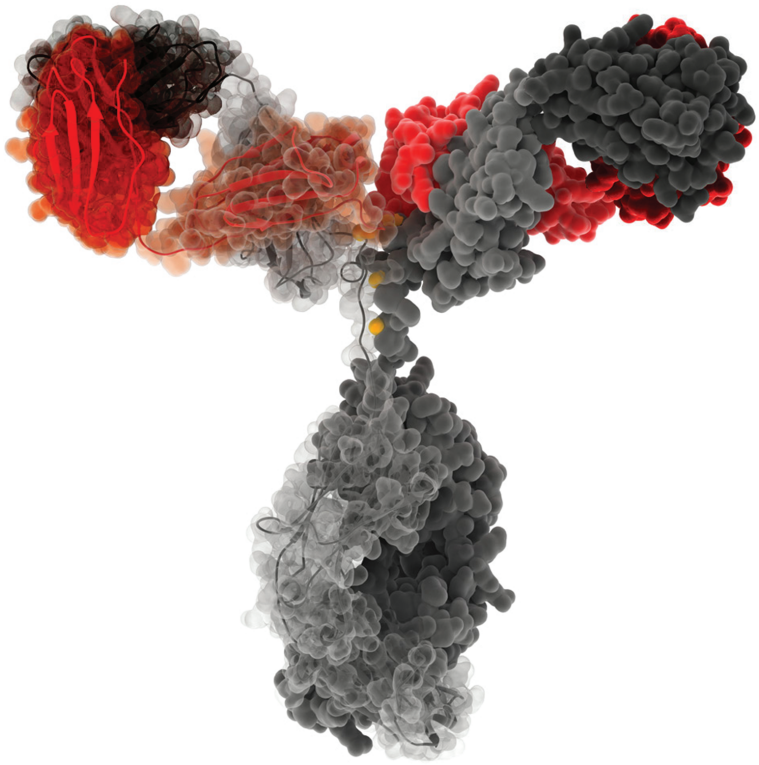

Figure 1.1: Crystal structure of an IgG. Heavy chains (grey), light chains (red) and interchain disulfide bonds (yellow) are depicted. Left heavy and light chains are semi-transparent and contain ribbon diagrams. Variable regions have a darker tone than constant regions. © http://visualscience.ru, 2011

THERAPEUTIC MONOCLONAL ANTIBODIES

Monoclonal antibodies (MAbs) are single types of antibodies directed against a single specific epitope. They are normally produced by a single clone of B cells or a single cell line (e.g. hybridoma, CHO, Per.C6) [11-13]. The first therapeutic MAb approved by the U.S. Food and Drug Administration (FDA) was the Muromonab-CD3 in 1986, a murine IgG_2a used as an immunosuppressive drug for transplants [14]. In 1996, only two MAbs were approved for therapeutic use in humans. Nowadays, about 30 MAbs have been approved by the FDA (Table 1.1) and hundreds are entering clinical trials every year [15]. MAbs are the fastest growing class of drugs and their importance tends to grow every year.

Table 1.1: List of FDA-approved MAbs to date (2011).*

Antibody	Brand name	Approval date	Type	Target	Main therapeutic indication
Muromonab-CD3	Orthoclone OKT3	1986	murine	T cell CD3 receptor	Transplant rejection
Abciximab	ReoPro	1994	chimeric	Inhibition of glycoprotein IIb/IIIa	Cardiovascular disease
Daclizumab	Zenapax	1997	humanized	IL-2Rα receptor (CD25)	Transplant rejection
Rituximab	Rituxan, Mabthera	1997	chimeric	CD20	Non-Hodgkin lymphoma
Basiliximab	Simulect	1998	chimeric	IL-2Rα receptor (CD25)	Transplant rejection
Infliximab	Remicade	1998	chimeric	Inhibition of TNF-α signaling	Several autoimmune disorders
Palivizumab	Synagis	1998	humanized	An epitope of the RSV F protein	Respiratory Syncytial Virus
Trastuzumab	Herceptin	1998	humanized	ErbB2	Breast cancer
Gemtuzumab	Mylotarg	2000	humanized	CD33	Acute myelogenous leukemia
Alemtuzumab	Campath	2001	humanized	CD52	Chronic lymphocytic leukemia
Efalizumab	Raptiva	2002	humanized	CD11a	Psoriasis
Adalimumab	Humira	2002	human	Inhibition of TNF-α signaling	Several auto-immune disorders
Ibritumomab tiuxetan	Zevalin	2002	murine	CD20	Non-Hodgkin lymphoma
Tositumomab	Bexxar	2003	murine	CD20	Non-Hodgkin lymphoma
Cetuximab	Erbitux	2004	chimeric	Epidermal growth factor receptor	Colorectal cancer, head and neck cancer
Bevacizumab	Avastin	2004	humanized	Vascular endothelial growth factor	Colorectal cancer, Age related macular degeneration
Omalizumab	Xolair	2004	humanized	IgE	Mainly allergy-related asthma
Natalizumab	Tysabri	2006	humanized	Alpha-4 (α4) integrin,	Multiple sclerosis and Crohn's disease
Ranibizumab	Lucentis	2006	humanized	Vascular endothelial growth factor A	Macular degeneration
Panitumumab	Vectibix	2006	human	Epidermal growth factor receptor	Colorectal cancer
Eculizumab	Soliris	2007	humanized	Complement system protein C5	Paroxysmal nocturnal hemoglobinuria

Certolizumab pegol	Cimzia	2008	humanized	Inhibition of TNF-α signaling	Crohn's disease
Canakinumab	Ilaris	2009	human	IL-1β	Cryopyrin-associated periodic syndromes
Ofatumumab	Arzerra	2009	human	CD20	Chronic lymphocytic leukemia
Golimumab	Simponi	2009	human	TNF-α inihibitor	Rheumatoid arthritis, Psoriatic arthritis, and Ankylosing spondylitis
Denosumab	Prolia , Xgeva	2010	human	RANK Ligand inhibitor	Postmenopausal osteoporosis , Solid tumor's bony metasteses
Tocilizumab	Actemra/ RoActemra	2010	humanised	Anti- IL-6R	Rheumatoid arthritis
Belimumab	Benlysta	2011	human	Inihibition of B- cell activating factor	Systemic lupus erythematosus
Brentuximab vedotin	Adcetris	2011	chimeric	CD30	Anaplastic large cell lymphoma and Hodgkin lymphoma
Ipilimumab	Yervoy	2011	human	Blocks CTLA-4	Melanoma

*Adapted from T.A Waldmann [17], P.A. Scolnik [18] and updated by consulting FDA databases [19].

The efficacy of Muromonab-CD3 in the prevention and treatment of transplant rejection was obvious in many cases, but various adverse reactions were reported in some patients [16]. Based on the hypothesis that reducing the extent of, or eliminating, mouse-derived sequences would reduce MAb immunogenicity, murine antibodies started being engineered to become more human-like [20]. Chimeric antibodies are composed of murine variable regions fused onto human constant regions and humanized antibodies are human antibodies with murine hypervariable domains of the Fab region. In 2002, the first fully-human antibody (adalimumab) was approved by the FDA for therapeutic use against TNF-α, bearing high expectations regarding (low) immunogenicity levels. However, clinical studies revealed that repeated administration of adalimumab induced ADAs in a high percentage of patients and in most cases the treatment had to be discontinued [21, 22]. It is now clear that humanization of therapeutic MAbs does not solve immunogenicity issues.

Among the factors that are known to play a role in immunogenicity of therapeutic proteins, the presence of protein aggregates has been indicated as one of the main product-related risk factors [23]. One of the main challenges of developing and commercializing therapeutic MAbs, as nearly all other therapeutic proteins, is

circumventing their aggregation during manufacturing, storage and administration steps [24, 25]. Even though several studies have shown that protein aggregates have the propensity to trigger an antibody response against the monomeric form of the protein, little is known about the particularities that make them immunogenic.

AIM AND OUTLINE OF THE THESIS

The work presented in this thesis focuses mainly on aggregate characterization and aggregate-related immunogenicity of MAb formulations, using a monoclonal human IgG_1 with κ light chains as a model. The use of emerging analytical techniques for the characterization of IgG aggregates is evaluated; non-native aggregation mechanisms of IgG are studied; the fate of fluorescently labeled IgG aggregates upon contact with human biological fluids *in vitro* and upon injection in mice is investigated; and the correlation between type and amount of IgG aggregates with their immunogenic potential is studied in transgenic (TG) mice (containing the human genes for Ig heavy and light chains) and their nontransgenic (NTG) counterparts.

In **Chapter 2** a general overview on protein immunogenicity and relevant immunological background are provided. The current literature on aggregate-related immunogenicity is reviewed and the different aspects relating protein aggregates to immunogenicity are then discussed.

In **Chapter 3** an emerging analytical method - nanoparticle tracking analysis (NTA) - is evaluated for the measurement of submicron protein aggregates and compared with dynamic light scattering (DLS). In order to do so, standard polystyrene beads of sizes ranging from 60 to 1,000 nm and physical mixtures thereof, drug delivery nanoparticles and protein aggregates are analyzed with NTA and DLS. Moreover, heat-induced IgG aggregation is followed with NTA over time.

In **Chapter 4** the use of native electrospray ionization time-of-flight mass spectrometry (ESI-TOF MS) for the analysis of low-order oligomers of IgG is tested. Fractions of IgG aggregates, induced by subjecting this protein to consecutive pH jumps (pH-shifts), are isolated by size exclusion chromatography (SEC) and analyzed by ESI-TOF MS.

The mechanism of IgG aggregation induced by pH-shift is investigated in **Chapter 5**. The aggregation process that follows this low-pH exposure is monitored over time using a wide range of complementary analytical techniques. The role of molten globules in such non-native aggregation process is studied and the most likely aggregation pathways are discussed.

In **Chapter 6** the potential of an emerging analytical technique - fluorescence single particle tracking (fSPT) - for the characterization of submicron protein aggregates in human serum and plasma is evaluated. Covalent aggregates of a fluorescently labeled IgG are diluted in buffer, serum and plasma, and their size distribution is analyzed by fSPT. In a separate experiment, IgG and HSA, fluorescently labeled with different dyes, are mixed, subjected to heat stress and analyzed by fSPT using a dual color mode.

The fate of different types of IgG aggregates upon contact with human serum in vitro is investigated in **Chapter 7**. Fluorescently labeled subvisible IgG aggregates, induced by applying heat or pH-shift stress, are analyzed with different complementary analytical techniques immediately after addition to human serum, and after 24 hours. Size distribution changes and interactions with serum components are investigated.

Chapter 8 describes a pilot study performed to test the feasibility of following over time the fate of fluorescently labeled IgG and recombinant human interferon alpha (IFN-α) aggregates in TG mice (respectively containing the human genes for these proteins). IFN-α aggregates induced by metal-catalyzed oxidation and IgG aggregates induced by shaking stress are injected intraperitoneally in mice and in vivo fluorescence images are captured over time.

In **Chapter 9** the correlation between the type and amount of IgG aggregates with their immunogenic potential is investigated. IgG aggregates are obtained by freeze-thawing cycles, pH-shift cycles, heating, shaking and metal-catalyzed oxidation. The size, amount, morphology and type of intermolecular bonds of aggregates, as well as structural changes and epitope integrity are assessed. These formulations are then injected in TG mice and their NTG counterparts, and anti-drug antibody titers are determined by a bridging enzyme-linked immunosorbent assay (ELISA).

Chapter 10 summarizes the findings and conclusions of this thesis and discusses the perspectives for further research on the correlation between aggregates and immunogenicity of MAbs.

REFERENCES

1. H. Schellekens. Bioequivalence and the immunogenicity of biopharmaceuticals. Nat Rev Drug Discov. 1:457-462 (2002).
2. P. Bork, L. Holm, and C. Sander. The immunoglobulin fold. Structural classification, sequence patterns and common core. Journal of molecular biology. 242:309-320 (1994).
3. W. Wang, S. Singh, D.L. Zeng, K. King, and S. Nema. Antibody structure, instability, and formulation. Journal of pharmaceutical sciences. 96:1-26 (2007).
4. B. Al-Lazikani, A.M. Lesk, and C. Chothia. Standard conformations for the canonical structures of

immunoglobulins. Journal of molecular biology. 273:927-948 (1997).
5. C. Janeway, P. Travers, M. Walport, and M. Shlomchik. Immunobiology, Garland Publishing, New York, 2001.
6. H. Liu, G. Gaza-Bulseco, D. Faldu, C. Chumsae, and J. Sun. Heterogeneity of monoclonal antibodies. Journal of pharmaceutical sciences. 97:2426-2447 (2008).
7. T. Mizuochi, T. Taniguchi, A. Shimizu, and A. Kobata. Structural and numerical variations of the carbohydrate moiety of immunoglobulin G. Journal of immunology. 129:2016-2020 (1982).
8. R.C. Grebenau, D.M. Goldenberg, C.H. Chang, G.A. Koch, D.V. Gold, A. Kunz, and H.J. Hansen. Microheterogeneity of a purified IgG_1 due to asymmetric Fab glycosylation. Molecular immunology. 29:751-758 (1992).
9. W. Jiskoot, G. van de Werken, J.M. Martin, B.N. Green, E.C. Beuvery, and D.J. Crommelin. Application of electrospray mass spectrometry (ES-MS) for the analysis of monoclonal antibody Fc subunits. Pharm Res. 9:945-951 (1992).
10. H. Leibiger, D. Wustner, R.D. Stigler, and U. Marx. Variable domain-linked oligosaccharides of a human monoclonal IgG: structure and influence on antigen binding. The Biochemical journal. 338 (Pt 2):529-538 (1999).
11. P.M. O'Callaghan, J. McLeod, L.P. Pybus, C.S. Lovelady, S.J. Wilkinson, A.J. Racher, A. Porter, and D.C. James. Cell line-specific control of recombinant monoclonal antibody production by CHO cells. Biotechnology and bioengineering. 106:938-951 (2010).
12. M. Kuczewski, E. Schirmer, B. Lain, and G. Zarbis-Papastoitsis. A single-use purification process for the production of a monoclonal antibody produced in a PER.C6 human cell line. Biotechnology journal. 6:56-65 (2011).
13. Z.H. Jin, L.Z. Zhao, Y. Zhang, and W. Zhang. An anti-DLK1 monoclonal antibody produced using ELISA and hybridoma techniques. Hybridoma. 28:441-445 (2009).
14. C. Emmons and L.G. Hunsicker. Muromonab-CD3 (Orthoclone OKT3): the first monoclonal antibody approved for therapeutic use. Iowa medicine : journal of the Iowa Medical Society. 77:78-82 (1987).
15. A.L. Nelson, E. Dhimolea, and J.M. Reichert. Development trends for human monoclonal antibody therapeutics. Nature reviews Drug discovery. 9:767-774 (2010).
16. W.G. Byerlyand R. Winslow. Adverse reaction from topical exposure to muromonab-CD3. Am J Hosp Pharm. 48:1442 (1991).
17. T.A. Waldmann. Immunotherapy: past, present and future. Nature medicine. 9:269-277 (2003).
18. P.A. Scolnik. mAbs: a business perspective. mAbs. 1:179-184 (2009).
19. FDA. Drugs@FDA online database. http://www.accessdata.fda.gov/scripts/cder/drugsatfda/ (accessed 15 December 2011).
20. M. Stern and R. Herrmann. Overview of monoclonal antibodies in cancer therapy: present and promise. Critical reviews in oncology/hematology. 54:11-29 (2005).
21. N.K. Bender, C.E. Heilig, B. Droll, J. Wohlgemuth, F.P. Armbruster, and B. Heilig. Immunogenicity, efficacy and adverse events of adalimumab in RA patients. Rheumatol Int. 27:269-274 (2007).
22. T. Levalampi, M. Korpela, K. Vuolteenaho, and E. Moilanen. Etanercept and adalimumab treatment in patients with rheumatoid arthritis and spondyloarthropathies in clinical practice: adverse events and other reasons leading to discontinuation of the treatment. Rheumatol Int. 28:261-269 (2008).
23. A.S. Rosenberg. Effects of protein aggregates: an immunologic perspective. The AAPS journal. 8:E501-507 (2006).
24. M.E. Cromwell, E. Hilario, and F. Jacobson. Protein aggregation and bioprocessing. The AAPS journal. 8:E572-579 (2006).
25. J.S. Bee, T.W. Randolph, J.F. Carpenter, S.M. Bishop, and M.N. Dimitrova. Effects of surfaces and leachables on the stability of biopharmaceuticals. Journal of pharmaceutical sciences (2011).

Chapter 2

Aggregation and immunogenicity of therapeutic proteins

Vasco Filipe[1,2], Andrea Hawe[1], Huub Schellekens[2], Wim Jiskoot[1]

[1] Division of Drug Delivery Technology, Leiden/Amsterdam Center for Drug Research, Leiden University, P.O. Box 9502, 2300 RA Leiden, The Netherlands

[2] Department of Pharmaceutics, Utrecht Institute for Pharmaceutical Sciences (UIPS), Utrecht University, P.O. Box 80082, 3508 TB, Utrecht, The Netherlands

Book chapter in: Aggregation of therapeutic proteins, John Wiley & Sons, 2010: pp 403-433.

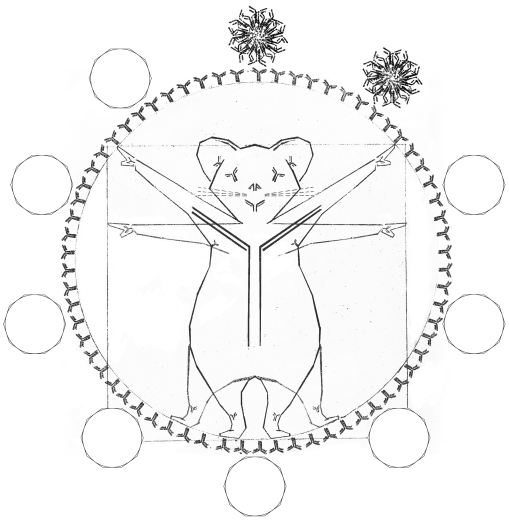

ABSTRACT

The aim of this chapter is to summarize the state of the art regarding knowledge on the role of protein aggregates in unwanted immunogenicity of therapeutic proteins. A general overview on protein immunogenicity and the relevant immunological background are provided, in order to better understand aggregate-related immunogenicity. Different aspects relating protein aggregates to immunogenicity are then discussed and our current understanding about this subject is summarized.

2.1 INTRODUCTION

Therapeutic proteins have proven efficacy in treating a wide range of diseases and are now established as a major drug class. However, a major concern associated with the use of these drugs is that repeated administration of such proteins to patients often leads to the induction of undesirable anti-drug antibodies (ADAs). These can be classified as binding or neutralizing antibodies, each of which can lead to a wide range of consequences, varying from none to life-threatening situations.

Unwanted immunogenicity has been a major issue ever since proteins were first used as therapeutics. Although some advancement has been made in understanding immunogenicity of therapeutic proteins, opinions are often conflicting, and to a large extent based on assumptions rather than facts. Among the several factors playing a role in immunogenicity, the presence of impurities, in particular aggregates, has been put forward as a major concern. Several studies have suggested that formulations with a high amount of aggregates tend to be more immunogenic [1]. However, little is known about the nature of the aggregate species responsible for such effects.

2.2 IMMUNOGENICITY OF THERAPEUTIC PROTEINS

2.2.1 Incidence of immunogenicity during therapy

The first reports of unwanted immunogenicity go alongside with the first use of therapeutic proteins, more than a century ago, when animal antiserum was introduced in humans for the treatment and prevention of infections. A few decades later, more precisely in 1922, insulin from bovine and porcine origin started to be used in the treatment of diabetes mellitus. All these products triggered immune responses involving ADAs, even after a single or few injections, and sometimes led

to fatal anaphylactic reactions [2]. These effects were at that time explained by the protein's foreign nature and impurities present in the formulations. In fact, the most severe adverse reactions to porcine and bovine insulin decreased after purification of the products.

The identification of new therapeutic targets, associated with the need to reduce unwanted immunogenicity, led to the next generation of therapeutic proteins, this time from human origin. Examples of these proteins include the plasma-derived clotting factors and growth hormone isolated from the pituitary glands of cadavers. However, these proteins also induced a strong antibody response in many patients [3, 4]. This was ascribed to the high level of impurities present in these products. Moreover, given that many of the patients were treated with these products because they had an innate deficiency of an endogenous protein, they also lacked the immune tolerance to the therapeutic protein.

Profiting from the advancement of recombinant DNA techniques and sequencing of the human genome, most therapeutic proteins introduced in the market nowadays are at least human homologues, with some even produced in human cell lines. However, in contrast to initial expectations, these proteins still induce ADAs, and in some cases in the majority of patients. Therapeutic proteins for which cases of immunogenicity after repeated administration have not been reported are extremely rare. It is now clear that a highly pure and stable formulation of a fully human therapeutic protein is not enough to avoid ADA formation.

Clinical ADA formation outcome is very difficult to predict and it often contradicts well accepted hypotheses. For example infliximab, a chimeric monoclonal antibody (MAb) against the tumor necrosis factor-alpha (TNFα), shows good results in treating diseases like rheumatoid arthritis and Crohn's disease. However, after a few months of treatment this drug has an antibody formation rate that ranges from 20-60%, depending on the studies [5, 6]. One may think that the mouse component can be the main reason for these high values, but similar results have been observed with recently approved fully human antibodies like adalimumab. This MAb has the same therapeutic target as infliximab, and has shown levels of ADA formation of about 20% [7].

2.2.2 Consequences of protein immunogenicity for patients

Immunogenicity of therapeutic proteins is mainly characterized by the formation of binding or neutralizing antibodies. The biological and clinical consequences

of these antibodies vary according to their levels, specificity, and the role of the therapeutic protein. Binding antibodies bind to the drug in sites that may or may not interfere with its pharmacokinetic/pharmacodynamic (PK/PD) behavior. Neutralizing antibodies interfere directly or indirectly with the active site of the drug, neutralizing its therapeutic effect. In some cases these antibodies can cross-react or even neutralize endogenous proteins, and this can have very serious consequences [8].

In many cases, the formation of ADAs has very little biological and clinical consequences. The most severe general immune reactions, such as acute and delayed infusion-like reactions, have become less common, owing in part to the high purity of new products. Acute infusion reactions normally occur within the first 48 hours after an infusion and include type I hypersensitivity, nausea, flushing, and dyspnea. Late infusion reactions typically occur after a longer period of treatment and they are more frequent, particularly for high-dosed MAbs. They include serum sickness-like reactions and other type III and delayed-type hypersensitivity reactions [9].

The most common biological effect of ADAs is loss of efficacy. In some cases this might be overcome by increasing the dose, for instance with factor VIII in the treatment of hemophilia A patients [10]. Normally, the interference of binding antibodies leads to a reduced half-life of the drug, resulting in lower activity. However, some cases have been reported where binding antibodies actually increase the half-life of therapeutic proteins and thereby increase their activity, as reported for human growth hormone [11]. Persistent levels of neutralizing antibodies lead to complete loss of activity. In such cases, the treatment has to be stopped and alternative treatments, if available, should be considered. The most dramatic consequences of immunogenicity occur when neutralizing antibodies neutralize an endogenous protein with an essential biological function.

One of the most severe cases of unwanted immunogenicity registered in the last decade occurred with erythropoietin (EPO), a hormone that regulates erythropoiesis and is normally used to treat anemia. When neutralizing antibodies start to cross-react with native EPO, patients cease the production of red blood cells and may develop pure red cell aplasia (PRCA) [12]. Although the percentage of patients that develop neutralizing antibodies against EPO is low, the consequences of this incident can be disastrous.

Concerns about unwanted immunogenicity have to consider both probability and consequences, with higher relevance on the second consideration. In the case of

therapeutic insulin, which has relatively high rates of ADA incidence, it is not fully understood why they seem to have no major effect on the drug's performance [13]. However, despite these high incidence rates, the low consequences attenuate the concern regarding the immunogenicity of this protein. In contrast, despite its low rates of antibody formation, EPO has been the center of many immunogenicity discussions, especially after an upsurge in the incidence of antibody-mediated PRCA between 2000 and 2002 [14]. Therefore, the levels and rates of antibody formation against a certain therapeutic protein have to be carefully balanced with the impact they may have in the patient and the progression of the disease.

2.2.3 Factors playing a role in protein immunogenicity

There have been several product, treatment, and analysis related factors identified and discussed to play a role in unwanted immunogenicity (Fig. 2.1). The particular relevance and the relative contribution of each of these factors to immunogenicity, and the underlying mechanisms, have not been fully elucidated. Moreover, there may also be unknown factors playing a role in this area.

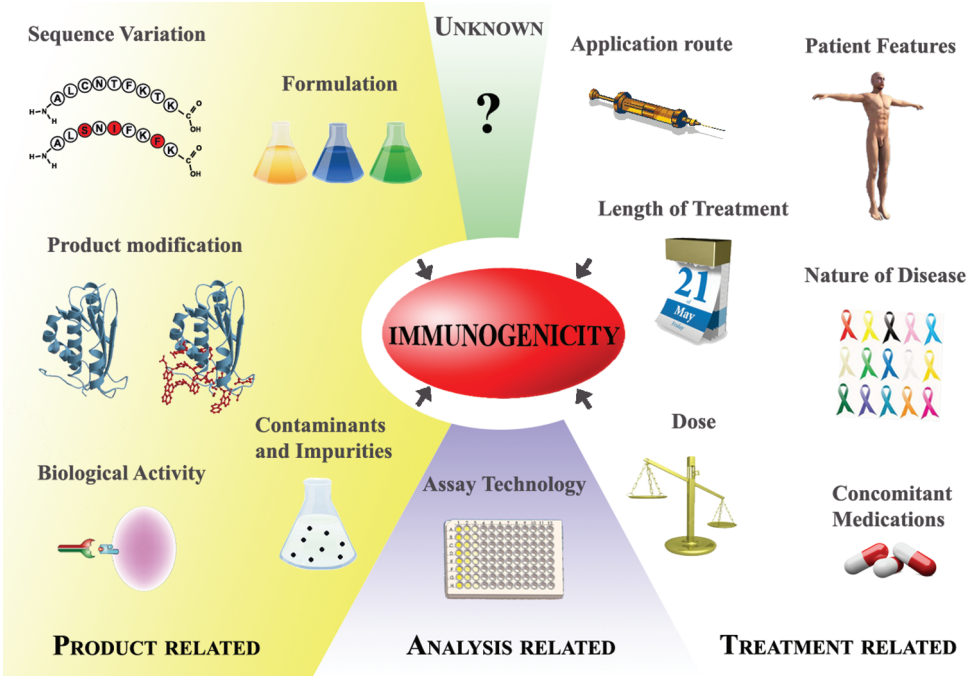

Figure 2.1: Factors influencing immunogenicity of therapeutic proteins (adapted from reference [15]).

Product Related

It is well known that the human immune system reacts against non-human proteins and that sequence variation can explain the high immunogenicity of therapeutic proteins like streptokinase [16], bovine adenosine deaminase [17], and salmon calcitonin [18]. However, as mentioned earlier in this chapter, similarity to the human sequence does not necessarily imply a lack of immunogenicity. Conversely, there are several examples of recombinant therapeutic proteins with sequences differing from the naturally occurring human sequence that have not led to an increased immune response [19, 20].

Product modification intended to increase half-life can have a positive or negative impact on immunogenicity. De-glycosylation of glycoproteins may expose new epitopes that are normally hidden by the glycan or expose new hydrophobic regions of the protein and alter its solubility, thereby affecting immunogenicity [21,22]. Moreover, post-translational modifications by the host cell, such as the addition of functional groups or structural changes, may also affect immunogenicity. Both natural glycosylated interferon $\alpha 2$ (IFN-$\alpha 2$) and interleukin-2 (IL-2) were reported to be less immunogenic than their nonglycosylated counterparts made in *E. coli* [23, 24].

Pegylation is claimed to reduce immunogenicity of therapeutic proteins by shielding epitopes [25]. In fact, this was verified in some non-human PEGylated proteins like bovine adenosine deamidase and asparginase [26]. However, there are reports of high immunogenicity of pegylated human proteins, such as megakaryocyte growth and differentiation factor (MGDF), but a comparison with unpegylated MGDF is lacking [27].

The biological activity of the therapeutic protein can also influence immunogenicity. An immune-stimulating protein is more likely to induce ADAs than an immune-suppressive protein. Monoclonal antibodies targeted to cell-bound epitopes are expected to induce a higher immune response than ones with a target in solution, allegedly due to their higher probability of gathering the necessary immunologic components to trigger an immune response [26].

The product formulation is another important factor for immunogenicity. For instance, human serum albumin (HSA) has been commonly added as a stabilizing agent, but it has been related with immunogenicity increase [28]. On the other hand, the replacement of HSA by glycine and polysorbate 80 in the formulation of EPO coincided with the upsurge of antibody-mediated PRCA outside the USA.

The integrity of therapeutic proteins profoundly depends on the formulation, and some degradation can occur during handling and storage. Degraded products have proven to be more immunogenic, as will be discussed later in this chapter. In particular, aggregates have shown to enhance immunogenicity and they are now one of the main concerns in the development of new therapeutic products. Ironically, downstream processing of a product can contribute to the introduction of impurities. For example, antibodies to factor VIII were associated with the introduction of a new pasteurization stage in the manufacturing process [29]. Although the purity of biopharmaceuticals has increased significantly over the last decades, impurities are still present in low amounts and they are thought to play an important role in immunogenicity.

Evidence for the importance of product variables can be found in significant variations in immunogenicity reported for different IFN-α products. For example, Avonex and Betaferon, which differ in formulation composition, level of impurities, sequence of amino acids, glycosylation, and producing cell type, have reported a percentage of patients with neutralizing antibodies of 13% for Avonex and 43% for Betaferon [30].

Treatment Related

There are various factors related to the treatment itself that can strongly influence unwanted immunogenicity. Several clinical and pre-clinical studies registered significant differences in ADAs according to the route of administration. Evidence suggests that subcutaneous (s.c.) administration is most likely to elicit an immune response, followed by intramuscular (i.m.) administration and intravenous (i.v.) administration, and the least immunogenic seems to be local (topical) administration [31]. For instance, it has been clinically shown that i.m. administration of IFN-β is less immunogenic than s.c. administration [32]. However, there have been no published cases whereby a change in the administration route completely eliminated the immunogenicity of a therapeutic protein [29].

The dose and duration of the treatment also play a role, since they determine the level of exposure to the immune system. Higher doses or prolonged duration of treatment increases exposure, thereby increasing the risk of immunogenicity. However, these two factors appear to be independent from each other. IFN-β formulations produced in *E. coli* and Chinese hamster ovary (CHO) cells both induced antibodies after 6-12 months of treatment, despite the ten fold difference in protein

amount between the two formulations [31].

Patient features like genetic background, gender, and age have all been reported to influence the incidence of ADAs [26], although for most of them the correlation is not consistent. Individuals who are deficient for functional genes may lack the immune tolerance for certain therapeutic proteins, making them more prone to develop an immune response. This may be the reason for the high immunogenicity levels reported for proteins used to treat genetic diseases, such as factor VIII and growth hormone [26].

Concomitant medications and the nature of the disease can also influence immunogenicity. For instance, the chimeric monoclonal antibody rituximab is practically nonimmunogenic in patients with non-Hodgkin's lymphoma, whereas the incidence of ADA formation against the same drug has been reported to be 27% and 65% in patients with primary Sjogren's syndrome and systemic lupus erythematosus, respectively [33]. Cancer patients are less likely to produce antibodies against therapeutic proteins. This is likely due to their compromised immune system, caused both by the disease and by immune-suppressive concomitant medications [26]. It has also been suggested that the average survival of cancer patients treated with therapeutic proteins may be too short to develop antibody responses.

Antibody Assay Related

Adopting an appropriate strategy for assessment of unwanted immunogenicity of therapeutic proteins is essential. A major factor leading to the highly variable and sometimes conflicting results concerning immunogenicity is most likely the assay technology used. For most cases, patient sera are first screened for the presence of binding antibodies. Positive samples are then submitted to confirmation assays and, if positive, antibody specificity and the presence of neutralizing antibodies are assayed. However, the lack of international standardization of assays and reference preparations makes it virtually impossible to compare test results from different laboratories [26].

For instance, screening of ADAs is extremely difficult in the presence of drug in the sample because it often prevents the ADAs to bind to the detection antibodies. This is particularly problematic for drugs with a long half-life, such as MAbs. The most recent assays for ADA screening include an acid pre-treatment of the collected serum before the detection step, in order to separate the binding or neutralizing antibodies from the drug [34]. Many immunogenicity studies from the past are now

being questioned and there is an urgent need for optimization and standardization of all immunogenicity assays.

2.3 IMMUNE MECHANISMS RELATED TO IMMUNOGENICITY OF THERAPEUTIC PROTEINS

The immune system constitutes a natural defense that has evolved to respond to all types of invasive threats, like bacteria and viruses. This defense is a complex system that involves the coordinated interaction of numerous elements. Many basic aspects of immunological functions have already been clarified to date, but there are still numerous questions to be answered. In order to better address the role of aggregates in immunogenicity of therapeutic proteins, it is important to understand the relevant immune responses possibly involved in this process.

From a classical point of view, the immune system can be divided into two arms: the innate and the adaptive immune system. The innate immune system comprises the cells and mechanisms that constitute the first line of defense against threats, in a fast and non-specific manner. Phagocytic cells, like macrophages that ingest and kill pathogens, together with the complement system, are primarily responsible for the innate immune response. The innate immune system strongly depends on pattern recognition receptors (PRRs) that have evolved to recognize highly conserved pathogen-associated molecular patterns (PAMPs). The most important and well characterized class of these receptors are the toll-like receptors (TLRs) [35].

The adaptive immune system is capable of mounting highly specific responses against pathogenic agents. It consists of a complex and diverse surveillance cell network, capable of developing long term memory cells against specific molecular determinants. The fundamental mechanisms of this type of response are mediated primarily by B- and helper T-lymphocytes. They circulate between the bloodstream, the lymph nodes, and peripheral lymphoid tissues in a state referred to as naïve cells. Upon contact with antigens they can get activated and transform into effector cells. Both lymphocytes carry unique antigen specific receptors on their surface. Through complex signaling mechanisms, B-cells are able to generate specific antibodies against any conceivable antigen. Given that unwanted immunogenicity of therapeutic proteins is primarily based on the detection of antibodies, this chapter will further focus on the adaptive arm of the immune system.

2.3.1 Immune responses to therapeutic proteins

Therapeutic proteins can activate the immune system through two different mechanisms: classical immune response and breaking of immune tolerance.

Classical Immune Response

The classical activation of the immune system is triggered by the presence of non-self epitopes: for example, those present in non-human therapeutic proteins like bacterial-derived asparginase and streptokinase [36]. The mechanism typically involves T-cell dependent activation of B-cells with subsequent production of different high affinity antibody isotypes and induction of memory cells. Resembling a vaccination-type immune reaction, the classical immune response may be enhanced by adjuvant equivalent "danger" signals, such as impurities or aggregates [37].

This type of immune response is also found in patients that lack immune tolerance to the therapeutic protein, e.g., due to a genetic defect, and is sometimes observed in patients treated with modified human proteins. In general, it is hard to predict if modified human proteins will trigger a classical immune response. Immunogenicity consequences of sequence deviation from the human amino acid sequence are less dependent on the level of divergence, and depend more on the type of amino acid changed and its location in the sequence [38].

The classical response usually originates a fast and robust immune reaction, often after the first injection. The ADAs formed are normally neutralizing antibodies and memory effect is very often observed. In most cases there is considerable loss of efficacy of the therapeutic, and sometimes the treatment has to be stopped due to anaphylactic type reactions. Similar to vaccines, re-treatment with the same product often triggers very fast and efficient immune responses [39].

Breaking of Immune Tolerance

The immune system has developed several mechanisms in order to tolerate self-proteins. Given that most recombinant human proteins are homologous to their endogenous counterparts, the immune response to such therapeutic proteins involves breaking of immune tolerance, the mechanism of which is not yet fully understood.

Antibody formation via this process is slow and it often takes several months of

chronic administration to break immune tolerance. ADAs normally disappear after stopping the treatment and sometimes disappear even during the treatment. ADA formation through this process often has no major consequences, but sometimes results in a reduction of efficacy, neutralization of activity, and neutralization of endogenous proteins [36].

2.3.2 Immune tolerance

T- and B-lymphocytes have the ability of randomly generating an infinite variety of receptors on their surface, commonly termed T-cell receptors (TCRs) and B-cell receptors (BCRs). This is achieved by random gene rearrangements in the receptor loci. It ensures a vast receptor repertoire providing recognition of any conceivable antigen. Very often a subset of these lymphocytes expresses self-reactive receptors and these cells must be downregulated in order to avoid autoimmune responses. A complex regulating mechanism, known as central tolerance, is responsible for verifying and suppressing self-reactive cells through several checkpoints in the pathway of lymphocyte differentiation, occurring in the thymus and bone marrow [40].

Despite the action of this mechanism, many auto-reactive lymphocytes manage to escape into the peripheral pool of circulating lymphocytes. Here, an additional regulation mechanism, not yet fully understood, is responsible for keeping them inactive, known as peripheral tolerance [40]. Auto-reactive circulating lymphocytes are thought to be either eliminated by apoptosis upon contact with self-antigens or to enter several possible states of anergy [41]. In any case, an immune reaction against a human protein requires breaking of this peripheral tolerance.

With concern to protein immunogenicity of human homologues, breaking of B-cell tolerance seems to be the most relevant mechanism [26]. Given that only B-cells are capable of producing antibodies, B-cell tolerance has to be broken for the production of self-antibodies to occur. This mechanism is not fully elucidated and many pieces of the puzzle seem to be missing. For example, the role of regulatory T-cells (Treg), which are known to have immune-suppressive regulatory functions over other cells, in breaking immune tolerance is not clear. Moreover, the impact of many signaling proteins still remains uncertain and several immunological pathways are still to be characterized. In any case, breaking of B-cell tolerance ultimately involves the activation of auto-reactive B-cells [26].

2.3.3 B-cell activation mechanisms

In order to understand the proposed models for immunogenicity of human homologues in therapy, it is important to realize that there are different ways of activating B-cells. These activation mechanisms can be classified as T-cell dependent (Td) or T-cell independent (Ti), depending on the contribution of helper CD4(+) T-cell.

T-Cell Dependent (Td)

Td activation of B-cells is normally triggered by antigens with a small number of copies of several different epitopes. Classical examples of these antigens include microbial proteins, several other nonself-proteins, and some altered self-proteins. This mechanism requires a sequence of coordinated events involving different cells types and several stimulatory signals (Fig. 2.2) [42].

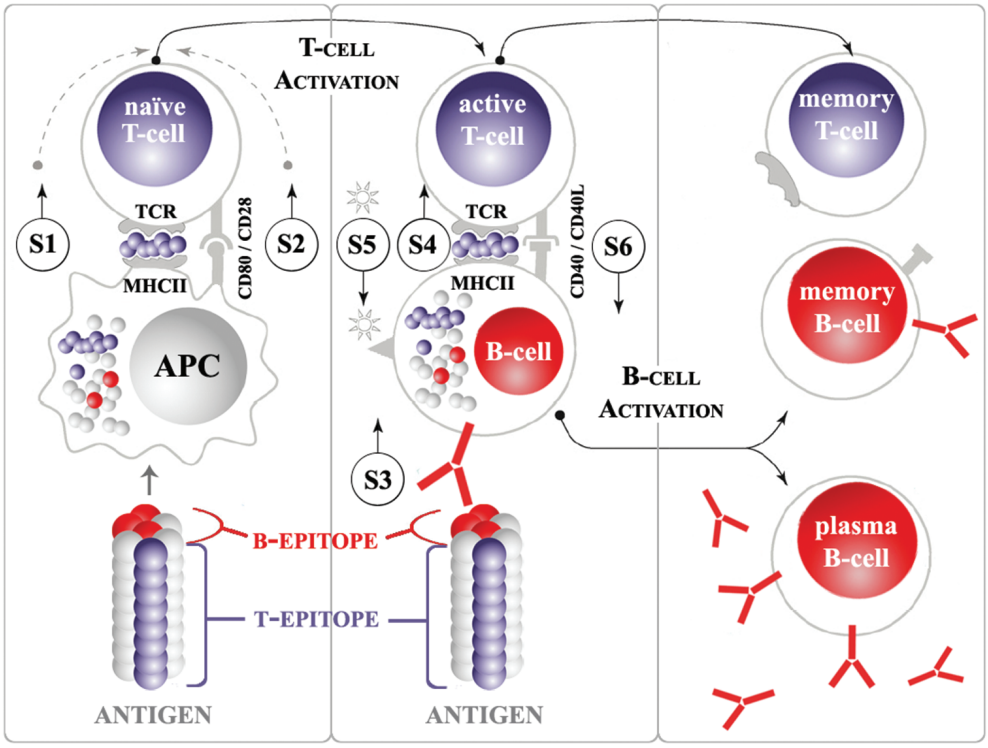

Figure 2.2: Common T-cell dependent B-cell activation mechanism (adapted from reference [42]). The first step in this process involves the nonspecific internalization of an antigen by a professional APC. It processes the antigen into peptides, which are then presented to a naïve T-cell, in major histocompatibility complex class II (MHC II) molecules on the surface of the APC. Two signals must be given by the APC for the T-cell to become fully

activated: the interaction of the MHC II–peptide complex with the TCR (S1); the interaction of co-stimulatory molecules from the APC, such as CD80 and CD86, with co-stimulatory molecules from the T-cell, such as CD28 (S2). Once fully activated, the T-cell divides and starts producing an array of cytokines with various activities. Meanwhile, activation of naïve B-cells starts with the recognition of the cognate antigen by BCRs (S3), more specifically IgM and IgD receptors. The B cell internalizes and processes the antigen–Ig complex and presents cognate T cell epitopes in MHC II molecules on its surface. Upon recognition of this MHC II–epitope complex by the effector T-cell (S4), two other signals must occur for complete activation of B-cells: the delivery of several cytokines from T-cells to B-cells (S5); the interaction of the CD40 co-stimulatory molecule from the B-cell with the recently expressed CD40L co-stimulatory molecule from the T-cell (S6). Once fully activated, the B-cell proliferates and differentiates into memory and antibody-secreting plasma cells, with the ability to perform antibody affinity maturation and isotype switching.

Td activation of B-cells requires antigens with epitopes capable of interacting with the protein-processing machinery of professional antigen presenting cells (APCs), such as dendritic cells (DCs), and both TCRs and BCRs. Any failure in delivering the stimulatory signals mentioned in Fig. 2.2 may lead to B- or T-cell anergy or apoptosis [42]. It is important to note that B-cells are also considered professional APCs and this fact adds some variants to the mechanism already described. The presentation of processed peptides by B-cells to naïve T-cells can activate both cells, resulting in an accelerated version of Td activation [43].

In general, the dependence on other cells and the requirement of several signaling steps make Td activation a slower process compared to Ti activation [1]. However, Td activation of B-cells normally results in a more robust immune response, exclusively leading to the formation of memory B- and T-cells [42]. It also promotes antibody affinity maturation and isotype switching, from the classes IgM and IgD into IgG, IgE and IgA [44].

T-Cell Independent (Ti)

Antigens that are expressed on the surface of pathogens in an organized and highly repetitive form can directly stimulate B-cells to produce antibodies without the help of T-cells. Examples of these antigens include both relatively simple polymers of peptides and polysaccharides, as well as higher order structures such as viral capsids, composed of repetitive arrays of multiple protein components [1]. This mechanism is not fully understood, as there are still several unknown signaling pathways. Currently, Ti activation of B-cells is divided in two different categories, commonly termed type 1 and type 2 activation (Fig. 2.3). Type 1 activation is also known as polyclonal B-cell activation, because these antigens are capable of directly inducing the proliferation and differentiation of several different B-cells into antibody-secreting cells [45]. This

mechanism is thought to involve the recognition of antigens by both BCRs and TLRs. The antibodies produced through this type of Ti activation are normally nonspecific and preferentially recognize heterologous antigens [45]. Despite being commonly classified as a Ti mechanism, polyclonal activation may also have some variants that require T-cell help [46]. Conversely, type 2 activation takes place when several antigen clusters are presented to B-cells in a manner that causes cross-linking of BCRs in a multivalent fashion [47]. This occurrence triggers a complex signaling pathway, such as the activation of Bruton's tyrosine kinases [48], eventually leading to B-cell activation (Fig. 2.3).

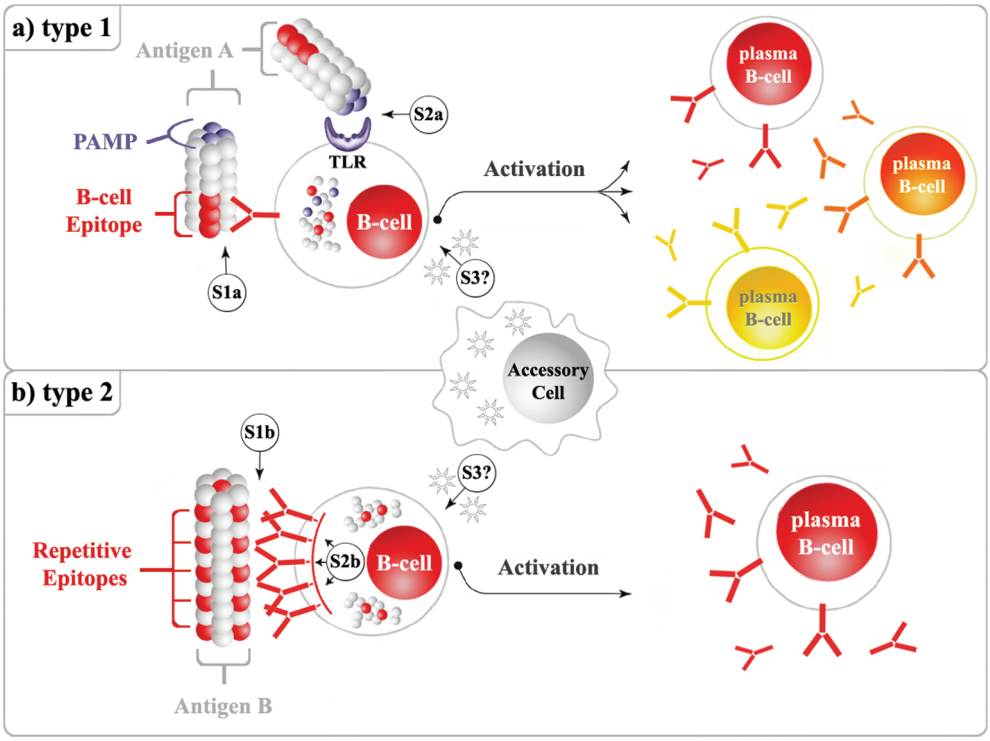

Figure 2.3: T-cell independent B-cell activation mechanisms. a) Type 1 activation requires the recognition of a polyclonal activator antigen (antigen A) by both BCRs (S1a) and TLRs (S2a), which leads to the production of several activation signals. B-cells are activated in a polyclonal fashion. b) Type 2 activation requires the recognition of a type 2 antigen (antigen B), which normally display repetitive epitopes, by BCRs (S1b). Clustering of bound BCRs leads to multivalent cross-linking (S2b), which triggers the production of several activation signals. In either case B-cells are activated, proliferate and become antibody-producing plasma B-cells. The contribution of external stimulatory factors by accessory cells, such as professional APCs, is not clear (S3?).

It has been reported that Ti activation of B-cells can be modulated by accessory cells, like macrophages and DCs, which can be stimulated via TLRs to produce several stimulatory signals [45]. Independence of T-cells and the direct activation of B-cells

by the antigen make this response much faster than Td responses [1]. However, Ti activation does not lead to affinity maturation or the generation of memory B-cells and it has often been mentioned that B-cells activated via this mechanism do not undergo isotype switching [42]. This last feature of B-cells is often associated with the engagement of CD40 on B-cells by CD40L on T-cells, a step exclusive for Td activation. However, some studies have suggested that isotype switching resulting from Ti activation is possible. HIV-1 envelope glycoproteins have been reported to directly activate B-cells, triggering isotype class switching from IgM to IgA or IgG, in a CD40-independent manner [49]. It has been described that several interleukins and activation factors such as interleukin-10 (IL10) and BAFF (B-cell Activating Factor belonging to the TNF Family), delivered by accessory cells play crucial roles in B-cell development and activation [49, 50]. However, knowledge regarding the exact targets and function of these proteins remains very limited. Still, these signals may hold the key to answer many questions about breaking immune tolerance by human protein homologues in therapy.

2.3.4 Breaking of B-cell immune tolerance

Over the last century, as the comprehension of the immune system increased, different models have been proposed to explain the immune response against therapeutic proteins. While the mechanisms of classical immune responses seem to be consensual, divergences start emerging with the mechanisms of breaking immune tolerance. It has already been shown that tolerance may be broken both by Td and Ti activation of auto-reactive B-cells [51]. The main task is now to clarify which of these two mechanisms is the most relevant for breaking immune tolerance during therapy and to identify the main trigger of this process.

Among the proposed silencing mechanisms of B-cell peripheral tolerance, the most feasible seems to be the induction of anergy [40]. Auto-reactive anergic B-cells may start to produce antibodies if they are given a certain “danger” signal as trigger. For example, bacterial endotoxins, capable of being recognized by TLRs, have proven to trigger the production of antibodies against self-antigens. However, this particular Td activation of B-cells has shown to result in a feeble immune response. When self-antigens are coupled to foreign T-cell epitopes, only a weak IgM response is induced, unless multiple high doses of antigen are given together with immune adjuvants [26].

Alternatively, the “danger” signal may be given to the B-cell in a Ti way. It has been

shown that the most potent way to induce high levels of IgG through Ti activation against a self-antigen is to present it arrayed on virus or virus-like particles (VLP) [52-54]. Ordered presentation of repetitive epitopes is characteristic of microbials and the immune system has apparently learned to react vigorously to this type of antigen presentation. Protein aggregates may also present epitopes in an array form and they are often pointed to as the most likely risk factor involved in breaking immune tolerance [26], as will be later described.

In any case, there is not enough evidence to fully support a higher emphasis of either the Ti or Td mechanism in breaking immune tolerance. Our current lack of knowledge regarding several pathways involved in breaking immune tolerance makes it very difficult to substantiate exact mechanisms and main triggers of this process. Nevertheless, several studies are now being carried out in this field supporting the relevance of protein aggregates in breaking immune tolerance.

2.4 AGGREGATES AND IMMUNOGENICITY

The ability of protein aggregates to trigger an antibody response against the monomeric form of the protein has been known for more than half a century. However, despite this obvious connection, little is known about the particularities that make protein aggregates potent inducers of the immune system.

It has been shown that not all aggregates are immunogenic [55] and, in fact, there are several intrinsic and extrinsic aspects to consider. Aggregate features such as size, molecular weight (MW), amount, solubility, and resemblance to microbial structures are each thought to play a role in their immunogenicity. Moreover, product-, treatment-, and host-related factors may also influence the immune response to protein aggregates. Examples of these factors include product origin, route of administration, host immune status and, in the case of therapeutic versions of endogenous proteins, the abundance and manner of presentation of the endogenous protein [1]. Unfortunately, for most cases the way these factors may affect an aggregate-related immune response is uncertain and their relevance remains unclear.

Protein aggregates can be formed by various mechanisms and there are several different ways to classify them. From an immunological point of view, and according to their propensity to trigger immune responses against the constituent monomer, aggregates can be roughly classified into three different types: (1) an assembly of native proteins in a polymeric-like structure; (2) an assembly of denatured or

partially denatured protein irreversibly associated (within the given environment); (3) covalently linked proteins, which could be either in a native or denatured state [1]. Given that the activity of microbial pathogenic proteins depends critically on the conformation of their active site, the immune system has evolved to preferentially make conformation-dependent antibodies for this site. This preference for making antibodies to conformational rather to linear determinants, i.e. independent of spatial arrangement, appears to be a general property of the immune system [56-58]. Regarding immunogenicity of therapeutic proteins, it has been documented that neutralizing antibodies to EPO tend to be conformation-dependent, since most of them fail to bind to completely denatured EPO containing mainly linear determinants [12]. Aggregate-induced antibodies that also bind to the monomeric protein are a major concern for immunogenicity of therapeutic proteins. For these reasons, native-like aggregates are thought to be more dangerous than conformationally changed aggregates [1].

In the field of protein vaccination, where a robust immune response to the administered protein is the desired effect, the presence of aggregates in the formulations can have diverse effects. Since most prophylactic and therapeutic vaccines aim to create antibodies against native state proteins, which can be presented in a monomeric state or organized in polymeric structures, it is important to ensure that the antibodies formed against aggregates can cross-react with the corresponding target protein. Vaccine formulations with high percentages of aggregates may elicit strong immune responses, but not necessarily with the desired outcome. Therefore, vaccine aggregation should only be allowed in a controlled and well characterized way.

The correlation between protein aggregates and both wanted and unwanted immunogenicity is a crucial topic for the pharmaceutical industry and it needs to be promptly clarified. Given that each protein is structurally unique and that aggregates can take countless forms, general conclusions can probably only be drawn based on a larger number of case-by-case studies. Understanding the effect of aggregates in immunogenicity requires far more research and it can only be achieved by extensive collaboration between academia, industry, and the regulatory authorities.

2.4.1 Evidence of aggregates as a risk factor for immunogenicity

Throughout the last century, several studies have drawn attention to relationships between protein aggregates and immunogenicity. In order to better understand these

concerns, some relevant clinical and nonclinical studies will be addressed.

Nonclinical

The first documented nonclinical studies directly relating therapeutic protein aggregates to immunogenicity date back to the 1960s, in which immunoglobulin (Ig) from different sources were injected in rodents. In the research performed by Dresser in 1962, while studying induced immunological paralysis in mice through small intraperitoneal injections of bovine γ globulin (BGG), he realized that immune responses could be eliminated by removing the high MW material from the preparations [59]. Accordingly, in 1963 Claman noticed that in order to properly induce immune tolerance to BGG in mice, the preparations had to be ultracentrifuged and the pellet removed [60]. Administration of the resuspended pellet resulted in high production of antibodies and fast clearance of the antigen. In 1966, Gamble decided to further study the correlation between the amount of soluble aggregates and the corresponding immune response [61]. Therefore, preparations of human γ globulin (HGG) with increasing amounts of heat-generated aggregates were injected in mice and the immune response was monitored. The results showed a clear dose-dependent correlation between the amount of aggregates administrated and the immune response intensity (Fig. 2.4). Once again, most mice treated with centrifuged HGG failed to induce a detectable immune response.

The choice of Ig as a model antigen for studying the effects of aggregates on the immune response was an interesting one, since these proteins differ from most other proteins in terms of complex immune system interactions. Ig can modify the immune response to itself through binding and colligation of multiple receptors on the B-cell surface [62]. Whether this may have influenced immunogenicity of the aggregated species in these studies is not certain, as the affinity and binding of human and bovine Ig with murine B-cell receptors is not clear. Nevertheless, these studies have drawn attention to the fact that high MW species are potent inducers of the immune system and they have emphasized the need to obtain more pure and aggregate-free therapeutic products.

Most nonclinical studies involving therapeutic proteins have involved the administration of foreign proteins. Based on the principles reviewed earlier in this chapter, this probably influences the immune response to aggregates. The ability of aggregates to elicit antibody responses to self-proteins was evaluated by Braun et al. in 1997 [63]. They used human interferon α (hIFN-α) transgenic mice

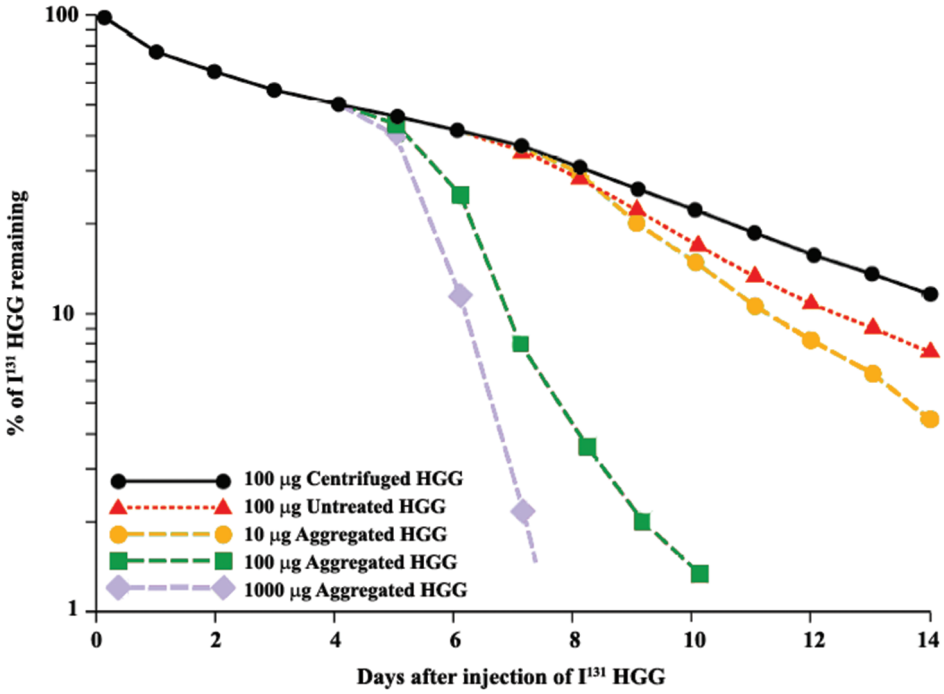

Figure 2.4: Immune elimination of iodine I-131 tagged HGG (I131 HGG) following administration of aggregated HGG in mice [61].

to study the capacity of aggregated hIFN-α products to break immune tolerance. Various administration routes were tested with two types of aggregates: hIFN-α cross-linked with either human or mouse serum albumin (IFN-α-albumin) and homogeneous aggregates of hIFN-α (IFN-α-IFN-α). IFN-α-albumin aggregates were prepared by artificial cross-linking with glutaraldehyde at a 1:1 molar ratio. IFN-α-IFN-α aggregates were obtained from a fraction of an old IFN-α bulk solution. The results clearly showed that both these aggregates were able to induce antibodies to hIFN-α in the transgenic mice, whereas monomeric hIFN-α failed to do so (within the timeframe of the study). It became clear that immune tolerance to self-proteins can be broken by aggregates. Unfortunately, the aggregate species responsible for this occurrence were not comprehensively characterized in the context of the study. However, the study provided valuable information regarding the role of aggregates, dosing frequency and route of administration on antibody induction to hIFN-α.

The propensity of different types of aggregates to elicit immune responses to self-proteins was further investigated by Hermeling et al. [64]. They evaluated the ability

of different well characterized degradation products of hIFN-α containing different types and amount of aggregates, to break immune tolerance of hIFN-α transgenic mice. The different types of aggregates were obtained by metal-catalyzed oxidation, hydrogen peroxide oxidation, glutaraldehyde cross-linking, and extreme-heat treatment. Only metal-catalyzed oxidized aggregates were found to break immune tolerance in transgenic mice. Oxidation through hydrogen peroxide treatment failed to generate aggregates and to induce antibodies against native hIFN-α in transgenic mice. Thus, the hIFN-α aggregates present in the metal-catalyzed oxidation product probably play an important role in breaking immune tolerance. It now remains to be evaluated if these findings for hIFN-α can be generalized for other proteins.

Clinical

Clinical evidence that aggregates in therapeutic protein products play a crucial role in immunogenicity was apparent from very early studies. In the 1950s and 1960s, HGG preparations containing substantially aggregated material were reported to trigger severe anaphylactic reactions in patients [65]. In 1969, Ellis et al. decided to more carefully study the correlation between the aggregates present in different available HGG preparations and antibody induction in patients [66]. They verified that antibody responses to these preparations were directed against the high MW fraction (i.e. the pellet after 2 hour centrifugation at 30,000 rpm). The antibodies were thought to be specific for novel or cryptic determinants present only on aggregated species. Also of relevance, immune responses to therapeutic HGG were far more potent and prevalent in antibody-deficient patients, which drew attention to the importance of immune tolerance in immunogenicity [65].

Anaphylactic reactions were also observed in patients treated with early commercial preparations of HSA and pasteurized plasma solutions (PP). In 1979, Ring et al. studied the immune responses of patients suffering from anaphylaxis upon administration of either of these therapeutic products [67]. All the administered preparations contained between 5 and 15% aggregates. ADAs detected in most patients appeared to be specific for these aggregates and failed to bind to monomeric HSA and de-aggregated PP.

One of the most intriguing clinical cases relating protein aggregates to immunogenicity occurred with human growth hormone (hGH). Originally purified from formalin-fixed pituary glands in the early 1960s, early therapeutic hGH preparations contained substantial amounts of aggregates (40-70%) and induced antibody

responses in up to 50% of the patients [11, 68]. After revising the manufacturing process and substantially reducing the level of aggregates down to 5-10%, the incidence of antibody formation decreased, yet prevailed. Interestingly, the level of aggregates appeared not to determine whether there would be an immune response, but rather the nature of the antibody response. In 1980, studies carried out by Moore et al. showed that patients treated with the heavily aggregated hGH product revealed persistent ADAs, whereas those treated with the less aggregated products developed transient ADAs [11]. Furthermore, the appearance of binding antibodies to hGH was far more frequent than that of neutralizing antibodies [69]. The latter type of antibodies was much more common in "knock out" patients for hGH, who lack immune tolerance to this protein.

Recombinant human IL-2 (rhIL-2) has been used for therapy since the 1980s and can be viewed as a good clinical model to test the general principles correlating aggregates and immunogenicity. rhIL-2 products have been reported to contain a high amount of small aggregates, with an average of more than 20 constituent monomers/aggregate, and to have an incidence of binding antibody responses of about 60% [1, 24]. However, despite the high immunogenicity rate verified for rhIL-2, induction of neutralizing antibodies seems to be uncommon. Interestingly, neutralizing antibodies largely arose in a group of patients treated with rhIL-2 in an immunologically provocative fashion, i.e., s.c. administration or concomitant treatment with IFN-α, and extensive treatment over a prolonged time period [24]. Nevertheless, neutralization *in vitro* did not seem to predict neutralization *in vivo*, as patients with antibody-mediated loss of response to rhIL-2 were extremely rare. Of interest, neutralizing antibodies responses generally arise several months after the appearance of binding antibodies, which may involve epitope spreading in a hypothetical Td activation scenario [1].

2.4.2 Proposed mechanisms of antibody induction by protein aggregates

Protein aggregates can activate the immune system through different mechanisms. Recognition and processing of aggregates has been reported to be accomplished through non-specific uptake by APCs [70, 71] and specific uptake by B-cells [43]. Protein aggregates are thought to play a key role in breaking immune tolerance, but they may also influence classical immune responses. However, the exact mechanisms by which aggregates may trigger unwanted immunogenicity of therapeutic proteins are still unknown.

The increased MW of aggregates compared to the monomeric protein has been pointed as one of the main causes for their elevated immunogenicity, since it fosters their exposition to the immune system and enhances their engulfment by APCs [72]. Interestingly, it has been described that some blood-borne DCs capture particulate (insoluble) antigens in the periphery, migrate to the spleen, and can induce splenic marginal zone B-cells and B1 B-cells to proliferate and produce antibodies in a Ti fashion [73, 74]. However, mass and size *per se* are not enough to justify the propensity of aggregates to influence immune responses to therapeutic proteins. Protein aggregates are believed to trigger immunogenicity because they are thought to originate a set of new characteristics that enhance their recognition by the immune system (Fig. 2.5). Aggregates can originate neo-epitopes, which may arise from their quaternary structure [75]. They are also thought to expose epitopes, usually hidden in the native protein (cryptic epitopes), as a result of partial or complete unfolding of their constituents [1]. However, the most concerning feature of aggregates seems to be the fact that they may present epitopes in a repetitive arrayed form [26]. Repetitive epitope presentation has been pointed as the most likely cause of aggregate-related immunogenicity, since it might mimic well conserved microbial patterns, to which the immune system has learned to vigorously react [54].

Intrinsic characteristics of aggregates may determine the mechanism by which they trigger the immune system. Protein aggregates containing neo-epitopes or exposed cryptic epitopes may enhance immunogenicity via presentation of these epitopes to T-cells by professional APCs or via direct recognition by B-cells. Nevertheless, ADAs formed against this type of aggregates are less likely to cross-react with the monomeric form, since native protein monomers will lack the referred neo-epitopes and exposed cryptic determinants. However, immune responses against these aggregates may be responsible for some cases of acute infusion reactions [67], more commonly associated with classical immune responses.

On the other hand, protein aggregates which present epitopes in a repetitive arrayed form, mimicking well conserved microbial patterns, may lead to multivalent cross-linking of BCRs [1, 26]. Once it occurs, the immune response can then follow two different pathways which may or may not require T-cell help. The first pathway results in acceleration of B-cell antigen processing and its presentation to T-cells, as a consequence of rapid targeting of BCR-aggregate complexes to the MHC II peptide loading compartment [43]. The second mechanism is T-cell independent and involves a complex signaling pathway, such as the activation of Bruton's tyrosine kinases, which mediate B-cell proliferation (Fig. 2.6) [48]. Protein aggregates

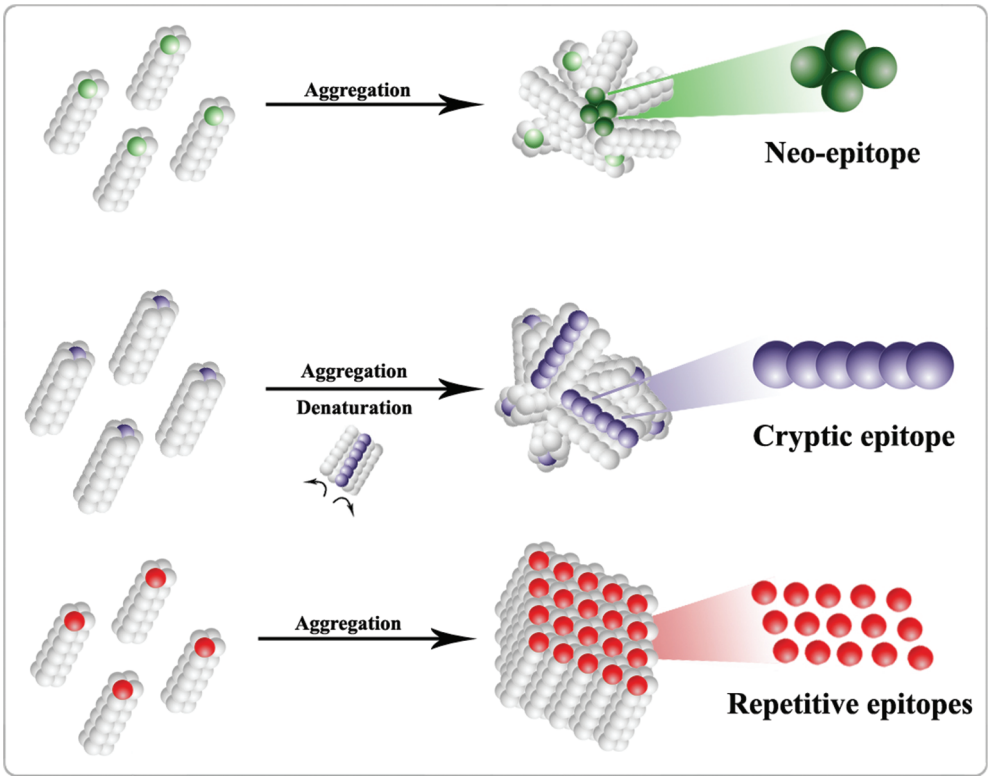

Figure 2.5: Main concerns regarding epitope presentation in protein aggregates.

exhibiting repetitive epitope presentation are more prone to trigger the formation of ADAs which can cross-react with the monomeric protein.

Therapeutic protein aggregates have been pointed to as the most likely risk factor necessary to break immune tolerance during therapy. Anergic self-reactive B-cells may become active upon cross-linking of BCRs by repetitive epitopes presented on self-protein aggregates. This theory would explain the late emergence of ADAs to human homologues during therapy and the frequent lack of memory cell induction. The probability of a protein aggregate which presents immunologically-relevant repetitive epitopes to be recognized by anergic self-reactive B-cells is so low, that it may take several months before breaking of immune tolerance occurs. On the other hand, in the eventual scenario of Ti type 2 B-cell activation, induction of a memory effect would be less likely [8]. The involvement of T-cells in this process still remains unclear, yet their eventual participation would also require breaking of T-cell tolerance. It has been reported that T-cell tolerance can be broken by auto-reactive B-cells whose tolerance had previously been broken by self-protein aggregates [76]. However, there is not enough evidence to either support or refute T-cell involvement

in breaking immune tolerance by therapeutic protein aggregates.

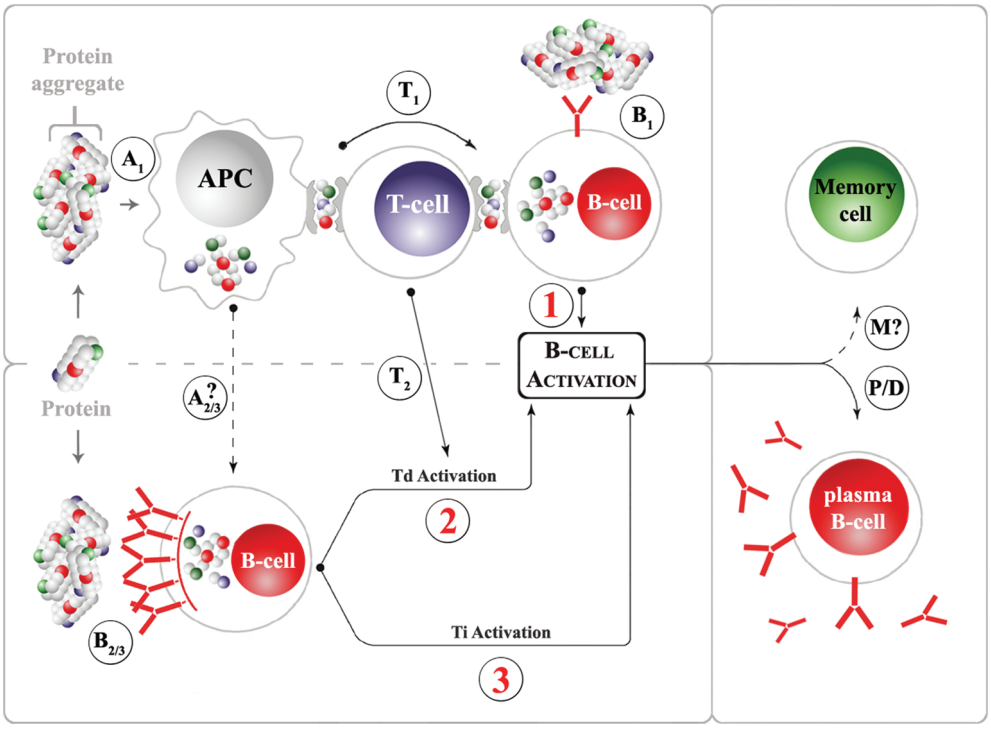

Figure 2.6: Proposed mechanisms of antibody induction by protein aggregates.

1) This mechanism follows a typical Td activation (see Fig. 2.2 for details). It involves the uptake and processing of protein aggregates by professional APCs (A1), followed by T-cell activation (T1), accompanied by aggregate uptake and processing by B-cells (B1), which eventually leads to B-cell proliferation and differentiation (P/D) and to the induction of memory cells (M?).

2) This mechanism occurs when aggregates trigger multivalent cross-linking of B-cell receptors (B2/3). B-cells may then receive activating signals from accessory cells (A2/3). T-cells are then recruited to activate B-cells (T2), which leads to their proliferation and differentiation (P/D) and possibly to the induction of memory cells (M?).

3) This mechanism also occurs when aggregates trigger multivalent cross-linking of B-cell receptors (B2/3), which triggers the production of several activation signals. B-cells may then receive additional signals from accessory cells (A2/3). T-cell help is not required for this type of B-cell activation. B-cells are then activated, which leads to their proliferation and differentiation (P/D). The induction of memory cells via this mechanism remains unclear (M?).

2.4.3 Possible factors responsible for immunogenicity of protein aggregates

Several intrinsic and extrinsic aspects are thought to play a role in the tendency of protein aggregates to trigger immune responses. Extrinsic factors which may affect

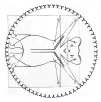

the immune response to protein aggregates are mostly the same as the ones affecting immunogenicity of proteins in general (see section 2.2.3). The presence of impurities, frequency and route of administration, host immune tolerance to the monomeric protein, activity of concomitant immunomodulators, and immunomodulatory activity of the protein itself are some of the extrinsic factors suggested to directly affect immune responses to protein aggregates [1]. Furthermore, intrinsic aggregate features such as size, amount, and other inherent characteristics are also expected to influence their immunogenicity and they will be thoroughly discussed below. However, very few studies have directly addressed this subject and the current knowledge originates mainly from vaccinology studies. For most cases, the way these intrinsic and extrinsic factors influence an aggregate-related immune response is poorly understood. Moreover, it is imperative to remember that each protein is unique to some degree and so are the aggregates that they may form. Thus, the search for general guidelines of aggregate-related immunogenicity is extremely challenging.

Both qualitative and quantitative factors are discussed to influence the immune responses to protein aggregates. However, it is very difficult to determine a maximum allowable “immunologically safe” dose limit of protein aggregates present in therapeutic products. Some products may have very low immunological consequences despite certain levels of aggregates, while for other products very small changes in aggregate levels may profoundly affect these consequences. As for qualitative factors, there are several aspects to consider.

One of the most important factors thought to influence aggregate-related immunogenicity is the conformation of the aggregate protein constituents. Aggregates formed by native-like proteins are expected to pose a higher threat for immunogenicity than the ones formed by denatured or partially denatured proteins [1]. Native-like conformation of aggregate constituents is considered to be crucial for cross-reactivity of aggregate-induced ADAs with the monomeric protein. Furthermore, as previously mentioned, the immune system has evolved to preferentially make antibodies to conformational rather to linear determinants. These assumptions were confirmed by Hermeling et al. in 2006, who challenged tolerant mice with progressively denatured aggregates of hIFN-α and observed that the more native-like aggregates exhibited a higher immunogenicity [77]. Conformational factors may also explain why aggregate-induced ADAs, triggered by challenging animal models with denatured protein aggregates obtained by extreme-heat stress, normally fail to cross-react with the native protein [55, 78].

The amino acid sequence of protein aggregate constituents is another factor

thought to play a role in their immunogenicity, as it determines the epitopes which will be exposed to the immune system. A single amino acid change has been reported to induce a completely new epitope [38], which may hypothetically have increased immunogenicity once presented in a repetitive manner on aggregated forms. Aggregates formed by already immunogenic proteins are also expected to be more efficient in triggering immune responses. Thus, aggregates of a foreign origin protein are expected to be more immunogenic than self-protein aggregates [1].

Protein aggregate size and solubility are also among the main factors believed to influence immune responses. However, little is known about the immunogenicity of small oligomers compared to large multimers. Nevertheless, multimerization seems to be crucial to immunogenicity, as larger-sized monomers are not necessarily more immunogenic than small monomeric proteins. Moreover, it has been long known that particulate antigens are rapidly endocytosed by APCs, which initiate immune responses [72].

The number of constituent monomers in an aggregate that is necessary to efficiently trigger immune responses remains a controversial issue. In 1990, clinical studies performed by Ratner et al. showed that pure crystalline dimers of human insulin were able to trigger immunogenicity in a dose dependent manner [79]. Conversely, the year before, while investigating the molecular requirements for Ti type 2 antibody responses to polymers carrying polysaccharides, Dintzis et al. verified that the presentation of at least 20 repetitive epitopes is required to successfully trigger an immune response [80]. They hypothesized that the B-cell stimulatory signal is "quantized" in that a minimum number of BCRs must be connected together in a spatially contiguous cluster, which they defined as an "immunon". In that study, the polymers had to have a MW higher than 100 kDa and possess a minimum of 20 epitope repeats in order to induce antibody formation via this mechanism. Thus, according to this theory, aggregates which present more than 20 repetitive epitopes on their surface and have a molecular weight bigger than 100 kDa may be more immunogenic, assuming that Ti type 2 B-cell activation is the preferred mechanism.

Successive work by many in the field has indicated that the generation of a signaling complex leading to Ti type 2 B-cell activation and antibody production depends also on epitope affinity, binding kinetics, and polymer rigidity [47]. Rigid polymers have proven to immobilize BCRs more efficiently than flexible polymers [52], which is a vital step for this type of B-cell activation. Accordingly, it is possible that rigid protein aggregates (i.e. with strong internal interactions) pose a higher immunological risk than flexible aggregates. However, one could also argue that

flexible aggregates may adapt more easily to bind to multiple BCRs, making them the most immunogenic type of aggregates.

Several studies have addressed the effect of self-antigen organization on antibody responses. In 1997, Bachmann and Zinkernagel extensively examined the effects of challenging viral coat protein (VCP) tolerant mice with differently organized VCP products. They verified that soluble monomeric VCP was toleragenic, poorly organized VCPs were able to trigger mainly Td responses and highly organized VCPs induced strong Ti responses [81]. They have proposed that repetitive determinants at a spacing of 5-10 nm are the most immunogenic presentation, since it is unique to microbial structures, to which the immune system has evolved to strongly respond [81-83]. More recently, Chackerian et al. observed that self-protein aggregates arrayed on virus-like particles (VLPs) in a dense and highly organized manner managed to trigger long-lasting high IgG titers, whereas less dense aggregate arrays failed [53]. Thus, according to these results, dense and organized aggregates with an average epitope spacing of 5-10 nm would be expected to be more immunogenic. However, in these studies the self-protein aggregate arrays were artificially created and involved viral components. Hence, the generalization of these findings to natural occurring aggregates should be addressed with caution.

Hydrophobicity of protein aggregates has also been suggested to play a role in their immunogenicity. It has been proposed that hydrophobic portions of biological molecules act, when exposed, as universal damage-associated molecular patterns to initiate repair, remodeling and immunity [84]. Thus, it is possible that more hydrophobic aggregates of therapeutic proteins represent a bigger threat for unwanted immunogenicity.

Another intrinsic factor that may affect aggregate-related immunogenicity is the aggregate nature, i.e. if they are formed only by the protein itself or by a mixture of protein and impurities, excipients, or degraded protein that may be present in the formulation. For example, protein adsorption to nano- or micro-particles, often released from pumps, pipes, vessels, filters, or primary packaging material may create aggregates with different epitope presentation than self-aggregates, and these may pose different immunogenicity risks. Moreover, glycosylation and pegylation may exert influence not only on the formation of aggregates, but also on aggregate-related immunogenicity [1]. However, identification of the immunological hazards posed by different aggregate types has not yet been explored.

2.4.4 Risk analysis of protein aggregates

The most relevant clinical risk posed by immune reactions to protein aggregates in therapeutic products may be narrowed down to the generation of cross-reacting antibodies that may affect the efficacy of the product or even neutralize an endogenous protein counterpart. For the formation of cross-reacting antibodies between aggregates and monomeric protein to occur, it is important that protein aggregate constituents maintain a native-like conformation. This requirement is more evident for neutralizing antibodies, which are directed against the active site of the protein. While aggregates of denatured protein may potently induce antibodies, they would not be expected to induce neutralizing antibodies because protein conformation was lost on denaturation. Antibodies directed to linear epitopes within the binding site of the protein could effectively neutralize it if they bind to a linear determinant critical in ligand-receptor binding, but this occurrence seems to be rare [1].

Epitope spreading has been suggested as a possible mechanism involved in the appearance of neutralizing antibody responses. Epitope spreading is normally defined as the diversification of epitope specificity from the initial dominant epitope-specific immune response to subdominant epitopes on that protein, normally derived by repetitive antigen presentation [85]. Thus, through epitope spreading, the presence of binding antibodies may facilitate the generation of neutralizing antibodies. In fact, for many therapeutic protein products, development of neutralizing antibodies is preceded by high titer and prolonged binding antibody responses. In such cases, according to this theory, preventing a neutralizing antibody response may be possible by limiting the titer and duration of the primary response [1].

The amount, size, and type of aggregates necessary to trigger immune responses are a major concern for pharmaceutical companies and regulatory agencies. In 2008, the hypothetical immunological significance of normally overlooked “subvisible particles” present in protein formulations was discussed by experienced researchers in the field [86]. Current USP particulate requirements state that particles >10 μm in size should be controlled bellow 6000 particles/container, but no regulations have been established for the smaller sizes. Therefore, it is possible that immunogenically relevant protein aggregates have been routinely ignored by these regulations. For every aggregate >10 μm present in a formulation, there can be considerable amounts of slightly smaller aggregates, and each may contain hundreds or thousands of protein units. Thus, given the lack of knowledge regarding the most immunogenic

aggregate sizes, it is important to develop instruments, protocols, and regulations which properly address a broader range of particle sizes, especially in the subvisible range.

2.4.5 Predictive models to access the immunogenicity of aggregates

Reliable models for prediction of aggregate-related immunogenicity are not available at the moment. The proper model would require a thorough understanding of the underlying mechanisms, and this is far from the current situation. There are some predictive models for unwanted immunogenicity of therapeutic proteins, but none of them has proven to be entirely effective and all of them have considerable downsides. Furthermore, the application of available techniques to predict the immunogenicity caused by protein aggregates is still very limited. The available models to predict immunogenicity may be divided into three classes: *in vitro*, *in silico* and *in vivo*. However, given that *in vitro* and *in silico* techniques are mostly based on the aptitude of proteins to actively interact with immune or innate cells, basically identifying T- or B-cell epitopes [87], these techniques are not suitable for predicting aggregate-related immunogenicity. Given the number of other factors that may equally influence immunogenicity, it seems very unlikely that these two methods may one day fully predict an immune response to either monomeric or aggregated therapeutic proteins [26].

The use of animal models to predict immunogenicity *in vivo* seems to be the most promising method to predict aggregate-related immune responses [77]. *In vivo* prediction has the advantage of including the entire immune machinery and environment necessary to better simulate the extremely complex scenario that results in complete immune responses, especially when protein aggregates are involved. Furthermore, with these models it is possible to include other immunogenicity influencing factors other than hazardous epitopes, such as route and frequency of administration, concomitant medication, and possibly disease state. However, the vast majority of proteins used for therapeutic purposes in humans are foreign to animals and this feature greatly affects their immune response. Therefore, in order to circumvent this problem, transgenic animal models have been developed and they have a promising predictive potential [26]. These animals may be tolerant to certain human homologues or may possess more human-like immunologic features, such as the case of transgenic mice expressing the human MHC II complex (HLA). Thus, in vivo testing with transgenic animal models may have the potential to predict

aggregate-related immunogenicity in the near future. However, much work still needs to be done before any type of model can properly predict immune responses to protein aggregates.

2.5 CONCLUSIONS

Protein aggregates are potent inducers of immune responses to therapeutic protein products. Thoroughly understanding the connection between aggregates and immunogenicity is extremely relevant to optimize the efficacy and safety of biopharmaceutical products. However, current knowledge regarding this subject is very limited and is mostly based on assumptions.

There are several aspects to consider when analyzing the impact of aggregates in immunogenicity of therapeutic proteins. According to current knowledge, high order multimeric protein aggregates containing native-like molecules with repetitive epitope presentation seem to be the most immunogenic type of aggregates. However, given that therapeutic proteins may have different aggregation profiles and pose unique immunological risks, a case-by-case approach is needed in order to better understand the immunogenicity of aggregates.

The risk caused by the presence of aggregates should be evaluated not only by the tendency of aggregates to trigger ADAs, but also by the clinical consequences that these ADAs may have. Antibodies against aggregates may not bind to the monomeric active form of the drug and, in case they do, it may not have relevant clinical consequences.

According to the type of immunogenic threat posed by protein aggregates, several immunological mechanisms have been proposed, which may or may not require T-cell help. The development of reliable predictive models to assess the immunogenicity of protein aggregates is highly necessary, but is dependent on the elucidation of these mechanisms.

REFERENCES

[1] A. S. Rosenberg, “Effects of protein aggregates: an immunologic perspective,” Aaps J, vol. 8, pp. E501-7, 2006.
[2] G. Schernthaner, “Immunogenicity and allergenic potential of animal and human insulins,” Diabetes Care, vol. 16 Suppl 3, pp. 155-65, Dec 1993.
[3] R. D. Milner, “Growth hormone 1985,” Br Med J (Clin Res Ed), vol. 291, pp. 1593-4, Dec 7 1985.
[4] M. G. Jacquemin and J. M. Saint-Remy, “Factor VIII immunogenicity,” Haemophilia, vol. 4, pp. 552-7, Jul 1998.
[5] A. B. Gottlieb, R. Evans, S. Li, L. T. Dooley, C. A. Guzzo, D. Baker, M. Bala, C. W. Marano, and A. Menter, “Infliximab induction therapy for patients with severe plaque-type psoriasis: a randomized, double-blind, placebo-controlled trial,” J Am Acad Dermatol, vol. 51, pp. 534-42, Oct 2004.
[6] F. Baert, M. Noman, S. Vermeire, G. Van Assche, D. H. G, A. Carbonez, and P. Rutgeerts, “Influence of immunogenicity on the long-term efficacy of infliximab in Crohn’s disease,” N Engl J Med, vol. 348, pp. 601-8, Feb 13 2003.
[7] R. L. West, Z. Zelinkova, G. J. Wolbink, E. J. Kuipers, P. C. Stokkers, and V. D. W. CJ, “Immunogenicity negatively influences the outcome of adalimumab treatment in Crohn;s disease,” Aliment Pharmacol Ther, Aug 8 2008.
[8] A. S. De Groot and L. Moise, “Prediction of immunogenicity for therapeutic proteins: state of the art,” Curr Opin Drug Discov Devel, vol. 10, pp. 332-40, May 2007.
[9] A. Cheifetz, M. Smedley, S. Martin, M. Reiter, G. Leone, L. Mayer, and S. Plevy, “The incidence and management of infusion reactions to infliximab: a large center experience,” Am J Gastroenterol, vol. 98, pp. 1315-24, Jun 2003.
[10] P. A. Patten and H. Schellekens, “The immunogenicity of biopharmaceuticals. Lessons learned and consequences for protein drug development,” Dev Biol (Basel), vol. 112, pp. 81-97, 2003.
[11] W. V. Moore and P. Leppert, “Role of aggregated human growth hormone (hGH) in development of antibodies to hGH,” J Clin Endocrinol Metab, vol. 51, pp. 691-7, Oct 1980.
[12] Casadevall, J. Nataf, B. Viron, A. Kolta, J. J. Kiladjian, P. Martin-Dupont, P. Michaud, T. Papo, V. Ugo, I. Teyssandier, B. Varet, and P. Mayeux, “Pure red-cell aplasia and antierythropoietin antibodies in patients treated with recombinant erythropoietin,” N Engl J Med, vol. 346, pp. 469-75, Feb 14 2002.
[13] A. Meager, “Human antibodies to insulin in diabetes,” J Interferon Res, vol. 14, pp. 181-2, Aug 1994.
[14] H. Schellekens, “Immunologic mechanisms of EPO-associated pure red cell aplasia,” Best Pract Res Clin Haematol, vol. 18, pp. 473-80, 2005.
[15] H. Schellekens, “Bioequivalence and the immunogenicity of biopharmaceuticals,” Nat Rev Drug Discov, vol. 1, pp. 457-62, Jun 2002.
[16] U. Rosenschein, R. Lenz, J. Radnay, T. Ben Tovim, and L. A. Rozenszajn, “Streptokinase immunogenicity in thrombolytic therapy for acute myocardial infarction,” Isr J Med Sci, vol. 27, pp. 541-5, Oct 1991.
[17] S. Chaffee, A. Mary, E. R. Stiehm, D. Girault, A. Fischer, and M. S. Hershfield, “IgG antibody response to polyethylene glycol-modified adenosine deaminase in patients with adenosine deaminase deficiency,” J Clin Invest, vol. 89, pp. 1643-51, May 1992.
[18] A. Grauer, K. Frank-Raue, J. Schroth, F. Raue, and R. Ziegler, “[Neutralizing antibodies against salmon calcitonin. The cause of a treatment failure in Paget’s disease],” Dtsch Med Wochenschr, vol. 119, pp. 507-10, Apr 8 1994.
[19] P. Kontsek, H. Liptakova, and E. Kontsekova, “Immunogenicity of interferon-alpha 2 in therapy: structural and physiological aspects,” Acta Virol, vol. 43, pp. 63-70, Feb 1999.

[20] F. Girard and M. Gourmelen, "Clinical experience with Somatonorm," Acta Paediatr Scand Suppl, vol. 325, pp. 29-32, 1986.
[21] J. G. Gribben, S. Devereux, N. S. Thomas, M. Keim, H. M. Jones, A. H. Goldstone, and D. C. Linch, "Development of antibodies to unprotected glycosylation sites on recombinant human GM-CSF," Lancet, vol. 335, pp. 434-7, Feb 24 1990.
[22] M. Karpusas, A. Whitty, L. Runkel, and P. Hochman, "The structure of human interferon-beta: implications for activity," Cell Mol Life Sci, vol. 54, pp. 1203-16, Nov 1998.
[23] G. Antonelli, E. Simeoni, M. Currenti, F. De Pisa, V. Colizzi, M. Pistello, and F. Dianzani, "Interferon antibodies in patients with infectious diseases. Anti-interferon antibodies," Biotherapy, vol. 10, pp. 7-14, 1997.
[24] O. Prummer, "Treatment-induced antibodies to interleukin-2," Biotherapy, vol. 10, pp. 15-24, 1997.
[25] F. M. Veronese and G. Pasut, "PEGylation, successful approach to drug delivery," Drug Discov Today, vol. 10, pp. 1451-8, Nov 1 2005.
[26] H. Schellekens, "How to predict and prevent the immunogenicity of therapeutic proteins," Biotechnol Annu Rev, vol. 14, pp. 191-202, 2008.
[27] S. Vadhan-Raj, "Clinical experience with recombinant human thrombopoietin in chemotherapy-induced thrombocytopenia," Semin Hematol, vol. 37, pp. 28-34, Apr 2000.
[28] A. V. Palleroni, A. Aglione, M. Labow, M. J. Brunda, S. Pestka, F. Sinigaglia, G. Garotta, J. Alsenz, and A. Braun, "Interferon immunogenicity: preclinical evaluation of interferon-alpha 2a," J Interferon Cytokine Res, vol. 17 Suppl 1, pp. S23-7, Jul 1997.
[29] H. Schellekens, "Factors influencing the immunogenicity of therapeutic proteins," Nephrol Dial Transplant, vol. 20 Suppl 6, pp. vi3-9, Jun 2005.
[30] A. Sominanda, U. Rot, M. Suoniemi, F. Deisenhammer, J. Hillert, and A. Fogdell-Hahn, "Interferon beta preparations for the treatment of multiple sclerosis patients differ in neutralizing antibody seroprevalence and immunogenicity," Mult Scler, vol. 13, pp. 208-14, Mar 2007.
[31] C. Ross, K. M. Clemmesen, M. Svenson, P. S. Sorensen, N. Koch-Henriksen, G. L. Skovgaard, and K. Bendtzen, "Immunogenicity of interferon-beta in multiple sclerosis patients: influence of preparation, dosage, dose frequency, and route of administration. Danish Multiple Sclerosis Study Group," Ann Neurol, vol. 48, pp. 706-12, Nov 2000.
[32] P. Perini, A. Facchinetti, P. Bulian, A. R. Massaro, D. D. Pascalis, A. Bertolotto, G. Biasi, and P. Gallo, "Interferon-beta (INF-beta) antibodies in interferon-beta1a- and interferon-beta1b-treated multiple sclerosis patients. Prevalence, kinetics, cross-reactivity, and factors enhancing interferon-beta immunogenicity *in vivo*," Eur Cytokine Netw, vol. 12, pp. 56-61, Mar 2001.
[33] I. Van Walle, Y. Gansemans, P. W. Parren, P. Stas, and I. Lasters, "Immunogenicity screening in protein drug development," Expert Opin Biol Ther, vol. 7, pp. 405-18, Mar 2007.
[34] D. Sickert, K. Kroeger, C. Zickler, E. Chokote, B. Winkler, J. M. Grenet, F. Legay, and A. Zaar, "Improvement of drug tolerance in immunogenicity testing by acid treatment on Biacore," J Immunol Methods, vol. 334, pp. 29-36, May 20 2008.
[35] S. Akira and K. Takeda, "Functions of toll-like receptors: lessons from KO mice," C R Biol, vol. 327, pp. 581-9, Jun 2004.
[36] H. Schellekens, "Immunogenicity of therapeutic proteins," Nephrol Dial Transplant, vol. 18, pp. 1257-9, Jul 2003.
[37] P. Matzinger, "Tolerance, danger, and the extended family," Annu Rev Immunol, vol. 12, pp. 991-1045, 1994.
[38] J. L. Ottesen, P. Nilsson, J. Jami, D. Weilguny, M. Duhrkop, D. Bucchini, S. Havelund, and J. M. Fogh, "The potential immunogenicity of human insulin and insulin analogues evaluated in a transgenic mouse model," Diabetologia, vol. 37, pp. 1178-85, Dec 1994.

[39] S. Hermeling, D. J. Crommelin, H. Schellekens, and W. Jiskoot, "Structure-immunogenicity relationships of therapeutic proteins," Pharm Res, vol. 21, pp. 897-903, Jun 2004.
[40] I. H. Tarner and C. G. Fathman, "Does our current understanding of the molecular basis of immune tolerance predict new therapies for autoimmune disease?," Nat Clin Pract Rheumatol, vol. 2, pp. 491-9, Sep 2006.
[41] N. J. Singh and R. H. Schwartz, "Primer: mechanisms of immunologic tolerance," Nat Clin Pract Rheumatol, vol. 2, pp. 44-52, Jan 2006.
[42] A. S. De Groot and D. W. Scott, "Immunogenicity of protein therapeutics," Trends Immunol, vol. 28, pp. 482-90, Nov 2007.
[43] P. C. Cheng, C. R. Steele, L. Gu, W. Song, and S. K. Pierce, "MHC class II antigen processing in B cells: accelerated intracellular targeting of antigens," J Immunol, vol. 162, pp. 7171-80, Jun 15 1999.
[44] K. Silver and R. J. Cornall, "Isotype control of B cell signaling," Sci STKE, vol. 2003, p. pe21, May 27 2003.
[45] C. L. Montes, E. V. Acosta-Rodriguez, M. C. Merino, D. A. Bermejo, and A. Gruppi, "Polyclonal B cell activation in infections: infectious agents' devilry or defense mechanism of the host?," J Leukoc Biol, vol. 82, pp. 1027-32, Nov 2007.
[46] P. G. Stevenson and P. C. Doherty, "Non-antigen-specific B-cell activation following murine gammaherpesvirus infection is CD4 independent *in vitro* but CD4 dependent *in vivo*," J Virol, vol. 73, pp. 1075-9, Feb 1999.
[47] Q. Vos, A. Lees, Z. Q. Wu, C. M. Snapper, and J. J. Mond, "B-cell activation by T-cell-independent type 2 antigens as an integral part of the humoral immune response to pathogenic microorganisms," Immunol Rev, vol. 176, pp. 154-70, Aug 2000.
[48] A. C. Fluckiger, Z. Li, R. M. Kato, M. I. Wahl, H. D. Ochs, R. Longnecker, J. P. Kinet, O. N. Witte, A. M. Scharenberg, and D. J. Rawlings, "Btk/Tec kinases regulate sustained increases in intracellular Ca2+ following B-cell receptor activation," Embo J, vol. 17, pp. 1973-85, Apr 1 1998.
[49] B. He, X. Qiao, P. J. Klasse, A. Chiu, A. Chadburn, D. M. Knowles, J. P. Moore, and A. Cerutti, "HIV-1 envelope triggers polyclonal Ig class switch recombination through a CD40-independent mechanism involving BAFF and C-type lectin receptors," J Immunol, vol. 176, pp. 3931-41, Apr 1 2006.
[50] F. Mackay, P. Schneider, P. Rennert, and J. Browning, "BAFF AND APRIL: a tutorial on B cell survival," Annu Rev Immunol, vol. 21, pp. 231-64, 2003.
[51] F. Melchers and A. R. Rolink, "B cell tolerance--how to make it and how to break it," Curr Top Microbiol Immunol, vol. 305, pp. 1-23, 2006.
[52] M. F. Bachmann, U. H. Rohrer, T. M. Kundig, K. Burki, H. Hengartner, and R. M. Zinkernagel, "The influence of antigen organization on B cell responsiveness," Science, vol. 262, pp. 1448-51, Nov 26 1993.
[53] B. Chackerian, P. Lenz, D. R. Lowy, and J. T. Schiller, "Determinants of autoantibody induction by conjugated papillomavirus virus-like particles," J Immunol, vol. 169, pp. 6120-6, Dec 1 2002.
[54] T. Fehr, M. F. Bachmann, E. Bucher, U. Kalinke, F. E. Di Padova, A. B. Lang, H. Hengartner, and R. M. Zinkernagel, "Role of repetitive antigen patterns for induction of antibodies against antibodies," J Exp Med, vol. 185, pp. 1785-92, May 19 1997.
[55] S. Hermeling, L. Aranha, J. M. Damen, M. Slijper, H. Schellekens, D. J. Crommelin, and W. Jiskoot, "Structural characterization and immunogenicity in wild-type and immune tolerant mice of degraded recombinant human interferon alpha2b," Pharm Res, vol. 22, pp. 1997-2006, Dec 2005.
[56] H. O. Ito, T. Nakashima, T. So, M. Hirata, and M. Inoue, "Immunodominance of conformation-dependent B-cell epitopes of protein antigens," Biochem Biophys Res Commun, vol. 308, pp. 770-6, Sep 5 2003.
[57] A. Nath, E. Hall, M. Tuzova, M. Dobbs, M. Jons, C. Anderson, J. Woodward, Z. Guo, W. Fu, R. Kryscio, D. Wekstein, C. Smith, W. R. Markesbery, and M. P. Mattson, "Autoantibodies to amyloid

beta-peptide (Abeta) are increased in Alzheimer's disease patients and Abeta antibodies can enhance Abeta neurotoxicity: implications for disease pathogenesis and vaccine development," Neuromolecular Med, vol. 3, pp. 29-39, 2003.
[58] B. O'Nuallain and R. Wetzel, "Conformational Abs recognizing a generic amyloid fibril epitope," Proc Natl Acad Sci U S A, vol. 99, pp. 1485-90, Feb 5 2002.
[59] D. W. Dresser, "Specific inhibition of antibody production. II. Paralysis induced in adult mice by small quantities of protein antigen," Immunology, vol. 5, pp. 378-88, May 1962.
[60] H. N. Claman, "Tolerance to a Protein Antigen in Adult Mice and the Effect of Nonspecific Factors," J Immunol, vol. 91, pp. 833-9, Dec 1963.
[61] C. N. Gamble, "The role of soluble aggregates in the primary immune response of mice to human gamma globulin," Int Arch Allergy Appl Immunol, vol. 30, pp. 446-55, 1966.
[62] A. Getahun and B. Heyman, "How antibodies act as natural adjuvants," Immunol Lett, vol. 104, pp. 38-45, Apr 15 2006.
[63] A. Braun, L. Kwee, M. A. Labow, and J. Alsenz, "Protein aggregates seem to play a key role among the parameters influencing the antigenicity of interferon alpha (IFN-alpha) in normal and transgenic mice," Pharm Res, vol. 14, pp. 1472-8, Oct 1997.
[64] S. Hermeling, W. Jiskoot, D. Crommelin, C. Bornaes, and H. Schellekens, "Development of a transgenic mouse model immune tolerant for human interferon Beta," Pharm Res, vol. 22, pp. 847-51, Jun 2005.
[65] S. Barandun, P. Kistler, F. Jeunet, and H. Isliker, "Intravenous administration of human gamma-globulin," Vox Sang, vol. 7, pp. 157-74, 1962.
[66] E. F. Ellis and C. S. Henney, "Adverse reactions following administration of human gamma globulin," J Allergy, vol. 43, pp. 45-54, Jan 1969.
[67] J. Ring, W. Stephan, and W. Brendel, "Anaphylactoid reactions to infusions of plasma protein and human serum albumin. Role of aggregated proteins and of stabilizers added during production," Clin Allergy, vol. 9, pp. 89-97, Jan 1979.
[68] L. E. Underwood, S. J. Voina, and J. J. Van Wyk, "Restoration of growth by human growth hormone (Roos) in hypopituitary dwarfs immunized by other human growth hormone preparations: clinical and immunological studies," J Clin Endocrinol Metab, vol. 38, pp. 288-97, Feb 1974.
[69] S. D. Frasier, "Human pituitary growth hormone (hGH) therapy in growth hormone deficiency," Endocr Rev, vol. 4, pp. 155-70, Spring 1983.
[70] M. R. Daha, E. L. van, H. M. Hazevoet, and A. Kijlstra, "Degradation of soluble immunoglobulin aggregates *in vitro* by monocytes from normal subjects and from patients with systemic lupus erythematosus," Scand J Immunol, vol. 16, pp. 117-22, Aug 1982.
[71] R. B. Weltzien and J. S. Pachter, "Visualization of beta-amyloid peptide (Abeta) phagocytosis by human mononuclear phagocytes: dependency on Abeta aggregate size," J Neurosci Res, vol. 59, pp. 522-7, Feb 15 2000.
[72] P. C. Frei, B. Benacerraf, and G. J. Thorbecke, "Phagocytosis of the Antigen, a Crucial Step in the Induction of the Primary Response," Proc Natl Acad Sci U S A, vol. 53, pp. 20-3, Jan 1965.
[73] M. Balazs, F. Martin, T. Zhou, and J. Kearney, "Blood dendritic cells interact with splenic marginal zone B cells to initiate T-independent immune responses," Immunity, vol. 17, pp. 341-52, Sep 2002.
[74] F. Martin, A. M. Oliver, and J. F. Kearney, "Marginal zone and B1 B cells unite in the early response against T-independent blood-borne particulate antigens," Immunity, vol. 14, pp. 617-29, May 2001.
[75] D. C. Robbins, S. M. Cooper, S. E. Fineberg, and P. M. Mead, "Antibodies to covalent aggregates of insulin in blood of insulin-using diabetic patients," Diabetes, vol. 36, pp. 838-41, Jul 1987.
[76] M. J. Mamula, R. H. Lin, C. A. Janeway, Jr., and J. A. Hardin, "Breaking T cell tolerance with foreign and self co-immunogens. A study of autoimmune B and T cell epitopes of cytochrome c," J Immunol, vol. 149, pp. 789-95, Aug 1 1992.

[77] S. Hermeling, H. Schellekens, C. Maas, M. F. Gebbink, D. J. Crommelin, and W. Jiskoot, "Antibody response to aggregated human interferon alpha2b in wild-type and transgenic immune tolerant mice depends on type and level of aggregation," J Pharm Sci, vol. 95, pp. 1084-96, May 2006.
[78] V. S. Purohit, C. R. Middaugh, and S. V. Balasubramanian, "Influence of aggregation on immunogenicity of recombinant human Factor VIII in hemophilia A mice," J Pharm Sci, vol. 95, pp. 358-71, Feb 2006.
[79] R. E. Ratner, T. M. Phillips, and M. Steiner, "Persistent cutaneous insulin allergy resulting from high-molecular-weight insulin aggregates," Diabetes, vol. 39, pp. 728-33, Jun 1990.
[80] R. Z. Dintzis, M. Okajima, M. H. Middleton, G. Greene, and H. M. Dintzis, "The immunogenicity of soluble haptenated polymers is determined by molecular mass and hapten valence," J Immunol, vol. 143, pp. 1239-44, Aug 15 1989.
[81] M. F. Bachmann and R. M. Zinkernagel, "Neutralizing antiviral B cell responses," Annu Rev Immunol, vol. 15, pp. 235-70, 1997.
[82] M. F. Bachmann, T. M. Kundig, D. E. Speiser, K. McKall-Faienza, K. Kishara, T. W. Mak, and P. S. Ohashi, "T-cell-independent antiviral B cell responses in CD45-deficient mice," Cell Immunol, vol. 175, pp. 12-5, Jan 10 1997.
[83] M. F. Bachmann and R. M. Zinkernagel, "The influence of virus structure on antibody responses and virus serotype formation," Immunol Today, vol. 17, pp. 553-8, Dec 1996.
[84] S. Y. Seong and P. Matzinger, "Hydrophobicity: an ancient damage-associated molecular pattern that initiates innate immune responses," Nat Rev Immunol, vol. 4, pp. 469-78, Jun 2004.
[85] P. V. Lehmann, E. E. Sercarz, T. Forsthuber, C. M. Dayan, and G. Gammon, "Determinant spreading and the dynamics of the autoimmune T-cell repertoire," Immunol Today, vol. 14, pp. 203-8, May 1993.
[86] J. F. Carpenter, T. W. Randolph, W. Jiskoot, D. J. Crommelin, C. R. Middaugh, G. Winter, Y. X. Fan, S. Kirshner, D. Verthelyi, S. Kozlowski, K. A. Clouse, P. G. Swann, A. Rosenberg, and B. Cherney, "Overlooking subvisible particles in therapeutic protein products: Gaps that may compromise product quality," J Pharm Sci, Aug 14 2008.
[87] E. L. Roggen, N. K. Soni, and G. R. Verheyen, "Respiratory immunotoxicity: an *in vitro* assessment," Toxicol In Vitro, vol. 20, pp. 1249-64, Dec 2006.

Chapter 3

Critical evaluation of nanoparticle tracking analysis (NTA) by NanoSight for the measurement of nanoparticles and protein aggregates

Vasco Filipe[1,2], Andrea Hawe[1], Wim Jiskoot[1]

[1] Division of Drug Delivery Technology, Leiden/Amsterdam Center for Drug Research, Leiden University, P.O. Box 9502, 2300 RA Leiden, The Netherlands

[2] Department of Pharmaceutics, Utrecht Institute for Pharmaceutical Sciences (UIPS), Utrecht University, P.O. Box 80082, 3508 TB, Utrecht, The Netherlands

Pharmaceutical Research, 27(5):796-810 (2010).

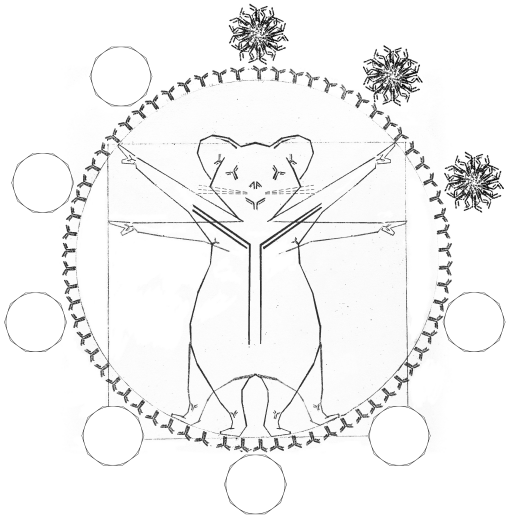

ABSTRACT

Purpose. To evaluate the nanoparticle tracking analysis (NTA) technique, compare it with dynamic light scattering (DLS) and test its performance in characterizing drug delivery nanoparticles and protein aggregates.

Methods. Standard polystyrene beads of sizes ranging from 60 to 1000 nm and physical mixtures thereof were analyzed with NTA and DLS. The influence of different ratios of particle populations was tested. Drug delivery nanoparticles and protein aggregates were analyzed by NTA and DLS. Live monitoring of heat-induced protein aggregation was performed with NTA.

Results. NTA was shown to accurately analyze the size distribution of monodisperse and polydisperse samples. Sample visualization and individual particle tracking are features that enable a thorough size distribution analysis. The presence of small amounts of large (1000 nm) particles generally does not compromise the accuracy of NTA measurements and a broad range of population ratios can easily be detected and accurately sized. NTA proved to be suitable to characterize drug delivery nanoparticles and protein aggregates, complementing DLS. Live monitoring of heat-induced protein aggregation provides information about aggregation kinetics and size of submicron aggregates.

Conclusion. NTA is a powerful characterization technique that complements DLS and is particularly valuable for analyzing polydisperse nanosized particles and protein aggregates.

INTRODUCTION

Most macromolecular drugs such as proteins, peptides, DNA and RNA cannot be administrated via the traditional oral route of administration, due to their susceptibility to enzymatic degradation or low absorption efficiency [1, 2]. To be effective these drugs have to be delivered in most cases via injection and/or through a drug delivery system (DDS).

DDS not only protect the therapeutic drug or antigen from degradation and/or increase their absorption, but may also allow controlled release or the precise delivery to a specific target [3]. Common examples of DDS include polymer-based particles, lipid-based carriers and virus-like particles. Given that most of these DDS are nanosized colloidal particles, it is essential to have reliable characterization tools to ensure their quality and colloidal stability.

Another pharmaceutically important field that requires adequate tools for the analysis of particles in the nanometer size range is the characterization of protein aggregates. Therapeutic proteins are prone to several chemical and physical

degradation pathways, which often lead to aggregation [4]. The presence of aggregates in a protein formulation compromises product quality and may lead to unwanted immunogenicity [5]. Thorough aggregate characterization is crucial to better understand the underlying mechanism of aggregate-related immunogenicity and ensure the quality of protein therapeutics. An accurate determination of the size and size distribution of aggregated protein formulations is not straightforward, as protein aggregates are typically very heterogeneous, with sizes ranging from a few nanometers to several micrometers [6-8]. Recently the importance of analyzing subvisible protein aggregates with sizes in the nanometer till low micrometer range has become recognized [9].

The most commonly used techniques for the analysis of nanoparticles and protein aggregates include dynamic light scattering (DLS), scanning electron microscopy (SEM), size exclusion chromatography (SEC), gel electrophoresis, asymmetrical flow field-flow fractionation (AF4) and analytical ultracentrifugation (AUC) [10-12]. From the mentioned techniques, DLS is the most user friendly and it yields relatively accurate and consistent results that can be obtained in a rather short period of time [10]. Therefore, DLS has become the preferred technique to routinely determine the size of nanoparticles.

Despite being a powerful and accessible tool, DLS is also known to have several drawbacks, which are mainly inherent to the principles of the technique. Particle size is determined from fluctuations in scattered light intensity due to the Brownian movement of the particles [13]. The fact that the intensity of the scattered light is proportional to the sixth power of the particle diameter makes this technique very sensitive to the presence of large particles [14]. This can be an advantage if the purpose is to detect small amounts of large particles, but it can be a major drawback for accurate size determination. Dust particles or small amounts of large aggregates can impede the size determination if the main component exhibits a distinctly smaller size [15].

Nanoparticle tracking analysis (NTA), which was first commercialized in 2006, is an innovative system for sizing particles from about 30 to 1000 nm, with the lower detection limit being dependent on the refractive index of the nanoparticles. This technique combines laser light scattering microscopy with a charge coupled device (CCD) camera, which enables the visualization and recording of nanoparticles in solution. The NTA software is then able to identify and track individual nanoparticles moving under Brownian motion and relates the movement to a particle size according to the following formula derived from the Stokes-Einstein equation (I) [16]:

$$\overline{(x,y)^2} = \frac{2k_B T}{3r_h \pi \eta} \quad \text{(I)}$$

where k_b is the Boltzmann constant and $\overline{(x,y)^2}$ is the mean-squared distance traveled by a particle at a temperature T, in a medium of viscosity η with a hydrodynamic radius of r_h.

Our aim was to explore the potential of nanoparticle tracking analysis (NTA) for the analysis of nanosized particles and protein aggregates. A direct comparison with DLS was made in order to reveal the advantages and pitfalls of a technique that is now making its first steps in the field of characterization of nanoparticles and submicron protein aggregates.

MATERIALS AND METHODS

Chemicals

Poly (lactic-co-glycolic acid) 50:50 (PLGA) and 4-(2-hydroxyethyl)-1-piperazine-ethanesulfonic acid (HEPES) were obtained from Sigma-Aldrich (Steinheim, Germany), chitosan (deacetylation degree 92%, MW 120 kDa) from Primex (Siglufjordur, Iceland) and egg L-α-phosphatidyl choline (EPC) from Lipoid GmbH (Ludwigshafen, Germany). 1,2-dioleoyl-sn-glycero-3-phospho ethanolamine (DOPE) and 1,2-dioleoyl-3-trimethyl ammonium-propane (DOTAP) were supplied by INstruchemie (Delfzijl, The Netherlands). Chloroform was purchased from Biosolve (Valkenswaard, The Netherlands). All other chemicals used were from Sigma-Aldrich (Steinheim, Germany), unless mentioned otherwise.

Preparation of polystyrene bead samples

Polystyrene nanometer standard beads with sizes of 60, 100, 200, 400 and 1000 nm were purchased from Thermo Scientific (Fremont, USA). They were diluted from the supplied package in deionized water until the concentration was acceptable for NTA measurements, i.e. between 10^7 and 10^9 total particles/ml. Thus, from the supplier's recipient, a 1:30000 volume based dilution was made for the 60-nm beads; 1:1000 dilution for the 100-nm beads; 1:250 dilution for the 200-nm beads;

1:25 dilution for the 400-nm beads and 1:100 dilution for the 1000-nm beads. All polystyrene bead measurements were performed with these samples, either alone or mixed at different volume ratios or number ratios based on NTA particle counts, as stated in the results section.

The 100-nm and 400-nm beads mixture used for the spiking experiments contained about $1.7*10^8$ beads/ml. For these experiments, 2 or 40 µl of a suspension of 1000-nm beads (ca. $1.6*10^8$ particles/ml) were added to 500 µl of the 100-nm and 400-nm beads mixture, which resulted in a 1000-nm beads concentration of about $6.4*10^5$ beads/ml and $1.2*10^7$ beads/ml, respectively. The resulting number ratios of 1000-nm beads to the beads in the initial mixture was 1:267 for the 2 µl spike (small spike) and 1:13 for the 40 µl spike (substantial spike).

Preparation of drug delivery nanoparticles

N-trimethyl chitosan (TMC) with a degree of quaternization of 15% was prepared from chitosan and used to make TMC nanoparticles, as described in the literature [17]. In short, TMC was dissolved in a 5 mM HEPES buffer (pH 7.4) and pentasodium tripolyphosphate (TPP) was added under continuous stirring to a weight ratio TMC:TPP of 10:1.8. Nanoparticles were collected by centrifugation (30 min, 15,000 g) on a glycerol bed, to avoid aggregation, and resuspended in 5 mM HEPES buffer (pH 7.4). The sample was diluted 1000 fold with deionized water before the measurements.

PLGA nanoparticles were prepared by an “oil-in-water” solvent evaporation method, using polysorbate 20 as emulsifying agent. Briefly, 1 ml of dichloromethane containing 50 mg of PLGA and 2 ml 1% (w/v) polysorbate 20 were emulsified using an ultrasonic processor for 15 sec at 70 W (Branson Instruments, Connecticut, USA). The emulsion was transferred to 50 ml of 0.02% (w/v) polysorbate 20 in water, and stirred at 50°C for 1 hr. The resulting PLGA nanoparticles were collected by centrifugation (8,000 g for 10 min) and washed twice in distilled water to remove excess polysorbate 20. The sample was diluted 2000 fold with deionized water before the measurements.

Cationic liposomes were prepared by the film-hydration-rehydration method, and sized by sonication. In detail, a lipid film was formed by solvent evaporation of a chloroform solution of EPC, DOPE and DOTAP in a rotary evaporator at 37°C. To prepare 1 ml of liposome dispersion, a total amount of 28 µmol lipid was used at a EPC/DOPE/DOTAP molar ratio of 4/2/1. The film was hydrated in 1 ml of 20 mM HEPES, 5% glucose, pH 7.4, and the dispersion was equilibrated for 1 hr at

room temperature. The dispersion was then sonicated twice for 30 sec, with 30 sec interval, using a Branson Sonifier 250 (Branson Ultrasonics, Danbury, UK), with 3 mm microtip at 20 mW energy output. The sample was diluted 10000 fold with deionized water before the measurements.

All the buffers used in this section were filtered using a 0.22-μm PES low binding syringe driven filter unit (Millex™ GP, Millipore, Ireland) and the absence/very low content of submicron particles was confirmed by their visualization in the NanoSight sample chamber.

Preparation of protein aggregates

A recombinant human monoclonal antibody of the IgG_1 subclass (IgG) was used for preparing IgG aggregates. The IgG was formulated at a concentration of 1.0 mg/ml in 10 mM sodium citrate (Merck, Darmstadt, Germany), 5% (w/v) sucrose (Sigma-Aldrich, Buchs, Switzerland), pH 6.0. The IgG formulation was filtered using a 0.22-μm PES low binding syringe driven filter unit. One ml of the filtered IgG formulation was placed in 1.5-ml reaction tubes (Eppendorf, Hamburg, Germany) and incubated for 15 minutes at 74°C in a heating block (Eppendorf, Hamburg, Germany). The sample was diluted 50 fold with the formulation buffer before each measurement.

Recombinant human insulin (insulin) was formulated in 10 mM sodium phosphate, pH 7.4, and the formulation was filtered using the same filter unit as for the IgG formulation. Insulin aggregation was induced via a metal-catalyzed oxidation reaction by the addition of copper chloride (0.04 mM), followed by ascorbic acid (4 mM). The formulation was incubated at room temperature for three hours and the reaction was stopped by the addition of 1 mM ethylenediaminetetraacetic acid (EDTA).

All the buffers used in this section were filtered using a 0.22-μm PES low binding syringe driven filter unit and the absence/very low content of submicron particles was confirmed by their visualization in the NanoSight sample chamber.

Dynamic light scattering (DLS)

DLS measurements were performed with a Malvern Zetasizer Nano ZS (Malvern, Herrenberg, Germany) equipped with a 633-nm He-Ne laser and operating at an angle of 173°. The software used to collect and analyze the data was the Dispersion Technology Software version 6.01 from Malvern. 500 μl of each sample was

measured in single-use polystyrene half-micro cuvettes (Fisher Emergo, Landsmeer, The Netherlands) with a pathlength of 10 mm.

The measurements were made at a position of 4.65 mm from the cuvette wall, with an automatic attenuator and at a controlled temperature of 25°C. For each sample 15 runs of 10 seconds were performed, with three repetitions for all the polystyrene beads and six repetitions for the polymer nanoparticles and protein aggregates. The intensity size distribution, the Z-average diameter (Z-ave) and the polydispersity index (PdI) were obtained from the autocorrelation function using the "general purpose mode" for the monodisperse polystyrene beads and polymer samples, the "multiple narrow mode" for the mixtures of polystyrene beads and the "protein analysis mode" for the protein aggregates. The default filter factor of 50% and the default lower threshold of 0.05 and upper threshold of 0.01 were used. The error bars displayed on the DLS graphs were obtained by the standard deviation (SD) of three or six measurements of the same sample.

Nanoparticle tracking analysis (NTA)

NTA measurements were performed with a NanoSight LM20 (NanoSight, Amesbury, United Kingdom), equipped with a sample chamber with a 640-nm laser and a Viton fluoroelastomer O-ring. The samples were injected in the sample chamber with sterile syringes (BD Discardit II, New Jersey, USA.) until the liquid reached the tip of the nozzle. All measurements were performed at room temperature except the live monitoring protein heat stress measurements (see section below).

The software used for capturing and analyzing the data was the NTA 2.0 Build 127. The samples were measured for 40 seconds with manual shutter and gain adjustments. The "single shutter and gain mode" was used to capture the monodisperse polystyrene beads, the 60 and 100 nm beads mixture, the TMC particles and the protein aggregates. The "extended dynamic range mode", which splits the capture video into two videos with independent shutter and gain settings, was used for all the other mixtures of monodisperse polystyrene beads, the PLGA particles and the insulin aggregates. Three measurements of the same sample were performed for all the polystyrene beads and six measurements for the polymer nanoparticles and protein aggregates. The error bars displayed on the NTA graphs were obtained by the standard deviation of the different measurements of each sample. The mean size and SD values obtained by the NTA software correspond to the arithmetic values calculated with the sizes of all the particles analyzed by the

software.

Live monitoring of protein heat stress

For the live monitoring of protein aggregation, the above mentioned IgG was formulated at a concentration of 1.0 mg/ml in 100 mM sodium citrate (Merck, Darmstadt, Germany), pH 7.6. Unstressed IgG was inserted in the NanoSight sample chamber at room temperature and the heating block was then set to 50°C. Once the chamber had reached the set temperature, which took about 10 minutes, a video was recorded for 40 seconds (t_0), followed by three time points with the same video length, at 15, 25 and 35 minutes. The videos of the first three time points were captured with the "single shutter and gain mode" and of the last time point with the "extended dynamic range mode", because of the high sample polydispersity observed for this time point.

RESULTS AND DISCUSSION

Evaluation of NTA performance and comparison to DLS

Monodisperse polystyrene beads

In order to verify the accuracy of NTA to size monodisperse samples, standard polystyrene beads of 60 nm, 100 nm, 200 nm, 400 nm and 1000 nm were analyzed with NTA and the results were compared to DLS (Fig. 3.1). While NTA requires particle concentrations of 10^7-10^9/ml, the DLS concentration range is less critical and depends upon a number of instrumental and sample properties [18]. For most of the samples used in this study the DLS concentration was about 10^8-10^{12} particles/ml (data not shown). Given the difference in concentration range between the two techniques, a concentration suitable for both techniques was selected for each bead size.

Contrary to DLS, NTA enables sample visualization and provides approximate particle concentrations, which are very useful features. Both techniques showed good sizing accuracy and relatively narrow distributions for all monodisperse samples. Nevertheless, it is possible to observe a tailing of all DLS size distributions towards larger sizes, mostly due to the immense contribution of a few large particles to the overall scattering [14].

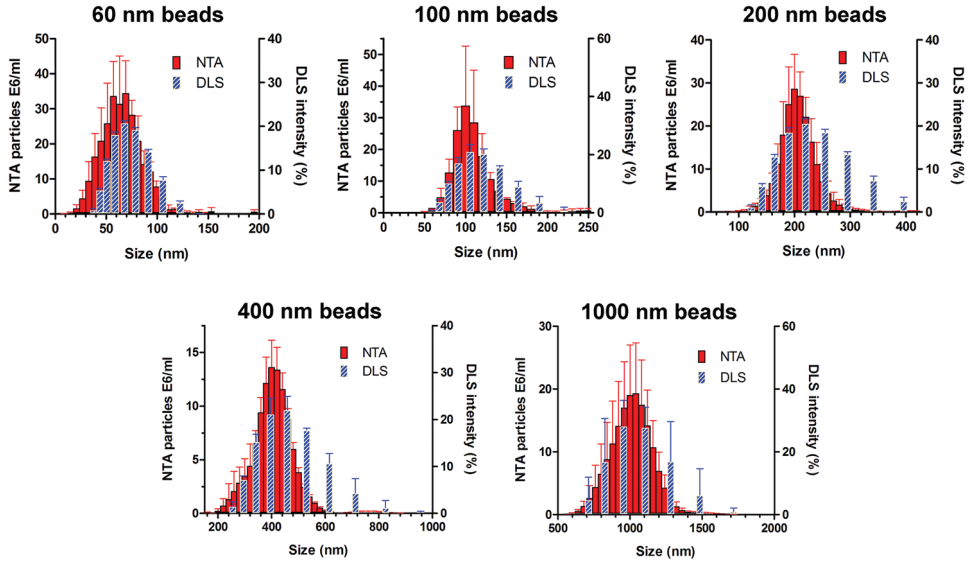

Figure 3.1: Size distribution from NTA and DLS measurements of monodisperse polystyrene beads. Error bars represent standard deviations obtained from three measurements of the same sample.

The mean size values obtained by NTA are slightly smaller and closer to the expected values than the Z-ave given by DLS, but all values are close to the bead size specified by the manufacturer (Table 3.1). However, the error bars of the size distribution obtained for each sample are smaller with DLS (Fig. 3.1), which is a consequence of the large amount of statistical data collected by DLS when compared to NTA. In fact, these high error bars in the NTA results are mostly caused by different particle counts between each measurement. The size distributions are practically the same, but the software sometimes detects slightly more or slightly less particles between each measurement of the same sample. This variation in the number of particles detected by NTA brings attention to the imprecision of the particle concentration given by this technique. Still, though not the primary aim of NTA, its capability to provide approximate submicron particle counts is an obvious advantage of the method over DLS.

While DLS measurements are fast and rather straightforward, NTA requires several optimization steps by a skilled operator, e.g. with respect to indentifying suitable settings for the video capture and analysis. Whereas DLS can automatically adjust the attenuator to adapt to a wide range of sample concentrations, the search for the right sample concentration for a successful NTA measurement can be time consuming, as it may require various dilution steps. However, NTA proved to be

slightly more accurate than DLS for sizing monodisperse samples.

Table 3.1: Mean size and size distribution of monodisperse polystyrene beads from NTA and DLS measurements.

Bead size (nm)	DLS		NTA		
	Z-ave (nm)	PdI	Mean (nm)	SD (nm)	Particle conc. (E^8/ml)
60	68 ± 1	0.04 ±0.01	66 ±2	20 ± 1	7.70
100	112 ± 4	0.13 ±0.07	105 ±6	30 ±10	1.87
200	218 ± 1	0.04 ±0.01	200 ±5	30 ± 5	2.32
400	443 ± 5	0.13 ±0.03	394 ±7	62 ± 6	1.08
1000	1056 ±164	0.36 ±0.08	989 ±51	117 ±14	1.64

Mixtures of monodisperse polystyrene beads: fixed number ratio

One of the well-known pitfalls of DLS is its low peak resolution, i.e. it can only resolve particle populations that differ in size at least by a factor of 3 [19]. Thus, with the purpose of testing the resolution of NTA, the monodisperse polystyrene standard beads analyzed in the previous section were mixed at a fixed number ratio (60 nm and 100 nm; 100 nm and 200 nm; 200 nm and 400 nm; 400 nm and 1000 nm) and analyzed with both techniques. The two-dimensional (2D) size distributions of DLS and NTA, with the corresponding NTA video frames and three-dimensional (3D) graphs (size vs. intensity vs. concentration) are shown in Fig. 3.2.

From these results, the difficulty of DLS in resolving peaks of polydisperse samples becomes apparent, as it was not possible to separate the two bead sizes of any of the mixtures. On the other hand, NTA was able to resolve and distinguish the two size populations in all mixtures and yielded accurate size estimations of the beads in the mixtures (Table 3.2). The 2D size distributions show that DLS only gives a single peak for the mixtures shifted towards the larger particle size present, which is again related to its bias to larger particles. The error bars of the DLS results of the two mixtures with the larger bead size (Fig. 3.2c and 3.2d) are larger than the ones of the NTA results. This is related to the difficulty that the DLS software has to fit the data of an autocorrelation curve of a sample that has two populations with size differences smaller than the peak resolution limit of this technique. As a result, the single peak as calculated by the DLS software is prone to changes in shape and position from measurement to measurement, giving rise to relatively large error bars in the average result.

The two different bead sizes with different scattering intensities can be observed in the NTA video frames, 2D size distribution graphs and can be clearly distinguished

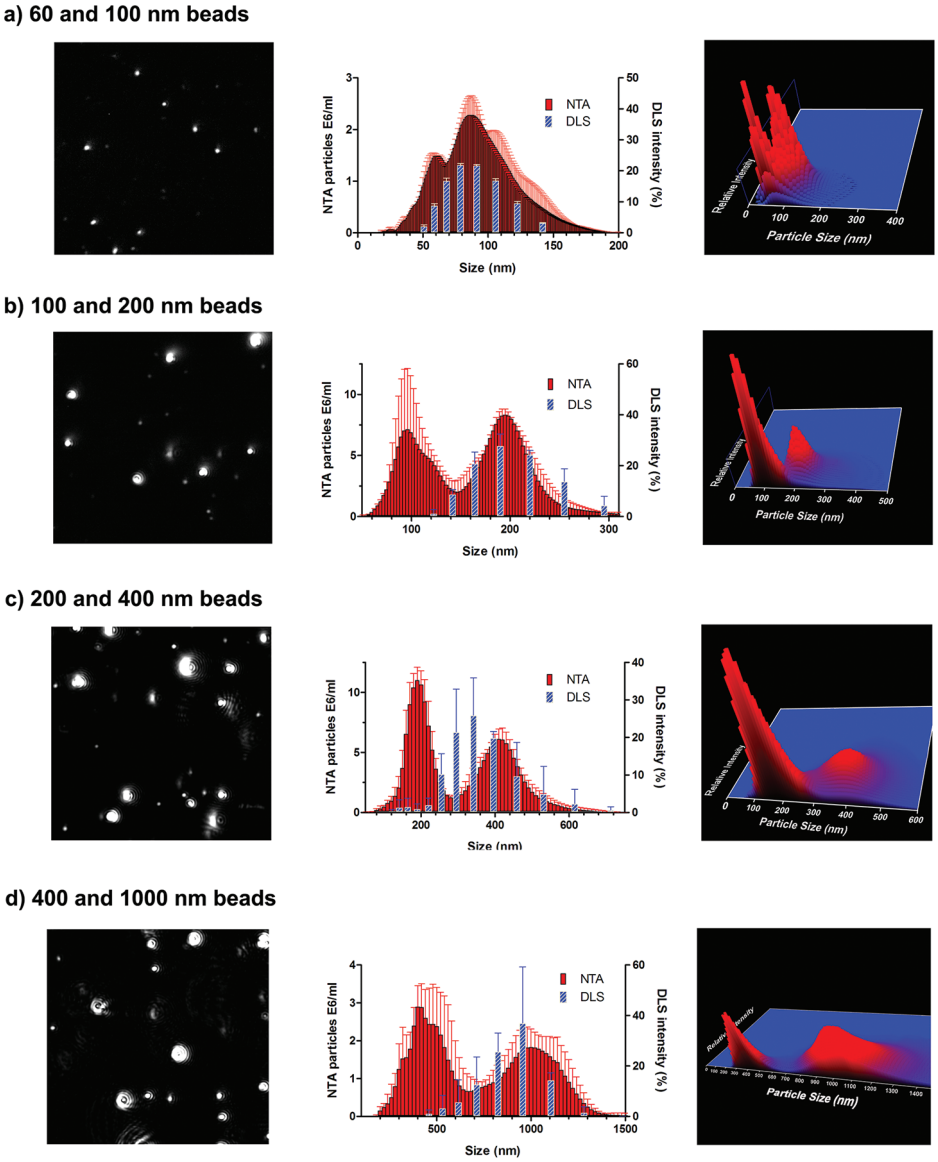

Figure 3.2: Size distribution from NTA and DLS measurements of mixtures of monodisperse polystyrene beads (middle panels) with the corresponding NTA video frame (left panels) and 3D graph (size vs. intensity vs. concentration; right panels). a) 60-nm/100-nm beads at a 4:1 number ratio; b) 100-nm/200-nm beads at a 1:1 number ratio; c) 200-nm/400-nm beads at a 2:1 number ratio; d) 400-nm/1000-nm beads at a 1:1 number ratio.

in the 3D graphs (Fig. 3.2). Despite having a 60-nm/100-nm bead number ratio of 4:1 (Fig 3.2a), NTA analysis of this mixture shows more 100-nm beads than 60-nm beads. This is mainly caused by a masking effect of the larger beads over

the smaller beads, explained in detail on the influence of small numbers of large particles section, combined with the fact that some of the 60-nm beads move so fast that they often move out of focus in the detection area before they can be tracked long enough to be considered for the final result. Nevertheless, the difference in scattering intensities displayed by the 3D graphs proves to be very useful to confirm the presence of different populations of similar sizes, such as in this 60-nm/100-nm bead mixture. While the 2D graph shows a peak at 100 nm and a shoulder at 60 nm, the 3D graph shows two distinct size populations, clearly confirmed by the higher light scattering intensity of the 100-nm particles compared to the 60-nm ones. Thereby, the third dimension (scattering intensity) in NTA contributes not only to the resolution of particle populations, but also provides information about the nature of the particles: for particles with equal refractive index the larger ones should scatter more light, proportional to the diameter to the power six.

Measuring the mixture of monodisperse beads with DLS is as easy and fast as measuring the standard polystyrene beads alone, but the results do not reflect the samples' real content. On the other hand, NTA analysis of two different particle sizes implies in most cases the use of the "extended dynamic range mode", which adds a complex variable to the analysis. This mode allows the recording of a set of two videos at the same time with different shutter and gain settings, enabling the simultaneous analysis of large and small particles in one measurement. A big advantage of NTA is the unbiased high peak resolution for polydisperse samples, which is not possible by DLS.

Mixtures of monodisperse polystyrene beads: effect of number ratio

In the field of nanoparticle characterization, it is important to have tools that are able to detect and characterize small amounts of a certain particle size population, different from the main population. Thus, to elucidate the ratio detection limits of NTA, 100 and 400 nm polystyrene beads were mixed at 100-nm/400-nm bead number ratios of 3:1, 6:1, 15:1, 150:1 and 300:1, and analyzed with NTA and DLS (Fig. 3.3). The ratios were based on the particle concentration of the individual bead samples obtained by NTA.

The selection of the distinct sizes of beads for these measurements took into consideration the DLS theoretical peak resolution of 3:1 in size. Nonetheless, DLS was not able to distinguish the two bead sizes for the lower 100-nm/400-nm bead number ratios of 3:1 and 6:1, for which mainly the larger beads were detected. When the number ratio reached 300:1 the larger particles were no longer shown by DLS.

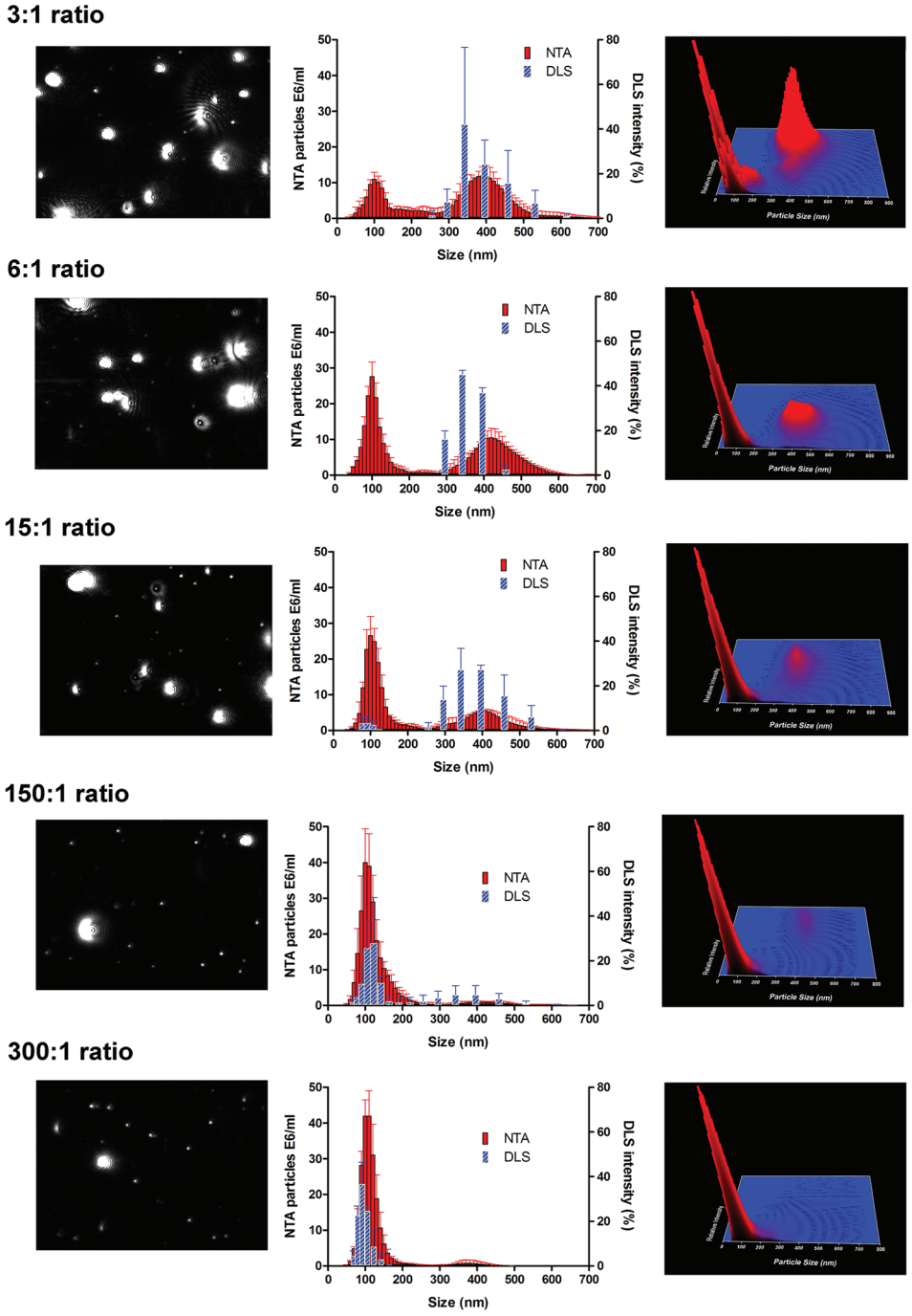

Figure 3.3: Influence of different number ratios of 100-nm/400-nm monodisperse beads in NTA and DLS measurements (middle panels) with the corresponding NTA video frame (left panels) and normalized 3D graph (size vs. intensity vs. concentration; right panels).

On the other hand, analysis with NTA enabled accurate sizing and a clear distinction of the two size populations for all the ratios analyzed. The presence of the two distinct size populations is very clear in the video frames of Fig. 3.3. In fact, being able to see the sample and search for the desired location where the video is recorded enables the operator the choice of including or excluding certain particles. Therefore, the appearance of the 400 nm peak for ratios bigger than 300:1 depends on the operator. Being able to see and scan the sample is a useful feature of NTA, but it should be used prudently to avoid false of biased results.

Influence of small numbers of large particles

One of the main concerns of DLS is the influence that a small amount of large particles, such as dust, may have on the outcome. The NTA technique is based on the tracking of single particles, whereas DLS measures a bulk of particles with a strong bias to the largest particles present in the sample. Therefore, the performance of NTA is expected to be less sensitive than DLS to the presence of minute amounts of large particles. To compare the influence of large particles on NTA and DLS results, a mixture of 100-nm and 400-nm polystyrene beads was spiked with two different amounts of 1000-nm beads. The resulting number ratios of 1000-nm beads to the beads in the initial mixture was 1:267 for the small spike and 1:13 for the big spike (Fig. 3.4).

The small spike was sufficient to cause an increase of about 40 nm in the Z-ave and of about 0.05 in the PdI determined by DLS (Table 3.2). The same spike made the NTA analysis slightly more complicated because the highly scattering 1000-nm beads made the 100-nm beads slightly more difficult to detect. However, with optimized settings (Table 3.3), all bead types present in the sample could be detected and accurately sized by NTA (Fig. 3.4b). However, after the spike the number of 100-nm beads detected by NTA decreased by about 70% and the number of 400-nm beads by about 20%. The intense light scattering of large particles makes the small particles more difficult to detect and prevents some of them from being tracked by the NTA software.

The big spike increased the Z-ave of DLS from 430 to 698 nm, but curiously decreased the PdI from 0.29 to 0.14. The lower PdI of this spiked sample is most likely a consequence of the masking effect of the 1000 nm beads over the smaller beads in DLS measurements. These DLS values could have suggested that it was a fairly monodisperse 700 nm sample, when in fact it contained three distinct size populations of 100, 400 and 1000 nm. Such misinterpretation was not made when

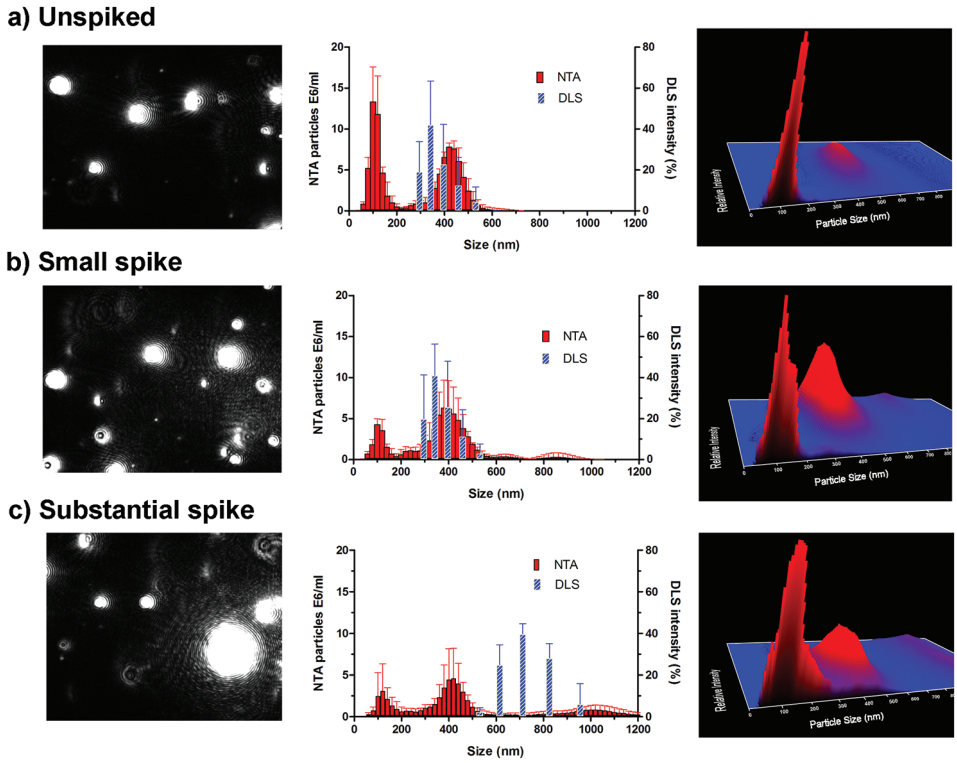

Figure 3.4: Influence of large particles (1000-nm beads) in a mixture of 100-nm and 400-nm monodisperse beads on NTA and DLS measurements. The size distribution (middle panels) with the corresponding NTA video frame (left panels) and normalized 3D graph (size vs. intensity vs. concentration; right panels) are shown. a) no 1000-nm beads; b) 1:267 number ratio of 1000-nm beads to the other beads in the mixture; c) 1:13 number ratio of 1000-nm beads to the other beads in the mixture.

using NTA, since the presence of different populations was clearly detected by sample visualization. Although the substantial spike made the NTA measurements considerably more complex, all the beads in the sample could still be visualized and accurately sized (Fig. 3.4c). However, also in this case spiking with large particles resulted in the underestimation of the number of smaller beads. After this spike the number of 100-nm beads detected by NTA decreased by about 80% and that of the 400-nm beads by about 35%.

Effect of settings in NTA software on particle size data

As already mentioned, NTA involves several adjustment steps during the video capture and analysis, which are essential to obtain accurate measurement results. The power of choice given to the operator may be seen as a great advantage, but also

Table 3.2: Mean size and size distribution of mixtures of monodisperse polystyrene beads from NTA and DLS measurements.

Bead size (nm)	DLS			NTA				
	Z-ave (nm)	PdI	Peak (nm)	Mean (nm)	SD (nm)	Peak 1 (nm)	Peak 2 (nm)	Peak 3 (nm)
60+100	84 ± 1	0.08 ±0.01	83± 7	90 ± 3	33 ± 4	58± 4	91± 9	-
100+200	195 ± 2	0.40 ±0.20	194± 5	162 ±13	60 ± 6	98± 2	196± 2	-
200+400	347 ±42	0.19 ±0.03	359± 32	298 ±20	122 ± 9	195± 5	410±10	-
400+1000	952 ±31	0.26 ±0.05	912± 75	712 ±36	296 ±20	427± 46	1067± 94	-
100+400	430 ±34	0.29 ±0.08	363±29	265 ±16	157 ±11	98± 5	419± 12	-
100+400+ S. Spike	467 ±22	0.35 ±0.05	378±32	338 ±36	163 ±23	99± 10	384± 12	850± 83
100+400+ B. Spike	698 ±26	0.14 ±0.07	750±65	527 ±101	353 ±11	106± 4	420± 22	997±31

Abreviations: Z-ave, Z-average; PdI, polydispersity index; SD, standard deviation calculated by the NTA software; S. Spike, small spike with 1000-nm beads to a 100-nm/400-nm beads mixture; B. Spike, big spike with 1000 nm beads to a 100 nm and 400 nm beads mixture. Numbers represent average values ± standard deviation (n = 3 measurements). See materials and methods for details. The peaks correspond to the highest value observed for a certain size.

raises concerns. The operator can easily choose settings that ignore or emphasize the presence of certain particles, which makes the veracity of the results dependent on individual judgment and experience.

To obtain accurate results one should: (i) thoroughly search with the microscope for the presence of all particle size classes in the sample; (ii) optimize the video settings in order to capture all these identified particle sizes; and (iii) adjust the analytical settings to unbiasedly track all moving particles captured by the video. With the purpose of clarifying the weight of the different software setting on the result, the influence of each parameter was carefully analyzed, as summarized in Table 3.3.

As the quality of NTA data will be dependent on the software settings used, which in turn depend on sample properties, as well as on the experience and decisions of the operator, NTA will be very difficult to qualify as a quality control method. Instead, NTA is –like DLS– very useful as characterization tool, as will be demonstrated in the applications discussed below.

NTA APPLICATIONS

DRUG DELIVERY NANOPARTICLES

In order to evaluate the analytical performance of NTA for nanoparticles commonly

Table 3.3: Effect of the most important NTA software settings on size analysis.

Parameter	Description	Impact on the measurement	
		Incorrect settings	Optimal settings
Shutter/Gain*	The shutter determines the length of time that the camera shutter is open and the gain regulates the sensitivity of the camera	- Underexposed videos omit smaller particles - Overexposed videos show particles as untraceable wobbling light flares	All particles appear as clear moving dots, traceable by the software
Capture Duration	Determines the length of the captured video	Too short videos result in inaccurate and statistically poor size distributions	Statistically robust and reproducible size distributions
Blur	Smoothens the captured video, eliminating visual noise from around and within the particle	- Excessive blur makes small particles disappear - Insufficient blur leaves false light scattering centers	Removes false light scattering centers and helps the software to track real particles
Detection Threshold*	Determines the minimum gray scale value of a dot necessary for it to qualify as a traceable particle	- Too high thresholds result in loss of small particles - Too low thresholds result in loss of large particles or mistracking of visual noise	All particles in the video are tracked and visual noise is ignored
Minimum Expected Particle Size (MEPS)	Determines the area around the particle where the software searches for it in the following frame (large particles – slow movements– small areas; small particles – fast movements - large areas)	Too high MEPS result in loss of small particles because they move outside of the search area - Too low MEPS result in loss of particles in general due to search area overlap	Most of the particles in the video are tracked long enough to be included in the final result

* Parameters that require thorough optimization and that have a major impact in the final outcome.

used in the pharmaceutical field, PLGA particles, TMC particles and liposomes were analyzed with NTA and the results compared to DLS (Fig. 3.5).

DLS analysis resulted in a Z-ave of 411 nm and a PdI of 0.09 for the TMC particles, indicating a relatively monodisperse sample. This was confirmed by the visualization of the particles in the NanoSight sample chamber (Fig. 3.5a) and by the relatively low standard deviation (91 nm) given by NTA. However, the mean size obtained by NTA was 320 nm, which is about 90 nm smaller than the Z-ave given by DLS, which points to a certain degree of polydispersity. The systematic size distribution shift towards larger sizes by DLS is more accentuated for the TMC particles than for the monodisperse polystyrene beads. This shift can be explained by the fact that size distributions obtained by DLS are intensity distributions, whereas NTA provides number distributions, which results in a larger shift in case of higher polydispersity.

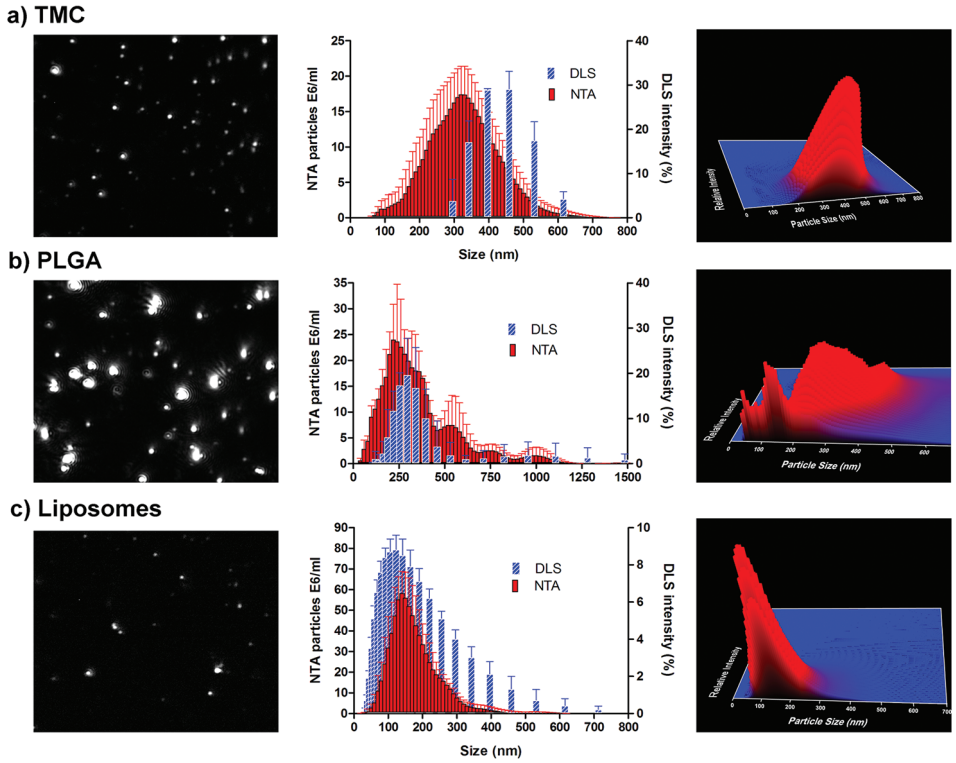

Figure 3.5: Drug delivery nanoparticles measured with NTA and DLS. The size distribution (middle panels) with the corresponding NTA video frame (left panels) and 3D graph (size vs. intensity vs. concentration; right panels) are shown.

The PLGA particles analyzed by DLS exhibited a Z-ave of 308 nm and a PdI of 0.22. This PdI value suggests that the PLGA particles were more polydisperse than the TMC particles. The relatively high polydispersity of the PLGA particles became very clear during the visualization of the sample by NTA (Fig. 3.5b) and was confirmed by the high standard deviation (182 nm) obtained for the PLGA particles. The main population of these particles given by DLS was shifted to larger sizes as compared to NTA. However, contrary to most samples analyzed in this evaluation, the mean value observed with NTA (322 nm) was slightly higher than the Z-ave given by DLS (Fig. 3.5). This may be due to the inherent difficulty for DLS to properly analyze polydisperse samples.

DLS analysis of the liposomes resulted in a Z-ave of 117 nm and a PdI of 0.248, suggesting that this sample was more polydisperse than the PLGA sample. Surprisingly, the visualization of the liposomes with NTA revealed a fairly monodisperse sample

and the standard deviation obtained was 77 nm, which is even smaller than that of TMC particles. The mean size value obtained with NTA was 154 nm, which is again larger than the Z-ave given by DLS. This time the peak given by DLS is shifted to smaller sizes as compared to the one obtained by NTA. Given that DLS has a lower detection limit than NTA, it is possible that smaller particles (< 30 nm) present in the formulation decreased the Z-ave in DLS, which would also explain the relatively high PdI. Other analytical techniques would have been necessary to clarify this observation.

Protein aggregates

A heat stressed IgG formulation and a metal-oxidized insulin formulation were used to evaluate the analytical performance of NTA with protein aggregates (Fig. 3.6). The difference in the lower detection limits of the two techniques was evident when it came to the characterization of protein aggregates. DLS was able to detect not only the monomeric IgG (~11 nm) but also the sucrose molecules (~1 nm) present in the buffer, as was early described by others [20, 21]. Given that the lower detection limit of NTA for proteins is about 30 nm, protein monomers and aggregates smaller than this are not detected by this technique. Nevertheless, in the stressed IgG formulation the IgG aggregate size distribution obtained by DLS and NTA was similar, with a main peak at around 200 nm. The Z-ave obtained by DLS was 47 nm and the PdI 0.5, while the average size according to NTA was 175 nm and the standard deviation 76 nm. The difference in the mean size values is most likely due to the fact that DLS considers aggregates, monomer and sucrose for the Z-ave (also explaining the high PdI), while NTA considers only aggregates for calculating the mean particle size (Fig. 3.6a).

The visualization of the aggregated IgG sample with NTA allowed the distinction of two or more light scattering centers in very large aggregates (> 1 μm), which suggests that they were formed by the assembly of smaller aggregates. However, the brightness of such large particles interferes with the optimization of the instrument settings, because it makes smaller aggregates more difficult to detect. The monomer present in the sample increases the background light and also makes smaller aggregates more difficult to detect.

In the aggregated insulin sample, the native insulin was only detected by DLS and found to have an average size of about 6 nm, consistent with literature data for insulin at neutral pH [22]. Also for this sample, the aggregate size distribution was consistent between the two techniques, with a broad peak centered around 160 nm

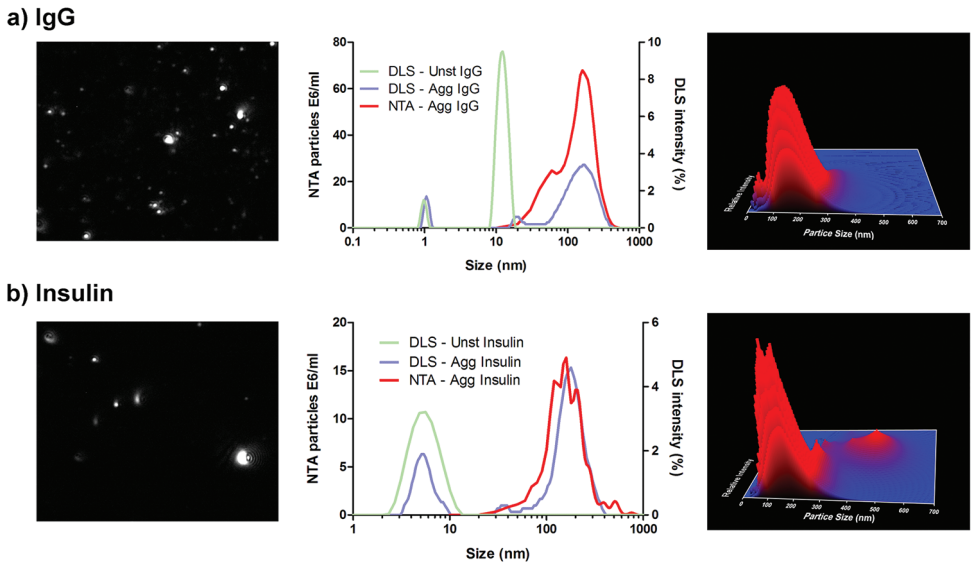

Figure 3.6: IgG aggregates (obtained by heat stress) and insulin aggregates (obtained by metal catalyzed oxidation) measured with NTA and DLS. The size distribution (middle panels) with the corresponding NTA video frame (left panels) and 3D graph (size vs. intensity vs. concentration; right panels) are shown.

(Fig. 3.6b). The Z-ave given by DLS was 70 nm and the PdI 1.0, while the mean given by NTA was 199 nm and the standard deviation 103 nm. Such a high PdI given by DLS suggested that the aggregates in the sample were very polydisperse, which can be confirmed by sample visualization and high standard deviation provided by NTA. Once again, the difference in mean value and Z-ave given by the two techniques is most likely due to the fact that DLS considers native insulin and aggregates, while NTA considers only aggregates.

Several factors are known to induce protein aggregation and some characterization techniques have been reported to induce or disturb the aggregation state [8]. During NTA measurements, the sample is in contact with glass, stainless steel, a Viton fluoroelastomer O-ring and nylon tubing. Moreover, the samples are submitted to a slight shear during the injection into the measurement cell. It has been reported that the synergistic effect of adsorption of a monoclonal antibody to stainless steel and shear can create small amounts of aggregates [23]. In fact, we noticed that some stressed IgG formulations slightly increase the amount and size of aggregates if left in the sample chamber for more than 30 min (data not shown). This phenomenon became more evident if the sample was moved back and forth in the measurement cell with the syringe piston. While DLS size measurements are usually performed in

disposable (polystyrene) cuvettes, the NanoSight sample chamber has to be manually cleaned and reused. Furthermore, as previously mentioned, NTA measurements often require sample dilution, which may destroy or create new aggregates and affect the size distribution [8]. In general, the effect of sample dilution on the sample is related to the instability of the submicron particles and is more likely to affect protein aggregates than drug delivery nanoparticles.

Overall, DLS sample treatment seems to be less aggressive than NTA, which is an advantage for unstable samples, such as protein aggregates. However, the high peak resolution and suitability for polydisperse samples make NTA a very useful technique to analyze protein aggregates.

Live monitoring of heat-induced protein aggregation

The heating block of NanoSight allows NTA measurements at temperatures ranging from room temperature to 50°C, which enables the live monitoring of protein aggregation at elevated temperatures. This feature is also possible with DLS, but the possibility of visualizing the aggregates being formed with NTA gives a more complete overview of the aggregation process.

An IgG formulation was heated at 50°C for 45 minutes in the NanoSight heating block, while movies were being recorded (Fig. 3.7). Since NTA is not capable of detecting particles smaller than about 30 nm, it was not possible to see the formation of dimers, trimers or any small oligomers. At t_0 the sample had already been exposed to some heat stress for about 10 min, the time required for the temperature to rise from room temperature to 50°C, and some polydisperse aggregates of about 50-350 nm were detected. At t_1 the number of aggregates had increased and distinct subpopulations became apparent around 50 nm, 100 nm and 200 nm. After about 20 minutes the number of aggregates rapidly increased. Even though the number of aggregates had slightly increased at t_2, it does not reflect this sudden increase of aggregates observed, because the background scattering (visible in the video frame of t_2) made particle tracking more difficult for the NTA software. After 35 minutes of heat stressing the number of aggregates reached the upper concentration limit of NTA and especially the number of aggregates with sizes around 50 nm increased significantly. After 45 minutes very large (> 5 μm) aggregates were visible and they made accurate NTA size measurements impossible, because the light they scattered masked the smaller traceable aggregates (<1 μm). These large aggregates contained several intense light scattering centers (results not shown), which were probably formed by the assembly of several smaller aggregates. Unfortunately, aggregate

assembly process was not detectable by this technique since the aggregates were constantly entering and leaving the view area.

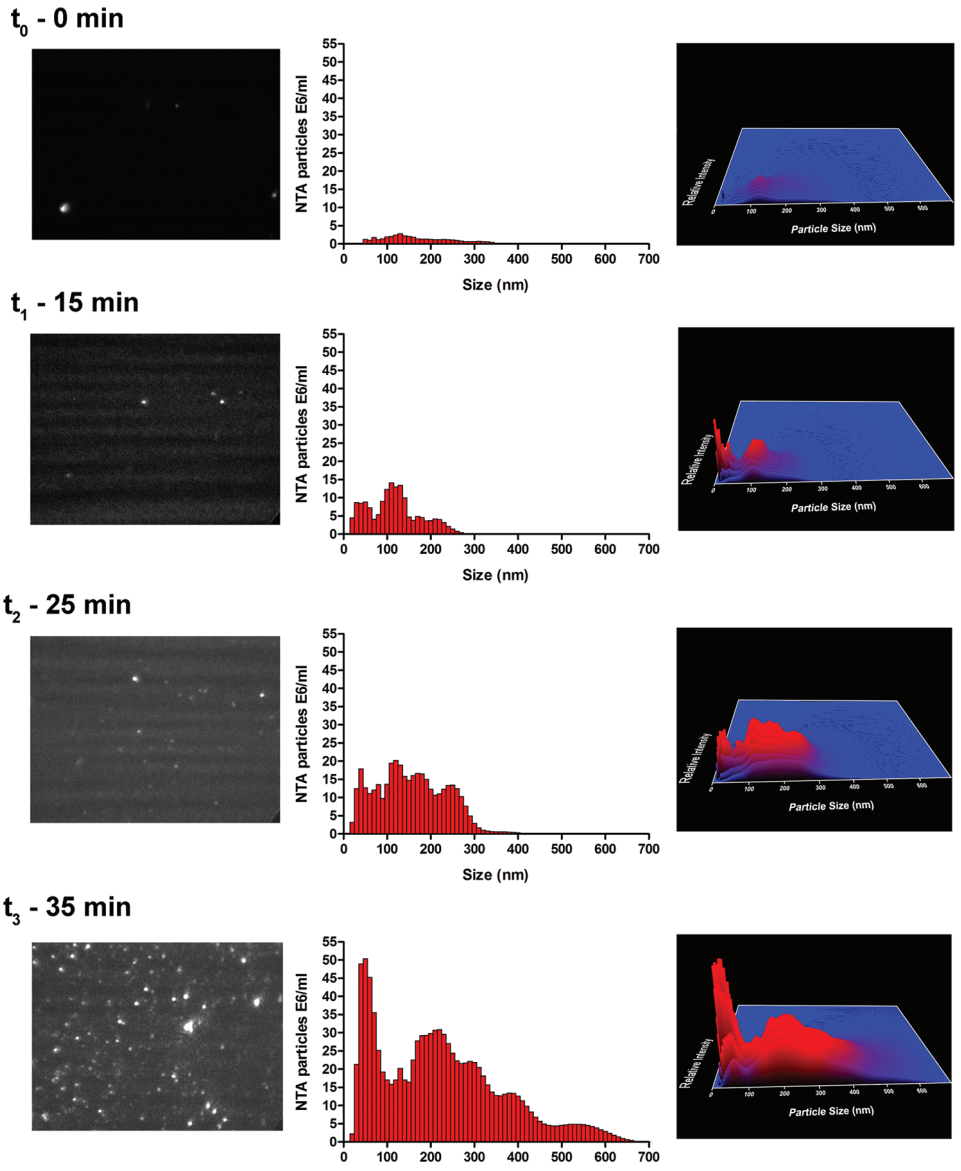

Figure 3.7: Live monitoring of IgG aggregation at 50 °C in the NanoSight sample chamber. The size distribution (middle panels) with the corresponding NTA video frame (left panels) and 3D graph (size vs. intensity vs. concentration; right panels) are shown.

CONCLUSIONS

In this work we evaluated NTA as a new characterization method for nanoparticle analysis and compared it to DLS. The differences between the two techniques are summed in Table 3.4. NTA can be time consuming and requires some operational skills for the adjustment all software settings, but has some clear advantages over DLS. NTA enables the visualization of the sample, gives an approximate particle concentration and obtains size information based on the Brownian motion of individual particles. NTA is very accurate for sizing both monodisperse and polydisperse samples and has a substantially better peak resolution. The presence of few large particles in a sample has a little impact on NTA sizing accuracy, but reduces the number of small particles detected by the software. Different population ratios in standard polystyrene bead mixtures are easily detected and do not affect the sizing accuracy.

NTA proved to be very suitable for analyzing drug delivery nanoparticles. This technique is also very suitable for analyzing protein aggregates, but care should be taken that sample preparation does not influence the aggregate distribution in the measurement cell. It also gives the possibility of live monitoring heat-induced aggregation, providing information about the aggregation kinetics.

AKNOWLEDGEMENTS

This research is supported by the Dutch Technology Foundation STW, applied science division of NWO and the Technology Program of the Ministry of Economic Affairs. The authors are grateful to Bram Slütter and Ana Silva for the preparation of the TMC nanoparticles and PLGA particles, to Myrra Carstens for the preparation of the liposomes and to Riccardo Torosantucci and Olubukayo Oladunjoye for preparing the aggregated protein samples.

Table 3.4: Comparison of NTA with DLS.

	DLS	NTA
CHARACTERISTICS		
Size accuracy	Accurate for monodisperse samples, inaccurate for polydisperse samples	Accurate for both monodisperse and polydisperse samples
Peak resolution	Low (>3 fold difference in diameter)	High (< 0.5 fold difference in diameter)
Size range	Ca. 1-1000 nm	Ca. 30-1000 nm
Concentration range (particles/ml)	Broad (about 10^8-10^{12})	Limited (10^7-10^9)
Population ratio	Narrow range Large influence on size accuracy and distribution	Very broad range Very little influence on size accuracy and little influence on size distribution
Reproducibility	More reproducible	Less reproducible
Contaminations	Large particles can seriously compromise the results	Dust, microorganisms or aggregates are easily detected. Large particles have little influence.
OPERATIONAL		
Device handling	Very user friendly Little sample handling Possibility of using disposable cuvettes	Requires several parameter adjustments Sample handling may affect size distribution Sample chamber must be cleaned after each sample Experienced operator required
Time consumption	Between 2 to 5 min per measurement	Between 5 min to 1 hour per measurement
Particular output	Approximate size distribution Intensity distribution Z-ave PdI	Individual particle sizing Number distribution Approximate concentrations Individual particle intensity
Sample visualization	No	Yes
APPLICATIONS		
Drug delivery nanoparticles	Accurate sizing Approximate size distribution Hard detection of contaminants	Accurate sizing More reliable size distribution Easy detection of contaminants
Protein aggregates	Approximate size distribution Includes protein monomers and some excipients Presence of very large aggregates has a big impact on the result	Accurate size distribution Protein monomer and small aggregates excluded Aggregate architecture information Interference of large aggregates may sometimes be overcome

REFERENCES

[1] R. I. Mahato, A. S. Narang, L. Thoma, and D. D. Miller, "Emerging trends in oral delivery of peptide and protein drugs," Crit Rev Ther Drug Carrier Syst, vol. 20, pp. 153-214, 2003.
[2] C. A. Lipinski, "Drug-like properties and the causes of poor solubility and poor permeability," J Pharmacol Toxicol Methods, vol. 44, pp. 235-49, Jul-Aug 2000.
[3] W. Jiskoot, R. M. van Schie, M. G. Carstens, and H. Schellekens, "Immunological risk of injectable drug delivery systems," Pharm Res, vol. 26, pp. 1303-14, Jun 2009.
[4] M. E. Cromwell, E. Hilario, and F. Jacobson, "Protein aggregation and bioprocessing," Aaps J, vol. 8, pp. E572-9, 2006.
[5] H. Schellekens, "Bioequivalence and the immunogenicity of biopharmaceuticals," Nat Rev Drug Discov, vol. 1, pp. 457-62, Jun 2002.
[6] H. C. Mahler, W. Friess, U. Grauschopf, and S. Kiese, "Protein aggregation: pathways, induction factors and analysis," J Pharm Sci, vol. 98, pp. 2909-34, Sep 2009.
[7] S. Frokjaer and D. E. Otzen, "Protein drug stability: a formulation challenge," Nat Rev Drug Discov, vol. 4, pp. 298-306, Apr 2005.
[8] J. S. Philo, "A critical review of methods for size characterization of non-particulate protein aggregates," Curr Pharm Biotechnol, vol. 10, pp. 359-72, Jun 2009.
[9] J. F. Carpenter, T. W. Randolph, W. Jiskoot, D. J. Crommelin, C. R. Middaugh, G. Winter, Y. X. Fan, S. Kirshner, D. Verthelyi, S. Kozlowski, K. A. Clouse, P. G. Swann, A. Rosenberg, and B. Cherney, "Overlooking subvisible particles in therapeutic protein products: gaps that may compromise product quality," J Pharm Sci, vol. 98, pp. 1201-5, Apr 2009.
[10] A. Bootz, V. Vogel, D. Schubert, and J. Kreuter, "Comparison of scanning electron microscopy, dynamic light scattering and analytical ultracentrifugation for the sizing of poly(butyl cyanoacrylate) nanoparticles," Eur J Pharm Biopharm, vol. 57, pp. 369-75, Mar 2004.
[11] P. H. Brown and P. Schuck, "Macromolecular size-and-shape distributions by sedimentation velocity analytical ultracentrifugation," Biophys J, vol. 90, pp. 4651-61, Jun 15 2006.
[12] W. Fraunhofer, G. Winter, and C. Coester, "Asymmetrical flow field-flow fractionation and multiangle light scattering for analysis of gelatin nanoparticle drug carrier systems," Anal Chem, vol. 76, pp. 1909-20, Apr 1 2004.
[13] B. J. Frisken, "Revisiting the method of cumulants for the analysis of dynamic light-scattering data," Appl Opt, vol. 40, pp. 4087-91, Aug 20 2001.
[14] J. Demeester, S. Smedt, N. Sanders, and J. Haustraete, "Light Scattering," in Methods for structural analysis of protein pharmaceuticals, W. Jiskoot and D. J. Crommelin, Eds., ed Arlington VA: AAPS Press, 2005.
[15] B. Berne and R. Pecora, Dynamic light scattering with applications to chemistry, biology, and physics. Mineola, NY: Dover Publications, 2000.
[16] (26/09/2009). Applications of Nanoparticle Tracking Analysis (NTA) in Nanoparticle Research. Available: http://www.schaefer-tec.com/fileadmin/user_upload/sortiment/nanopartikel/NanoSight/NANOSIGHT_Application_Review_NTA_April_2009_M201B.pdf
[17] B. Slutter, L. Plapied, V. Fievez, M. A. Sande, A. des Rieux, Y. J. Schneider, E. Van Riet, W. Jiskoot, and V. Preat, "Mechanistic study of the adjuvant effect of biodegradable nanoparticles in mucosal vaccination," J Control Release, vol. 138, pp. 113-21, Sep 1 2009.
[18] (22/09/2009). Minimum DLS concentration?: Malvern support FAQ. Available: http://www.malvern.com/malvern/kbase.nsf/allfaqbyno/KB000795?opendocument
[19] (22/09/2009). Can DLS resolve oligomer mixtures?: Malvern support FAQ. Available: http://www.malvern.com/malvern/kbase.nsf/allfaqbyno/KB001102

[20] H. C. Mahler, R. Muller, W. Friess, A. Delille, and S. Matheus, “Induction and analysis of aggregates in a liquid IgG1-antibody formulation,” Eur J Pharm Biopharm, vol. 59, pp. 407-17, Apr 2005.
[21] M. Kaszuba, D. McKnight, M. T. Connah, F. K. McNeil-Watson, and U. Nobbmann, “Measuring sub nanometre sizes using dynamic light scattering,” J Nanopart Res, vol. 10, pp. 823-829, 2007.
[22] S. Hvidt, “Insulin association in neutral solutions studied by light scattering,” Biophys Chem, vol. 39, pp. 205-13, Feb 1991.
[23] J. S. Bee, J. L. Stevenson, B. Mehta, J. Svitel, J. Pollastrini, R. Platz, E. Freund, J. F. Carpenter, and T. W. Randolph, “Response of a concentrated monoclonal antibody formulation to high shear,” Biotechnol Bioeng, vol. 103, pp. 936-43, Aug 1 2009.

Chapter 4

Mass spectrometric analysis of intact human monoclonal antibody aggregates fractionated by size-exclusion chromatography

Başak Kükrer[1], Vasco Filipe[1,2], Esther van Duijn[3], Piotr Kasper[4], Rob J. Vreeken[4,5], Albert J.R. Heck[3], Wim Jiskoot[1]

[1] Division of Drug Delivery Technology, Leiden/Amsterdam Center for Drug Research, Leiden University, P.O. Box 9502, 2300 RA Leiden, The Netherlands

[2] Department of Pharmaceutics, Utrecht Institute for Pharmaceutical Sciences (UIPS), Utrecht University, P.O. Box 80082, 3508 TB, Utrecht, The Netherlands

[3]Biomolecular Mass Spectrometry and Proteomics Group and Netherlands Proteomics Center, Faculty of Science, Utrecht University, Padualaan 8, 3584 CH Utrecht, The Netherlands

[4]Netherlands Metabolomics Center, Einsteinweg 55, 2333 CC Leiden, The Netherlands

[5]Division of Analytical Biosciences, Leiden/Amsterdam Center for Drug Research, Leiden University, P.O. Box 9502, 2300 RA Leiden, The Netherlands

Pharmaceutical Research, 27(10):2197-2204 (2010)

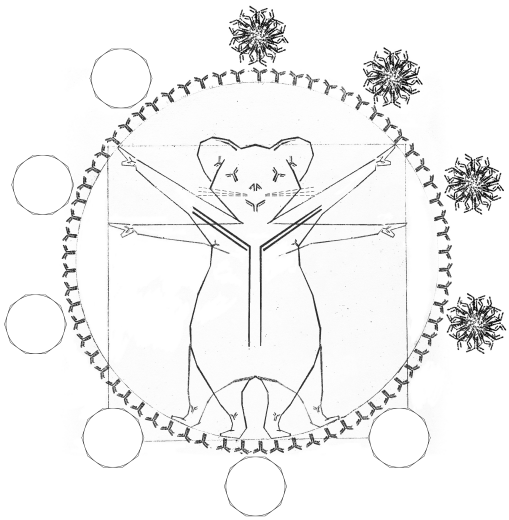

ABSTRACT

Purpose. The aim of this study was to develop a method to characterize intact soluble monoclonal IgG_1 antibody (IgG) oligomers by mass spectrometry.

Materials and methods. IgG aggregates (dimers, trimers, tetramers and high-molecular-weight oligomers) were created by subjecting an IgG formulation to several pH jumps. Protein oligomer fractions were isolated by high performance size exclusion chromatography (HP-SEC), dialyzed against ammonium acetate pH 6.0 (a mass spectrometry-compatible volatile buffer), and analyzed by 'native' electrospray ionization time-of-flight mass spectrometry (ESI-TOF MS).

Results. Monomeric and aggregated IgG fractions in the stressed IgG formulation were successfully isolated by HP-SEC. ESI-TOF MS analysis enabled us to determine the molecular weight of the monomeric IgG as well as the aggregates, including dimers, trimers and tetramers. HP-SEC separation and sample preparation proved to be necessary for good quality signal in ESI-TOF MS. Both the HP-SEC protocol and the ESI-TOF mass spectrometric technique were shown to leave the IgG oligomers largely intact.

Conclusions. ESI-TOF MS is a useful tool complementary to HP-SEC to identify and characterize small oligomeric protein aggregates.

INTRODUCTION

Monoclonal antibodies (mAb), also known as immunoglobulins (Ig), are glycoproteins used as therapeutics for the treatment of several life-threatening conditions including cancer, inflammatory diseases, complications upon organ transplantation, and infectious and cardiovascular diseases [1-3]. Among the five different classes of Ig, IgG is the most abundant one and widely used for therapeutic purposes. The IgG class is further divided into several subclasses — IgG_1, IgG_2, IgG_3, and IgG_4 (in order of relative abundance in human plasma). The structural differences among these subtypes are the number and location of inter-chain disulfide bonds and the length of the hinge region [3].

Like all other protein therapeutics, mAb can undergo various degradation processes during production, storage, transport etc. [4]. Aggregation is a common degradation process for therapeutic proteins and can occur during production, formulation and storage [5], e.g. due to pH changes, temperature variations and agitation [6-8]. Partial unfolding or other types of conformational changes in the protein structure may cause aggregate formation [9-12]. Aggregation of therapeutic proteins is highly undesired since it can lead to activity loss, decreased solubility, and

enhanced unwanted immunogenicity [13-15]. Therefore, there is a great interest in unraveling aggregation pathways and analyzing the quantity and characteristics of protein aggregates.

Aggregation of mAbs due to various types of stress factors has been studied extensively [3, 6-8, 11, 14, 16-18]. Structural characterization of mAb aggregates involves multiple complementary techniques. High performance size-exclusion chromatography (HP-SEC) is commonly used for measuring and separating protein aggregates according to their size [19, 20]. However, for the identification of these separated compounds, other analytical techniques are required [17, 21, 22] Molecular weight determination is a common way in the identification and characterization of oligomeric mAb species. For this purpose sodium dodecyl sulfate/ polyacrylamide gel electrophoresis (SDS-PAGE) and on-line multi-angle laser light scattering detection are accepted techniques, however, both methods suffer from relatively low mass accuracy and precision. These limitations can be overcome by using mass spectrometry (MS), especially electrospray ionization time-of-flight mass spectrometry (ESI-TOF MS), a method that can accurately assign the molecular mass of proteins and aggregates thereof. In specific, "native" ESI-TOF MS is particularly useful for structural characterization of intact protein aggregates due to the ability of preserving quaternary protein structures, maintaining non-covalent protein interactions and its theoretically unlimited mass range [23-25].

Native MS combines the advantages of ESI by replacing the commonly used volatile polar solvents (e.g. water, acetonitrile, methanol etc.) with the MS-compatible volatile aqueous buffer solutions like ammonium acetate [26-29]. With native MS, we are able to determine both the mass of large protein complexes such as ribosomes and whole viruses [30] and the structure, topology and architecture of protein complexes, which cannot be obtained with high-throughput interactomics methods [26, 31]. With native MS we do not obtain detailed molecular structure information (which can still surpass the other tools by its diversity in methodology and applications), however; its sensitivity, speed, selectivity and ability to simultaneously measure several species present in a mixture is clearly advantageous in comparison with traditional structural biology methods such as NMR spectroscopy or X-ray crystallography [26, 32]. Additionally, in combination with more proteomics based MS, i.e., profiling of post-translational modifications, whole pictures of intact biological machineries can be generated.

As in case of many analytical techniques, the quality of the sample is the key for the outcome of the experimental results. Native MS requires typically 100–500

pmol for the sample optimization and multiple analysis. However, sample purity/homogeneity should be high for native MS experiments [23, 25, 27]. Therefore, the method development is essential to answer the particular question.

The coupling of chromatographic separation techniques such as HP-SEC directly to ESI-TOF MS for the analysis of antibody monomers has been previously reported [33]. As for IgG aggregates, Remmele et al. [18] and Van Buren et al. [11] used ESI-MS on IgG dimers that were enzymatically digested after chromatographic separation. However, to our knowledge, we are the first group combining HP-SEC with native MS for the detection of intact monoclonal antibody aggregates. In this paper, we present a protocol to identify intact IgG oligomers (dimers, trimers, and tetramers), induced by pH stress on a monomeric monoclonal IgG_1 (IgG), using native ESI-TOF MS. We analyzed and fractionated the aggregates by HP-SEC, dialyzed the isolated fractions to aqueous ammonium acetate and then analyzed them by ESI-TOF MS. We demonstrate that native ESI-TOF MS makes it possible to characterize IgG dimers, trimers and tetramers.

MATERIALS AND METHODS

Protein and other materials

A monoclonal human antibody of the IgG_1 subclass (IgG), kindly provided by Biogen (Cambridge, MA USA), was formulated at 65 mg/ml in 10 mM sodium citrate buffer containing 5% sucrose, pH 6.0. It was diluted in a similar formulation buffer containing 10 mM sodium citrate with 5% sucrose, pH 6.0. 150 mM ammonium acetate (puriss p.a., for mass spectrometry, Fluka, Sigma-Aldrich Steinheim, Germany) was used as the buffer solution for mass spectrometric analysis. The formulations were filtered using 0.22 µm PES (polyethersulfone) low binding syringe driven filter units (Millex™ GP, Millipore, Ireland).

Sodium citrate dihydrate and glycine were from Merck (Merck KGaA, Darmstadt, Germany), NaH_2PO_4 dihydrate, Na_2HPO_4 dihydrate, tris(hydroxymethyl)aminomethane (Tris), β-mercaptoethanol and hydrochloric acid (HCl) were from Sigma (Sigma, Sigma-Aldrich Steinheim, Germany), sodium hydroxide from Boom (Boom BV. Meppel, The Netherlands), glycerol and sodium dodecyl sulfate (SDS) from Merck (Merck Darmstadt and Merck, Hohenbrunn, Germany), cesium iodide and sodium azide from Fluka (Fluka, Sigma-Aldrich Steinheim, Germany), bromophenol blue from Bio-Rad (Bio-Rad Hercules, USA) and 5% polyacrylamide tris-HCl ready gel, pre-

stained broad range molecular weight markers, silver stain kit from Bio-Rad (Bio-Rad Veenendaal, The Netherlands).

Amicon 10 kDa molecular-weight cut-off filters were purchased from Millipore (Millipore SA, Molsheim, France). Deionized water was obtained from a MilliQ water purification system (Millipore, USA).

Preparation of Protein Aggregates

The sample under investigation was prepared by diluting the monoclonal antibody formulation with the 10 mM sodium citrate buffer, pH 6.0 to a final concentration of 1 mg/ml IgG. To apply the pH stress, 1 M HCl was slowly added drop wise with a pipette to the antibody solution to change the pH from 6.0 to 1.0. Then, 1 M NaOH was added to adjust the pH to 10.0. Finally, 1 M HCl was added again to adjust the pH back to 6.0. There was approximately 1 minute waiting time between the pH shifts, while constant stirring at 500 rpm. No precipitation was observed after the pH stress treatments.

High performance size exclusion chromatography (HP-SEC)

Unstressed and pH-stressed samples were analyzed with HP-SEC for the detection and separation of IgG oligomers. For this purpose, we used a TSK Gel 3000 SWXL column (300x7.8 mm, 5.0 µm particle size) with a TSK Gel 3000 pre-column (TOSOH Bioscience, Stuttgart, Germany) combined with a Thermo UV detector and a Gilson 234 Autoinjector. The separation was performed at a flow rate of 0.5 mL/min and 300 µL of sample was injected. The elution buffer was composed of 100 mM sodium phosphate, 100 mM sodium sulfate, 0.05% (w/v) sodium azide at pH 7.2. The elution buffer was freshly prepared, filtered and degassed prior to use. Elution was monitored by UV detection (280 nm). Monomer, dimer, trimer/tetramer and high molecular weight oligomer fractions were collected in separate vials after UV detection.

Native mass spectrometry

All samples were dialyzed against 150 mM ammonium acetate at pH 6.0 using 10-kDa molecular-weight cut-off Slide-A-Lyzer dialysis cassettes (Thermo Fisher Scientific, Pierce Biotechnology, Rockford, USA). The dimer and trimer/tetramer

solutions were further washed with 150 mM ammonium acetate buffer solution pH 6.0, using Amicon ultracentrifuge filters (10 kDa) prior to MS analysis. The sample was centrifuged at 14.000 x g for 15 min at 4°C. The same devices were used to finally concentrate the protein to about 5 mg/ml.

The obtained protein samples were measured with a modified Waters Micromass nano-ESI-TOF MS (positive ion mode). Needles were made from borosilicate glass capillaries (Kwik-Fil, World Precision Instruments, USA) on a P-97 puller (Sutter Instruments, USA), coated with a thin gold layer by using an Edwards Scancoat six Pirani 501 sputter coater (Edwards Laboratories, USA). To produce intact gas phase ions the source was operated at an elevated pressure (~7 mbar). The created droplet size is 1 micron. The typical spray concentrations of the proteins are 5 micromoles with 2 microliters. Mass spectra were recorded with a capillary voltage of 1.2 kV and a cone voltage of 150 V. The pressure in the time-of-flight was 2.7 10^{-6} mbar. All spectra were calibrated using 25 mg/ml cesium iodide solution. Further details can be found elsewhere [34].

SDS-PAGE

Approximately 24 μg of unstressed and pH-stressed IgG and about 3 μg of dimer (fraction 2) and high-molecular-weight oligomers (fraction 4) collected from HP-SEC were mixed with non-reducing denaturing sample buffer at a 1:4 volume ratio in 0.5 ml reaction vials (Eppendorf, Hamburg, Germany). The non-reducing sample buffer contained 0.06 M tris(hydroxymethyl)aminomethane (Tris), 25% (v/v) glycerol, 2% (w/v) sodium dodecyl sulfate (SDS) and 0.1% (w/v) bromophenol blue. The samples were treated for 2 minutes at 98°C in an Eppendorf Thermomixer Confort (Hamburg, Germany) and loaded in a 5% polyacrylamide tris-HCl ready gel, alongside with pre-stained broad range molecular weight markers.

Gel electrophoresis was performed in a Bio-Rad Mini-PROTEAN 3 cell equipped with a Bio-Rad PowerPac 300 power supply (Bio-Rad, Veenendaal, The Netherlands). The electrophoresis buffer containing 0.3% (w/v) Tris, 1.44 % (w/v) glycine and 0.1% SDS, pH 8.3. Separation was performed at a constant current of 100 V and at maximally 50 mA for about 1 hour. The gel was stained using the Bio-Rad silver stain kit.

RESULTS AND DISCUSSION

HP-SEC ANALYSIS OF IgG OLIGOMERS

IgG aggregates were prepared according to the procedure described in the Materials and Methods section. We initially compared unstressed IgG and pH-stressed IgG in formulation buffer (citrate buffer) with HP-SEC. As can be seen from the chromatograms in Fig. 4.1, it is evident that an applied pH stress on an IgG sample results in the formation of number of additional peaks that are attributed to soluble IgG aggregates. The unstressed IgG was predominantly monomeric (peak at 17.7 min), with a minor peak at 14.8 min (Fig. 4.1, red line), whereas pH-stressed IgG was shown to contain substantial amounts of soluble aggregates (Fig. 4.1, black line), having distinct peaks at 15.1, and 14.0, 13.2 and 12.1 min. Presumably these peaks belong to the dimer, trimer, tetramer and high-molecular-weight (HMW) oligomers of IgG, respectively. The observed slight shifts in retention times of unstressed and pH-stressed IgG monomers and dimers are indicative of different interactions with the column material, perhaps due to partial unfolding and increased hydrophobicity of these species.

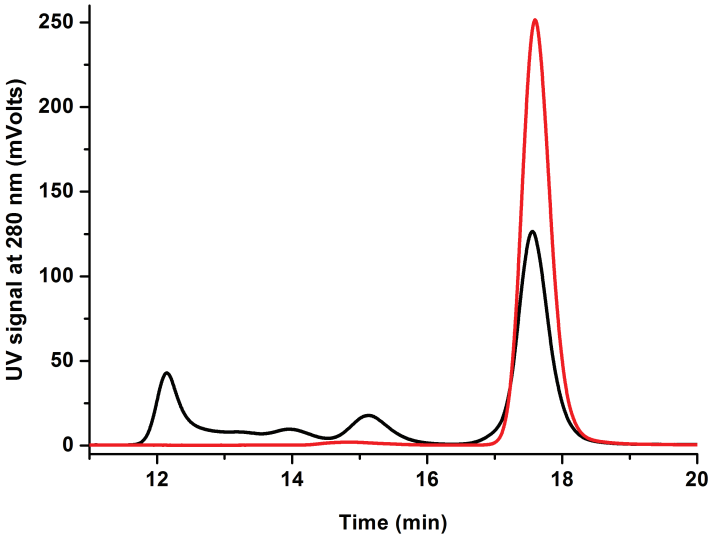

Figure 4.1: Size-exclusion chromatograms of unstressed IgG (red) vs. pH-stressed IgG (black) in 10 mM citrate buffer pH 6.0.

Mass spectrometric analysis of IgG oligomers

While HP-SEC is ideal for initial screening of IgG oligomers, MS is far more suitable for accurate molecular weight determinations. ESI-MS produces multiply charged protein ions, resulting in a charge state distribution in the spectrum. From this distribution the molecular weight of the protein can be determined using computer algorithms for the deconvolution of the charge envelope. However, ESI-MS sets stringent constraints on the sample buffer. Most buffer solutions used in structural biology and pharmaceutical formulations are not compatible with ESI-MS. The sample solution for ESI-MS needs to be free of any interfering charged species, such as salts and metal ions, as they may obstruct the protein ionization process [27, 35]. For this purpose, aqueous ammonium acetate solution has been introduced previously as an ESI-MS–compatible 'volatile buffer'. This volatile buffer easily desolvates, evaporation of solvents leading to the formation of gas-phased ions of protein molecules, and in the meantime the original quaternary structure of the protein is usually preserved [26, 27].

Among many other approaches to identify the proteins by MS, we have followed a "top-down" method for the identification of intact protein aggregates [36]. In this approach, the protein sample, dissolved in aqueous ammonium acetate buffer, is directly injected to ESI-TOF MS instrument without any chemical or enzymatic treatment. This results in a molecular mass of the intact protein and/or protein aggregates and their major post-translational modifications.

Fig. 4.2 shows the mass spectra of unstressed IgG (top) and pH-stressed IgG (bottom). These spectra represent characteristic charge envelopes belonging to the protein species. Peaks distributed between m/z 5000 to 7000 represent the different charged states of monomeric IgG, both in unstressed and pH-stressed samples. At first glance the spectra are very similar. Detailed analysis however shows that the spectrum of unstressed IgG contains 99.8% monomer and 0.2% dimer (top panel, zoomed inset), whereas that of pH-stressed IgG shows 90.1% monomer, 9.5% dimer, and 0.4% trimer (Fig. 4.2, lower panel, zoomed inset). These percentages were calculated using the peak intensities of the entire charge state distribution for all species present.

Mass spectrometric analysis of HP-SEC fractions

As can be seen in previous section, the monomer signal is very abundant in pH-

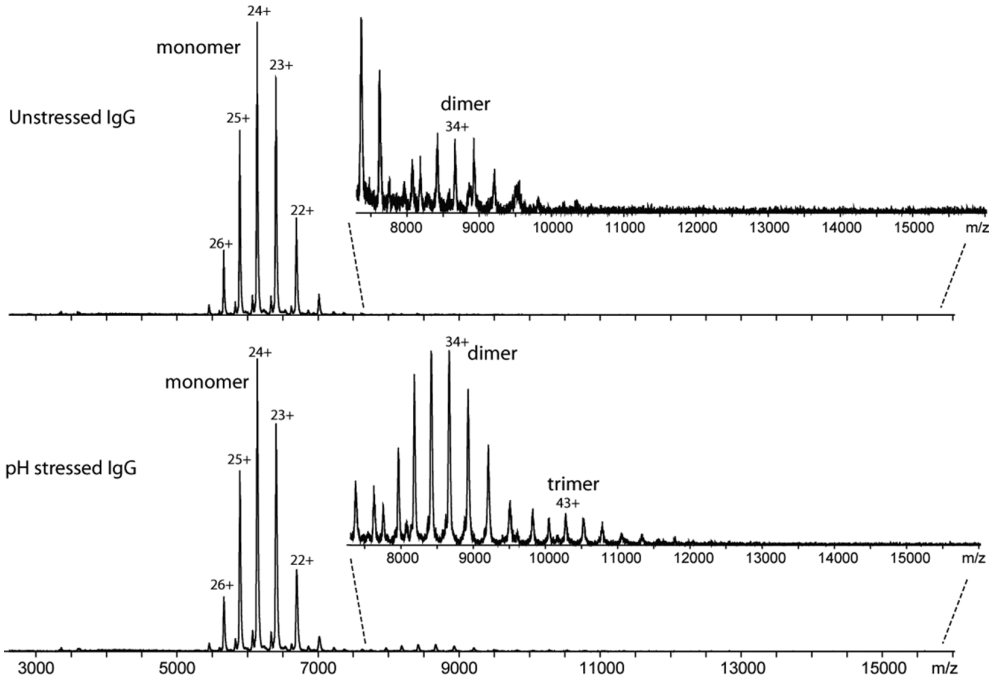

Figure 4.2: ESI-TOF MS spectra of unstressed (top) and pH-stressed (bottom) IgG solutions, without HP-SEC separation. Samples are in 150 mM ammonium acetate buffer pH 6.0.

stressed IgG solution and it suppresses the MS signals deriving from the other (higher oligomer) species in the solution. However, HP-SEC clearly showed the existence of other species. Therefore, chromatographic separation and purification of the individual fractions was performed. In this way, we can isolate and individually study the structural information and possible conformational variants within the dimers, trimers, and other oligomers.

HP-SEC was used to isolate the monomer, dimer, trimer/tetramer and HMW oligomer fractions of the stressed IgG mixture. The stability and purity of these fractions were tested by re-analyzing them with the same HP-SEC method (Fig. 4.3). Clearly, isolation of the individual species was successful: four fractions presumably corresponding to monomer, dimer, trimer/tetramer and HMW oligomers were obtained. The trimer and tetramer species were collected simultaneously because of the difficulty in separating the two species with this HP-SEC column. In addition, the results show that the separated products are largely irreversible as analysis of the individual fractions hardly shows other oligomeric forms or monomeric IgG in their respective chromatograms (Fig. 4.3).

Unfortunately mobile phases containing volatile salts, tested for HP-SEC coupled

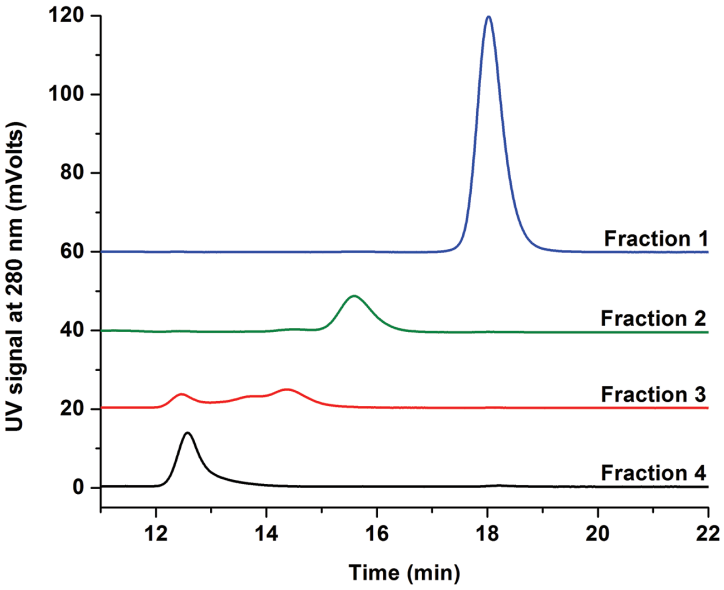

Figure 4.3: Size-exclusion chromatograms of collected fractions of pH-stressed IgG; HMW: High-molecular-weight aggregates (black), trimers/tetramers (red), dimers (green) and monomer (blue). Spectra are not normalized.

with MS analysis of a recombinant IgG product were shown to be poor in terms of chromatographic separation and mass spectrometric performance [36]. Similarly, prior to MS analysis, we dialyzed the oligomer fractions isolated by HP-SEC against an aqueous ammonium acetate solution as in case of non-fractioned samples. Re-analysis of the dialyzed samples by HP-SEC indicated that the oligomeric state of the different fractions was not measurably affected (data not shown).

Fig. 4.4 shows the deconvoluted MS spectra of the HP-SEC fractions containing intact IgG monomer, dimers and trimers/tetramers. Deconvolution of their charge envelopes resulted in mass values of 147,339 ± 101 Da for the monomer, 294,709 ± 93 Da for the dimer, 441,950 ± 313 Da for the trimer and 589,745 ±228 Da for the tetramer. We were not able to obtain good signals for fraction 4.

In Fig. 4.5, we compare the relative abundances of the species in each fraction. In addition to the expected oligomeric state, other species were detected as well. There was a trace amount of dimer (0.5%) present in the monomer fraction, whereas the MS spectrum of the dimer fraction showed ~ 15% monomer and 2% trimer. The spectrum of the trimer/tetramer fraction consisted of 57% trimer, 17% tetramer, 13% dimer and 13% monomer IgG.

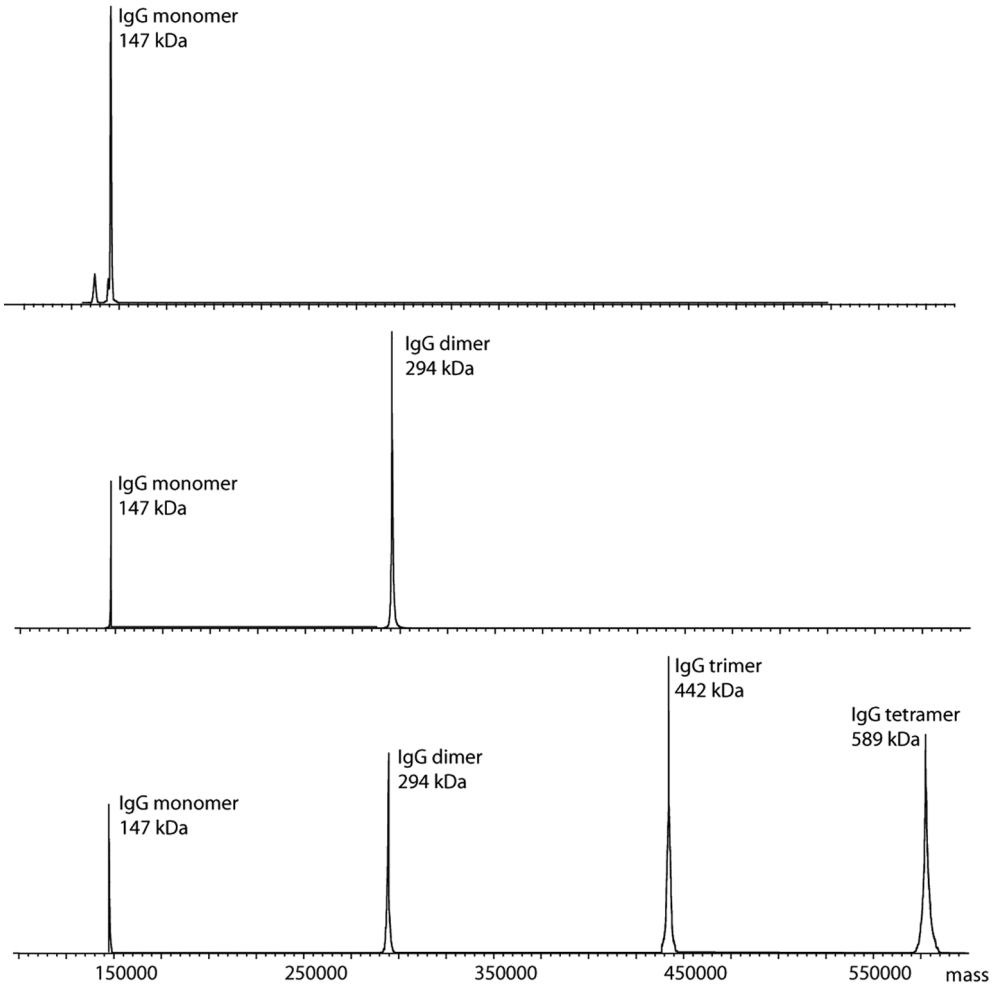

Figure 4.4: ESI-TOF MS of pH-stressed IgG fractions. Spectra are belonging to HP-SEC fractions 1 (top), fraction 2 (middle), and fraction 3 (bottom). The corresponding approximate molecular weights are depicted next to the peaks.

SDS-PAGE

SDS-PAGE is a well-established technique to investigate whether the aggregates formed were composed of covalently and/or non-covalently linked species [4, 38].

In the literature, the simultaneous formation of covalent and non-covalent dimers has been reported for different IgG mAbs [18, 39-41]. In addition, it has been observed that some short term stressed non-covalent antibody dimers can

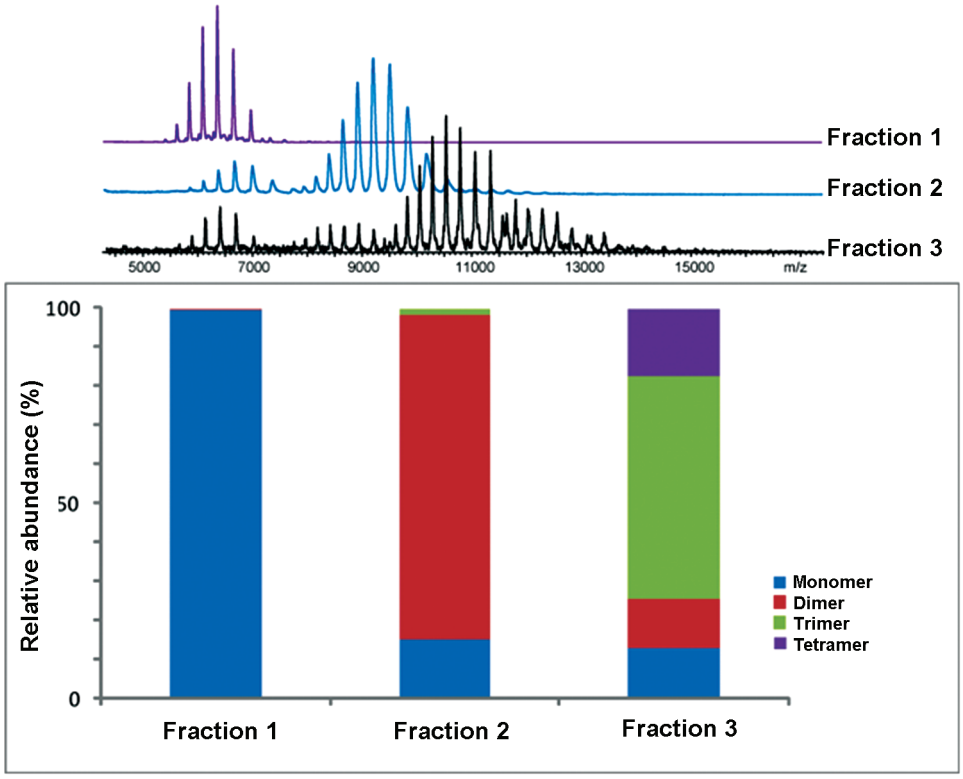

Figure 4.5: Bars representing the summed intensities for all IgG species observed in each fraction. For illustration, the raw MS spectra used to calculate the relative abundances are depicted above.

irreversibly convert into covalent dimers [18, 42]. The amount of non-covalent and covalent dimers formed by several IgG species depended on IgG type, solution conditions, and temperature [11].

We performed non-reducing and reducing SDS-PAGE on the unstressed IgG, the pH-stressed IgG, isolated fraction 2 and fraction 4, as depicted in Fig. 4.6. Given that the amount of dimer was less abundant compared to monomer in both unstressed and pH-stressed IgG according to HP-SEC, an excessive amount of these samples was loaded in the slots of the gel in order to detect these dimers. This resulted in over exposure of the monomer band at ~150 kDa in lanes 2 and 3 (Fig. 4.6), while the dimer bands were visible at ~300 kDa. In fact, the dimer bands under non-reducing conditions are rather similar in intensity between these two samples, which indicates that the majority of dimers were non-covalently linked. This was confirmed by SDS-PAGE analysis of the dimer fraction (Fig. 4.6, lane 4), where most of the dimers collected by HP-SEC fractionation had dissociated into monomers under

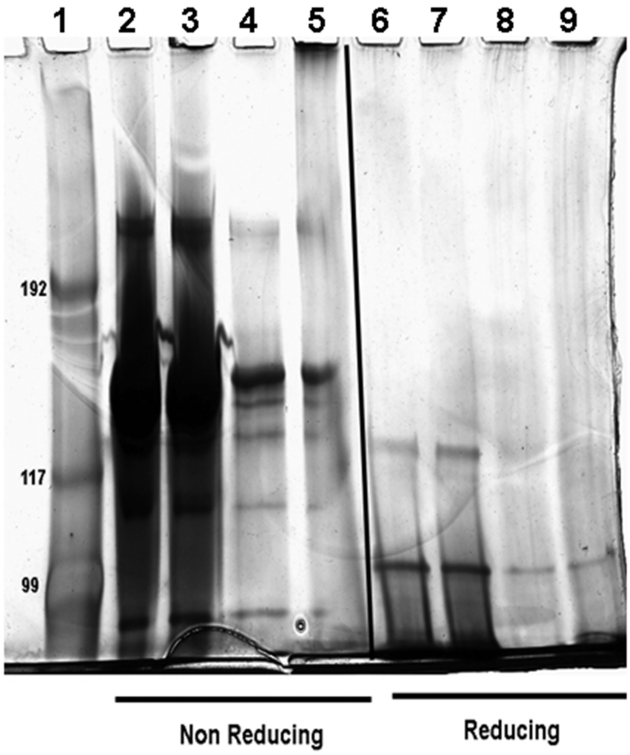

Figure 4.6: Silver-stained non-reduced and reduced SDS-PAGE gel. Lanes belong to standards (1), unstressed IgG (2 for non-reduced, 6 for reduced), pH-stressed IgG (3 for non-reduced, 7 for reduced), HP-SEC fraction 2 (4 for non-reduced, 8 for reduced) and HP-SEC fraction 4 (5 for non-reduced, 9 for reduced) of pH-stressed IgG (see Figure 3 for HP-SEC profiles of the fractions).

denaturing conditions. For the HMW oligomer fraction 4, a band can be observed at the top of lane 5 and another one at ~150 kDa, which means that this fraction contained both covalent and non-covalent oligomers. The reducing part of the gel showed the disappearance of the bands due to IgG aggregates under reducing condition, indicating that all the covalent disulfide bridges are broken effectively (Fig. 4.6, lanes 6-9). Nevertheless, the pH-stressed IgG dimers were strong enough to remain intact during HP-SEC analysis, dialysis, and subsequent ESI-TOF MS analysis.

CONCLUSION

In this paper, we have combined chromatographic separation of protein oligomers with intact protein characterization by “native” ESI-TOF MS. We have described a HP-SEC/buffer exchange protocol that enables “native” ESI-TOF MS analysis of

pH-stressed IgG samples. We have shown that proper sample preparation and chromatographic separation of monomer, dimer and trimer/tetramer fractions by HP-SEC have resulted in improved MS analysis, as compared to MS analysis prior to HP-SEC separation. Both the sample preparation and the native ESI-TOF MS technique leave the aggregates intact. In conclusion, ESI-TOF MS is a useful method that adds to our current analytical arsenal to identify and characterize mAb oligomers.

ACKNOWLEDGEMENTS

This research was supported by the Technology Foundation STW, the applied science division of NWO and technology program of the Dutch Ministry of Economic Affairs. A VENI grant was awarded to E van Duijn by the Netherlands Organization for Scientific Research (NWO) (VENI 700.58.402). We thank The Netherlands Proteomics Center for financial support.

REFERENCES

[1] P. J. Carter, "Potent antibody therapeutics by design," Nat. Rev. Immunol., vol. 6, pp. 343-357, 2006.
[2] D. Schrama, R. A. Reisfeld, and J. C. Becker, "Antibody targeted drugs as cancer therapeutics," Nat. Rev. Drug Discov., vol. 5, pp. 147-159, 2006.
[3] W. Wang, S. Singh, D. L. Zeng, K. King, and S. Nema, "Antibody structure, instability, and formulation " J. Pharm. Sci., vol. 96, pp. 1-26, 2007.
[4] M. E. M. Cromwell, E. Hilario, and F. Jacobson, "Protein aggregation and bioprocessing," AAPS Journal, vol. 8, pp. E572-579, 2006.
[5] H.-C. Mahler, W. Friess, U. Grauschopf, and S. Kiese, "Protein aggregation: pathways, induction factors and analysis," J. Pharm. Sci., vol. 98, pp. 2909-2934, 2009.
[6] A. W. Vermeer and W. Norde, "The thermal stability of immunoglobulin: Unfolding and aggregation of a multi-domain protein.," Biophys. J. , vol. 78, pp. 394-404, 2000.
[7] D. Ejima, K. Tsumoto, H. Fukada, R. Yumioka, K. Nagase, T. Arakawa, and J. S. Philo, "Effects of acid exposure on the conformation, stability, and aggregation of monoclonal antibodies," Proteins, vol. 66, pp. 954-962, 2007.
[8] W. Jiskoot, M. Bloemendal, B. v. Haeringen, R. v. Grondelle, E. C. Beuvery, J. N. Herron, and D. J. Crommelin, "Non-random conformation of a mouse IgG2a monoclonal antibody at low pH," Eur. J. Biochem. , vol. 201, pp. 223-232, 1991.
[9] R. Jaenicke, "Protein folding: Local structures, domains, subunits, and assemblies," Biochem., vol. 30, pp. 3147-3161, 1991.
[10] Y.-S. Kim, J. S. Wall, J. Meyer, C. Murphy, T. W. Randolph, M. C. Manning, and J. F. Carpenter, "Thermodynamic modulation of light chain amyloid fibril formation," J. Biol. Chem., vol. 276, pp. 1570-1574, 2000.
[11] N. v. Buren, D. Rehder, H. Gadgil, M. Matsamura, and J. Jacob, "Elucidation of two major aggregation pathways in an IgG2 antibody," J. Pharm. Sci., vol. 98, pp. 3013-3030, 2009.

[12] R. M. Fesinmeyer, S. Hogan, A. Saluja, S. R. Brych, E. Kras, L. O. Narhi, D. N. Brems, and Y. R. Gokarn, "Effects of ions on agitation and temperature induced aggregation reactions of antibodies," Pharma. Res., vol. 26, pp. 903-913, 2009.
[13] A. S. Rosenberg, "Effects of protein aggregates: an immunologic perspective," AAPS J., vol. 8, pp. 501-507, 2006.
[14] S. Hermeling, D. J. A. Crommelin, H. Schellekens, and W. Jiskoot, "Structure-immunogenicity relationships of therapeutic proteins," Pharm. Res., vol. 21, pp. 897-903, 2004.
[15] E. Y. Chi, S. Krishnan, T. W. Randolph, and J. F. Carpenter, "Physical stability of proteins in aqueous solution: Mechanism and driving forces in nonnative protein aggregation," Pharm. Res. , vol. 20, pp. 1325-1336, 2003.
[16] T. Jøssang, J. Feder, and E. Rosenqvist, "Heat aggregation kinetics of human IgG," J. Chem. Phys. , vol. 82, pp. 574-589, 1985.
[17] H.-C. Mahler, R. Muller, W. Frieß, A. Delille, and S. Matheus, "Induction and analysis of aggregates in a liquid IgG_1-antibody formulation," Eur. J. Pharm. Biopharm., vol. 59, pp. 407-417, 2005.
[18] R. L. Remmele JR., W. J. Callahan, S. Krisnanh, L. Zhou, P. V. Bondarenko, A. C. Nichols, G. R. Kleemann, G. D. Pipes, S. Park, S. Fodor, E. Kras, and D. N. Brems, "Active dimer of epratuzumab provides insight into the complex nature of an antibody aggregate," J. Pharm. Sci., vol. 95, pp. 126-145, 2006.
[19] C. B. Andersen, M. Manno, C. Rischel, M. Thorolfsson, and V. Martorana, "Aggregation of a multidomain protein: a coagulation mechanism governs aggregation of a model IgG1 antibody under weak thermal stress," Prot. Science, vol. 19, pp. 279-290, 2010.
[20] T. Arakawa, D. Ejima, T. Li, and J. S. Philo, "The critical role of mobile phase composition in size exclusion chromatography of protein pharmaceuticals," J. Pharm. Sci., vol. 99, pp. 1674-1692, 2009.
[21] A. Hawe, J. C. Kasper, W. Friess, and W. Jiskoot, "Structural properties of monoclonal antibody aggregates induced by freeze–thawing and thermal stress," European J. Pharma. Scien. , vol. 38, pp. 79-87, 2009.
[22] J. F. Carpenter, T. W. Randolph, W. Jiskoot, D. J. A. Crommelin, C. R. Middaugh, and G. Winter, "Potential inaccurate quantitation and sizing of protein aggregates by size exclusion chromatography: essential need to use orthogonal methods to assure the quality of therapeutic protein products," J. Pharm. Sci., vol. 99, pp. 2200-2208, 2010.
[23] E. v. Duijn, "Current limitations in native mass spectrometry based structural biology," J Am Soc Mass Spectrom, vol. 21, pp. 971-978, 2010.
[24] R. H. H. v. d. Heuvel, E. v. Duijn, H. Mazon, S. A. Synowsky, K. Lorenzen, C. Versluis, S. J. J. Brouns, D. Langridge, J. v. d. Oost, J. Hoyes, and A. J. R. Heck, "Improving the performance of a quadrupole Time-of-Flight instrument for macromolecular mass spectrometry," Anal Chem., vol. 78, pp. 7473-7483, 2006.
[25] K. Lorenzen, A. Vannini, P. Cramer, and A. J. R. Heck, "Structural biology of RNA polymerase III: mass spectrometry elucidates subcomplex architecture," Structure, vol. 15, pp. 1237-1245, 2007.
[26] A. J. R. Heck, "Native mass spectrometry: a bridge between interactomics and structural biology," Nat. Methods, vol. 5, pp. 927-933, 2008.
[27] H. Hernandez and C. V. Robinson, "Determining the stoichiometry and interactions of macromolecular assemblies from mass spectrometry," Nat. Protoc., vol. 2, pp. 715-726, 2007.
[28] A. R. McKay, B. T. Ruotolo, L. L. Ilag, and C. V. Robinson, "Mass measurements of increased accuracy resolve heterogeneous populations of intact ribosomes," J. Am. Chem. Soc. , vol. 128, pp. 11433-11442, 2006.
[29] E. W. Chung, D. A. Henriques, D. Renzoni, C. J. Morton, T. D. Mulhern, M. C. Pitkeathly, J. E. Ladbury, and C. V. Robinson, "Probing the nature of interactions in SH2 binding interfaces—Evidence from electrospray ionization mass spectrometry," Protein Sci., vol. 8, pp. 1962-1970, 1999.

[30] C. Uetrecht, R. J. Rose, E. v. Duijn, K. Lorenzen, and A. J. R. Heck, “Ion mobility mass spectrometry of proteins and protein assemblies,” Chem Soc Rev, vol. 39, pp. 1633-1655, 2010.
[31] R. H. v. d. Heuvel and A. J. R. Heck, “Native protein mass spectrometry: from intact oligomers to functional machineries,” Curr. Opin. Chem. Biol. , vol. 8, pp. 519-526, 2004.
[32] M. Oda, S. Uchiyama, M. Noda, Y. Nishi, M. Koga, K. Mayanagi, C. V. Robinson, K. Fukui, Y. Kobayashi, K. Morikawa, and T. Azuma, “Effects of antibody affinity and antigen valence on molecular forms of immune complexes,” Mol. Immun., vol. 47, pp. 357-364, 2009.
[33] L. J. Brady, J. Valliere-Douglass, T. Martinez, and A. Balland, “Molecular mass analysis of antibodies by on-line SEC-MS,” J. Am. Soc. Mass Spectrom., vol. 19, pp. 502-509, 2008.
[34] Van Duijn E, Bakkes PJ, Heeren RMA, Van den Heuvel RH, Van Heerikhuizen H, Van der Vies SM, et al. Monitoring macromolecular complexes involved in the chaperonin-assisted protein folding cycle by mass spectrometry. Nat Methods. ;2:371–6, 2005.
[35] T. Koschubs, K. Lorenzen, S. Baumli, S. Sandstrom, A. J. R. Heck, and P. Cramer, “Preparation and topology of the Mediator middle module,” Nuc. Acids Res., p. in press., 2010.
[36] Z. Zhang, H. Pan, and X. Chen, “Mass spectrometry for structural characterization of therapeutic proteins,” Mass Spec. Rev., vol. 28, pp. 147- 176, 2009.
[37] A. C. Lazar, L. Wang, W. A. Blattler, G. Amphlett, J. M. Lambert, and W. Zhang, “Analysis of the composition of immunoconjugates using size-exclusion chromatography coupled to mass spectrometry,” Rapid Commun. Mass Spectrom. , vol. 19, pp. 1806-1814, 2005.
[38] J. T. Ribarska, S. T. Jolevska, A. P. Panovska, and A. Dimitrovska, “Studying the formation of aggregates in recombinant human granulocyte-colony stimulating factor (rHuG-CSF), lenograstim, using size-exclusion chromatography and SDS-PAGE. ,” Acta Pharm., vol. 58, pp. 199-206, 2008.
[39] M. Paborji, N. L. Pochopin, W. P. Coppola, and J. B. Bogardus, “Chemical and physical stability of chimeric L6, a mouse-human monoclonal antibody,” Pharm. Res., vol. 11, pp. 764-771, 1994.
[40] J. M. Moore, T. W. Patapoff, and M. E. Cromwell, “Kinetics and thermodynamics of dimer formation and dissociation for a recombinant humanized monoclonal antibody to vascular endothelial growth factor,” Biochem., vol. 38, pp. 13960-13967, 1999.
[41] E. M. Yoo, L. A. Wims, L. A. Chan, and S. L. Morrison, “Human IgG2 can form covalent dimers,” J. Immunol., vol. 170, pp. 3134-3138, 2003.
[42] D. L. Tankersley, M. S. Preston, and J. S. Finlayson, “Immunoglobulin G dimer: An idiotype-antiidiotype complex,” Mol. Immunol., vol. 25, pp. 41-48, 1988.

Chapter 5

Transient molten globules and metastable aggregates induced by brief exposure of a monoclonal IgG to low pH

Vasco Filipe[1,2], Başak Kükrer[1], Andrea Hawe[1], Wim Jiskoot[1]

[1] Division of Drug Delivery Technology, Leiden/Amsterdam Center for Drug Research, Leiden University, P.O. Box 9502, 2300 RA Leiden, The Netherlands

[2] Department of Pharmaceutics, Utrecht Institute for Pharmaceutical Sciences (UIPS), Utrecht University, P.O. Box 80082, 3508 TB, Utrecht, The Netherlands

Accepted at Journal of Pharmaceutical Sciences. DOI: 10.1002/jps.23157 (2012)

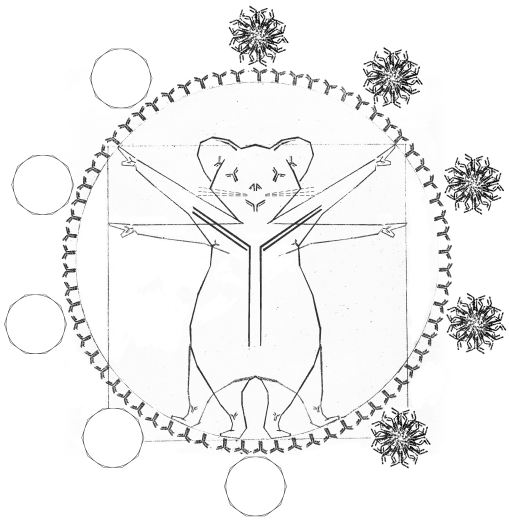

ABSTRACT

The presence of aggregates in therapeutic protein formulations is of great concern due to quality, safety and efficacy issues. Nonetheless, the mechanisms and kinetics of protein aggregation are only partly understood. In this study, metastable IgG aggregates induced by a brief exposure to pH 1, were kept at 4 °C and analyzed over time by size exclusion chromatography (SEC), nanoparticle tracking analysis, light obscuration, dynamic light scattering, fluorescence spectroscopy and circular dichroism.

The results show the formation of polydisperse aggregates (from dimers to 10-μm particles) shortly after the pH-shift stress. These aggregates increased in size and number over time until a pseudo-equilibrium was reached after 5-7 days. The presence of transient, partially unfolded monomers (molten globules) was detected by SEC with online fluorescent dye detection. The molten globules seemed to either refold into the native state or become involved in aggregation pathways. Seeding pH-shift induced aggregates into unstressed IgG did not accelerate aggregation during incubation for 3 weeks at 55 °C.

These results reinforce the role of partially unfolded species in the aggregation of therapeutic proteins. We conclude that the formation of pH-shift induced IgG aggregates is likely driven by downhill polymerization, as a consequence of successive additions of molten globular monomers.

INTRODUCTION

Monoclonal antibodies (mAb) have become invaluable in treating a wide range of diseases and are currently the fastest growing drug category [1, 2]. Similar to other protein-based pharmaceuticals, one of the main challenges of developing therapeutic mAbs is their propensity to aggregate during manufacturing, storage and administration [3, 4]. Protein aggregates have been indicated as one of the main causes for loss of therapeutic activity and adverse immune reactions [5]. Therefore, the presence of protein aggregates in biopharmaceutical products has become a main concern for the pharmaceutical industry and regulatory agencies. Preventing and monitoring the formation of aggregates has become a major effort during the development of these products [6].

The characterization of aggregated protein formulations may include parameters such as the size distribution, percentage of aggregates, particle counts, secondary and tertiary structure, as well as reversibility [7, 8]. It is well accepted that protein aggregates can be in an equilibrium state with monomers and/or aggregate

precursors [9]. Such an equilibrium may be disturbed by a wide set of variables such as temperature, pH, surface interactions, buffer type and protein concentration [10, 11]. Consequently, the characterization of protein aggregates is complex and requires a combination of different analytical techniques [12, 13].

Protein aggregation pathways are only partly understood and may vary according to the type of protein, formulation composition and stress factor [14]. Non-native aggregation pathways have been pointed out as the most naturally occurring aggregation mechanisms of several therapeutic proteins, including mAbs [9]. In these pathways, monomers with secondary or tertiary structures different from the native state act as intermediates in the aggregation process.

Proteins are flexible molecules that naturally oscillate between the lowest free energy conformational state (native state) and other thermodynamically metastable higher energy states, such as the molten globule [15, 16]. Molten globules conserve a native-like secondary structure but have significantly different tertiary structures, as a result of hydrophobic collapses [17]. These relatively short-lived transitional states may fold back into the native state or initiate a non-native aggregation process [18, 19]. A number of studies have shown that incubation at low pH induces the formation of molten globule-like structures [20-22].

Several kinetic models have been proposed to describe non-native aggregation pathways. In condensation models, two multimers of certain sizes can associate to form a larger aggregate without requiring a sequential addition of monomeric subunits [23]. In nucleated polymerization models, the aggregation process is thermodynamically unfavorable until a certain oligomerization number has been reached. Oligomers that reach this critical size start acting as clusters or “seeds” for other proteins to bind in a thermodynamically favorable way. According to this mechanism, the rate of aggregation can be accelerated by the addition of these seeds to the solution, which effectively bypasses the nucleation step [24]. Downhill polymerization models state that the thermodynamically unfavorable step is the monomer to dimer conversion. Once this step is overcome, the aggregation process becomes favorable and occurs by consecutive addition of monomers [25]. Recent studies report that a single mAb (IgG_1) may follow different non-native aggregation mechanisms, according to the pH of the solution [26].

Exposure of mAbs to low pH is often unavoidable during downstream processing, e.g. during chromatographic steps and viral clearance processes. Hence, it is important to understand the impact of short exposures to low pH on mAb aggregation. In the present work, a mAb of the IgG_1 subclass (IgG) was very briefly exposed to a

low pH and the consequent aggregation after neutralization was monitored over time by a set of analytical techniques. Size exclusion chromatography (SEC) equipped with UV and multiple angle light scattering (MALLS) detection, nanoparticle tracking analysis (NTA), light obscuration (LO) and dynamic light scattering (DLS) were used to provide information about the size distribution as well as the concentration of formed aggregates. Far-UV and near-UV circular dichroism (CD), steady-state fluorescence spectroscopy and SEC equipped with a fluorescence detector, in conjugation with 4,4'-dianilino-1,1'-binaphthyl-5,5'-disulfonic acid dipotassium salt (bis-ANS) as an extrinsic dye, were used to provide structural information about the aggregates and monomers.

This work aims to study how IgG monomers and aggregates evolve after a brief exposure to low pH by using a wide range of complementary analytical techniques. We show that molten globules are a key element for the aggregation process inherent to this type of stress and we speculate about the aggregation mechanisms involved in this process.

MATERIALS AND METHODS

Materials

A recombinant human monoclonal antibody of the IgG_1 subclass (IgG) was used at a concentration of 1 mg/ml. The formulation buffer contained 10 mM sodium citrate (Merck, Darmstadt, Germany), 5% (w/v) sucrose (Sigma-Aldrich, Buchs, Switzerland), pH 6.0. The buffer was filtered using a 0.22-μm PES low binding syringe-driven filter unit (Millex™ GP, Millipore, Ireland) prior to use.

NaH_2PO4 dihydrate, Na_2HPO_4 dihydrate, sodium azide, guanidine hydrochloride (GuHCl) and hydrochloric acid (HCl) were purchased from Sigma-Aldrich, sodium hydroxide (NaOH) from Boom BV (Meppel, The Netherlands) and the fluorescent dye 4,4'-dianilino-1,1'-binaphthyl-5,5'-disulfonic acid dipotassium salt (bis-ANS) from Fluka (Zwijndrecht, The Netherlands).

Aggregation procedure

The pH-shift stress consisted of changing the buffer pH from pH 6.0 to pH 1.0 and back to pH 6.0 at room temperature. Hydrochloric acid (5 M) was slowly added drop wise to the IgG formulation in order to change the pH from 6.0 to 1.0. The

samples were then kept for 1 minute at this low pH with constant stirring at 500 rpm. Then, sodium hydroxide (5 M) was added drop wise to adjust the pH back to 6.0. Stirring by itself did not induce aggregation, according to different techniques. After the pH-shift, the samples were kept at 4°C until further analysis. No precipitation was observed during the time course of the experiment.

In order to obtain unfolded IgG monomers to use as a control for SEC analysis, the IgG formulation was denatured by adding concentrated GuHCl to a final concentration of 6 M.

Spiking procedure

An IgG sample was pH-shifted according to the above protocol and after 24 hours at 4°C added (10% v/v) to an unstressed IgG formulation. This spiked sample was incubated for 3 weeks at 55°C in a water bath. The original sample (100% pH-shift) used for the spike and an unstressed sample were incubated under the same conditions and used as controls.

Size exclusion chromatography (SEC)

SEC was performed on an Agilent 1200 (Agilent Technologies, Palo Alto, CA, USA) combined with a Wyatt Eclipse (Wyatt Technology Europe GmbH, Dernbach, Germany). A TSK Gel 3000 SWXL column (300 mm × 7.8 mm) with a TSK Gel 3000 precolumn (Tosoh Bioscience, Montgomeryville, PA, USA) was used. Fifty µL of the formulations were injected and separation was performed at a flow rate of 0.5 ml/min. The elution buffer was composed of 100 mM sodium phosphate, 100 mM sodium sulfate, 0.05% (w/v) sodium azide at pH 7.2. For the online fluorescent dye detection SEC runs, bis-ANS was added to the elution buffer to a final concentration of 0.6 µM, as described by Hawe et al [27].

UV and fluorescence detection were performed with an Agilent 1200 apparatus. The UV signal was detected at 280 nm, whereas bis-ANS fluorescence detection was performed with the excitation and emission monochromators set at 385 nm and 490 nm, respectively. MALLS detection was performed with an 18-angle DAWN HELEOS detector (Wyatt Technology Europe, Dernbach, Germany) operating with a 50-nW solid-state laser at 658 nm. The molecular weight of the IgG peaks was calculated with the Astra software version 5.3.1.5 (Wyatt Technology Europe, Dernbach, Germany). An extinction coefficient of 1.69 (ml mg^{-1} cm^{-1}), a dn/dc of

0.185 (ml/g) and a second virial coefficient of 0 were used. The calculation of the molecular weight was based on the Zimm equation [28].

In order to calculate the percentage of monomer, dimers, larger oligomers and unrecovered protein, the areas under the curve (AUC) of the UV signal were used. All the percentages are relative to the total AUC of the unstressed sample.

Light obscuration (LO)

LO measurements were performed on a PAMAS SVSS system (PAMAS GmbH, Rutesheim, Germany) equipped with a HCB-LD-25/25 sensor and a 1-ml syringe. Each sample was measured three times, with each measurement consisting of a pre-run volume of 0.3 ml followed by three runs of 0.2 ml at a flow rate of 10 ml/min. The final results are a mean of the three runs and the error bars and numbers represent the standard deviation (SD) between them.

Nanoparticle particle tracking (NTA)

NTA measurements were performed with a NanoSight LM20 (NanoSight, Amesbury, United Kingdom), equipped with a sample chamber with a 640-nm laser and a Viton fluoroelastomer O-ring, as described by Filipe et al [29]. The software used for capturing and analyzing the data was the NTA 2.0 Build 127. The samples were measured for 40 seconds with manual shutter and gain adjustments. The stressed samples were measured undiluted for the 1, 3 and 5 hours' time points, 2 fold diluted for the 1 and 3 days' time points and 4 fold diluted for the 5 days' time point. Six measurements of each sample were performed and the mean was obtained.

Dynamic light scattering (DLS)

DLS measurements were performed with a Malvern Zetasizer Nano ZS (Malvern, Herrenberg, Germany) equipped with a 633-nm He-Ne laser and operating at an angle of 173°. The software used to collect and analyze the data was the Dispersion Technology Software version 6.01 from Malvern. Five hundred µl of each sample was measured undiluted in single-use polystyrene half-micro cuvettes (Fisher Emergo, Landsmeer, The Netherlands) with a pathlength of 10 mm. Each measurement consisted of 15 runs of 10 seconds and the Z-average diameter (Z_{ave}) and the

polydispersity index (PdI) were determined. Three measurements of each sample were made and the errors represent the SD between them.

Circular dichroism (CD)

CD was performed with a Jasco J-815 CD spectrometer in combination with a Jasco PTC- 423S temperature controller (Jasco International, Tokyo, Japan) at 25°C. The IgG samples were diluted to 0.1 mg/ml for far-UV CD and 0.5 mg/ml for near-UV CD measurements. The samples were measured in quartz cuvettes (Hellma GmbH, Muellheim, Germany) with a path length of 1 mm for far-UV CD and 10 mm for near-UV CD.

CD spectra were collected in a continuous scanning method from 200 to 250 nm for far-UV CD and from 250 to 320 nm for near-UV CD. The measurements were performed at a scanning speed of 50 nm/min, a response time of 2 s, a bandwidth of 1 nm, a sensitivity of 100 m°, steps of 0.5 nm and an accumulation of 10 scans. Using the Spectra Analysis Software (version 1.53.04, Jasco), the spectra were background corrected by subtracting the spectrum of the buffer and smoothed with GraphPad Prism® 5 with a 0th order polynomial smoothing and 4 neighbors on each value. Data were calculated as mean residue ellipticity according to Kelly et al., using a mean amino acid residue weight of 113 suggested by Aghaie et al. for IgG [30, 31].

Steady-state fluorescence spectroscopy

Steady-state fluorescence was measured with a Tecan Infinite M1000 plate reader (Tecan Benelux, Giessen, Netherlands) with 96-well plates (Greiner Bio-One, Alphen a/d Rijn, The Netherlands), a sample volume of 200 µl per well (n = 3), a gain of 188 and a Z-position of 21000 µm. Bis-ANS was added to the wells to a final concentration of 1 µM. The samples were excited at 385 nm and the emission spectra were recorded from 400 nm to 600 nm. The spectra of the 3 wells were averaged and the average was then smoothed in the GraphPad Prism® 5 software with a 0th order polynomial smoothing and 4 neighbors on each value.

RESULTS

Monomers and Oligomers

SEC is the most widely used method for analyzing aggregation of therapeutic proteins. Even though this technique has some recognized downsides, SEC provides valuable quantitative information about soluble protein aggregates [10, 32]. In the present work, this technique was applied with UV (SEC-UV) and MALLS (SEC-MALLS) detection to separate and quantify monomers and small oligomers present in the pH-shift stressed formulations. The evolution of the aggregation profile in these formulations was followed over time (Fig. 5.1) and the relative amounts of the separated aggregate species were calculated (Table 5.1). The results after 7 and 9 days were very similar to the ones observed after 5 days, so for clarity purposes they are not shown.

Table 5.1: Size distribution and quantitative data from SEC-UV, DLS, NTA and LO measurements of pH-shift stressed IgG over time and unstressed IgG. SEC-UV percentages are relative to the total AUC of the unstressed sample. The SEC-UV data is derived from Fig. 5.1a.

	SEC-UV (%)				DLS		NTA	LO
	Mon	Dim	L Olig	Unrecov Protein	Z_{ave} (nm)	PdI	Particles $\times 10^8$/ml	(Part > 1µm) $\times 10^3$/ml
Unst	99	1	0	N/A	8.4 ±0.1	0.18 ±0.03	0.3 ±0.1	1.4 ±0.2
1 h	54	16	18	12	14.7 ±0.2	0.31 ±0.06	1.7 ±0.3	33.6 ±3.2
3 h	52	15	23	10	16.3 ±2.4	0.32 ±0.07	3.5 ±1.7	30.7 ±3.8
5 h	53	15	24	9	17.8 ±3.1	0.37 ±0.10	3.7 ±0.8	38.6 ±3.0
1 D	52	13	27	8	22.9 ±6.2	0.41 ±0.11	8.6 ±1.9	72.1 ±6.9
2 D	52	13	28	7	26.4 ±7.2	0.39 ±0.13	12.8 ±1.0	81.4 ±5.4
5 D	53	13	29	5	45.5 ±26.7	0.34 ±0.08	17.8 ±2.5	100.7 ±10.4

Abreviations: Unst – unstressed; Mon – monomer; Dim – dimer; L Olig – larger oligomers; Unrecov – unrecovered; Z_{ave} – Z average; PdI – polydispersity index; Part – particles; N/A – not applicable.

The monomer eluted about 17.5 min after injection and the oligomers between 11.5 and 16 min. Both chromatograms show that the unstressed formulation contained mainly monomers and only about 1% of dimers (Table 5.1). The aggregation profile of unstressed IgG did not change over time (data not shown). The pH-shift stress formulations were characterized by the presence of aggregates, not only by the appearance of oligomer peaks, but also by substantial monomer peak

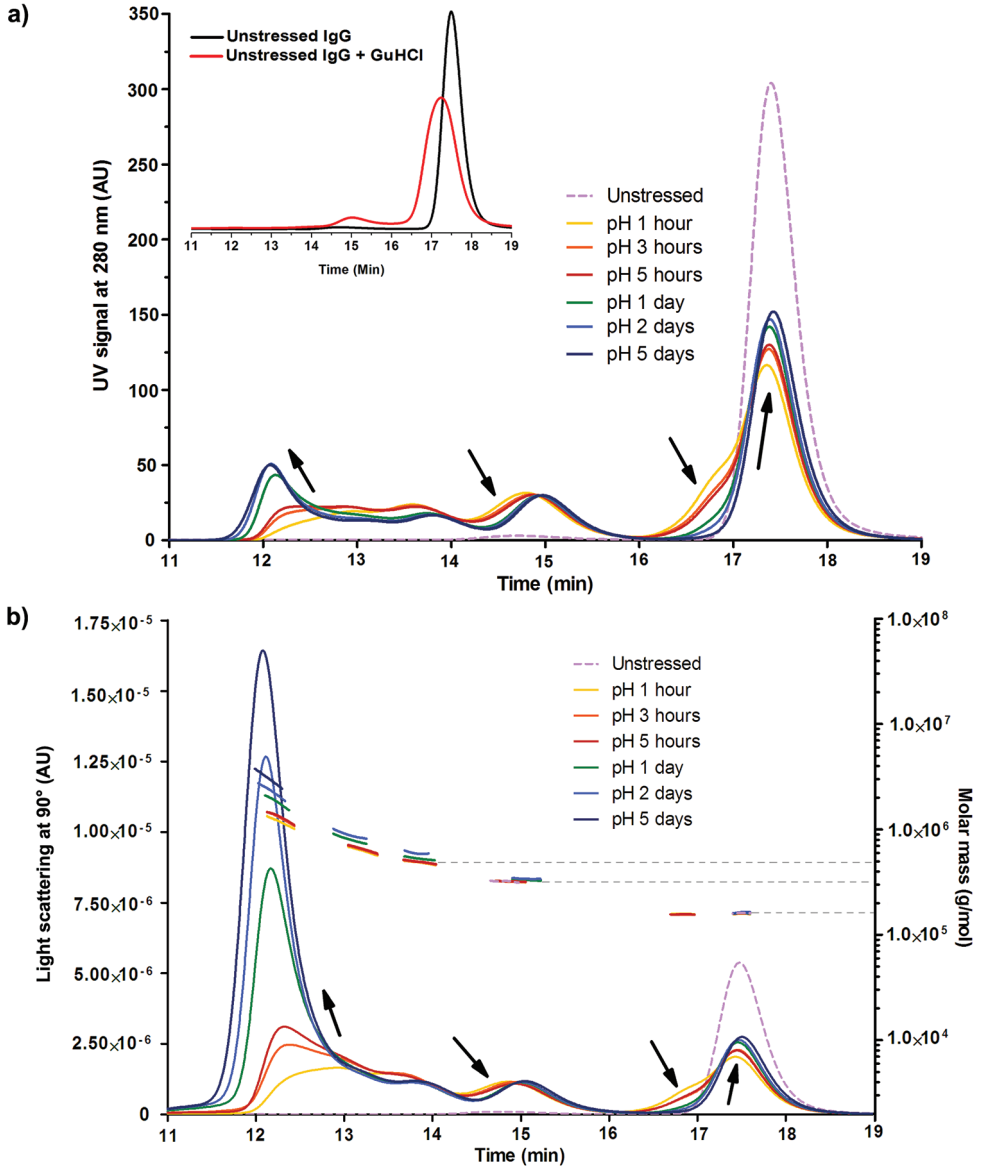

Figure 5.1: Representative SEC chromatograms of pH-shift stressed IgG over time and unstressed IgG with (a) UV detection at 280 nm and (b) MALLS detection and the estimated molar mass of each peak. The insert of (a) shows a SEC chromatogram with UV detection at 280 nm of unstressed and IgG in 6M GuHCl. The arrows indicate the direction in which the peaks evolve over time.

loss. It is important to notice that aggregates larger than the interstitial space of the stationary phase either pass through the void volume of the column, and appear as a single peak (ca. 12 min), or become trapped in the column due to their large size or interaction with the column material [10].

The size distribution of the aggregates and the amount of monomer in SEC evolved considerably during the first 5 days after stress. About 1 hour after the pH-shift stress, about 50% of the monomer peak was lost and a considerable amount of dimers (eluting at ca. 15 min) and oligomers (eluting between 14 and 12 min) was detected. The peak areas of the monomer and the larger oligomers increased over time in SEC-UV (Fig. 5.1a), while the one of dimers slightly decreased. As the days went by, the larger oligomers peak started appearing at earlier elution times (i.e., before 12 min), indicating that the hydrodynamic size of these oligomers increased over time. This increment can be better observed with SEC-MALLS (Fig. 5.1b), which shows that the light scattering signal and the calculated average molar mass of these oligomers increased significantly over time.

In SEC-UV (Fig. 5.1a), the monomer peaks of freshly stressed formulations have a prominent left shoulder (ca. 16.5 min). IgG eluting with this shoulder had the same molecular weight as the monomer (Fig. 5.1b) and eluted at approximately the same retention time as IgG treated with a denaturing agent (GuHCl), as shown in the insert of Fig. 5.1a. Thus, this shoulder most likely represents partially unfolded monomers that, due to their larger hydrodynamic volume, eluted slightly earlier than native state monomers. The shoulder was very prominent 1 hour after stress and then gradually disappeared over time. In fact, the dimers and trimers of freshly stressed formulations also eluted at slightly earlier times than the ones in the unstressed formulation, indicating that these two species were also partially unfolded. As the days passed, these peaks started eluting at later retention times, as if these species were all gradually refolding or the percentage of partially unfolded species gradually decreased.

Subvisible Aggregates

In order to analyze the presence of aggregates larger than the exclusion volume of SEC (subvisible aggregates), different complementary techniques were used: DLS, NTA and LO. DLS is a well-established technique that can measure the Z-average diameter (Z_{ave}) and the polydispersity index (PdI) of aggregates typically in the submicron range. This technique has a broad detection limit (ca. 1-1000 nm), but the results are biased to the larger particles and the method does not measure aggregate content [29]. NTA is an emerging technique that enables the sizing and quantification of particles in the submicron range. Compared with DLS, NTA has a narrower size range for proteinaceous material (ca. 40-1000 nm), but is more

suitable for polydisperse samples [29]. LO particle counting is a technique that can count and measure the size of micron-sized particles. NTA and LO size distribution graphs of the stressed formulations over time are displayed in Fig. 5.2, whereas the Z_{ave} and PdI of DLS measurements and the NTA and differential LO particle counts are shown in Table 5.1. The results after 7 and 9 days were again very similar to the ones observed after 5 days, so for clarity purposes they are not shown.

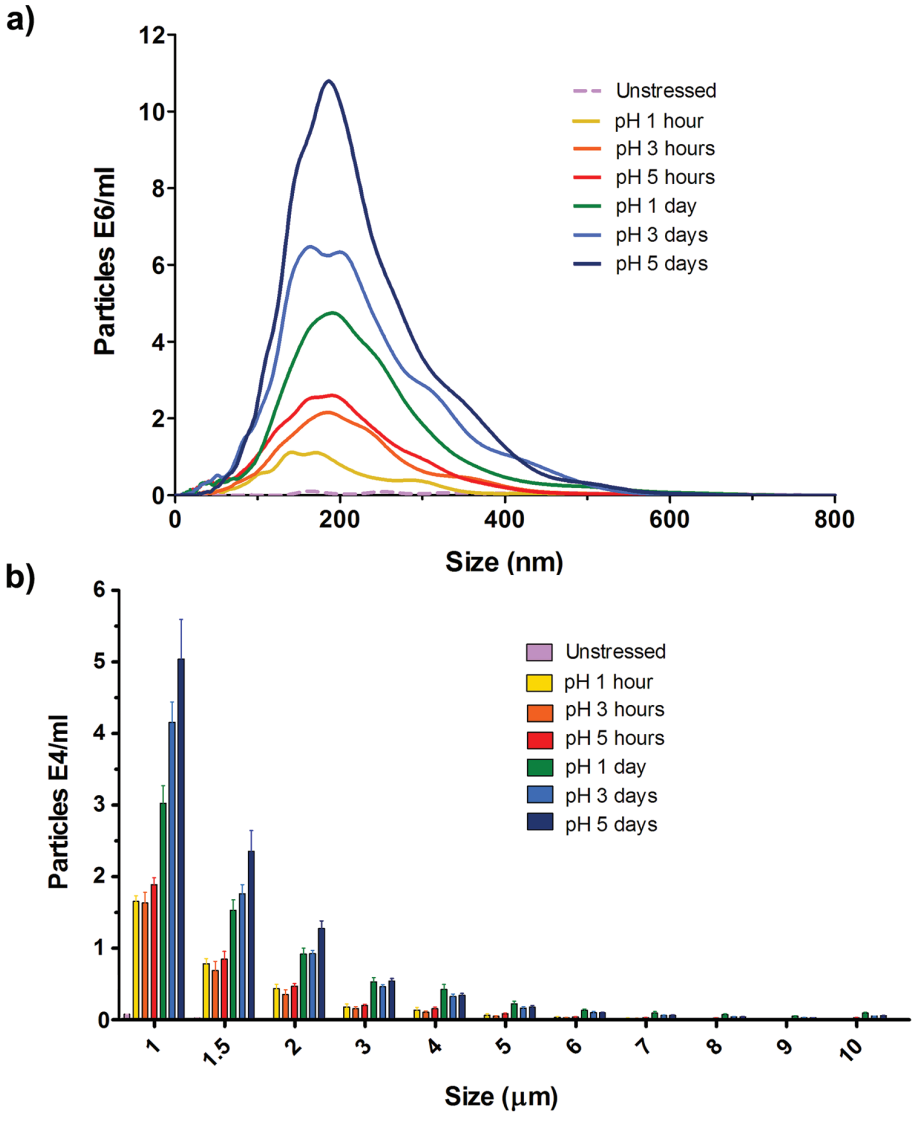

Figure 5.2: Size distribution of subvisible aggregates of pH-shift stressed IgG over time and unstressed IgG: (a) submicron particles (determined by NTA), (b) micron-sized particles (determined by LO).

The unstressed formulation had a Z_{ave} of 8.4 nm and a PdI of 0.18 according to DLS measurements. It is important to notice that the 5% sucrose present in the formulation buffer can be detected by DLS, yielding a peak at approximately 1 nm [29]. This likely explains the relatively low Z_{ave} observed for this unstressed formulation, compared with typical IgG Z_{ave} values described by others (ca. 11 nm) [13, 33]. About 1 hour after the pH-shift stress, the Z_{ave} of the formulation had increased to 14.7 nm and the PdI to 0.31. During the next 5 days, the Z_{ave} grew gradually until 45.5 nm, but the PdI remained practically unaltered. These results show that the average size of pH-shift induced aggregates increases with time, in concordance with the SEC results.

NTA measurements of the unstressed formulation revealed that it already contained a small amount of submicron aggregates (ca. 3×10^7 particles/ml). One hour after the pH-shift, the amount of aggregates detected by NTA was 1.7×10^8 particles/ml and the size average was around 200 nm. For the following time points, the amount of aggregates increased and after 5 days the stressed formulations contained about 1.8×10^9 particles/ml (Table 5.1, Fig. 5.2a). Remarkably, the size average of these aggregates did not significantly change over time. Some aggregates with sizes larger than 600 nm were observed in all stressed samples, but the NTA software was not able to properly track and size them. These aggregates contained multiple scattering centers, which added a rotational variable that cannot be analyzed correctly by the software, i.e., the tracking of such multiple centers resulted in seemingly small aggregates with very high scattering intensities. These incorrect measurements can be easily identified and were thus removed from the final result.

The concentration of micron-sized aggregates in the unstressed formulation was about 1400 particles/ml, most of which had a size in the low micrometer range, according to LO measurements (Table 5.1, Fig. 5.2b). Approximately 1 hour after stress, the amount of aggregates in this size range had increased to 33 600 particles/ml. The number of aggregates further increased over time, reaching a concentration of about 10^5 particles/ml after 5 days, but the aggregate size distribution remained practically unaltered. The main population of micron-sized aggregates was about 1 μm, which is the lower detection limit of this technique. The size distribution curve shown in Fig. 5.2b suggests that the main population of aggregates may be even smaller than 1 μm. However, according to NTA results, there are almost no aggregates larger than 600 nm. This apparent discrepancy may be explained by the 10^2 fold difference in particle concentration range detected by these techniques (cf. y-axis scales in Fig. 5.2) and by the difficulty of NTA to properly track and size

aggregates larger than 600 nm with multiple scattering centers, as explained above.

An estimate of the total mass of protein in these subvisible aggregates was calculated according to the method described by Barnard et al [34]. The submicron aggregates tracked by NTA equaled to an approximate protein concentration of 1 μg/ml about 1 hour after stress and 17 μg/ml after 5 days. The calculated protein concentration of micron-sized aggregates measured by LO was approximately 2 μg/ml 1 hour after stress and 6 μg/ml after 5 days. These rough estimates indicate that the amount of subvisible aggregates remained very small as compared to the total IgG content (1 mg/ml).

Structural Characterization

In order to obtain information about changes in the three-dimensional structure of the protein after stress, the formulations were analyzed by different structural analytical techniques over time. Secondary structure and tertiary structure of the overall formulation were analyzed by far-UV CD and near UV -CD spectroscopy, respectively (Fig. 5.3a and 5.3b). Steady-state fluorescence spectroscopy was applied with bis-ANS as an extrinsic fluorescent dye (Fig. 5.3c). Bis-ANS is a dye that fluoresces intensely only in hydrophobic environments, such as exposed hydrophobic pockets of proteins to which it can bind [35]. The CD and fluorescence results after 7 and 9 days were very similar to the ones observed after 5 days, and are therefore not shown.

The far-UV CD spectrum (Fig. 5.3a) of the unstressed IgG formulation has a negative minimum at around 220 nm and a positive maximum at 204 nm, indicative of a high β-sheet structure, which is typical for IgG [13, 36, 37]. The far-UV spectra of the pH-shift stressed samples are similar to the one of the unstressed formulation, indicating that the IgG had a fairly well conserved native-like secondary structure after stress. This similarity is more pronounced for wavelengths higher than 210 nm. It is important to remember that these stressed samples contained a high amount of large aggregates and these may have interfered with CD measurements, mainly due to light scattering [30]. Light scattering is inversely proportional to the wavelength and that may in part explain the differences observed for wavelength shorter than 210 nm. However, these spectral differences seem to become slightly less pronounced over time. Given that the samples at later time points contained more and larger aggregates, it is likely that these small spectral differences reflect real structural changes, rather than light scattering interference.

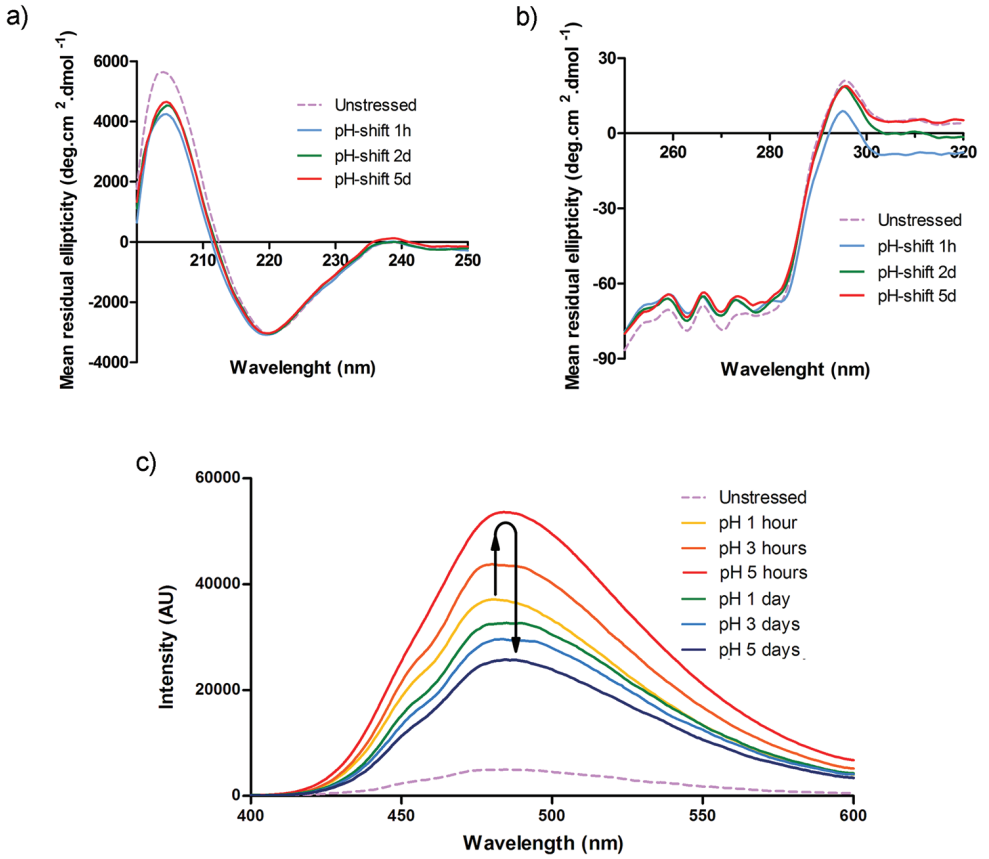

Figure 5.3: Structural characterization of pH-shift stressed IgG over time and unstressed IgG by (a) far-UV CD, (b) near-UV CD and (c) Bis-ANS fluorescence. The arrows in (c) show the evolution of the fluorescence intensity maximum over time.

The near-UV CD spectrum (Fig. 5.3b) of the unstressed formulation has a distinctive positive peak at 295 nm (tryptophan) and a negative band in the range between 250 and 290 nm (aromatic amino acid residues and cysteine), which is typical for IgG [36, 38]. The spectra of the pH-shift stressed formulations differ slightly from the unstressed one. A decreased mean residue ellipticity between 290 and 320 nm and lower negative ellipticity values for the shorter wavelengths were measured for the samples after stress. This indicates that the pH-shift stress induced small conformational changes of the IgG in solution. Since this technique gives an overall result, it is not possible to specify if these were severe changes of only a few IgG molecules or mild changes of all molecules. During the following days, the spectrum of the stressed IgG gradually shifted to a profile closer to the native-like spectrum profile.

All bis-ANS fluorescence spectra of pH-shift stressed IgG have an emission maximum at 486 nm (Fig. 5.3c). Compared with the spectrum of the unstressed formulation, the maximum fluorescence intensity increased 7 fold shortly after the pH-shift. This indicates that more hydrophobic regions were exposed after the stress, most likely as the result of IgG structural changes as also detected by CD. The fluorescence intensity kept increasing during the first few hours after stress, but decreased during the subsequent days. In fact, after 1 day the intensity value had become lower than the one observed 1 hour after stress. These results suggest partial refolding back to native states a few days after stress and/or the appearance of aggregates with relatively low-affinity bis-ANS binding sites. After 5 days (as well as 7 an 9 days) the fluorescence intensity did not reach the low original intensity value of the unstressed formulation, indicating that refolding was only partially reversible.

With the purpose of identifying which species had undergone the biggest structural changes and understanding the changes in the bis-ANS fluorescence intensity signal observed over time, SEC with online bis-ANS fluorescence detection (SEC-fluorescence) was used (Fig. 5.4). This recently developed method already proved to be efficient to detect both aggregation and structural changes of both monomeric and aggregated IgG in heat-stressed formulations [13, 27].

The SEC-fluorescence chromatogram of the unstressed formulation shows that the monomer eluting at 17.6 min has a considerably weak emission signal, as expected for IgG in the native state [27]. One hour after the pH-shift stress, a high bis-ANS fluorescence signal was observed not only for the oligomers but also for the monomer. This means that even 1 hour after stress, there was still a large amount of monomers with significant structural changes. It is important to notice that the bis-ANS-interactive monomer of this freshly stressed formulation eluted 0.5 minutes earlier than the unstressed monomer (cf. Fig. 5.1). The stressed monomer eluted at about the same time (17.1 min) as the unfolded monomer treated with GuHCl, as shown in the insert of Fig. 5.4. It seems that the shoulder observed with SEC-UV (between 16.5 and 17.0 min - Fig. 5.1) represents the left part of the peak of conformationally altered monomers observed with SEC-fluorescence.

For the following time points, SEC-fluorescence chromatograms show a gradually decreased emission signal and slightly later elution times for the monomers and small oligomers, which is particularly apparent from the chromatograms of pH-shift stressed IgG after 1-5 days (Fig. 5.4). However, the intensity signal of the larger oligomers slightly increased over time, suggesting that these aggregates contained conformationally altered IgG. These results suggest that structurally changed

monomers are the main trigger for pH-shift induced aggregation and their relatively long-lasting presence may explain the dynamics observed for these stressed samples over time.

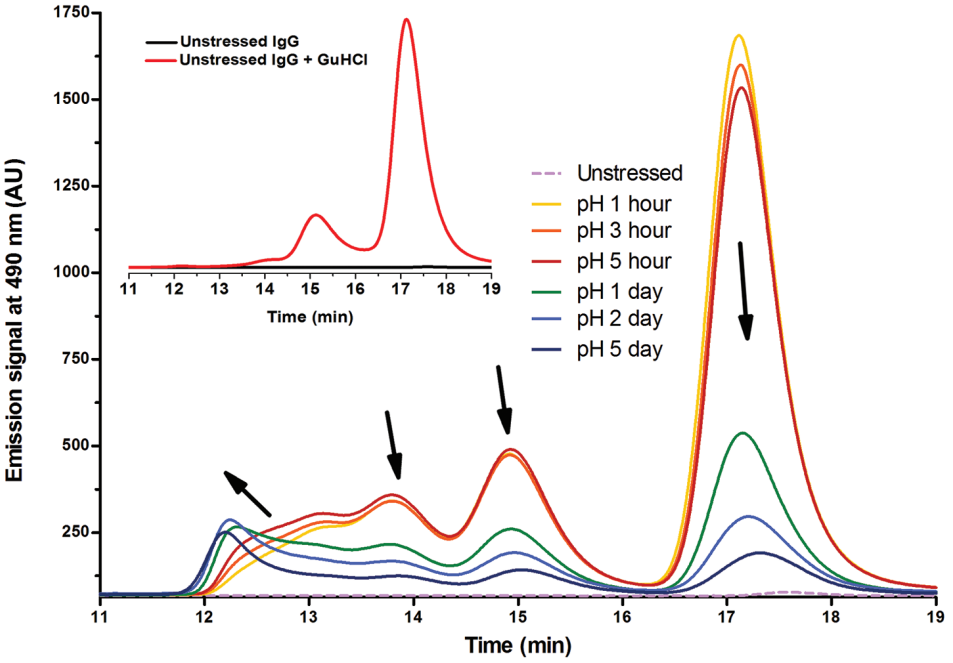

Figure 5.4: SEC chromatograms of the pH-shift stressed IgG formulation over time with bis-ANS fluorescence emission detection at 490 nm and excitation at 385 nm. The mobile phase contained 0.6 µM bis-ANS. The insert is a chromatogram with the same experimental conditions of unstressed and GuHCl stressed IgG. The arrows show the evolution of the peaks over time.

Spiking Study

A spiking study was conducted with the aim of getting more insight into the aggregation mechanism associated with the pH-shift stress. The occurrence of nucleation polymerization events was tested by spiking a pH-shift stressed formulation into an unstressed IgG formulation (10% v/v). Since the stressed formulation was 1 day old (after stress) at the time of the spike, the pseudo-equilibrium between monomers and aggregates had not been reached yet. Thus, the goal was to see if some of the wide range of aggregates present in this stressed sample would act as aggregation seeds in spiked formulations and lead to the formation of more and larger aggregates as compared to nonspiked unstressed IgG. The spiked formulation

was incubated at 55 °C for 3 weeks with the purpose of accelerating the aggregation process. The formulations were analyzed by SEC-UV, DLS and LO. A negative control (unstressed) and a positive control (100% pH-shift) were also incubated and analyzed. The LO size distribution graph is shown in Fig. 5.5 and quantitative information from SEC-UV, DLS and LO measurements is presented in Table 5.2.

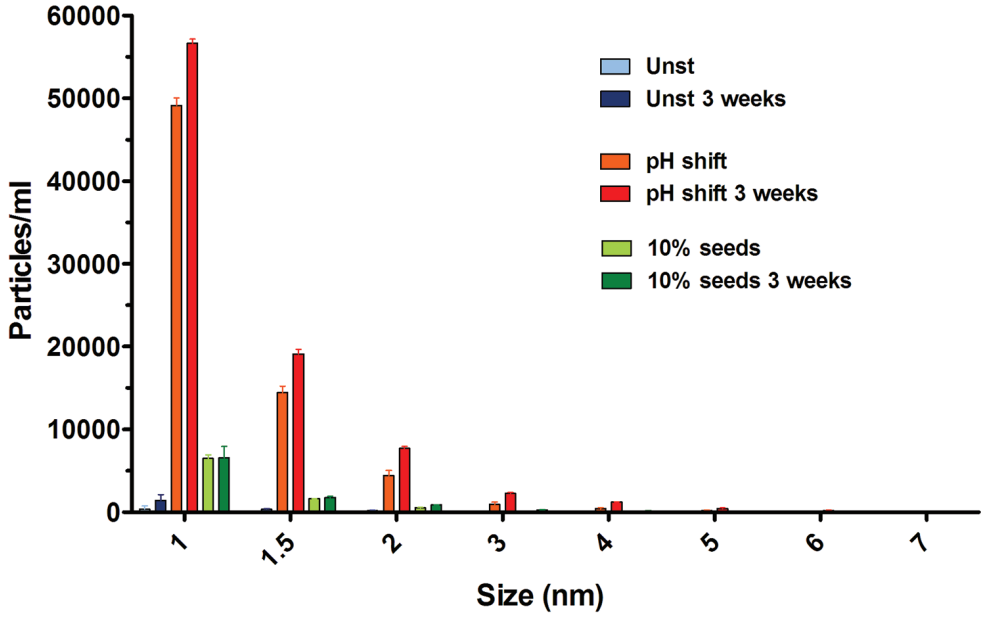

Figure 5.5: LO size distribution of micron-sized aggregates of unstressed, pH-shift stressed and spiked (10% seeds) formulations, before and after an incubation period of 3 weeks at 55 °C.

The average size of aggregates measured by LO remained practically unaltered after incubation. The unstressed and pH-shift formulations showed an increase in average particle count by about 1500 and 24000 particles/ml, respectively. However, the spiked formulation showed no significant particle count increase, since the increment value (900 particles/ml) is smaller than the SD observed for this sample after 3 weeks (ca. 1400 particles/ml).

The DLS results of the spiked formulation do not show progressive aggregation after incubation. In fact, the Z_{ave} and PdI of this sample slightly decreased after 3 weeks, suggesting the disappearance of some of the aggregates. For the positive and negative controls the number of micron-sized aggregates and Z_{ave} both increased after 3 weeks. The PdI of the unstressed formulation slightly increased, whereas the

one of the 100% pH-shift stressed formulation remained practically unaltered.

Table 5.2: Size distribution and quantitative data from SEC-UV, DLS, and LO measurements of unstressed, pH-shift stressed and spiked (10% seeds) IgG formulations, before and after an incubation period of 3 weeks at 55 °C. SEC-UV percentages are relative to the total AUC of the unstressed sample at t_0.

		SEC-UV (%)					DLS		LO
		Mon	Dim	L Olig	Frag	Unrecov Protein	Z_{ave} (nm)	PdI	(Part > 1µm) ×10^3/ml
Unstressed	t_0	97	2	0	1	N/A	8.4 ±0.1	0.21 ±0.03	0.9 ±0.3
	t_1	95	2	0	3	0	8.9 ±0.2	0.25 ±0.04	2.4 ±0.8
pH-shift	t_0	43	11	17	1	29	32.2 ±8.4	0.66 ±0.15	64.3 ±9.9
	t_1	37	7	11	19	27	34.3 ±9.8	0.65 ±0.12	88.4 ±8.2
10% seeds	t_0	92	3	1	1	4	10.8 ±1.1	0.36 ±0.08	9.0 ±0.5
	t_1	89	2	1	4	4	10.3 ±1.3	0.27 ±0.06	9.8 ±1.4

Abreviations: Mon – monomer; Dim – dimer; L Olig – larger oligomers; Frag – fragments, Unrecov - unrecovered; Zave – Z average; PdI – polydispersity index; N/A – not applicable.

The inconsistency observed between the DLS results of Table 5.1 for the sample after 1 day and Table 5.2 for the 100% corresponding sample (pH-shift t_0) is due to the variability inherent to the stress method. Even though the exposure time at pH 1 can be well controlled, the time of transition between pHs is harder to control and it leads to some variability in the initial amount of aggregates formed. DLS is very sensitive to the presence of aggregates and the sample used for spiking most likely contained more submicron aggregates than the one shown in Table 5.1 and that resulted in an increased Z_{ave} and PdI. This variation had a marginal effect on the SEC profiles (results not shown) and did not seem to affect the amount of micron sized aggregates (cf. LO data in Table 5.1 and Table 5.2).

Spiking also did not have an impact on the formation of larger oligomers or the unrecovered protein percentage, according to SEC-UV. The slight loss of monomers and dimers observed for the spiked sample after incubation were associated with an increased fragmentation. This was also observed for the unstressed and the 100% pH-shift stressed formulation, with the latter showing very high percentage of fragments after incubation. Some level of fragmentation has already been reported during exposures at elevated temperatures and this seems to be aggravated for solutions previously stressed by a low pH-shift [13]. It seems that, in the 100% pH-shift stressed sample, fragmentation occurred not only from monomers, but also from dimers and larger oligomers.

Altogether, these results indicate that the formation of pH-shift induced aggregates

is most likely not associated with nucleated polymerization.

DISCUSSION

In this study we have shown that a short exposure of an IgG to a low pH induces the immediate formation of a wide range of metastable aggregates that reach a pseudo-equilibrium state after 5-7 days when kept at 4 °C.

The pH-shift immediately caused structural changes in the IgG molecules, in particular at a tertiary structure level and less at a secondary structure level, as obvious from CD. With steady-state bis-ANS fluorescence the intensity signal increased up to 10 fold after stress, pointing towards an exposure of hydrophobic pockets due to the pH-shift induced structural changes. Moreover, conformationally changed monomers were detected by SEC-fluorescence. These monomers had a transient character and most of them disappeared during the next few days. These transient monomers seemed to be partially unfolded but, according to far-UV CD results, exhibited a fairly conserved native-like secondary structure, which is typical of molten globules [39]. These species have been reported to form under mild denaturing conditions, such as incubation at low or high pH values, changes in pressure or temperature, variations in solution ionic strengths or addition of chaotropic agents [40, 41]. This molten globule state seems to be the key element for the aggregation process of these metastable aggregates.

The combined protein concentration of the subvisible aggregates detected by NTA and LO was estimated to be about 3 μg/ml after 1 hour and 23 μg/ml after 5 days, i.e. 0.3% and 2.3%, respectively, of the total amount of IgG. It is possible that these percentages were in fact underestimated, since LO has been shown to count substantially less particles than other analytical techniques, such as flow imaging techniques [42, 43]. In any case, the amount of aggregates that were too large to enter the SEC column increased over time. However, the percentage of unrecovered protein decreased from 12% (after 1 hour) to 5% (after 5 days). These results suggest that the presence of large aggregates was not the main factor influencing the incomplete protein recovery observed, especially shortly after stress.

The presence of molten globules in stressed formulations can be easily observed in the SEC-UV chromatograms of Fig. 5.1a, as a left-shoulder on the monomer peak, and the enhanced bis-ANS fluorescence at the same elution position in SEC-fluorescence (Fig. 5.4). However, it is possible that the amount of molten globules was much higher than the one detected by this technique. Conformationally

changed proteins normally have more hydrophobic regions exposed than their native counterparts (as observed by SEC-fluorescence), which may lead to unspecific binding of these species to the stationary phase of SEC columns [32]. Thus, it may well be that some of the molten globules got retained in the resin of the column. This could explain to some extent the incomplete protein recovery in SEC. In fact, as the amount of molten globules diminished over time, the unrecovered protein fraction decreased (Table 1).

Molten globules are normally short-lived species that may either refold back to the native state or initiate an aggregation process [17, 19]. According to the SEC-fluorescence results, the amount of monomeric molten globules continuously decreased during the time course of the experiment. However, the overall bis-ANS fluorescence, detected by steady-state spectroscopy, increased during the first few hours and decreased during the following days. The interaction of bis-ANS with IgG and its aggregates is rather complex and depends not only on the number of binding sites, but also on their affinity. A wide range of binding affinities for the same type of IgG aggregates has been reported [44]. The increment of fluorescence intensity during the first few hours may thus be related with the formation of aggregates with high affinity for the dye, which compensated for the disappearance of lower-affinity molten globules. After 1 day, the amount of molten globule had diminished significantly (Fig. 5.1 and 5.4) and this was associated with an overall decrease of bis-ANS fluorescence (Fig. 5.3c). At the same time, the aggregates apparently evolved into larger oligomers with relatively low-affinity bis-ANS binding sites, which led to an overall lower fluorescence. This assumption is corroborated by the slight decrease of fluorescence observed for the larger oligomers fraction from day 2 to day 5 (Fig. 5.4).

The amount of subvisible aggregates increased over time, in both the submicron and the micron range. However, the size average of these aggregates remained practically unaltered. These results indicate that the formation of micron-sized aggregates is not the direct consequence of an association of submicron aggregates. Therefore, the aggregation process did not seem to be driven by condensation mechanisms as described by Speed et al [23].

The absence of nucleated polymerization mechanisms was inferred from the spiking study results. The pH-shifted sample selected for spiking (1 day after stress) contained a fair amount of protein oligomers and subvisible particles that could act as nucleation seeds. However, the presence of these species in the spiked sample did not lead to accelerated aggregation after incubation, as compared to a

nonspiked control.

By excluding the mechanisms discussed above, a downhill polymerization mechanism is likely responsible for the aggregation observed in this study [25]. In fact, downhill polymerization was facilitated in our study since the thermodynamically unfavorable step (monomer to dimer conversion) was bypassed by a massive formation of molten globules, induced by the pH-shift. The relatively large amount of these species in early stages after stress seemed to trigger a fast aggregation process, most likely by consecutive addition of molten globular monomers to already formed aggregates. As the amount of molten globules decreased, by either refolding back to the native state or by their incorporation in aggregates, the rate of aggregation also decreased. After 5 to 7 days, once almost all molten globules had disappeared from solution, the aggregation process practically stagnated and a pseudo-equilibrium was reached.

The aggregation profile evolution observed in this study is specific to this particular IgG, in this exact buffer and under these precise the experimental stress conditions. Nevertheless, the low pH-driven non-native aggregation mechanism described here is likely to occur with other IgGs and even other types proteins, since partial unfolding caused by low pH exposure is a phenomenon common to all proteins. In fact, in preliminary unpublished studies with polyclonal human IgG and rituximab we observed similar progressive aggregation and partial recovery of monomeric IgG in time after applying identical pH stress as employed in the present study.

CONCLUSION

We have shown that a short exposure of IgG to low pH results in the formation of a wide size range of non-native aggregates as well as a large amount of molten globules that seem to be the key element for the aggregation process. While some of these conformationally altered monomers fold back into the native state, others are converted into aggregates, presumably by a downhill polymerization mechanism. This is consistent with the observation that the aggregation process slows down when the amount of molten globules in solutions becomes scarce.

Altogether, these results highlight the role of partially unfolded species in the aggregation of therapeutic proteins. Since the exposure of mAbs to low pH is often unavoidable during purification processes, it is important to ensure that the structural integrity of the molecules remained intact, in order to avoid subsequent protein aggregation. Furthermore, this study illustrates that one should anticipate

time-dependent changes in a protein's aggregation profile after exposure to low pH or other stress conditions.

ACKNOWLEDGEMENTS

This research was supported by the Technology Foundation STW, the applied science division of NWO and technology program of the Dutch Ministry of Economic Affairs. We thank Mohamed Salah Rezk for analytical support. We also thank Stefan Romeijn for his technical support with the SEC-MALLS measurements.

REFERENCES

[1] G. Walsh, "Biopharmaceutical benchmarks 2006," Nature biotechnology, vol. 24, pp. 769-76, Jul 2006.
[2] S. Lawrence, "Pipelines turn to biotech," Nature biotechnology, vol. 25, p. 1342, Dec 2007.
[3] M. E. Cromwell, E. Hilario, and F. Jacobson, "Protein aggregation and bioprocessing," The AAPS journal, vol. 8, pp. E572-9, 2006.
[4] J. S. Bee, T. W. Randolph, J. F. Carpenter, S. M. Bishop, and M. N. Dimitrova, "Effects of surfaces and leachables on the stability of biopharmaceuticals," Journal of pharmaceutical sciences, Apr 26 2011.
[5] A. S. Rosenberg, "Effects of protein aggregates: an immunologic perspective," The AAPS journal, vol. 8, pp. E501-7, 2006.
[6] J. den Engelsman, P. Garidel, R. Smulders, H. Koll, B. Smith, S. Bassarab, A. Seidl, O. Hainzl, and W. Jiskoot, "Strategies for the assessment of protein aggregates in pharmaceutical biotech product development," Pharmaceutical research, vol. 28, pp. 920-33, Apr 2011.
[7] M. K. Joubert, Q. Luo, Y. Nashed-Samuel, J. Wypych, and L. O. Narhi, "Classification and characterization of therapeutic antibody aggregates," The Journal of biological chemistry, vol. 286, pp. 25118-33, Jul 15 2011.
[8] J. S. Laurence and C. R. Middaugh, "Fundamental structures and behaviours of proteins," in Aggregation of therapeutic proteins, W. Wang and C. J. Roberts, Eds., ed: Wiley, 2010, pp. 1-61.
[9] C. J. Roberts, "Non-native protein aggregation kinetics," Biotechnology and bioengineering, vol. 98, pp. 927-38, Dec 1 2007.
[10] J. S. Philo, "A critical review of methods for size characterization of non-particulate protein aggregates," Current pharmaceutical biotechnology, vol. 10, pp. 359-72, Jun 2009.
[11] L. A. Kueltzo, W. Wang, T. W. Randolph, and J. F. Carpenter, "Effects of solution conditions, processing parameters, and container materials on aggregation of a monoclonal antibody during freeze-thawing," Journal of pharmaceutical sciences, vol. 97, pp. 1801-12, May 2008.
[12] H. C. Mahler, W. Friess, U. Grauschopf, and S. Kiese, "Protein aggregation: pathways, induction factors and analysis," Journal of pharmaceutical sciences, vol. 98, pp. 2909-34, Sep 2009.
[13] A. Hawe, J. C. Kasper, W. Friess, and W. Jiskoot, "Structural properties of monoclonal antibody aggregates induced by freeze-thawing and thermal stress," European journal of pharmaceutical sciences : official journal of the European Federation for Pharmaceutical Sciences, vol. 38, pp. 79-87, Sep 10 2009.
[14] W. Wang, S. Nema, and D. Teagarden, "Protein aggregation--pathways and influencing factors,"

International journal of pharmaceutics, vol. 390, pp. 89-99, May 10 2010.
[15] S. S. Plotkin and J. N. Onuchic, "Understanding protein folding with energy landscape theory. Part I: Basic concepts," Quarterly reviews of biophysics, vol. 35, pp. 111-67, May 2002.
[16] K. A. Dill and H. S. Chan, "From Levinthal to pathways to funnels," Nature structural biology, vol. 4, pp. 10-9, Jan 1997.
[17] V. Daggett and M. Levitt, "A model of the molten globule state from molecular dynamics simulations," Proceedings of the National Academy of Sciences of the United States of America, vol. 89, pp. 5142-6, Jun 1 1992.
[18] N. B. Bam, J. L. Cleland, and T. W. Randolph, "Molten globule intermediate of recombinant human growth hormone: stabilization with surfactants," Biotechnology progress, vol. 12, pp. 801-9, Nov-Dec 1996.
[19] P. Hammarstrom, M. Persson, P. O. Freskgard, L. G. Martensson, D. Andersson, B. H. Jonsson, and U. Carlsson, "Structural mapping of an aggregation nucleation site in a molten globule intermediate," The Journal of biological chemistry, vol. 274, pp. 32897-903, Nov 12 1999.
[20] V. E. Bychkova, R. Berni, G. L. Rossi, V. P. Kutyshenko, and O. B. Ptitsyn, "Retinol-binding protein is in the molten globule state at low pH," Biochemistry, vol. 31, pp. 7566-71, Aug 25 1992.
[21] C. Redfield, R. A. Smith, and C. M. Dobson, "Structural characterization of a highly-ordered 'molten globule' at low pH," Nature structural biology, vol. 1, pp. 23-9, Jan 1994.
[22] S. Muzammil, Y. Kumar, and S. Tayyab, "Molten globule-like state of human serum albumin at low pH," European journal of biochemistry / FEBS, vol. 266, pp. 26-32, Nov 1999.
[23] M. A. Speed, J. King, and D. I. Wang, "Polymerization mechanism of polypeptide chain aggregation," Biotechnology and bioengineering, vol. 54, pp. 333-43, May 20 1997.
[24] Y. Farjoun and J. C. Neu, "Exhaustion of nucleation in a closed system," Physical review. E, Statistical, nonlinear, and soft matter physics, vol. 78, p. 051402, Nov 2008.
[25] A. R. Hurshman, J. T. White, E. T. Powers, and J. W. Kelly, "Transthyretin aggregation under partially denaturing conditions is a downhill polymerization," Biochemistry, vol. 43, pp. 7365-81, Jun 15 2004.
[26] R. K. Brummitt, D. P. Nesta, L. Chang, A. M. Kroetsch, and C. J. Roberts, "Nonnative aggregation of an IgG1 antibody in acidic conditions, part 2: nucleation and growth kinetics with competing growth mechanisms," Journal of pharmaceutical sciences, vol. 100, pp. 2104-19, Jun 2011.
[27] A. Hawe, W. Friess, M. Sutter, and W. Jiskoot, "Online fluorescent dye detection method for the characterization of immunoglobulin G aggregation by size exclusion chromatography and asymmetrical flow field flow fractionation," Analytical biochemistry, vol. 378, pp. 115-22, Jul 15 2008.
[28] B. H. Zimm, "The dependence of the scattering of light on angle and concentration in linear polymer solutions," The Journal of physical and colloid chemistry, vol. 52, pp. 260-7, Jan 1948.
[29] V. Filipe, A. Hawe, and W. Jiskoot, "Critical evaluation of Nanoparticle Tracking Analysis (NTA) by NanoSight for the measurement of nanoparticles and protein aggregates," Pharmaceutical research, vol. 27, pp. 796-810, May 2010.
[30] S. M. Kelly, T. J. Jess, and N. C. Price, "How to study proteins by circular dichroism," Biochimica et biophysica acta, vol. 1751, pp. 119-39, Aug 10 2005.
[31] A. Aghaie, A. A. Pourfathollah, S. Z. Bathaie, S. M. Moazzeni, H. K. Pour, and S. Banazadeh, "Structural study on immunoglobulin G solution after pasteurization with and without stabilizer," Transfusion medicine, vol. 18, pp. 62-70, Feb 2008.
[32] T. Arakawa, D. Ejima, T. Li, and J. S. Philo, "The critical role of mobile phase composition in size exclusion chromatography of protein pharmaceuticals," Journal of pharmaceutical sciences, vol. 99, pp. 1674-92, Apr 2010.
[33] H. C. Mahler, R. Muller, W. Friess, A. Delille, and S. Matheus, "Induction and analysis of aggregates in a liquid IgG1-antibody formulation," European journal of pharmaceutics and

biopharmaceutics : official journal of Arbeitsgemeinschaft fur Pharmazeutische Verfahrenstechnik e.V, vol. 59, pp. 407-17, Apr 2005.
[34] J. G. Barnard, S. Singh, T. W. Randolph, and J. F. Carpenter, "Subvisible particle counting provides a sensitive method of detecting and quantifying aggregation of monoclonal antibody caused by freeze-thawing: insights into the roles of particles in the protein aggregation pathway," Journal of pharmaceutical sciences, vol. 100, pp. 492-503, Feb 2011.
[35] C. G. Rosen and G. Weber, "Dimer formation from 1-amino-8-naphthalenesulfonate catalyzed by bovine serum albumin. A new fluorescent molecule with exceptional binding properties," Biochemistry, vol. 8, pp. 3915-20, Oct 1969.
[36] B. Demeule, M. J. Lawrence, A. F. Drake, R. Gurny, and T. Arvinte, "Characterization of protein aggregation: the case of a therapeutic immunoglobulin," Biochimica et biophysica acta, vol. 1774, pp. 146-53, Jan 2007.
[37] J. T. Pelton and L. R. McLean, "Spectroscopic methods for analysis of protein secondary structure," Analytical biochemistry, vol. 277, pp. 167-76, Jan 15 2000.
[38] W. Jiskoot, M. Bloemendal, B. van Haeringen, R. van Grondelle, E. C. Beuvery, J. N. Herron, and D. J. Crommelin, "Non-random conformation of a mouse IgG2a monoclonal antibody at low pH," European journal of biochemistry / FEBS, vol. 201, pp. 223-32, Oct 1 1991.
[39] K. S. Vassilenko and V. N. Uversky, "Native-like secondary structure of molten globules," Biochimica et biophysica acta, vol. 1594, pp. 168-77, Jan 31 2002.
[40] A. P. Bom, M. S. Freitas, F. S. Moreira, D. Ferraz, D. Sanches, A. M. Gomes, A. P. Valente, Y. Cordeiro, and J. L. Silva, "The p53 core domain is a molten globule at low pH: functional implications of a partially unfolded structure," The Journal of biological chemistry, vol. 285, pp. 2857-66, Jan 22 2010.
[41] V. N. Uversky and O. B. Ptitsyn, "Further evidence on the equilibrium "pre-molten globule state": four-state guanidinium chloride-induced unfolding of carbonic anhydrase B at low temperature," Journal of molecular biology, vol. 255, pp. 215-28, Jan 12 1996.
[42] C. T. Huang, D. Sharma, P. Oma, and R. Krishnamurthy, "Quantitation of protein particles in parenteral solutions using micro-flow imaging," Journal of pharmaceutical sciences, vol. 98, pp. 3058-71, Sep 2009.
[43] K. Wuchner, J. Buchler, R. Spycher, P. Dalmonte, and D. B. Volkin, "Development of a microflow digital imaging assay to characterize protein particulates during storage of a high concentration IgG1 monoclonal antibody formulation," Journal of pharmaceutical sciences, vol. 99, pp. 3343-61, Aug 2010.
[44] A. Hawe, T. Rispens, J. N. Herron, and W. Jiskoot, "Probing bis-ANS binding sites of different affinity on aggregated IgG by steady-state fluorescence, time-resolved fluorescence and isothermal titration calorimetry," Journal of pharmaceutical sciences, Oct 18 2010.

Chapter 6

Fluorescence single particle tracking (fSPT) for the characterization of submicron protein aggregates in biological fluids and complex formulations

Vasco Filipe[1,2], Robert Poole[1], Marika Kutscher[1], Katrien Forier[3], Kevin Braeckmans[3], Wim Jiskoot[1]

[1] Division of Drug Delivery Technology, Leiden/Amsterdam Center for Drug Research, Leiden University, P.O. Box 9502, 2300 RA Leiden, The Netherlands

[2] Department of Pharmaceutics, Utrecht Institute for Pharmaceutical Sciences (UIPS), Utrecht University, P.O. Box 80082, 3508 TB, Utrecht, The Netherlands

[3] Biophotonic Imaging Group, Laboratory of General Biochemistry and Physical Pharmacy, Faculty of Pharmacy, Ghent University, Harelbekestraat 72, 9000 Ghent, Belgium

Pharmaceutical Research, 28(5):1112-20 (2011).

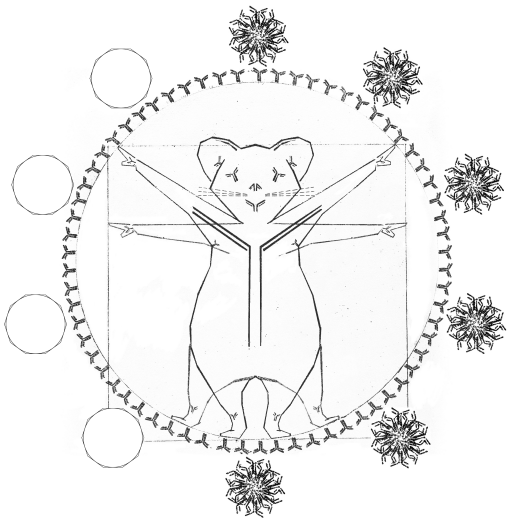

ABSTRACT

Purpose. To evaluate the potential of fluorescence single particle tracking (fSPT) for the characterization of submicron protein aggregates in human serum, plasma and in formulations containing human serum albumin (HSA).

Methods. A monoclonal IgG was covalently labeled with a fluorescent dye and cross-linked with glutaraldehyde. IgG aggregates and fluorescent beads of 0.1 μm (control) were diluted in buffer, serum and plasma, and their size distributions were analyzed by fSPT and nanoparticle tracking analysis (NTA). In a separate experiment, IgG and HSA, fluorescently labeled with different dyes, were mixed and subjected to heat-stress. The stressed sample was analyzed by fSPT using a *dual color mode* and by NTA.

Results. The accuracy and precision of fSPT proved to be comparable to NTA. fSPT was able to successfully measure all the samples in buffer, serum and plasma. The average size of the cross-linked protein aggregates showed a slight increase in biological fluids. Moreover, fSPT analysis showed that a significant proportion of the aggregates formed by subjecting an IgG/HSA mixture to heat-stress were composed of both proteins.

Conclusion. fSPT is a powerful technique for the characterization of submicron protein aggregates in biological fluids and complex formulations.

INTRODUCTION

Over the past few decades, therapeutic proteins have become established as a major drug class for the pharmaceutical industry. A major challenge in commercializing proteins as drug candidates is their inherent physical and chemical instability. Of the numerous degradation pathways, protein aggregation is a particular cause for concern [1, 2]. It is believed that protein aggregates may have the propensity in vivo to trigger an antibody response against the monomeric form of that protein, also known as unwanted immunogenicity [1, 3]. The presence of antibodies against a therapeutic protein can have serious clinical consequences, such as loss of therapeutic efficacy or even the neutralization of the equivalent endogenous protein [4]. Therefore, determination of the amount and type of aggregates necessary to allegedly trigger such immune reactions is of major importance both for pharmaceutical companies and regulatory agencies. With regard to their size, protein-containing samples can be very heterogeneous and individual aggregates can range in diameter from a few nanometers to several micrometers or larger [2, 5, 6].

A number of characterization tools are available for determining the size of protein aggregates, e.g. size exclusion chromatography and asymmetrical flow field-flow fractionation combined with UV and light scattering detectors, dynamic light scattering (DLS) and nanoparticle tracking analysis (NTA), analytical ultracentrifugation, light obscuration particle counting and micro flow imaging [7-11]. A major limitation of most of these techniques is that it is very difficult, if not impossible, to use them for analyzing therapeutic proteins or their aggregates in biological media. In fact, very little is known about the fate of protein pharmaceuticals following administration to a patient. To address this problem we set out to identify a new strategy and analytical tool that would allow us to characterize aggregates of a specific protein in the presence of serum or plasma.

Very recently, fluorescence Single Particle Tracking (fSPT) was suggested as a powerful method to size submicron matter in undiluted biological fluids [12]. Using fSPT, it was shown that the aggregation of fluorescently labeled liposomal drug carriers can be followed in real time in undiluted whole blood. In the present work we have evaluated the potential of the fSPT technique to detect and determine the size of submicron protein aggregates in serum and plasma. To this end we have covalently labeled the proteins of interest with a fluorescent probe. This strategy has previously been applied for the characterization of a specific protein interaction in human serum using analytical ultracentrifugation in an instrument modified to incorporate a fluorescence detection system [13]. The authors demonstrated that the fluorescence probe did not affect either the characteristics or the potency of the protein. The same labeling strategy may also be used to characterize the aggregates of therapeutic proteins in complex formulations, containing for example high amounts of stabilizing proteins, such as human serum albumin (HSA).

In this work, a monoclonal antibody (MAb) was fluorescently labeled without affecting its aggregation profile. Submicron MAb aggregates were generated by applying stress and these were successfully analyzed in biological fluids and in a formulation containing a large amount of HSA.

MATERIAL AND METHODS

Diluents

The formulation buffer used to prepare the polystyrene beads and proteins contained 10 mM sodium citrate (Merck, Darmstadt, Germany), 5% (w/v) sucrose

(Sigma-Aldrich, Buchs, Switzerland), pH 6.0. The formulation buffer was filtered using a 0.22-μm PES low binding syringe-driven filter unit (Millex™ GP, Millipore, Ireland).

Human serum and plasma were collected from three healthy volunteers free of medications. Serum was collected in Vacutainer SST tubes and plasma was collected in Vacutainer heparin tubes (Becton Dickinson, Franklin Lakes, USA). The plasma samples were centrifuged for 2 minutes at 2000 rpm with a Sigma 1-15 centrifuge (Osterode, Germany) mainly to spin down the red blood cells. The serum samples were centrifuged for 15 min at 3000 rpm in a Beckman Coulter Alegra X-12 centrifuge (Brea, USA) to remove all the blood cells and clotting factors. The serum and plasma samples were stored at 4°C for a maximum period of 48 hours before being used for measurements. The viscosities of the buffer, serum and plasma were measured in an AR-G2 rheometer from TA Instruments (New Castle, USA) at 37ºC. The average values used for sizing calculations are 0.80 cP, 1.29 cP and 1.30 cP for buffer, serum and plasma, respectively.

Preparation of fluorescent polystyrene beads

Polystyrene FluoSpheres carboxylate-modified microspheres with a nominal size of 0.1 μm, yellow-green fluorescent (excitation 505 nm/emission 515 nm), were purchased from Invitrogen (Merelbeke, Belgium) and covalently linked with methoxy-polyethylene glycol-amine (m-PEG-amine) (5000 daltons, Creative PEGWorks, Winston Salem, U.S.A.) polymer chains using a method adapted from Suh et al. in order to minimize interactions with serum components [14]. The fluorescent PEGylated beads were separately diluted with formulation buffer, serum and plasma until the concentration was acceptable for either NTA or fSPT measurements, i.e. 1:5,000 volume based dilution for NTA measurements and 1:1,000 volume based dilution for fSPT measurements.

Preparation of alexa fluor labeled IgG

Alexa Fluor 488, Alexa Fluor 546 and Alexa Fluor 594 carboxylic acid, N-hydroxysuccinimide esters were obtained from Invitrogen (Merelbeke, Belgium). IgG and HSA labeling was performed according to the manufacturer's instructions. In brief, a recombinant human MAb of the IgG_1 subclass [11] was prepared at a concentration of 10 mg/ml in 100 mM sodium phosphate (Fluka, Sigma-Aldrich, Buchs, Switzerland) pH 7.4. To this was added a solution of dye in DMSO (10 mg/ml)

to give a molar ratio of 4:1 (dye:protein). The same procedure was followed for HSA. A pH of 7.4 was chosen in order to achieve selective labeling of the amine termini. The samples were mixed and left for 1 hour at room temperature. The conjugates were purified by passing the samples through disposable PD10 desalting columns (GE Healthcare, Uppsala, Sweden) packed with Sephadex G25 medium that had been equilibrated with phosphate buffered saline (PBS). Finally the samples were dialyzed using a Float-A-Lyzer® G2 (Spectrum, Rancho Dominguez, USA) with a 100 kDa molecular weight cut-off membrane to remove excess of dye and to exchange the buffer from PBS back to the original formulation buffer (see Diluents subsection). The final labeling ratio achieved was about 4 Alexa Fluor 546 labels per IgG, about 2 Alexa Fluor 594 labels per IgG and about 2 Alexa Fluor 488 labels per HSA, according to the formula suggested by Invitrogen:

$$\frac{n_{Dye}}{n_{\mathrm{Pr}otein}} = \frac{A_{\max}}{\varepsilon_{Dye} \times c_{\mathrm{Pr}otein} \times l}$$

where n_{Dye} are the moles of dye, $n_{Protein}$ are the moles of protein, A_{max} is the measured absorbance at the dye's absorption maximum, ε_{Dye} is the molar extinction coefficient of the dye at its absorption maximum, $c_{Protein}$ is the molar protein concentration (determined by absorbance at 280 and corrected for the presence of dye, according to the correction formulas given by the dye supplier) and l is the path length.

Preparation of fluorescently labeled protein aggregates

Covalent aggregates of Alexa Fluor 546 labeled IgG (A546 IgG) were prepared by using glutaraldehyde (Sigma-Aldrich, Steinheim, Germany) as a cross-linker. The aggregates were obtained by incubating 0.5 mg/ml of A546 IgG with 0.2% (v/v) of glutaraldehyde for 2 minutes at room temperature. The cross-linking reaction was terminated by adding sodium borohydride (Sigma-Aldrich, Steinheim, Germany) at a final concentration of 0.008% (w/v). This reaction was then allowed to proceed for 24 h at room temperature. The sample was diluted 250 fold with the formulation buffer, serum or plasma before the fSPT analysis and 5 fold before the NTA measurements.

For the preparation of fluorescently labeled protein aggregates in a complex formulation, Alexa Fluor 594 labeled IgG (A594 IgG) was prepared at a concentration of 0.5 mg/ml in formulation buffer (see Diluents subsection) containing Alexa Fluor

488 labeled HSA (A488 HSA) at a concentration of 3.2 mg/ml. The sample was placed in a 1.5-ml reaction tube (Eppendorf, Hamburg, Germany) and incubated for 12 minutes at 74°C in a VWR Digital Heat Block (VWR, West Chester, USA). The sample was diluted 1,000 fold with the formulation buffer before the fSPT and 50 fold before the NTA measurements.

Nanoparticle tracking analysis (NTA)

NTA measurements were performed essentially as described before with a NanoSight LM20 (NanoSight, Amesbury, United Kingdom), equipped with a sample chamber with a 640-nm laser and a Viton fluoroelastomer O-ring [11]. The samples were injected in the sample chamber with sterile syringes (BD Discardit II, New Jersey, USA) and all measurements were performed at 37°C. The software used for capturing and analyzing the data was the NTA 2.0 Build 127. The samples were measured for 40 seconds with manual shutter and gain adjustments. Three measurements of the same sample were performed for the polystyrene beads and six measurements for the protein aggregates. The standard deviations of the mean size values were calculated from the values obtained in each measurement.

Light obscuration (LO)

LO measurements were performed on a PAMAS SVSS system (PAMAS GmbH, Rutesheim, Germany) equipped with a HCB-LD-25/25 sensor and a 1 ml syringe. Each sample was measured three times, with each measurement consisting of a pre-run volume of 0.3 ml followed by three runs of 0.2 ml at a flow rate of 10 ml/min. The measurement settings differ significantly from the United States Pharmacopeia (USP) method, but they were chosen in order to reduce sample volume, since it has been shown that small sampling volumes are appropriate for quantifying size and levels of subvisible particles at the amounts typically present in protein therapeutics [15]. The samples were diluted 100 fold with the formulation buffer before the measurements in order to keep the particle counts below the upper count limit of the device.

Fluorescence single particle tracking (fSPT)

The fSPT technique was recently described in detail elsewhere [12]. In short,

widefield laser illumination was provided to an inverted epi-fluorescence microscope (Nikon TE2000E, NIKON BELUX, Brussels, Belgium) for excitation of the fluorescently labeled sample. The fSPT setup was equipped with three solid state lasers: a 100 mW Calypso 491 nm (Cobolt, Solna, Sweden), a 75 mW Jive 561 nm (Cobolt) and a IQ1C 30 mW 636 nm (Power Technology, Little Rock, AR). Using a fast and sensitive electron-multiplying CCD camera (Cascade II:512; Roper Scientific, Tucson, AZ), videos were acquired (Nikon Elements R imaging software) of the fluorescently labeled protein aggregates diffusing in the medium (formulation buffer, serum, or plasma). A Nikon Plan Apochromat 100× NA1.4 oil immersion objective lens was used for imaging.

Using custom built software, diffusional motion trajectories were calculated for individual protein aggregates from the fSPT videos. Since the diffusion coefficient for each trajectory could be calculated, a distribution of diffusion coefficients was obtained by analyzing a large number of trajectories. A maximum entropy deconvolution algorithm was used to reduce statistical broadening and sampling noise in the distribution of diffusion coefficients. Finally, this distribution of diffusion coefficients was converted to a size distribution using the Stokes-Einstein equation for spherical particles:

$$d = \frac{kT}{3D\pi\eta}$$

where d is the particle diameter, k the Boltzmann constant, T the absolute temperature, η the dynamic viscosity of the solution and D the diffusion coefficient.

Each measurement consisted of the recording and analysis of ten videos of the same sample for the polystyrene beads and twenty videos for the protein aggregates. Each video was recorded for only 5 seconds in order to minimize photobleaching. The standard deviations of the mean size values were calculated from the values obtained in each video.

The upper and lower size and concentration limits of fSPT are hard to specify, since they are dependent on several complex analytical factors. The lower size limit for detecting a particle depends on the ratio between the background intensity and the number of photons that can be collected from that particle, which in turn is dependent on the brightness of the fluorescent label, the laser intensity and illumination time. Nevertheless, in our experiments particles as small as 50 nm could be successfully measured. The upper size limit is mostly related to the particle density and fluid viscosity, in such a way that particle sedimentation becomes the

limiting factor. In a general way, an upper size limit of about 1000 nm can be set for fSTP measurements.

With this technique, the upper limit of particle concentration is dictated by the optical resolution and the tracking algorithm, resulting in a maximum useful particle concentration that is typically in the nanomolar range [12]. Theoretically there is no lower limit of particle concentration, since the size is calculated for individual particles. However, it is clear that there should be a sufficient number of particles in the system to obtain good statistics within a reasonable time period.

Colocalization analysis

In order to verify whether IgG and HSA can form mixed aggregates, A594 IgG (red fluorescent) and A488 HSA (green fluorescent) were combined and the mixture was subsequently subjected to heat stress (12 minutes at 74°C). The resulting aggregate-containing solution was then analyzed by dual color fSPT.

Dual color is an fSPT mode in which videos can be recorded simultaneously in two different spectral ranges (green and red in this case), enabling separate video analysis and the detection of particle colocalization between both videos. Since aggregates are seen in fSPT videos as separate objects (spots of light), an object based algorithm was employed for quantification. For each frame of the movie, all green and red objects were identified by image processing (for details, see Braeckmans et al.) [16]. For each object, the contour and centre position was determined. A green object was considered colocalized with a red object if its center position fell within the contour of the red object. Vice versa, a red object was considered colocalized with a green object if its center position fell within the contour of the green object. By performing this analysis for all frames of a movie, the percentage of mixed aggregates relative to the pure IgG or HSA aggregates could be estimated.

RESULTS AND DISCUSSION

Fluorescent Polystyrene Beads in Biological Fluids

In line with previous studies we first verified that fSPT can accurately detect and size submicron particles in biological fluids [12]. PEGylated standard fluorescent polystyrene beads of 0.1 μm nominal size were separately diluted in buffer, serum and plasma, and the size distributions were then measured by fSPT (Fig. 6.1). The

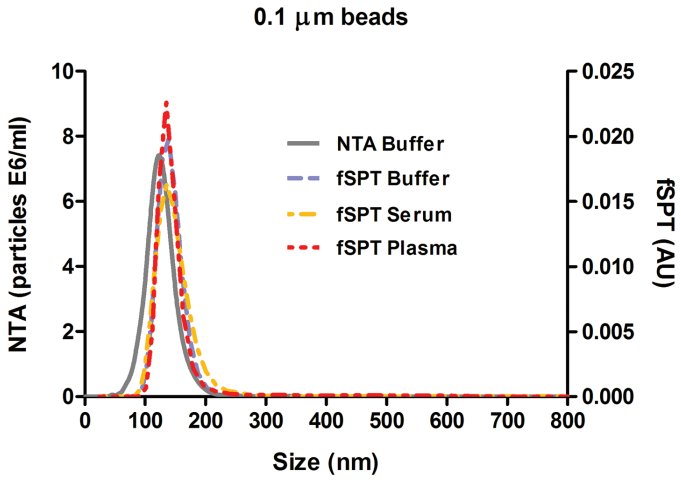

Figure 6.1: Size distribution from fSPT and NTA measurements of PEGylated fluorescent polystyrene beads in buffer, serum and plasma.

samples in buffer were also analyzed by NTA as a control, since both sizing techniques are based on the same principle of tracking individual particles and calculating the particle hydrodynamic size from the measured diffusion coefficient. However, the standard NTA instrument, as described by Filipe et al. [11], relies on light scattered by the particles and, therefore, cannot be used for biological media like serum or plasma which contain a variety of light scattering components.

The size distributions obtained by fSPT and NTA for the PEGylated beads in buffer are comparable, confirming the accuracy of fSPT to size nanoparticles. The mean size given by NTA was 129 ± 7 nm, while the mean sizes given by fSPT were 139 ± 10 nm in buffer, 143 ± 7 nm in serum and 142 ± 8 nm in plasma. The source of the small difference between the means given by the two techniques in buffer is unknown, but may have to do with the contribution of small impurities (between 50 and 120 nm) associated with the PEGylation process. Such impurities would decrease the NTA mean but can not be detected by fSPT, since they would not be fluorescent. In any case, the mean values are within the standard deviations obtained for both techniques. These standard deviations of the means are small and very similar between the two techniques, confirming the precision of fSPT.

The fSPT size distributions are also very similar in each of the media, indicating that the beads do not aggregate in biological fluids and that these fluids do not interfere with the fluorescence properties of the beads. Moreover, it can be concluded that the clotting factors, which are present in plasma and not in serum, have no major

effect on the size distribution of the beads. These results demonstrate the potential of this technique to measure the size distribution of nanoparticles in biological fluids.

Effect of Labeling on Aggregation Profile

With the aim of evaluating the effect of the fluorescent label on the aggregation profile of this specific IgG, a comparative aggregation study between A546 labeled and unlabeled IgG was performed. The samples were stressed by glutaraldehyde cross-linking under the same conditions and the aggregates were analyzed by NTA and LO (Fig. 6.2). Combined, these two techniques focus on the size range covered by fSPT (submicron range) and on the size range that can interfere with fSPT measurements (micron range).

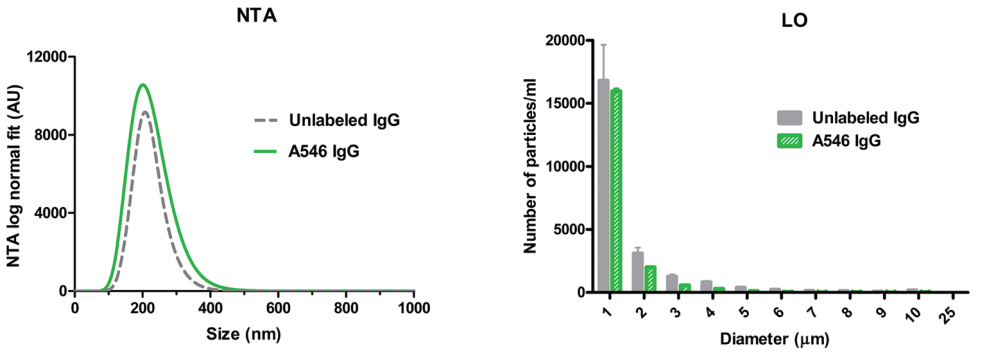

Figure 6.2: Size distribution from NTA and LO measurements in buffer of A546 IgG and unlabeled IgG aggregates induced by glutaraldehyde cross-linking.

The NTA size distribution of the labeled IgG samples is very similar to that of the unlabeled one. The height difference between the two peaks is within the variations inherent to the stress method itself and therefore should not be taken into account. The LO measurements also show a similar size distribution and particle count per size bin between the two samples. These results lead to the conclusion that this fluorescent label does not have a major impact on the aggregation profile in the subvisible and submicron range of this specific IgG with this particular stress method.

These findings should not be generalized for other proteins, other fluorescent labels or other stress methods. During optimization studies we verified that some fluorescent dyes may significantly change the aggregation profile of some proteins in certain given conditions (data not shown). Therefore, a case by case approach should be followed to evaluate the effect of a fluorescent label on a certain protein's

stability.

Covalent A546 IgG Aggregates in Biological Fluids

In order to evaluate the analytical performance of fSPT for protein aggregates in biological fluids, covalent submicron A546 IgG aggregates were analyzed in buffer, serum and plasma (Fig. 6.3). Glutaraldehyde cross-linked covalent aggregates were used since they cannot be dissociated and can be considered to be stable aggregates. Unstressed A546 IgG was also analyzed by fSPT in each of the media and was shown not to contain aggregates. As an additional control, the sample diluted in buffer was also measured by NTA. The size average of the A546 IgG aggregates in buffer measured with NTA was 215 ± 38 nm and with fSPT 198 ± 36 nm. The difference observed in peak width between the NTA and fSPT size distributions in

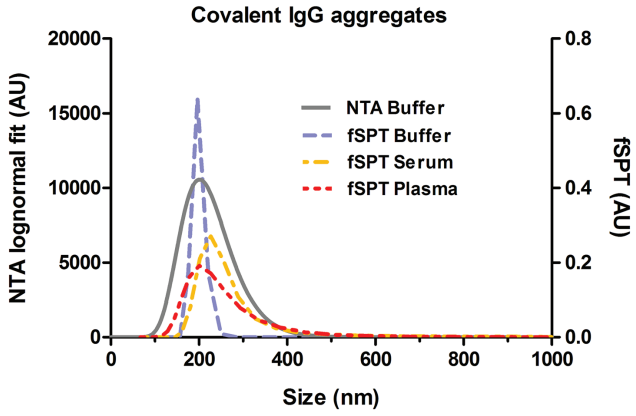

Figure 6.3: Size distribution from fSPT and NTA measurements of glutaraldehyde cross-linked A546 IgG in buffer, serum and plasma.

buffer can be attributed to a difference in the size analysis algorithm. In the fSPT sizing method used here, the raw size distribution as measured directly from the particle trajectories is refined by a maximum entropy deconvolution step that filters out statistical broadening and sampling noise so as to not over-interpret features in the distribution that are not statistically warranted by the data [12]. Although a similar function is available in the NTA software (model curve fitting), we chose to use the log-normal fit of the data for this sample, given that according to the manufacturer, this function should only be used for either very monodisperse or clearly bimodal samples. Another factor that can contribute to the difference in peak

width is the difference in optimal dilutions (50 fold) required for measurements with each technique, since higher dilutions may affect the aggregate size distribution [7].

These glutaraldehyde cross-linked aggregates showed an increase in their mean size in serum and plasma compared to buffer (198 ± 36 nm, 265 ± 38 nm and 245 ± 34 nm in buffer, serum and plasma, respectively). This size increase could be due self association of the aggregates or to interactions between the aggregates and other serum and plasma components, a phenomenon normally described as opsonization [17]. In general, opsonization is the adsorption of plasma components (i.e. opsonins) onto the surface of a foreign particle to render it more susceptible to phagocytosis. Opsonins include mainly immunoglobulins, blood clotting factors and components of the complement system [18, 19]. Given that the IgG used in this work is humanized and that IgG is one of the most abundant classes of proteins circulating in blood, one would not expect it to be opsonized. However, protein cross-linking with glutaraldehyde leads to a high amount of intermolecular and intramolecular cross-links, which normally lead to conformational changes [20-22]. Consequently, since opsonins bind to nanoparticles mainly via hydrophobic interactions, it is possible that these unnatural aggregates of conformationally changed IgG may lead to some opsonization [23].

Given that the size distribution of these aggregates is relatively the same in serum and in plasma, it is possible to conclude that the presence of clotting factors have little impact on the hypothetical opsonization, since they do not have a major effect on the size average of these aggregates.

A594 IgG Aggregates Formulated with A488 HSA

Over the last few decades, the need to stabilize therapeutic proteins progressively led to rather complex formulations containing sugars, surfactants, amino acids and even other proteins. However, such intricate environments often make the selective characterization of the therapeutic protein very difficult. For example, several therapeutic protein formulations contain high concentrations of HSA, which is known to act as a general stabilizer for liquid and lyophilized protein formulations by effectively inhibiting protein surface adsorption [24, 25]. Unfortunately, with most protein characterization tools it is virtually impossible to distinguish between the excipient HSA and the therapeutic protein without prior separation. When considering protein aggregates the situation becomes even more complex, as both the protein drug and HSA may form separate or mixed aggregates.

This section aims to show the potential of fSPT for the selective characterization of protein aggregates in formulations containing high amounts of HSA. For this purpose, A594 IgG was mixed with A488 HSA at an IgG:HSA concentration ratio of 1:6 (w/w); the mixture was heated in order to stimulate the formation of aggregates with diameters of the order of a hundred nanometers (monitored by fSPT). The sample was then analyzed by fSPT using dual color imaging (Fig. 6.4), whereby Alexa Fluor 488 and Alexa Fluor 594 labeled aggregates could be tracked simultaneously to examine whether HSA and IgG form mixed aggregates or not. The overall aggregate size was also measured by NTA, although it cannot distinguish between IgG aggregates, HSA aggregates or mixed aggregates (Fig. 6.4).

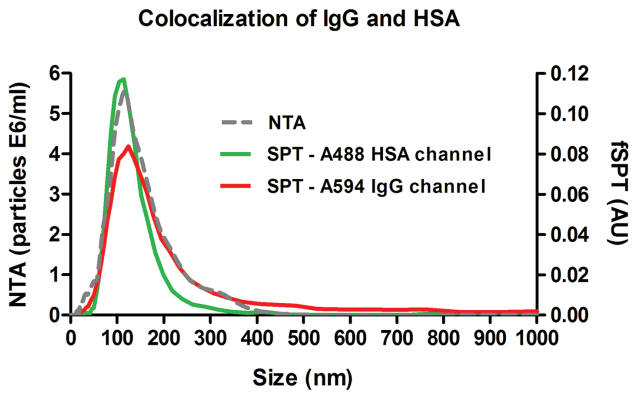

Figure 6.4: Size distribution from fSPT and NTA measurements of a heat-stressed mixture of A594 IgG and A488 HSA in buffer.

The average size of the aggregates determined by NTA was 152 nm. By fSPT, the average size of the IgG-containing and HSA-containing aggregates was 161 nm and 122 nm, respectively (Table 6.1). These results suggest that either the aggregates of both proteins have coincidently the same size range or that these aggregates are composed of both proteins. In order to clarify this uncertainty, the videos from both IgG (red fluorescence) and HSA (green fluorescence) channels were aligned and an object-based colocalization was calculated. A representative fSPT video frame is shown on Fig. 6.5, wherein colocalization is clearly visible (see also supplementary material for complete overlaid video). The results show that the IgG-containing aggregates colocalize significantly with the HSA-containing aggregates. About 70±9% of the aggregates tracked in the IgG channel were found to be colocalized with HSA-containing aggregates, while only about 36±4% of the aggregates tracked in the HSA channel colocalized with IgG-containing aggregates. The amount of aggregates

tracked in the HSA channel was approximately twice the amount of aggregates tracked in the IgG channel. This indicates that there were more HSA-containing aggregates than IgG-containing aggregates and this explains the low colocalization observed for the aggregates in the HSA channel. The fact that there were more HSA aggregates is not surprising considering the IgG:HSA concentration ratio of 1:6 (w/w). An example of this occurrence can be seen in Fig. 6.5, where two out of five HSA aggregates do not colocalize with IgG aggregates.

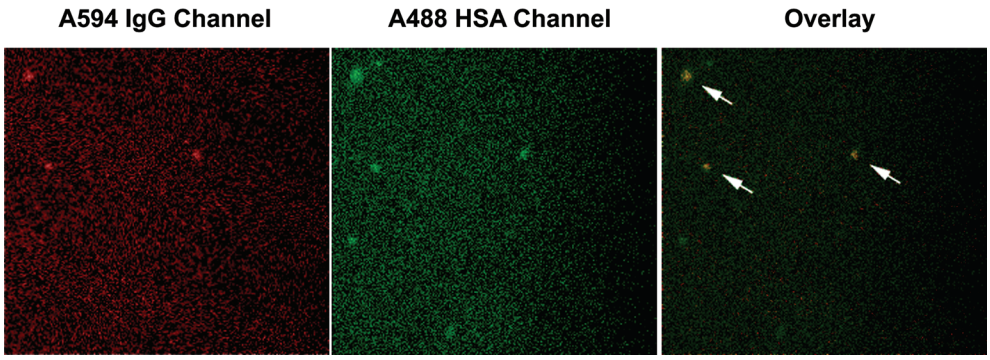

Figure 6.5: A video frame containing aggregates captured in the IgG and HSA channels using the *dual color mode* of fSPT, with the corresponding overlay image.

Table 6.1: Mean size from NTA and fSPT measurements of a heat-stressed mixture of A594 IgG and A488 HSA in buffer.

	fSPT		NTA
	Mean (nm)	**Colocalization (%)**	**Mean (nm)**
Scattering	-	-	152
A488 HSA Channel	122	36±4	-
A594 IgG Channel	161	70±9	-

Previous studies have already suggested the interaction between therapeutic proteins and HSA to form mixed-aggregates in solution, mainly by enzyme-linked immunosorbent assays [26, 27]. In the present study, using dual color fSPT, we were for the first time able to visualize and get a clear glimpse at the aggregation profile of therapeutic proteins in formulations containing HSA. Here, we have clearly demonstrated that under conditions of heat-stress, HSA can form mixed-aggregates with the therapeutic protein; in this case, IgG. Given that heat stress induces protein denaturation and consequently exposure of hydrophobic regions, it is likely that HSA starts to bind to the partially denatured intermediates of the therapeutic protein

and ends up involved in the overall aggregation process [25, 28]. In fact, the same heat stress was applied to the A594 IgG in a formulation without A488 HSA, and it resulted in a much higher amount of IgG aggregates with a higher size average, confirming the stabilizing properties of HSA in solution (data not shown).

It should be noted that control experiments in buffer with only one of the two proteins labeled indicated that the labeling of HSA or IgG did not change the size distribution. However, labeling of HSA (but not IgG) substantially reduced the amount of submicron aggregates (as measured by NTA), even though the amount of micron-sized aggregates (as measured by LO) remained approximately the same (data not shown). This may be due to the hydrophobic nature of the label and/or the (random) HSA labeling procedure. Further studies with other labels or different, site-specific labeling strategies should be done in order to understand and avoid this problem.

CONCLUDING REMARKS

In this work, we evaluated the potential of fSPT for the characterization of protein aggregates in biological fluids and HSA-containing formulations. fSPT gave comparable size distributions to NTA for aggregates and particles in buffer and has the added advantage that it can also be applied to look at samples in serum and plasma. It seems that some serum components adsorb to the beads and protein aggregates once these come into contact with biological fluids. fSPT has also been shown to be suitable for selectively analyzing protein aggregates in complex formulations, such as those containing HSA. Using dual color fSPT it was possible to verify that most of the IgG aggregates created by heat stress in a HSA-containing formulation were in fact composed of a mixture of IgG and HSA.

The requirement for prior labeling of the protein of interest with a fluorescent probe may be seen as a drawback of this technique. However, if it can be proven that the stability and aggregation profile of the proteins remain unaltered after the labeling, the potential of this technique to reveal the fate of protein aggregates in biological fluids is evident. This paves the way for several research areas, such as formulation and immunogenicity studies, where it is important to know if a certain therapeutic protein aggregates once injected into the blood stream or if certain types of aggregates disappear or change their size in biological fluids.

AKNOWLEDGEMENTS

This research is supported by the Dutch Technology Foundation STW, applied science division of NWO and the Technology Program of the Ministry of Economic Affairs. The authors are grateful to Mies van Steenbergen from the Utrecht Institute for Pharmaceutical Sciences for the viscosity measurements of all the diluents.

REFERENCES

[1] M. E. Cromwell, E. Hilario, and F. Jacobson, "Protein aggregation and bioprocessing," Aaps J, vol. 8, pp. E572-9, 2006.

[2] H. C. Mahler, W. Friess, U. Grauschopf, and S. Kiese, "Protein aggregation: pathways, induction factors and analysis," J Pharm Sci, vol. 98, pp. 2909-34, Sep 2009.

[3] A. S. Rosenberg, "Effects of protein aggregates: an immunologic perspective," Aaps J, vol. 8, pp. E501-7, 2006.

[4] H. Schellekens, "Bioequivalence and the immunogenicity of biopharmaceuticals," Nat Rev Drug Discov, vol. 1, pp. 457-62, Jun 2002.

[5] A. Hawe, J. C. Kasper, W. Friess, and W. Jiskoot, "Structural properties of monoclonal antibody aggregates induced by freeze-thawing and thermal stress," Eur J Pharm Sci, vol. 38, pp. 79-87, Sep 10 2009.

[6] J. F. Carpenter, T. W. Randolph, W. Jiskoot, D. J. Crommelin, C. R. Middaugh, G. Winter, Y. X. Fan, S. Kirshner, D. Verthelyi, S. Kozlowski, K. A. Clouse, P. G. Swann, A. Rosenberg, and B. Cherney, "Overlooking subvisible particles in therapeutic protein products: gaps that may compromise product quality," J Pharm Sci, vol. 98, pp. 1201-5, Apr 2009.

[7] J. S. Philo, "A critical review of methods for size characterization of non-particulate protein aggregates," Curr Pharm Biotechnol, vol. 10, pp. 359-72, Jun 2009.

[8] C. T. Huang, D. Sharma, P. Oma, and R. Krishnamurthy, "Quantitation of protein particles in parenteral solutions using micro-flow imaging," J Pharm Sci, vol. 98, pp. 3058-71, Sep 2009.

[9] W. Fraunhofer and G. Winter, "The use of asymmetrical flow field-flow fractionation in pharmaceutics and biopharmaceutics," Eur J Pharm Biopharm, vol. 58, pp. 369-83, Sep 2004.

[10] T. Arakawa and J. Wen, "Size-exclusion chromatography with on-line light scattering," Curr Protoc Protein Sci, vol. Chapter 20, p. Unit 20 6, Nov 2001.

[11] V. Filipe, A. Hawe, and W. Jiskoot, "Critical Evaluation of Nanoparticle Tracking Analysis (NTA) by NanoSight for the Measurement of Nanoparticles and Protein Aggregates," Pharm Res, Mar 4 2010.

[12] K. Braeckmans, K. Buyens, W. Bouquet-Geerardyn, C. Vervaet, P. Joye, F. De Vos, L. Plawinski, L. Doeuvre, E. Angles-Cano, N. Sanders, J. Demeester, and S. De Smedt, "Sizing nanomatter in biological fluids by fluorescence Single Particle Tracking," Nano Lett, 2010.

[13] B. Demeule, S. J. Shire, and J. Liu, "A therapeutic antibody and its antigen form different complexes in serum than in phosphate-buffered saline: a study by analytical ultracentrifugation," Anal Biochem, vol. 388, pp. 279-87, May 15 2009.

[14] J. Suh, K. L. Choy, S. K. Lai, J. S. Suk, B. C. Tang, S. Prabhu, and J. Hanes, "PEGylation of nanoparticles improves their cytoplasmic transport," Int J Nanomedicine, vol. 2, pp. 735-41, 2007.

[15] S. Cao, Y. Jiang, and L. Narhi, "A light-obscuration method specific for quantifying subvisible particles in protein therapeutics," Pharmacop Forum, vol. 36, pp. 824–34, 2010.

[16] K. Braeckmans, D. Vercauteren, J. Demeester, and S. C. De Smedt, “Single Particle Tracking in Nanoscopy multidimensional optical fluorescence microscopy,” A. Diaspro, Ed., ed: Taylor and Francis 2010.
[17] J. W. Yoo, E. Chambers, and S. Mitragotri, “Factors that Control the Circulation Time of Nanoparticles in Blood: Challenges, Solutions and Future Prospects,” Curr Pharm Des, vol. 16, pp. 2298-2307, 2010.
[18] S. M. Moghimi, A. C. Hunter, and J. C. Murray, “Long-circulating and target-specific nanoparticles: theory to practice,” Pharmacol Rev, vol. 53, pp. 283-318, Jun 2001.
[19] M. M. Frank and L. F. Fries, “The role of complement in inflammation and phagocytosis,” Immunol Today, vol. 12, pp. 322-6, Sep 1991.
[20] D. T. Cheung and M. E. Nimni, “Mechanism of crosslinking of proteins by glutaraldehyde II. Reaction with monomeric and polymeric collagen,” Connect Tissue Res, vol. 10, pp. 201-16, 1982.
[21] R. Usha and T. Ramasami, “Structure and conformation of intramolecularly cross-linked collagen,” Colloids Surf B Biointerfaces, vol. 41, pp. 21-4, Mar 10 2005.
[22] S. Hermeling, L. Aranha, J. M. Damen, M. Slijper, H. Schellekens, D. J. Crommelin, and W. Jiskoot, “Structural characterization and immunogenicity in wild-type and immune tolerant mice of degraded recombinant human interferon alpha2b,” Pharm Res, vol. 22, pp. 1997-2006, Dec 2005.
[23] A. Gessner, R. Waicz, A. Lieske, B. Paulke, K. Mader, and R. H. Muller, “Nanoparticles with decreasing surface hydrophobicities: influence on plasma protein adsorption,” Int J Pharm, vol. 196, pp. 245-9, Mar 10 2000.
[24] W. Wang, “Lyophilization and development of solid protein pharmaceuticals,” Int J Pharm, vol. 203, pp. 1-60, Aug 10 2000.
[25] P. McGoff and D. S. Scher, “Solution formulation of proteins/peptides,” in Protein Formulation and Delivery. vol. 175, E. J. McNally and J. E. Hastedt, Eds., ed New York: Informa Healthcare USA, Inc., 2000.
[26] A. Braun and J. Alsenz, “Development and use of enzyme-linked immunosorbent assays (ELISA) for the detection of protein aggregates in interferon-alpha (IFN-alpha) formulations,” Pharm Res, vol. 14, pp. 1394-400, Oct 1997.
[27] R. Kumarasamy, J. Bausch, D. Kopcha, S. Patel, and E. McGonigle, “An enzyme-linked immunosorbent assay (ELISA) for quantitation of adducts of granulocyte-macrophage colony stimulating factor (GM-CSF) and human serum albumin (HSA) in stressed solution mixtures,” Pharm Res, vol. 11, pp. 365-71, Mar 1994.
[28] W. Wang, S. Nema, and D. Teagarden, “Protein aggregation-Pathways and influencing factors,” Int J Pharm, Feb 24 2010.

SUPPLEMENTARY MATERIAL

http://www.ncbi.nlm.nih.gov/pmc/articles/PMC3073042/bin/11095_2011_374_MOESM1_ESM.avi

Chapter 7

Detection and characterization of subvisible aggregates of monoclonal IgG in serum

Vasco Filipe[1,2], Robert Poole[1], Olubukayo Oladunjoye[1], Kevin Braeckmans[3,4], Wim Jiskoot[1]

[1] Division of Drug Delivery Technology, Leiden/Amsterdam Center for Drug Research, Leiden University, P.O. Box 9502, 2300 RA Leiden, The Netherlands

[2] Department of Pharmaceutics, Utrecht Institute for Pharmaceutical Sciences (UIPS), Utrecht University, P.O. Box 80082, 3508 TB, Utrecht, The Netherlands

[3] Biophotonic Imaging Group, Laboratory of General Biochemistry and Physical Pharmacy, Faculty of Pharmacy, Ghent University, Harelbekestraat 72, 9000 Ghent, Belgium

[4] Center for Nano- and Biophotonics, Harelbekestraat 72, 9000 Ghent, Belgium

Accepted at the Journal of Pharmaceutical Research. DOI: 10.1007/s11095-012-0749-x (2012)

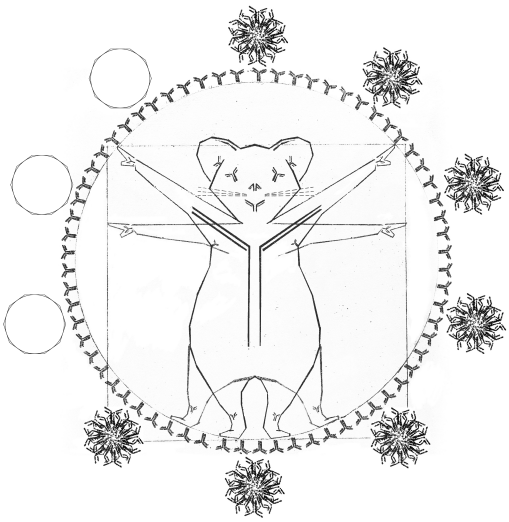

ABSTRACT

Purpose. To detect and characterize the aggregation of therapeutic monoclonal antibodies in undiluted biological fluids.

Methods. Fluorescently labeled subvisible IgG aggregates formed by applying either heat stress or by pH-shift were investigated immediately after addition to human serum, and after 24 hours. Unstressed and stressed IgG formulations were analyzed by fluorescence single particle tracking, confocal laser scanning microscopy and flow cytometry.

Results. Unstressed formulations remained free from subvisible aggregates in serum, whereas heat-stressed and pH-shift stressed formulations showed dissimilar aggregation behaviors. The aggregation profile of the heat-stressed formulation diluted in serum remained practically the same as the one diluted in buffer, even after the 24 hours incubation period. The pH-shift stressed formulation had strikingly smaller and more numerous subvisible aggregates immediately after dilution in serum compared to buffer. These aggregates became noticeably larger in both diluents after 24 hours, but in serum they appeared to be formed by other types of constituents than the labeled protein itself.

Conclusion. These results show that subvisible therapeutic protein aggregates may undergo changes in number, type and size distribution upon contact with human serum. This emphasizes the importance of analytical strategies for monitoring aggregation in undiluted biological fluids.

INTRODUCTION

Therapeutic proteins are an increasingly important class of drugs. However, their inherent tendency to aggregate during manufacture, shipping, storage and delivery remains a problem that hinders their development and commercialization [1-4]. The presence of aggregates in protein formulations is undesirable, not only because of reduced therapeutic efficacy due to loss of the active (usually monomeric) form of the protein, but also because it is believed that aggregates can trigger unwanted immunological responses once administered to patients [5-7]. The development of an immune response against a therapeutic protein can have serious clinical consequences, such as loss of therapeutic efficacy or even the neutralization of an equivalent endogenous protein [6]. Monitoring the amount and type of aggregates present in protein formulations has become a main concern for pharmaceutical companies and regulatory agencies over the last few decades.

Among the numerous types of protein aggregates, subvisible aggregates have received a lot of attention recently because of their potential immunogenicity in conjunction with the fact that they have been analytically overlooked until recent

years [3, 8]. Subvisible aggregates are typically between 0.1 and 50 μm in size and in the present work they are divided into micron- (1-50 μm) and submicron-sized (0.1-1 μm) aggregates. Such aggregates are a particular cause for concern because they mimic highly immunogenic viruses and bacteria both in terms of size range and in terms of the presence of closely spaced repetitive epitopes at their surface [9-11]. However, there remain no regulations against the presence of subvisible particles under the size of 10 μm in protein formulations and other parenteral solutions.

The characterization of protein aggregates is complex and requires the use of many different analytical techniques [3, 4, 12]. Until only a few years ago, subvisible aggregates posed a particular analytical challenge, mostly due to the lack of suitable techniques for their size range. This is now changing with the continuing development of new analytical techniques such as nanoparticle tracking analysis (NTA), flow microscopy and Taylor dispersion analysis (TDA) [13-17]. However, methods to investigate subvisible aggregates in serum are still lacking and very little is known about the fate of protein pharmaceuticals and their aggregates following administration to patients. The size and affinity of complexes between a therapeutic IgG and its antigen have shown to be different in buffer and serum [18], which reinforces the importance of studying therapeutic protein aggregates also in biological fluids.

The main obstacle that must be overcome in order to analyze aggregates of a specific therapeutic protein in biological fluids is that such fluids contain an extremely high amount of various proteins and other biological components, which have a camouflaging effect for most conventional analytical techniques. To overcome this problem we covalently labeled our protein of interest (IgG) to a fluorescent probe (Alexa Fluor® 488) in order to make it distinguishable from all the other biological components. A wide size range of protein aggregates was obtained by the individual manipulation of two pharmaceutically relevant stress factors: temperature and pH. Stressed and unstressed formulations were then introduced in undiluted human serum and subvisible aggregates were analyzed by three different fluorescence-based techniques: fluorescence single particle tracking (fSPT), confocal laser scanning microscopy (CLSM) and flow cytometry (FCM).

fSPT is an emerging technique for sizing fluorescent particles from about 50 nm to 1 μm. This technique combines a fluorescence microscope with widefield laser illumination and an electron-multiplying charge-coupled device camera, which enables the visualization, recording and size measurement of fluorescent particles moving under Brownian motion. fSPT has already proven to be efficient to size

submicron particles in undiluted biological fluids [19, 20].

CLSM is a powerful imaging technique that manages to eliminate out-of-focus light in areas that are thicker than the focal plane (ca. 0.75 μm). In this work we decided to use CLSM to monitor the aggregates in serum because this technique removes a great percentage of the background light coming from A488-IgG monomers, which enabled us to have clear images of the aggregates.

FCM is a well-established technique that has the capacity of simultaneously analyzing different parameters of individual particles at a very fast rate, ignoring all other particles that do not meet certain chosen criteria, i.e. serum components in our case. Even though FCM is most commonly used for cells and particles in the micron range, the potential of this technique for analyzing submicron particles is well-known and it has been explored to analyze nanoparticles in biological fluids [21-23].

This work shows that it is possible to answer some of the questions about the fate of biopharmaceuticals upon administration to patients. Monitoring the fate of therapeutic proteins and their aggregates in biological media may provide crucial information for drug development at various phases and help to understand some of the adverse reactions observed for some these drugs.

MATERIALS AND METHODS

IgG AND DILUENTS

A recombinant human monoclonal antibody of the IgG_1 subclass was used for this experiment at an initial concentration of 1 mg/ml. The buffer used to formulate and dilute the IgG contained 10 mM sodium citrate (Merck, Darmstadt, Germany), 5% (w/v) sucrose (Sigma-Aldrich, Buchs, Switzerland), pH 6.0. The buffer was filtered using a 0.22-μm PES low binding syringe-driven filter unit (Millex™ GP, Millipore, Ireland).

Human serum was collected from four healthy volunteers free of medications. The serum was collected in Vacutainer SST tubes (Becton Dickinson, Franklin Lakes, NJ, USA) and centrifuged for 15 min at 3000 rpm in a Beckman Coulter Alegra X-12 centrifuge (Brea, CA, USA) to remove all the blood cells and clotting factors. The serum samples were stored at 4 °C for a maximum period of six hours before being used for the experiment. The viscosity of the buffer and serum was measured in an AR-G2 rheometer from TA Instruments (New Castle, DE, USA) at 37 °C. The average

values obtained for buffer were 0.8 cP and for the four collected sera were 1.23, 1.29, 1.30 and 1.34 cP. These values were used for fSPT measurements, in order to obtain accurate size distributions in each diluent. The results in serum displayed in fSPT, CLSM and FCM graphs were chosen from a representative donor in each case.

Fluorescent labeling

Alexa Fluor 488 carboxylic acid, N-hydroxysuccinimide ester was obtained from Invitrogen (Merelbeke, Belgium). The IgG labeling was performed according to the manufacturer's instructions, using an IgG concentration of 10 mg/ml and a molar ratio of 4:1 (dye:IgG). A pH of 7.4 was chosen for the labeling buffer, in order to achieve selective labeling of the amine termini. The A488-IgG was dialyzed using a Float-A-Lyzer® G2 (Spectrum, Rancho Dominguez, CA, USA) with a 100 kDa molecular weight cut-off membrane to remove excess of dye and to exchange from the labeling buffer back to the original formulation buffer. The final A488-IgG concentration was 1 mg/ml and the labeling ratio achieved was about 2 A488 labels per IgG.

Preparation of IgG aggregates

The IgG aggregates were obtained by either heat or pH-shift stress. Both labeled and unlabeled IgGs were stressed at a concentration of 1 mg/ml. The heat stress consisted of incubating the A488-IgG at 74 °C for 12 minutes and the unlabeled IgG at 74 °C for 18 minutes. One ml of IgG formulation was placed in 1.5-ml reaction tubes (Eppendorf, Hamburg, Germany) and the incubation was performed on an Eppendorf Thermomixer® R (Hamburg, Germany). The pH-shift stress consisted of changing 5 times the buffer pH from pH 6 to pH 1 and back to pH 6 at room temperature. For each pH-shift cycle, hydrochloric acid (5 M) (Sigma-Aldrich, Steinheim, Germany) was slowly added drop wise to the IgG formulation in order to change the pH from 6.0 to 1.0. The samples were then kept for 1 minute at this low pH with constant stirring at 400 rpm with a stirring bar. Then, sodium hydroxide (5 M) (Sigma) was added drop wise to adjust the pH back to 6.0. Stirring by itself did not induce aggregation, according to different techniques. All stressed samples were kept at 4 °C until further use. A488-IgG stressed and unstressed formulations were diluted 50-fold in either buffer or serum before fSPT, CLSM and FCM measurements. These samples were analyzed right after the dilution and after an incubation period of 24 hours at 37 °C in a INB 400 Memmert incubator (Memmert, Schwabach, Germany).

Size exclusion chromatography (SEC)

SEC was performed on a TSK Gel 3000 SWXL column (Tosoh Bioscience, Montgomeryville, PA, USA), using a Thermo Separation Products Spectra System P4000 gradient pump (Thermo Scientific, Breda, The Netherlands), a Waters 717 plus autosampler (Waters, Milford, MA, USA) and a Spectra-Physics UV150 UV detector (Spectra-Physics, Irvine, CA, USA) at a 280 nm wavelength. The data was collected using ADChrom software version 3.5 (Agilent Technologies, Santa Clara, CA, USA). Fifty µl of each sample was injected and separation was performed at a flow rate of 0.5 ml/min. The running buffer was composed of 25 mM phosphate, 125 mM arginine, 0.025% (w/v) sodium azide at pH 7 (Sigma-Aldrich, Steinheim, Germany).

Sodium dodecyl sulfate polyacrylamide gel electrophoresis

SDS-PAGE was performed with a Biorad Mini-Protean 3 module (Bio-Rad, Hercules, CA, USA), as described previously [24]. Briefly, a 4–20% linear gradient Tris-HCl Ready Gel from Bio-Rad was run under non-reducing and reducing (sample buffer containing 5% (v/v) β-mercaptoethanol) conditions at 150 V at room temperature. The bands were detected by Coomassie Brilliant Blue R-250 staining and the gel was scanned with a Bio-Rad GS-800 densitometer and Quantity One software.

Nanoparticle tracking analysis

NTA measurements were performed with a NanoSight LM20 (NanoSight, Amesbury, United Kingdom), equipped with a sample chamber with a 640-nm laser and a Viton fluoroelastomer O-ring, as described previously [15]. Briefly, the samples were injected in the sample chamber with sterile BD Discardit II syringes (Becton, Dickinson and Company, Franklin Lakes, NJ, USA) until the liquid reached the tip of the nozzle. The software used for capturing and analyzing the data was the NTA 2.0 Build 127. The samples were measured for 40 seconds with manual shutter and gain adjustments. Six measurements of each sample were performed and the mean was obtained. The error shadows represent the standard deviations between the measurements. Stressed formulations were diluted 50-fold with buffer before each measurement.

Light obscuration (LO)

LO measurements were performed on a PAMAS SVSS system (PAMAS GmbH, Rutesheim, Germany) equipped with a HCB-LD-25/25 sensor and a 1- ml syringe. Each sample was measured three times, with each measurement consisting of a pre-run volume of 0.3 ml followed by three runs of 0.2 ml at a flow rate of 10 ml/ min. The final results are a mean of the three runs and the error bars represent the standard deviation between them. Stressed formulations were diluted 50-fold with buffer before each measurement.

Fluorescence single particle tracking

The fSPT technique was recently described in detail by Braeckmans et al [19]. The measurements were performed with an inverted epi-fluorescence microscope (Nikon TE2000E, NIKON BELUX, Brussels, Belgium) equipped with a Nikon Plan Apochromat 100× NA1.4 oil immersion objective lens, a 100 mW Calypso 491 nm laser (Cobolt, Solna, Sweden), an electron-multiplying CCD camera (Cascade II:512; Roper Scientific, Tucson, AZ) and the results were processed with Nikon Elements R imaging software combined with custom build software. Each measurement consisted of the recording and analysis of 10 or 20 videos of the same sample, with the number of videos depending on the amount of aggregates in each sample. Each video was recorded at 35 frames per second for 5 s only in order to minimize photobleaching. At least 3 measurements from each stressed formulation were performed in buffer and 1 measurement for each blood donor.

Confocal laser scanning microscopy

CLSM images were obtained using the Argon blue laser (488 nm) from a Bio-Rad Radiance 2100 MP confocal laser scanning system (Bio-Rad, Hercules, CA, USA) equipped with a Nikon Eclipse TE2000-U inverted fluorescence microscope and a 60x A/1.4 oil Nikon objective (Nikon, Tokyo, Japan). LaserSharp 2000 v6.0 software (Bio-Rad, Hercules, CA, USA) was used for image acquisition and Adobe Photoshop CS5 (Adobe, San Jose, CA, USA) for image processing. A 4 µl drop of each sample was placed on a well of a 24 well Greiner SensoPlate (Greiner Bio-One, Alphen a/d Rijn, The Netherlands), covered with a glass coverslip (Menzel-Gläser, Braunschweig,

Germany) and immediately analyzed. Triplicates of each sample in buffer and serum from each donor were analyzed. The scans were made at a distance of about 10 μm from the glass surface, with the same settings for all submicron aggregates in both diluents. The settings had to be individually adjusted for each micron-sized aggregate in order to obtain sharp images. A rough estimation of the amount of aggregates bigger than ca. 5 μm/ml (i.e. aggregates that had a defined shape) was obtained by extrapolating the average amount of these aggregates present in each well (4 μl). At least 3 wells from each stressed formulation in buffer and serum were considered for these estimations.

Flow cytometry

FCM was performed with a BD FACSCanto II flow cytometer (Becton, Dickinson and Company, Franklin Lakes, NJ, USA). The data was collected with the BD FACSDiva 6.2 software and processed with the FlowJo 7.6.4 software (Tree Star, Ashland, OR, USA). The samples were analyzed with the lowest flow rate and the window extension was set to the minimum value (0.5) in order to minimize coincidence of particles in front of the detectors. The measurements were stopped after 2 minutes of data collection so that the number of events could be compared between samples. At least 3 measurements from each stressed formulation were performed in buffer and 1 measurement for each blood donor. The events were detected by the 530/30 (FITC) and 488/10 (side scatter) photomultiplier tubes (PMTs). Given that most of the aggregates present in our stressed formulations were in the submicron range, the PMT voltages were adjusted for this size range. A threshold of 300 was set for the FITC-PMT in order to eliminate background events from serum.

Yellow-green fluorescent (excitation 505 nm/emission 515 nm) polystyrene standards of 200, 500 and 2000 nm (Invitrogen, Merelbeke, Belgium) were used to optimize PMT voltages for submicron particles. These beads were also used to obtain an approximate size calibration for the protein aggregates, by direct comparison of side scatter intensity and by pulse width calibration (supplementary figure) [22, 25]. These two approaches gave similar aggregate size averages.

RESULTS

A first step in any study involving fluorescently labeled proteins is to identify if and how the presence of the fluorescent probe affects the behavior of the protein. In this

case the effect on the aggregation behavior was evaluated.

Labeling effect on protein aggregation

In this study Alexa Fluor® 488 (A488) was covalently linked to a humanized monoclonal antibody of the IgG_1 subclass (IgG). Incubation at a high temperature (heat stress) and short exposures to low pH (pH-shift stress) were the two stress methods used to obtain subvisible aggregates of both A488-IgG and unlabeled IgG. The effect that this fluorescent label had on the aggregation profile of this protein was monitored by complementary methods covering a broad size range: SEC, NTA and LO (Fig. 7.1).

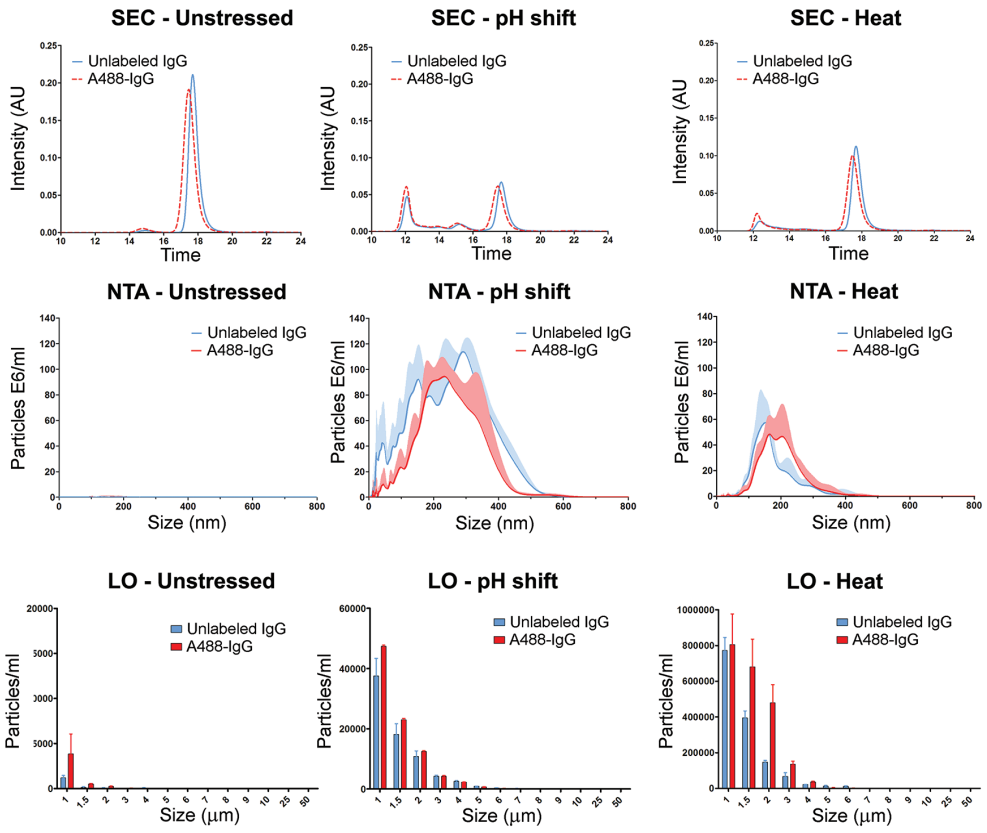

Figure 7.1: Aggregation profile of A488-IgG and unlabeled IgG formulations, after pH-shift and heat stresses. The top row graphs are chromatograms obtained by SEC with UV absorption detection at 280 nm. The middle row graphs show the aggregate size distribution obtained by NTA (submicron range) and the lower row graphs the distribution obtained by LO (micron range). The NTA and LO graphs contain standard deviations, represented by shadows and error bars, respectively.

These results show very similar aggregation profiles between the A488-IgG and unlabeled IgG, for both stressed and unstressed formulations. SEC results show approximately the same amount of monomer loss and the same pattern of aggregation after the stresses. The 0.2 min left-shift observed in all the SEC chromatograms of the A488-IgG is most likely associated with the slightly increased molecular weight caused by the fluorescent label. NTA and LO results show small differences in size distribution and particle counts between the A488-IgG and the unlabeled IgG aggregates, but they are within the errors associated with the stress methods and analytical procedure.

Aggregation profile characterization

The SEC chromatograms in Fig. 7.1 show that pH-shift stress induced a large monomer loss associated with the formation of dimers, trimers and larger oligomers. Heat stress led to a slightly smaller monomer loss and the formation of larger oligomers. It is important to notice that with SEC, aggregates larger than 500 kDa either pass through the void volume of the column and appear as a single peak (eluting at ca. 12 minutes) or they become trapped in the column due to their large size or non-specific binding [26]. In fact the protein recovery of the stressed samples was about 70% and 50% for the pH-shift and the heat stress samples, respectively. In order to obtain the size distribution of the larger oligomers, NTA and LO were used.

From the NTA results, it is clear that pH-shift stress induced a slightly higher amount and a more polydisperse distribution of submicron aggregates than heat stress. The NTA size averages of the pH-shift and heat-stressed formulations were about 280 nm and 180 nm, respectively. The LO results show a much higher amount of micron-sized aggregates induced by heat than by pH-shift stress. The main reason for the apparent absence of aggregates between 500 nm and 1 μm, when comparing NTA and LO results, is the 10^2 fold difference in the concentration range detected by these techniques. This means that most aggregates of these stressed formulations are in the submicron range.

Both stressed formulations were analyzed by sodium dodecyl sulfate polyacrylamide gel electrophoresis (SDS-PAGE) in order to detect the presence of covalent aggregates (Fig. 7.2).

Under non-reducing conditions all the formulations show a pronounced band at around 150 kDa, which corresponds to the molecular weight of IgG monomers. It is also possible to distinguish a clear band at the top of the heat stress lane, which

corresponds to covalent aggregates that due to their large size could not enter the gel matrix and therefore deposited on top of the gel. The lack of band at the top of the pH-shift lane suggests that the aggregates formed by this stress method were not covalent and therefore dissociate under the denaturing conditions caused by the presence of SDS.

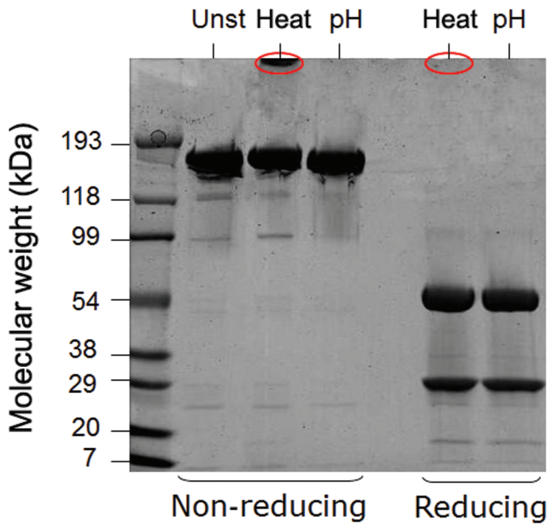

Figure 7.2: SDS-PAGE gel of unstressed (Unst), heat-stressed (Heat) and pH-shift (pH) stressed formulations under reducing and non-reducing conditions.

Under reducing conditions the intramolecular disulfide bonds of the IgG monomers break, originating two bands at around 25 kDa and 50 kDa, which correspond to the light and heavy chains, respectively. Moreover, the absence of a heat-stressed aggregate band (visible on top of the non-reducing gel) under reducing conditions substantiates the covalent, disulfide bond mediated nature of these aggregates.

Strategy to monitor subvisible aggregates in serum

In order to monitor the aggregation profile of A488-IgG in serum, unstressed, heat-stressed and pH-shift stressed formulations were diluted at 1:50 (v/v) ratio in buffer and human serum, and analyzed by fSPT, CLSM and FCM. The final IgG concentration after dilution in this experiment (0.02 mg/ml) is in the same order of magnitude as typical concentrations reached by therapeutic IgGs administered intravenously to humans [27, 28]. The samples were analyzed immediately after

dilution and after an incubation period of 24 hours at 37 °C.

Fluorescence single particle tracking

fSPT measurements of A488-IgG stressed formulations in buffer and serum are shown in Fig. 7.3. The unstressed formulation did not contain measurable amounts of submicron aggregates in either buffer or serum, even after the incubation period at 37 °C.

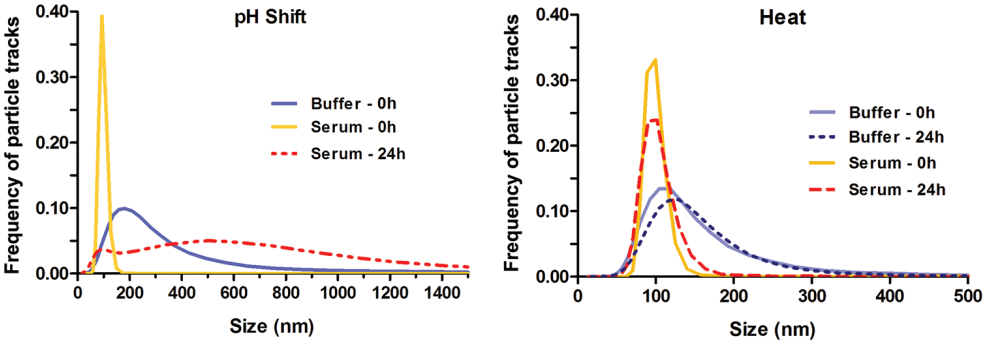

Figure 7.3: fSPT measurements of stressed A488-IgG formulations in buffer and in serum, immediately after dilution and after a 24 h at 37 °C.

The fSPT aggregate size distributions in buffer are consistent with the ones obtained by NTA, with size averages for the pH-shift and heat-stressed formulations of 292 nm and 137 nm, respectively (Table 7.1). The differences in size distribution smoothness given by these techniques are mostly due to their different approaches of data handling, as described previously [15, 19].

The size average of the aggregates in the pH-shifted formulation considerably decreased after dilution in serum, from 292 nm to 110 nm. In fact, the amount of aggregates observable through the microscope of this device was strikingly higher in serum right after dilution, but most of them were actually too small and faint for the software to track them properly. This suggests that most of these aggregates were smaller than 50 nm and/or composed of a mixture of A488-IgG and serum components, which would have resulted in aggregates with lower fluorescence intensity. Surprisingly, after the incubation period of 24 h at 37 °C most aggregates in buffer were micron-sized, i.e. beyond the range of fSPT to determine their size. In serum, most of the pH-shift aggregates also became bigger (ca. 460 nm), but not as much as in buffer.

In contrast, the heat-stressed aggregates showed only a small size average decrease when diluted in serum, from 137 nm to 102 nm. However, given that the error of these measurements is about 30 nm, the decrement is not noteworthy. These aggregates seemed to be stable after the 24 hours incubation period in both buffer and serum.

Confocal laser scanning microscopy

Even though CLSM is primarily used for imaging optical sections of micron-sized structures, the lower size limit of this technique can go beyond the typical optical microscope resolution (ca. 200 nm) if the particles analyzed are bright enough. In this study, while submicron aggregates were captured as mere dots, micron-sized aggregates displayed well-resolved shapes (Fig. 7.4). This enabled us to also monitor possible morphology and size changes of micron-sized aggregates in serum. It was not possible to distinguish any aggregates for the unstressed formulation in either buffer or serum, even after the incubation period at 37 °C.

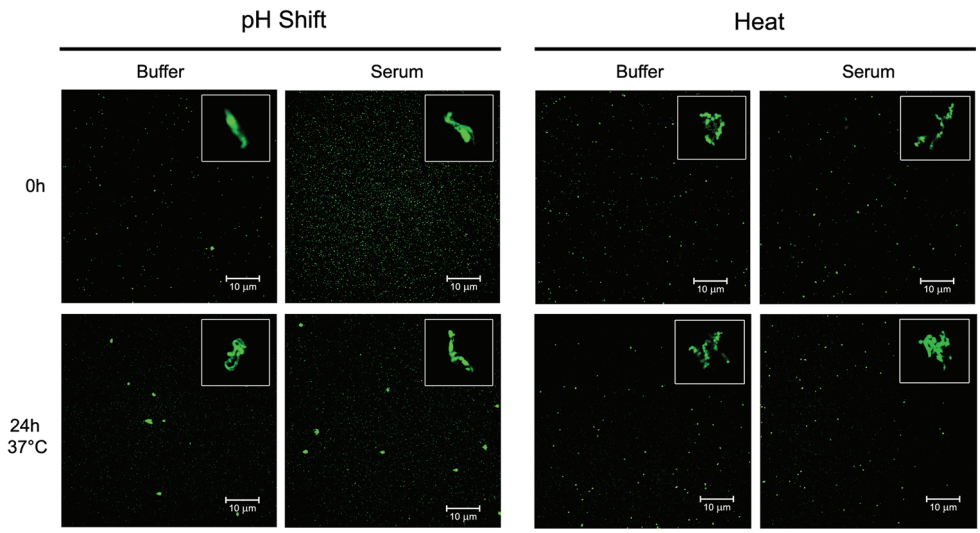

Figure 7.4: CLSM images of stressed A488-IgG formulations in buffer and serum, immediately after dilution (upper row) and after an incubation period of 24 h at 37 °C (lower row). A representative micron-sized aggregate is shown on the right upper corner of each image (same size scale).

The CLSM images show clear differences at time 0 h between the pH-shifted submicron aggregates in buffer and in serum. It is possible to observe that these

aggregates became smaller and more numerous immediately after being diluted in serum. After 24 hours at 37 °C these aggregates became visibly larger in both diluents, but in this case there were no obvious differences between them. On the other hand, heated submicron aggregates did not seem to change once diluted in serum, even after the incubation period. These observations are consistent with the size distributions obtained by fSPT.

The micron-sized pH-shift aggregates appear to have different morphology from the heat-induced aggregates. pH-shift seems to induce the formation of aggregates resembling clouds or popped balloons, whereas heat-induced aggregates appear to be assemblies of compact smaller units. The morphology and amount (Table 7.1) of these micron-sized aggregates seem to remain approximately the same in buffer and in serum, even after the incubation period.

Flow cytometry

Fluorescence vs. side scatter (SSC) plots of stressed formulations in buffer and serum are shown in Fig. 7.5. The unstressed formulation gave less than the minimum amount of displayable events for both diluents and both incubation times.

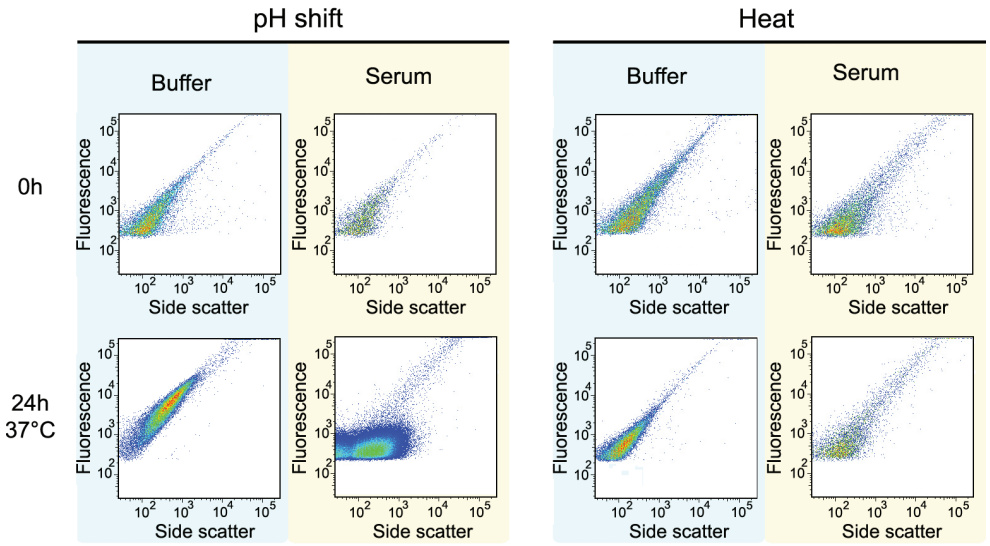

Figure 7.5: Fluorescence vs. side scatter FCM plots of stressed A488-IgG formulations in buffer and serum, immediately after dilution (upper row) and after an incubation period of 24 h at 37 °C (lower row). The dot density color gradient goes from blue (sparse) to red (very dense).

For submicron particles, SSC proved to be the most accurate indicator of particle size, whereas fluorescence intensity served as the selective parameter to distinguish A488-IgG aggregates from other serum components. An approximate calibration with fluorescent standard beads suggested that events with SSC signal of 10^2 are about 200 nm, 10^3 are about 500 nm and 10^4 are micron-sized (supplementary figure). Although light scatter also depends on the refractive index of the particles, in agreement with fSPT results FCM indicates that most aggregates present in both stressed formulations at time 0 h are about 200 nm. All plots at time 0 h display a linear positive correlation between fluorescence and SSC, indicating that as the size of the aggregates increases, their fluorescence also increases, as expected.

Table 7.1: fSPT mean size distribution and average aggregate concentrations from CLSM and FCM measurements of stressed A488-IgG formulations in buffer and serum, immediately after dilution and after an incubation period of 24 h at 37 °C. The errors represent the standard deviation between 3 different dilutions in buffer or between the measurements in serum of the different blood donors.

Analytical Method	Sample	pH-shift	Heat
fSPT mean (nm)	Buffer 0h	292 ±47	137 ±38
	Serum 0h	110 ±32	102 ±27
	Buffer 24h	N/A	150 ±46
	Serum 24h	463 ±81	112 ±41
CLSM [(particles>5μm) ×10^3/ml]	Buffer 0h	10 ±2	33 ±7
	Serum 0h	12 ±3	40 ±5
	Buffer 24h	9 ±3	35 ±4
	Serum 24h	11 ±3	35 ±7
FCM (counts×10^3)	Buffer 0h	12 ±2	11 ±2
	Serum 0h	4 ±1	6 ±2
	Buffer 24h	30 ±8	10 ±3
	Serum 24h	90 ±42	5 ±2

Both stressed formulations show the same dot distribution in serum as in buffer at time 0 h, but the number of events of the pH-shifted and heated formulations in serum is 3 and 2 times lower, respectively (Table 7.1). This occurrence was also observed for fluorescent standard beads, in which the number of events was about 2 times lower in serum than in buffer. Serum seems to have some sort of a masking effect for this technique, most likely caused by its translucent properties. The presence of serum components might lead to secondary scattering and absorption of both the incoming light beam and the scattered or emitted light from the aggregates, eventually resulting in a smaller amount of particle counts.

After the 24 hours incubation period, the heat-stressed plot does not suffer any significant changes in both the position of the main population and the number of events (Table 7.1). On the other hand, the main population of the pH-shifted formulation shows a clear shift towards higher values of SSC and fluorescence in buffer after the incubation period, which confirms the formation of larger aggregates. Surprisingly, in serum, the main population shows a shift towards higher SSC, but the fluorescence signal remains the same. The different position of the main population in the 24 h pH-shift plots suggests that the large aggregates formed in serum are somehow different from the ones formed in buffer. Moreover, the number of events after the incubation period increased and it is about 3 times higher in serum than in buffer (Table 7.1).

DISCUSSION

According to the SDS-PAGE results (Fig. 7.2), heat stress led to the formation of covalent IgG aggregates, whereas pH-shift stress did not. The nature of these covalent bonds is probably disulfide mediated, as the aggregates were not detected by SDS-PAGE under reducing conditions. Both heat and pH-shift stress conditions are expected to induce at some degree of unfolding, but through distinct driving forces. Protein unfolding normally results in the exposure of hydrophobic regions and eventually, in the case of IgG, free cysteins [29]. Protein unfolding is normally followed by aggregation, mostly mediated by hydrophobic effects [30]. In the case of heat stress, the formation of intermolecular disulfide bonds is probably facilitated by the high temperature, either by two free cysteins or by thiol-disulfide exchange. Disulfide bonds have smaller dissociation energies than other covalent bonds in the protein and are susceptible to breakage under the reducing conditions used in SDS-PAGE [31]. On the other hand, for the pH-shift sample, the low pH prevents the dissociation of thiol groups and consequently the formation of disulfide bonds is hindered [32]. This may explain the lack of covalent aggregates at the top of the gel under non-reducing conditions for the pH-shift sample.

The effect that a fluorescent label and a stress factor may have on the aggregation profile of therapeutic proteins, and how this will affect their fate in serum, may vary significantly according to the type of protein, label, stress factor and stress conditions [33-35]. Therefore, the results obtained in this study should not be generalized for other proteins or fluorescent labels and a case-by-case approach should be followed.

From all the fluorescent dyes previously tested for this study (Alexa Fluor® 488,

546, 555, 594 and 700), A488 was the one that least changed the aggregation behavior of this IgG for the chosen stress methods (data not shown). However, during optimization studies we noticed that the heat-induced aggregation kinetics of the A488-IgG was slightly different from the unlabeled IgG. At the same temperature, the evolution of the aggregate size distribution was the same, but the A488-IgG had the tendency to arrive faster to these aggregation states. Thus, in order to obtain stressed formulations of labeled IgG with a similar aggregate size distribution as the unlabeled IgG, the heating time of A488-IgG was a few minutes shorter than the one used for unlabeled IgG. Nevertheless, a comparable aggregate size distribution for heated A488-IgG and unlabeled IgG was achieved.

Interestingly, heat-stressed aggregates turned out to be the most measurably stable aggregates in both serum and buffer throughout the incubation period. Therefore, even though the presence of the fluorescent label led to a slightly lower degree of stability of this IgG, this does not seem to have significant consequences for the aggregation state of this protein in serum.

The subvisible aggregates of the pH-shifted formulation were very unstable in serum. The size reduction immediately after dilution in serum was consistently shown by fSPT and CLSM. FCM results did not clearly show this size reduction, most probably because most of them fall under the detection limits of this technique. This size reduction was quite surprising, since in our previous work, in which we tested the potential of fSPT to monitor glutaraldehyde cross-linked covalent aggregates in biological fluids, a slight size increase in serum and plasma was observed, presumably because of adsorption of serum components to these aggregates [20]. In the present work, pH-shift aggregates not only became smaller but also much more numerous immediately after dilution in serum. Also the heat-stressed aggregates showed a slight size decrease in serum according to fSPT, although to a lesser extent, which may be due to the partly covalent nature of these aggregates (Fig. 7.2). These results suggest that something more complex is happening with non-covalent IgG aggregates upon dilution in serum.

The appearance of a very large amount of submicron aggregates in the pH-shifted formulation immediately after dilution in serum was remarkable. Such a high amount suggests that these aggregates derived not only from preexisting aggregates but probably also from unstable monomers. At extreme pH's proteins are heavily charged, which eventually leads to chemical changes and at least partial unfolding of every monomer in solution [30]. When the pH is restored to the original formulation buffer, it is likely that some of these monomers remain partially

unfolded. Heat stress also leads to chemical changes and the formation of unfolded states, but by different processes [36]. Thus, it is possible that in our case the heat-induced unfolded states were more reversible than the ones caused by pH-shift stress. The presence of unstable pH-shifted monomers and aggregates could then have triggered a multitude of pathways in serum that could have led to the formation of these numerous small submicron aggregates.

The formation of larger subvisible aggregates in both serum and buffer after the incubation period for the pH-shift formulation was also surprising. The aggregation profile of these aggregates had proven to be stable for several weeks, but something as trivial as a dilution with the same buffer induced an aggregate-size increase. This occurrence shows how complex and unpredictable aggregated species can be. This A488-IgG aggregate size increase upon dilution after 24 h was confirmed with unlabeled IgG and it also happened at 4 °C, but to a lesser extent (data not shown). These results support the concerns about on the one hand analytical techniques for protein aggregates involving dilutions, such as SEC and field flow fractionation, and on the other hand changes that may occur after e.g. intravenous administration which is followed by rapid dilution [37].

FCM results suggest that the large pH-shift aggregates formed in serum after the incubation time had a different composition from the ones in buffer. The observation that large aggregates formed in serum were considerably less fluorescent than the ones formed in buffer, led to the hypothesis that the former are composed of a mixture of A488-IgG and other, non-fluorescing serum components. Adsorption of serum proteins to nanoparticles and other biological materials upon dilution in a physiological environment has been reported [38]. In fact, pure self-association of A488-IgG molecules in such complex environments is highly unlikely, since specific binding between monomers of the same IgG is not to be expected.

Immunoglobulins are the second most abundant protein in blood and the amount of physiological pathways in which IgG can be involved is enormous [39]. Thus, identifying the components responsible for the pH-shift aggregate changes in serum can be very challenging. Nevertheless, we decided to briefly investigate if human serum albumin (HSA) or complement factor C1q could be involved in these changes. We chose these proteins because: HSA is the most abundant protein present in blood and is known for being a carrier for several proteins; C1q is known to bind to IgG only when it is aggregated, in order to activate the classical pathway of the complement system [39, 40]. The pH-shift formulation was diluted in buffer containing these proteins at their approximate serum concentration (HSA - 40 mg/ml; C1q - 0.1 mg/

ml), but no conclusive results were obtained (data not shown) [39, 41]. It is likely that a combination of several serum components is required to induce the changes observed in serum. This underscores the need for more research to understand the causes of the observed changes in the subvisible aggregate profile in serum.

The fact that micron-sized aggregates of both stressed formulations did not seem to change throughout the entire experiment is intriguing. Nevertheless, small changes in this size range could have been overlooked by CLSM. Therefore, all samples were also analyzed by FCM with settings optimized for the micrometer range, but no clear differences in particle counts, fluorescence intensity or scattering signal were observed (data not shown). Altogether, it seems that pH-shift induced micron-sized aggregates are more stable than submicron aggregates in serum.

The only condition stipulated by the United States Pharmacopeia (USP) for the presence of subvisible particles in therapeutic protein formulations as well as other parenteral solutions (standard <788>) states that particles > 10 μm should be controlled below 6000 particles/container and particles > 25 μm below 600 particles/container. However, there are no studies that would support the idea that submicron and micron-sized aggregates are less immunogenic than visible precipitates (>50 μm) [8]. In fact, our stressed samples would have passed USP standards and yet most of the product is under the form of potentially immunogenic aggregates, which subsist after dilution in serum.

CONCLUSIONS

The fate and behavior of subvisible IgG aggregates in biological fluids has been investigated. Whilst unstressed IgG remains apparently unchanged in serum, i.e. it does not spontaneously aggregate, certain aggregates of the same protein do change. Aggregates formed by pH-shift appear particularly susceptible, whereas the ones formed by heat stress seem to be stable. These results indicate that the aggregation profile of therapeutic proteins may drastically change once the formulation is administered, emphasizing the importance of analytical strategies for monitoring aggregation in undiluted biological fluids.

REFERENCES

[1] M. E. Cromwell, E. Hilario, and F. Jacobson, “Protein aggregation and bioprocessing,” The AAPS journal, vol. 8, pp. E572-9, 2006.

[2] J. S. Bee, T. W. Randolph, J. F. Carpenter, S. M. Bishop, and M. N. Dimitrova, “Effects of surfaces

and leachables on the stability of biopharmaceuticals," Journal of pharmaceutical sciences, Apr 26 2011.
[3] H. C. Mahler, W. Friess, U. Grauschopf, and S. Kiese, "Protein aggregation: pathways, induction factors and analysis," Journal of pharmaceutical sciences, vol. 98, pp. 2909-34, Sep 2009.
[4] J. den Engelsman, P. Garidel, R. Smulders, H. Koll, B. Smith, S. Bassarab, A. Seidl, O. Hainzl, and W. Jiskoot, "Strategies for the assessment of protein aggregates in pharmaceutical biotech product development," Pharmaceutical research, vol. 28, pp. 920-33, Apr 2011.
[5] A. S. Rosenberg, "Effects of protein aggregates: an immunologic perspective," The AAPS journal, vol. 8, pp. E501-7, 2006.
[6] H. Schellekens, "Bioequivalence and the immunogenicity of biopharmaceuticals," Nature reviews. Drug discovery, vol. 1, pp. 457-62, Jun 2002.
[7] S. Hermeling, D. J. Crommelin, H. Schellekens, and W. Jiskoot, "Structure-immunogenicity relationships of therapeutic proteins," Pharmaceutical research, vol. 21, pp. 897-903, Jun 2004.
[8] J. F. Carpenter, T. W. Randolph, W. Jiskoot, D. J. Crommelin, C. R. Middaugh, G. Winter, Y. X. Fan, S. Kirshner, D. Verthelyi, S. Kozlowski, K. A. Clouse, P. G. Swann, A. Rosenberg, and B. Cherney, "Overlooking subvisible particles in therapeutic protein products: gaps that may compromise product quality," Journal of pharmaceutical sciences, vol. 98, pp. 1201-5, Apr 2009.
[9] V. Filipe, A. Hawe, H. Schellekens, and W. Jiskoot, "Aggregation and immunogenicity of therapeutic proteins," in Aggregation of therapeutic proteins, W. Wang and C. J. Roberts, Eds., ed New Jersey: John Wiley & Sons, 2010, pp. 403-433.
[10] W. Jiskoot, R. M. van Schie, M. G. Carstens, and H. Schellekens, "Immunological risk of injectable drug delivery systems," Pharmaceutical research, vol. 26, pp. 1303-14, Jun 2009.
[11] H. M. Dintzis, R. Z. Dintzis, and B. Vogelstein, "Molecular determinants of immunogenicity: the immunon model of immune response," Proceedings of the National Academy of Sciences of the United States of America, vol. 73, pp. 3671-5, Oct 1976.
[12] A. Hawe, J. C. Kasper, W. Friess, and W. Jiskoot, "Structural properties of monoclonal antibody aggregates induced by freeze-thawing and thermal stress," European journal of pharmaceutical sciences : official journal of the European Federation for Pharmaceutical Sciences, vol. 38, pp. 79-87, Sep 10 2009.
[13] S. K. Singh, N. Afonina, M. Awwad, K. Bechtold-Peters, J. T. Blue, D. Chou, M. Cromwell, H. J. Krause, H. C. Mahler, B. K. Meyer, L. Narhi, D. P. Nesta, and T. Spitznagel, "An industry perspective on the monitoring of subvisible particles as a quality attribute for protein therapeutics," Journal of pharmaceutical sciences, vol. 99, pp. 3302-21, Aug 2010.
[14] A. Hawe, W. L. Hulse, W. Jiskoot, and R. T. Forbes, "Taylor Dispersion Analysis Compared to Dynamic Light Scattering for the Size Analysis of Therapeutic Peptides and Proteins and Their Aggregates," Pharmaceutical research, May 11 2011.
[15] V. Filipe, A. Hawe, and W. Jiskoot, "Critical evaluation of Nanoparticle Tracking Analysis (NTA) by NanoSight for the measurement of nanoparticles and protein aggregates," Pharmaceutical research, vol. 27, pp. 796-810, May 2010.
[16] J. G. Barnard, S. Singh, T. W. Randolph, and J. F. Carpenter, "Subvisible particle counting provides a sensitive method of detecting and quantifying aggregation of monoclonal antibody caused by freeze-thawing: insights into the roles of particles in the protein aggregation pathway," Journal of pharmaceutical sciences, vol. 100, pp. 492-503, Feb 2011.
[17] K. Wuchner, J. Buchler, R. Spycher, P. Dalmonte, and D. B. Volkin, "Development of a microflow digital imaging assay to characterize protein particulates during storage of a high concentration IgG1 monoclonal antibody formulation," Journal of pharmaceutical sciences, vol. 99, pp. 3343-61, Aug 2010.
[18] B. Demeule, S. J. Shire, and J. Liu, "A therapeutic antibody and its antigen form different

complexes in serum than in phosphate-buffered saline: a study by analytical ultracentrifugation," Analytical biochemistry, vol. 388, pp. 279-87, May 15 2009.
[19] K. Braeckmans, K. Buyens, W. Bouquet, C. Vervaet, P. Joye, F. De Vos, L. Plawinski, L. Doeuvre, E. Angles-Cano, N. N. Sanders, J. Demeester, and S. C. De Smedt, "Sizing nanomatter in biological fluids by fluorescence single particle tracking," Nano letters, vol. 10, pp. 4435-42, Nov 10 2010.
[20] V. Filipe, R. Poole, M. Kutscher, K. Forier, K. Braeckmans, and W. Jiskoot, "Fluorescence single particle tracking for the characterization of submicron protein aggregates in biological fluids and complex formulations," Pharmaceutical research, vol. 28, pp. 1112-20, May 2011.
[21] H. Mach, A. Bhambhani, B. K. Meyer, S. Burek, H. Davis, J. T. Blue, and R. K. Evans, "The use of flow cytometry for the detection of subvisible particles in therapeutic protein formulations," Journal of pharmaceutical sciences, vol. 100, pp. 1671-8, May 2011.
[22] C. Tamerler and M. Sarikaya, "Genetically designed Peptide-based molecular materials," ACS nano, vol. 3, pp. 1606-15, Jul 28 2009.
[23] T. W. Odom and C. L. Nehl, "How gold nanoparticles have stayed in the light: the 3M's principle," ACS nano, vol. 2, pp. 612-6, Apr 2008.
[24] M. M. van Beers, M. Sauerborn, F. Gilli, V. Brinks, H. Schellekens, and W. Jiskoot, "Aggregated recombinant human interferon Beta induces antibodies but no memory in immune-tolerant transgenic mice," Pharmaceutical research, vol. 27, pp. 1812-24, Sep 2010.
[25] K. Seale, C. Janetopoulos, and J. Wikswo, "Micro-mirrors for nanoscale three-dimensional microscopy," ACS nano, vol. 3, pp. 493-7, Mar 24 2009.
[26] J. S. Philo, "A critical review of methods for size characterization of non-particulate protein aggregates," Current pharmaceutical biotechnology, vol. 10, pp. 359-72, Jun 2009.
[27] L. Peyrin-Biroulet, C. Laclotte, and M. A. Bigard, "Adalimumab maintenance therapy for Crohn's disease with intolerance or lost response to infliximab: an open-label study," Alimentary pharmacology & therapeutics, vol. 25, pp. 675-80, Mar 15 2007.
[28] D. Shealy, A. Cai, K. Staquet, A. Baker, E. R. Lacy, L. Johns, O. Vafa, G. Gunn, 3rd, S. Tam, S. Sague, D. Wang, M. Brigham-Burke, P. Dalmonte, E. Emmell, B. Pikounis, P. J. Bugelski, H. Zhou, B. Scallon, and J. Giles-Komar, "Characterization of golimumab, a human monoclonal antibody specific for human tumor necrosis factor alpha," mAbs, vol. 2, Jul 8 2010.
[29] C. Chumsae, G. Gaza-Bulseco, and H. Liu, "Identification and localization of unpaired cysteine residues in monoclonal antibodies by fluorescence labeling and mass spectrometry," Analytical chemistry, vol. 81, pp. 6449-57, Aug 1 2009.
[30] W. Wang, S. Nema, and D. Teagarden, "Protein aggregation--pathways and influencing factors," International journal of pharmaceutics, vol. 390, pp. 89-99, May 10 2010.
[31] J. Zhao, D. Xu, K. Zhang, and X. Cheng, "Quantum chemical study of C–SH bond dissociation energies for some thiol compounds," Comp. Theor. Chem., vol. 909, pp. 9-12, 2009.
[32] B. Alvarez, G. Ferrer-Sueta, B. A. Freeman, and R. Radi, "Kinetics of peroxynitrite reaction with amino acids and human serum albumin," The Journal of biological chemistry, vol. 274, pp. 842-8, Jan 8 1999.
[33] D. B. Volkin and C. R. Middaugh, "Vaccines as physically and chemically well-defined pharmaceutical dosage forms," Expert review of vaccines, vol. 9, pp. 689-91, Jul 2010.
[34] R. E. Crandall, J. Janatova, and J. D. Andrade, "The effects of radioiodination and fluorescent labelling on albumin," Preparative biochemistry, vol. 11, pp. 111-38, 1981.
[35] W. Wang, N. Li, and S. Speaker, "External factors affecting protein aggregation," in Aggregation of therapeutic proteins, W. Wang and C. J. Roberts, Eds., ed New Jersey: John Wiley & Sons, 2010, pp. 119-204.
[36] Q. Luo, M. K. Joubert, R. Stevenson, R. R. Ketchem, L. O. Narhi, and J. Wypych, "Chemical modifications in therapeutic protein aggregates generated under different stress conditions," The

Journal of biological chemistry, Apr 25 2011.
[37] J. S. Philo, “Is any measurement method optimal for all aggregate sizes and types?,” The AAPS journal, vol. 8, pp. E564-71, 2006.
[38] P. Aggarwal, J. B. Hall, C. B. McLeland, M. A. Dobrovolskaia, and S. E. McNeil, “Nanoparticle interaction with plasma proteins as it relates to particle biodistribution, biocompatibility and therapeutic efficacy,” Advanced drug delivery reviews, vol. 61, pp. 428-37, Jun 21 2009.
[39] M. W. Turner and B. Hulme, The plasma proteins: an introduction. London: Pitman Medical & Scientific Publishing 1970.
[40] W. Augener, H. M. Grey, N. R. Cooper, and H. J. Muller-Eberhard, “The reaction of monomeric and aggregated immunoglobulins with C1,” Immunochemistry, vol. 8, pp. 1011-20, Nov 1971.
[41] R. J. Ziccardi and N. R. Cooper, “The subunit composition and sedimentation properties of human C1,” Journal of immunology, vol. 118, pp. 2047-52, Jun 1977.

SUPPLEMENTARY FIGURE

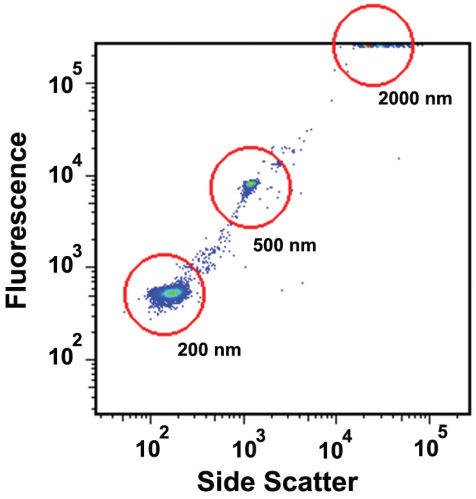

Fluorescence vs side scatter FCM plot of a mixture of 200, 500 and 2000 nm fluorescent beads in buffer. The dot density color gradient goes from dark blue (sparse), light blue (dense) to red (very dense).

Chapter 8

In vivo fluorescence imaging of IgG and IFN-α aggregates: a feasibility study

Vasco Filipe[1,2], Grzegorz Kijanka[2], Vera Brinks[2],
Huub Schellekens[2], Wim Jiskoot[1]

[1] Division of Drug Delivery Technology, Leiden/Amsterdam Center for Drug Research, Leiden University, P.O. Box 9502, 2300 RA Leiden, The Netherlands

[2] Department of Pharmaceutics, Utrecht Institute for Pharmaceutical Sciences (UIPS), Utrecht University, P.O. Box 80082, 3508 TB, Utrecht, The Netherlands

Pilot study

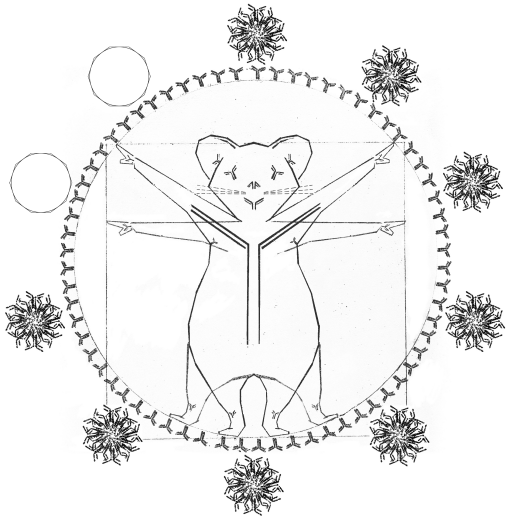

SUMMARY

Protein aggregation is a major concern as it may induce immunogenicity and thereby compromise the safety and efficacy of biopharmaceuticals. However, the mechanisms by which protein aggregates can elicit immune responses are largely unknown. The aim of this pilot study was to investigate the feasibility of *in vivo* fluorescence imaging of Alexa Fluor® 700 labeled protein (aggregates) in mice and to compare the localization of intraperitoneally injected non-aggregated and aggregated formulations of a human monoclonal antibody (IgG) and recombinant human interferon alpha 2a (IFN-α) over time. The formation of IFN-α aggregates was induced by metal-catalyzed oxidation and IgG aggregates by shaking stress. Stressed and unstressed formulations were analyzed by size exclusion chromatography (SEC) and light obscuration (LO). They were then injected intraperitoneally in mice and images were captured with a fluorescence optical imaging (FOI) system over time. SEC results indicated that the stressed IgG formulation contained about 58% aggregates and the IFN-α stressed formulation about 84%. A considerably high amount of micron-sized aggregates was detected by LO in the IgG stressed formulation, but not in the IFN-α stressed formulation. For both proteins, images captured by FOI showed differences in elimination rates and accumulation regions between aggregated and non-aggregates formulations. These results show that *in vivo* fluorescence imaging of fluorescently labeled protein aggregates is possible and that the presence of protein aggregates likely affects the biodistribution of therapeutic proteins, but clearly more research is needed in order to confirm these results and to obtain quantitative data. The fluorescent labeling of protein (aggregates) combined with FOI may help us to understand the connection between pharmacokinetics, biodistribution and immunogenicity of (aggregated) proteins.

INTRODUCTION

The vast majority of biopharmaceuticals elicit anti-drug antibodies (ADAs) in patients. Among all the factors influencing the incidence of immunogenicity, the presence of protein aggregates in therapeutic protein formulations has been put forward as a major concern [1]. Nevertheless, the immunological mechanism of antibody formation by protein aggregates is largely unknown. In fact, very little is known about fate of protein aggregates following administration to patients.

The presence of aggregates may affect pharmacokinetic/pharmacodynamic (PK/PD) properties of protein therapeutics. The loss of the active (usually monomeric) protein to aggregated species may result in decreased biological activity and, consequently, in reduced therapeutic efficacy [2]. The presence of particulates in drugs administered intravenously has been shown to decrease microcirculation as

a consequence of the mechanical blockage of capillaries [3] and the same situation may occur with aggregates of therapeutic proteins. It is known that ADAs may drastically change PK/PD properties of therapeutic drugs [4], but it may well be that the other way around also occurs, i.e. altered PK/PD properties (eventually caused by the presence of aggregates) may contribute to the formation of ADAs. For example, increased drug half-life means that the therapeutic protein will remain visible to the immune system for a longer period, which may increase the probabilities of an immune response.

This chapter summarizes a pilot study performed to test the feasibility of following over time the fate of fluorescently labeled IgG and recombinant human interferon alpha 2a (IFN-α) aggregates in immune tolerant transgenic (TG) mice. Size exclusion chromatography (SEC) and light obscuration were used to confirm the presence of aggregates in stressed formulations. Using a fluorescence optical imaging (FOI) system, the localization/bioaccumulation and elimination of therapeutic protein aggregates were observed and compared with the ones of the corresponding monomers.

MATERIAL AND METHODS

Materials

A recombinant human monoclonal antibody of the IgG_1 subclass was formulated in 10 mM sodium citrate (Merck, Darmstadt, Germany), 5% (w/v) sucrose (Sigma-Aldrich, Buchs, Switzerland), pH 6.0. Recombinant human IFN-α 2a was formulated in sodium phosphate buffer (PBS) (Braun Medical B.V., Oss, The Netherlands). The buffers were filtered using a 0.22-μm PES low binding syringe-driven filter unit (Millex™ GP, Millipore, Ireland). Sodium phosphate, sodium sulfate, sodium azide, copper chloride, ascorbic acid and ethylenediaminetetraacetic acid (EDTA) were purchased from Sigma-Aldrich.

Fluorescent labeling

Alexa Fluor® 700 carboxylic acid, N-hydroxysuccinimide ester was obtained from Invitrogen (Merelbeke, Belgium). The labeling of both IgG and IFN-α was performed according to the manufacturer's instructions, using a protein concentration of 10 mg/ml and a molar ratio of 4:1 (dye:protein). A pH of 7.4 was chosen for the labeling

buffer, in order to achieve selective labeling of the amine termini. Labeled proteins were dialyzed using a 3.5 kDa MWCO Slide-A-Lyzer Cassette (Perbio Science, Etten-Leur, The Netherlands) to remove excess of dye and to exchange from the labeling buffer back to the respective formulation buffers. The final labeled IgG concentration was 3.1 mg/ml and the labeling ratio achieved was about 2 labels per IgG. The final concentration of labeled IFN-α was 6.6 mg/ml and the labeling ratio achieved was about 1 label per IFN-α. Both labeled proteins were diluted to 0.5 mg/ml with the respective formulation buffers and stored at 4°C.

Stressing procedures

The IgG was stressed in an IKA KS 4000i control shaker (IKA WORKS, Wilmington, NC, USA) by placing 1 ml of IgG solution (0.5 mg/ml) in 2-ml reaction tubes (Eppendorf, Hamburg, Germany) and shaking with orbital agitation at 400 rpm for 3 hours at RT. The tubes were placed horizontally in the shaker to increase the turbulence inside. The metal-catalyzed oxidation was achieved by incubating IFN-α (0.5 mg/ml) with 4 mM ascorbic acid and 0.04 mM $CuCl_2$ for 3 h at room temperature according to Li et al. [5]. The reaction was stopped by adding 100 mM EDTA to a final concentration of 1 mM. This sample was dialyzed extensively against PBS with a 3.5 kDa MWCO Slide-A-Lyzer Cassette (Perbio Science). All formulations were stored at 4°C until being analyzed or injected.

Visual inspection

Stressed samples were inspected visually for the presence of visible particles. Formulation buffer (transparent and uncolored) was used as a reference.

Size exclusion chromatography (SEC)

SEC was performed on a TSK Gel 3000 SWXL column (Tosoh Bioscience, Montgomeryville, PA, USA), using a Thermo Separation Products Spectra System P4000 gradient pump (Thermo Scientific, Breda, The Netherlands), a Waters 717 plus autosampler (Waters, Milford, MA, USA) and a Waters 2475 fluorescence detector (Waters). The samples were excited at 700 nm and the emission spectra were recorded at 720 nm. The data was collected using ADChrom software version 3.5 (Agilent Technologies, Santa Clara, CA, USA). One hundred µl of each sample

was injected and separation was performed at a flow rate of 0.5 ml/min. The running buffer was composed of 100 mM sodium phosphate, 100 mM sodium sulfate and 0.05% (w/v) sodium azide at pH 7.1.

Light obscuration (LO)

LO measurements were performed on a PAMAS SVSS system (PAMAS GmbH, Rutesheim, Germany) equipped with a HCB-LD-25/25 sensor and a 1 ml syringe. Each sample was measured three times, with each measurement consisting of a pre-run volume of 0.3 ml followed by three runs of 0.2 ml at a flow rate of 10 ml/min. The final results are a mean of the three runs and the error bars represent the standard deviation between them. The IgG stressed formulation was diluted 5-fold with formulation buffer before the measurement.

Animal experiment

A total of 6 mice were included: 2 TG mice tolerant for human IgG - five-feature translocus mice [6] (carrying the human Ig heavy and both κ- and λ-light chain transloci; 2 TG mice immune tolerant for IFN-α [according to Hermelling et. al [7]] and 2 non-transgenic (NTG) controls. All animals had access to water and food (Hope Farms, Woerden, the Netherlands) *ad libitum*. Each mouse was injected intraperitoneally with 100 μl of protein solution (50 μg of protein/injection) and fluorescence optical images were taken. All protein formulations were homogenized by mildly vortexing prior to injections. This experiment was approved by the Institutional Ethical Committee (Utrecht University).

Fluorescence optical imaging (FOI)

Images were captured with a Biospace Lab photon imager (Biospace Lab, Paris, France) right before (basal) and several time points (0h, 2h, 4h and 1,2,3,4 and 7 days) after injection. All the animals had their abdomen, chest and back fur removed. The mice were anesthetized with isoflurane and placed in the imaging device with their abdominal area upwards. Images were captured with the Photon Acquisition software (Biospace Lab), using the default settings for Alexa Fluor® 700 and setting the fluorescence acquisition time to 5 seconds. Image processing was performed with the M3 Vision™ software (Biospace Lab).

RESULTS

Aggregation level

SEC with fluorescence detection and LO were used as complementary techniques to evaluate the extent of aggregation induced by the stress methods. SEC focuses on small oligomers and may provide approximate (total) percentage of aggregation by quantifying monomer loss after stress. LO particle counting is a technique that can count and measure the size of micron-sized particles (1-200 μm). SEC and LO size distribution graphs of the unstressed and stressed formulations are displayed in Fig. 8.1.

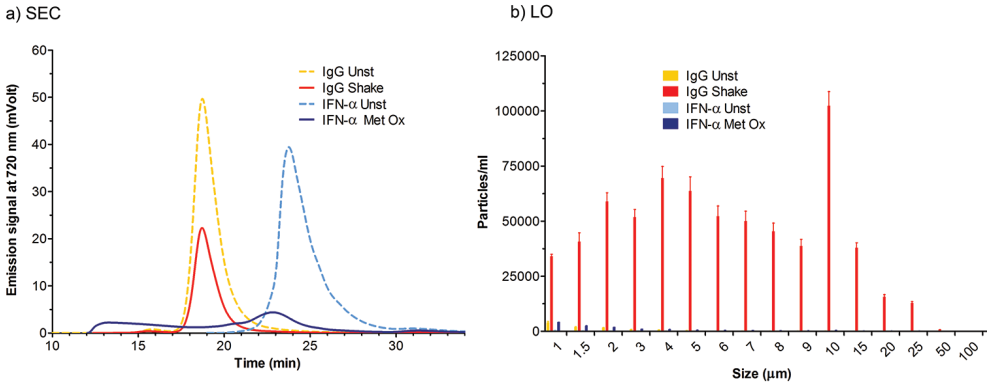

Figure 8.1: SEC chromatograms and LO size distributions of shaken (Shake) IgG, metal-catalyzed oxidized (Metal Ox) IFN-α and the respective unstressed (Unst) formulations.

Fig. 8.1a shows that both stressed formulations suffered considerable monomer loss, but only the IFN-α stressed sample contained oligomers detectable by SEC. Monomer loss usually reflects the presence of aggregates that are larger than the interstitial space of the stationary phase and become trapped in the column, but may also reflect unspecific protein binding to the column matrix [8]. Assuming that the former has a greater impact, the aggregation percentages, based on the area under the curve of these chromatograms, were 58% for the stressed IgG formulation and 84% for the IFN-α stressed formulation.

LO results show that shaking induced the formation of a high amount of micron-sized aggregates in the IgG formulation. Even though the IFN-α stressed formulation

suffered the most drastic monomer loss, the amount of micron-sized aggregates in this sample was relatively low, indicating that most of the aggregates were in the submicron size range.

Visual inspection revealed that the IgG stressed sample contained very small visible particles right after shaking stress. Most of these precipitates remained adsorbed to the air bubbles caused by the stress, to pipette tips and to the container walls, indicating a high degree of hydrophobicity of these aggregates. The air bubbles disappeared by the time of injection/analysis, when only a small white deposit was observable. The IFN-α stressed sample remained free of visible particles during the time course of the experiment.

In vivo fluorescence imaging of IgG

Aggregated and non-aggregated (monomeric) IgG formulations were injected intraperitoneally in TG mice and they were imaged during a time period of 7 days (Fig. 8.2).

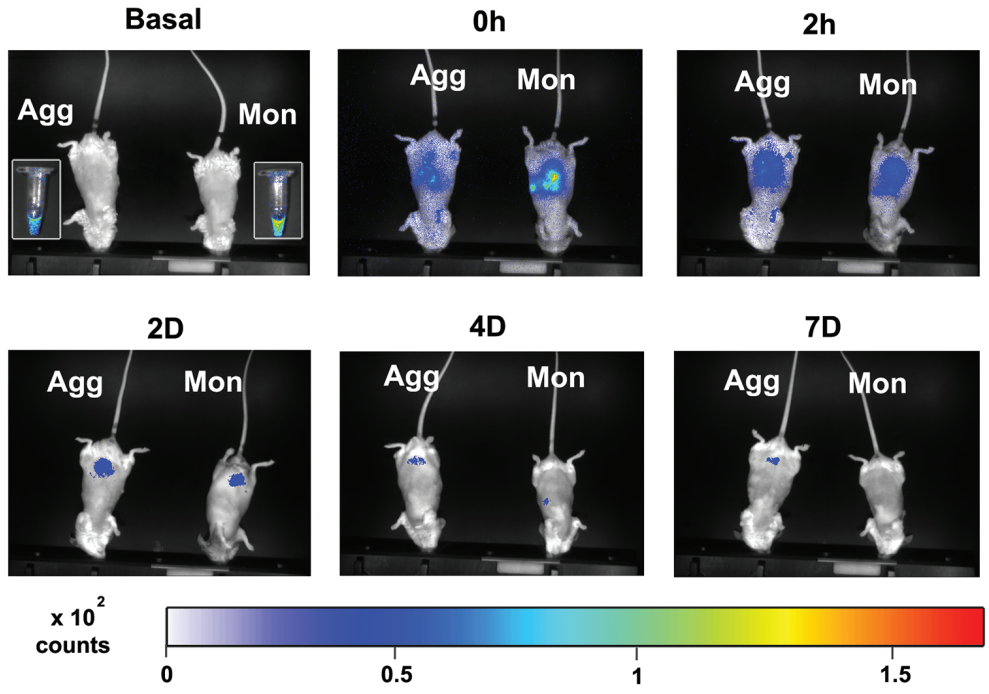

Figure 8.2: Fluorescence optical images of transgenic mice injected intraperitoneally with either unstressed (Mon) or shaken (Agg) IgG over time. The tubes used for injections are shown as insets in the basal picture.

The sample tubes of the "Basal" picture show that the unstressed formulation had a stronger fluorescence signal than the shaken formulation. This is likely related to loss of protein to surfaces during sample handling after stress due to the high apparent hydrophobicity of the visible aggregates in this sample (see previous section). Another possible explanation could be related to fluorophore damage due to the mechanical stress applied to this sample.

Fluorescence was successfully observed in these mice after injection, meaning that fluorescent labeling of protein (aggregates) combined with FOI is a feasible approach to study the fate of IgG aggregates *in vivo*. The difference in fluorescence signal intensity between aggregated and non-aggregated was also observed in mice right after injection (0h). However, after 2 hours this difference was no longer visible and after 7 days only the mouse injected with aggregated IgG had measurable fluorescence. These results suggest that the aggregates exhibit a lower elimination rate than the monomeric IgG.

The injection site is clearly visible in the mouse treated with non-aggregated IgG at time 0h. After 2 days, most of the protein seemed to accumulate in a central lower abdominal area in both mice. In fact, with the experimental conditions used in this study, it is impossible to know if this accumulation was in the lower intraperitoneal cavity, the intestines or the bladder. During the following days, the mouse treated with aggregated IgG continued showing fluorescence in the same lower abdominal area, whereas the one treated with monomeric IgG showed fluorescence in the upper left part of the abdominal area, where the spleen, the stomach, one kidney and part of the liver are located [9].

In vivo fluorescence imaging of IFN-α

Aggregated and non-aggregate (monomeric) IFN-α formulations were injected intraperitoneally in TG and NTG mice. Since the type of immune response between NTG and TG tolerant mice to therapeutic proteins is expected to be different [7, 10], NTG mice were also included in this pilot study. The mice were imaged during a time period of 4 days (Fig. 8.3).

The sample tubes show that the stressed formulation had a stronger fluorescence signal than the unstressed sample. This is probably related to a difference in protein concentration caused by the dialysis step. Metal-catalyzed oxidation did not seem to negatively affect the fluorescent properties of the label.

Once again, fluorescence was detected in all mice right after injection (0h),

showing that this approach is also suitable to study the fate of IFN-α aggregates *in vivo*. The mice injected with the aggregated formulation showed fluorescence in a more spread and lower area than the mice injected with unstressed formulation (times 0h and 2h). Since differences are already observed right after injection, this might be due to a variation between injections rather than PK/PD differences between aggregated and non-aggregated protein.

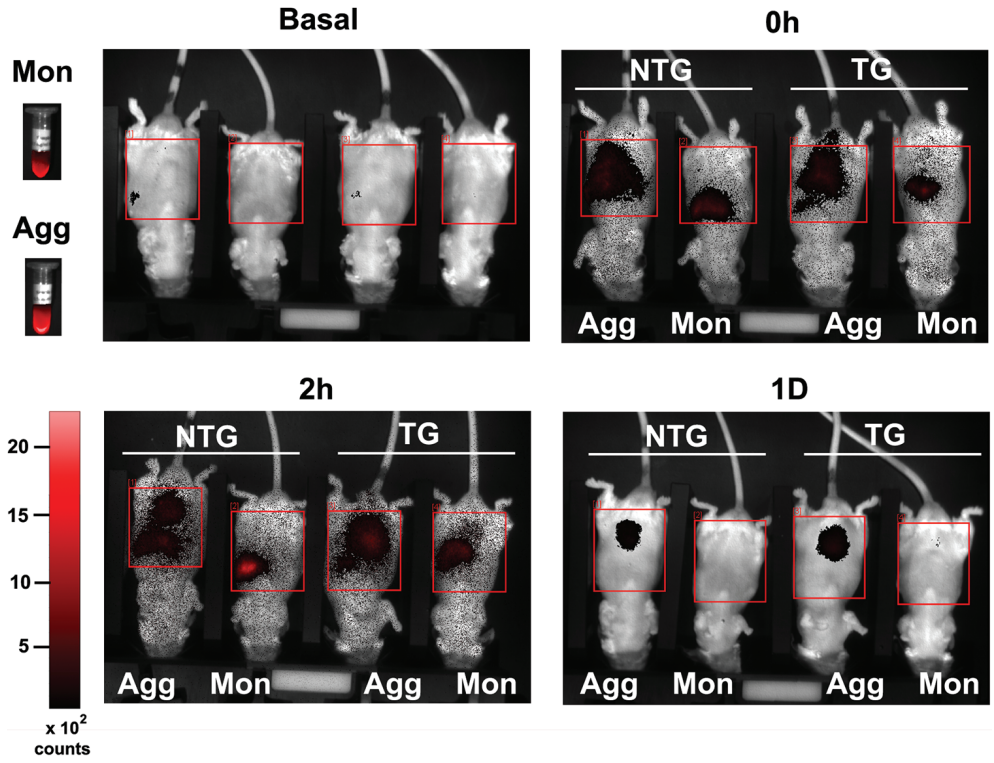

Figure 8.3: Fluorescence optical images over time of transgenic (TG) and non-transgenic (NTG) mice injected intraperitoneally with either unstressed (Mon) or metal oxidized (Agg) IFN-α. The tubes used for injections are shown on the left.

In any case, similar to the IgG samples, the lower abdominal region accumulation and the lower elimination rate of the aggregated formulation were also observed for IFN-α. Moreover, no major differences were observed between the images of TG and NTG mice. The images captured 2 days after injection showed no fluorescence signal in any of the mice.

DISCUSSION

SEC and LO analysis show that both stressed formulations contained a large amount of aggregates as compared with unstressed formulations. Shaking stress was chosen for the IgG formulation because it induced the formation of a high amount of very large aggregates. We chose metal-catalyzed oxidation as the stress method to aggregate IFN-α, since it has been shown to significantly increase the immunogenicity of this protein in both TG and NTG mice [7, 11]. However, the amount of large (micron-sized) aggregates was relatively small compared with that obtained for the stressed IgG formulation.

Despite having small group sizes, a different elimination rate between aggregated and monomeric protein was observed for both proteins. However, it is not possible to directly attribute the long-lasting fluorescence to the aggregates, because the experimental settings used in this pilot study do not allow the distinction between aggregates and monomer accumulated in certain organs or tissues.

The two most commonly used routes of administration for therapeutic proteins are intravenous and subcutaneous injection, which certainly will result in different biodistribution profiles than the one obtained by intraperitoneal administration. In any case, both drugs were able to successfully exit the peritoneal cavity and reach the circulatory system, as shown by the sparse fluorescence dots observed all over the body of all mice at times 0h and 2h.

Interestingly, both aggregated formulations seemed to accumulate in the lower abdominal area at late time points. Recent studies have shown that intestinal capillaries selectively restrict macromolecules to a greater degree than the continuous type of capillaries of many other organs [12]. It is thus unlikely that large protein aggregates could have diffused through intestinal capillaries to accumulate in the intestinal tract. Accumulation in the bladder is also unlikely, since protein in the urinary tract should also result in kidney fluorescence and that was not observed. Proteins injected in the peritoneal cavity are thought to pass the peritoneal wall by hydrostatic pressure-driven diffusion and convection, and the rate of this type of transport is inversely related to the size of the solute [13, 14]. Therefore, it is more likely that the fluorescence detected at later time points is due to protein aggregates that could not exit the peritoneal cavity and somehow accumulated in the lower abdominal region.

CONCLUSION

Labeling of protein with Alexa Fluor® 700 enables *in vivo* fluorescence imaging of monomeric and aggregated protein formulations in mice. Aggregated IFN-α and IgG formulations appeared to have decreased elimination rates as compared with the correspondent non-aggregated formulations. Protein present in aggregated formulations accumulated in the lower abdominal region, but it is impossible to know exactly in which organ/tissue. Clearly more research is needed to clarify and understand these preliminary results and to provide statistical strength to the observations made in this pilot study. Further research in this subject may help to establish correlations between biodistribution and immunogenicity of therapeutic proteins.

ACKNOWLEDGEMENTS

This research was supported by the Technology Foundation STW, the applied science division of NWO and technology program of the Dutch Ministry of Economic Affairs. We thank Amar Oedit for his help with protein labeling and optimization of the stress methods.

REFERENCES

[1] A. S. Rosenberg, "Effects of protein aggregates: an immunologic perspective," The AAPS journal, vol. 8, pp. E501-7, 2006.
[2] V. A. Bumelis, Z. Bumeliene, G. Gedminiene, V. Smirnovas, J. Sereikaite, and I. Medelyte, "Analysis of the physical homogeneity and biological activity of recombinant human interferon-gamma," Biotechnologija, vol. 2, pp. 51-53, 2003.
[3] H. A. Lehr, J. Brunner, R. Rangoonwala, and C. J. Kirkpatrick, "Particulate matter contamination of intravenous antibiotics aggravates loss of functional capillary density in postischemic striated muscle," American journal of respiratory and critical care medicine, vol. 165, pp. 514-20, Feb 15 2002.
[4] I. Mahmood and M. D. Green, "Pharmacokinetic and pharmacodynamic considerations in the development of therapeutic proteins," Clin Pharmacokinet, vol. 44, pp. 331-47, 2005.
[5] S. Li, T. H. Nguyen, C. Schoneich, and R. T. Borchardt, "Aggregation and precipitation of human relaxin induced by metal-catalyzed oxidation," Biochemistry, vol. 34, pp. 5762-72, May 2 1995.
[6] I. C. Nicholson, X. Zou, A. V. Popov, G. P. Cook, E. M. Corps, S. Humphries, C. Ayling, B. Goyenechea, J. Xian, M. J. Taussig, M. S. Neuberger, and M. Bruggemann, "Antibody repertoires of four- and five-feature translocus mice carrying human immunoglobulin heavy chain and kappa and lambda light chain yeast artificial chromosomes," Journal of immunology, vol. 163, pp. 6898-906, Dec 15 1999.
[7] S. Hermeling, L. Aranha, J. M. Damen, M. Slijper, H. Schellekens, D. J. Crommelin, and W. Jiskoot, "Structural characterization and immunogenicity in wild-type and immune tolerant mice of degraded

recombinant human interferon alpha2b," Pharmaceutical research, vol. 22, pp. 1997-2006, Dec 2005.
[8] J. S. Philo, "A critical review of methods for size characterization of non-particulate protein aggregates," Current pharmaceutical biotechnology, vol. 10, pp. 359-72, Jun 2009.
[9] K. O. Vasquez, C. Casavant, and J. D. Peterson, "Quantitative whole body biodistribution of fluorescent-labeled agents by non-invasive tomographic imaging," PloS one, vol. 6, p. e20594, 2011.
[10] S. Hermeling, W. Jiskoot, D. Crommelin, C. Bornaes, and H. Schellekens, "Development of a transgenic mouse model immune tolerant for human interferon Beta," Pharmaceutical research, vol. 22, pp. 847-51, Jun 2005.
[11] S. Hermeling, H. Schellekens, C. Maas, M. F. Gebbink, D. J. Crommelin, and W. Jiskoot, "Antibody response to aggregated human interferon alpha2b in wild-type and transgenic immune tolerant mice depends on type and level of aggregation," Journal of pharmaceutical sciences, vol. 95, pp. 1084-96, May 2006.
[12] D. N. Granger and A. E. Taylor, "Permeability of intestinal capillaries to endogenous macromolecules," The American journal of physiology, vol. 238, pp. H457-64, Apr 1980.
[13] M. F. Flessner, R. L. Dedrick, and J. C. Reynolds, "Bidirectional peritoneal transport of immunoglobulin in rats: compartmental kinetics," The American journal of physiology, vol. 262, pp. F275-87, Feb 1992.
[14] M. F. Flessner, "Transport of protein in the abdominal wall during intraperitoneal therapy. I. Theoretical approach," American journal of physiology. Gastrointestinal and liver physiology, vol. 281, pp. G424-37, Aug 2001.

Chapter 9

Immunogenicity of different stressed monoclonal IgG formulations in immune tolerant transgenic mice

Vasco Filipe[1,2], Wim Jiskoot[1], Abdul Hafid Basmeleh[2], Andhyk Halim[2], Huub Schellekens[2], Vera Brinks[2]

[1] Division of Drug Delivery Technology, Leiden/Amsterdam Center for Drug Research, Leiden University, P.O. Box 9502, 2300 RA Leiden, The Netherlands

[2] Department of Pharmaceutics, Utrecht Institute for Pharmaceutical Sciences (UIPS), Utrecht University, P.O. Box 80082, 3508 TB, Utrecht, The Netherlands

In preparation

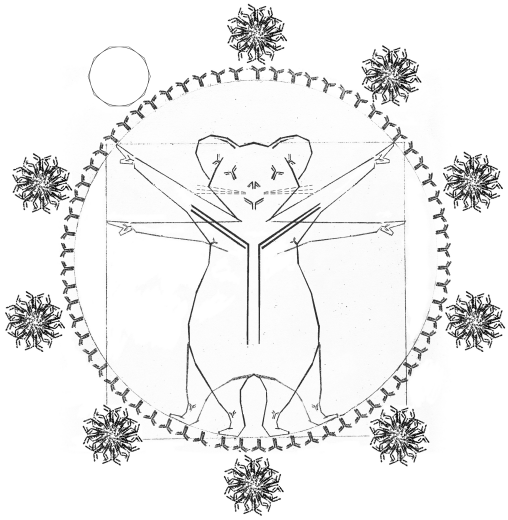

SUMMARY

The presence of protein aggregates in biopharmaceutical formulations is of great concern for safety and efficacy reasons. The aim of this study was to correlate the type and amount of monoclonal IgG aggregates with their immunogenic potential. IgG degradation was obtained by freeze-thawing cycles, pH-shift cycles, heating, shaking and metal-catalyzed oxidation. The size, amount, morphology and type of intermolecular bonds of aggregates, as well as structural changes and epitope integrity were characterized. These formulations were injected in mice transgenic (TG) for human genes for Ig heavy and light chains and their nontransgenic (NTG) counterparts. Anti-drug antibody (ADA) titers were determined by a bridging ELISA. Unstressed IgG and the freeze-thawed formulation, containing a relatively large amount of micron-sized aggregates, did not induce measurable ADA levels. A mild antibody response was obtained in a fairly small percentage of mice, by injecting them with a large amount of (i) visible and subvisible aggregates caused by shaking stress, (ii) sub-micron aggregates induced by heating or (iii) polydisperse subvisible aggregates caused by pH-shift cycles. The metal-catalyzed oxidized IgG formulation was the most immunogenic one, in both ADA titers and number of responders. This formulation contained no visible aggregates, a relatively small amount of subvisible aggregates, a large amount of fragments and fragment-derived oligomers, and presumably a large amount of oxidized species, as compared with other stressed formulations. The overall titers of NTG responders were significantly higher than the ones produced by TG mice, whereas there was no significant difference between the overall number of TG and NTG responders. This study reinforces the important role of protein aggregates on immunogenicity of therapeutic proteins and provides new insight into the immunogenic potential of different types of IgG aggregates.

INTRODUCTION

Monoclonal antibodies (MAbs) are used to treat a wide range of diseases and are currently the fastest growing drug category [1]. However, a major concern associated with the use of MAbs, as nearly all other therapeutic proteins, is that their repeated administration to patients often leads to the induction of anti-drug antibodies (ADAs). The development of ADAs in patients may influence pharmacokinetics and significantly lower efficacy, as has been observed, e.g., for anti-TNF-α antibodies used for the treatment of rheumatoid arthritis [2, 3]. In some cases, the formation of ADAs leads to severe adverse effects and life-threatening situations [4].

Among the several factors playing a role in immunogenicity, the presence of aggregates in formulations has been put forward as a major concern [5]. Several studies have suggested that formulations with a high amount of aggregates tend to

be more immunogenic [6, 7]. Thus, the presence of aggregates in biopharmaceutical products has become a main concern for the pharmaceutical industry and regulatory agencies. However, little is known about the nature of the aggregate species responsible for immune reactions.

The characterization of protein aggregates is complex and requires the use of many different analytical techniques [8, 9]. Until recently, the presence of visible aggregates (> 100 μm) and relatively large (> 10 μm) subvisible particles in parenteral formulations had been the main concern for adverse reactions, whereas subvisible aggregates < 10 μm and submicron (< 1 μm) aggregates had been largely overlooked. However, it seems increasingly likely the latter type of aggregates is involved in the development of immunogenicity [10]. Until only a few years ago, subvisible aggregates posed a particular analytical challenge, mostly due to the lack of suitable techniques for their size range. This is now changing with the continuing development of new analytical techniques such as nanoparticle tracking analysis (NTA), flow microscopy, Taylor dispersion analysis, and the revival of Coulter counter methodology [11-16].

Several predictive models for immunogenicity of therapeutic proteins have been suggested. The available methods to predict immunogenicity involve *in vitro*, *in silico* and *in vivo* approaches. *In vitro* and *in silico* techniques are mostly based on the aptitude of proteins to actively interact with immune or innate cells, basically identifying T- or B-cell epitopes [17, 18]. Therefore, these two approaches are not suitable for predicting aggregate-related immunogenicity [19]. The use of animal models to predict immunogenicity *in vivo* seems to be the most promising approach to predict aggregate-related ADA responses [6, 20-22].

In vivo assessment of immunogenicity has the advantage that the complex interplay between different aspects of the immune system (i.e., immune cells, cytokines) is accounted for. This is of importance when studying the immunogenicity of aggregates, in which the underlying immune mechanisms leading to antibody formation are mostly unknown. However, the vast majority of proteins used for therapeutic purposes in humans are foreign to animals. Per definition they will develop a classical immune response against a foreign protein when exposed to protein drugs, which is not necessarily the type of response observed in patients. Therefore, in order to circumvent this problem, transgenic animal models that express the human protein of interest have been developed [23]. These mice are, like humans, immune tolerant to a specific human protein and provide the opportunity to study the factors that underlie immunogenicity of therapeutic proteins, including

breaking/circumventing of immune tolerance.

The risk that aggregates pose for immunogenicity has been studied for a number of different therapeutic proteins in transgenic mice [24-26], however the immunogenicity of MAbs using an appropriate TG mouse model has never been systematically studied. In this work, a humanized MAb of the IgG_1 subclass was aggregated by different pharmaceutically relevant stress factors and the resulting formulations were characterized by different complementary analytical methods. These samples were then injected in a TG mouse strain carrying human IgG genes, the five-feature translocus mice [27], for *in vivo* immunogenicity testing.

EXPERIMENTAL PROCEDURES

Materials

A recombinant human monoclonal antibody of the IgG_1 subclass was used for this experiment at an initial concentration of 0.5 mg/ml. The buffer used to formulate and dilute the IgG contained 10 mM sodium citrate (Merck, Darmstadt, Germany), 5% (w/v) sucrose (Sigma-Aldrich, Buchs, Switzerland), pH 6.0. The buffer was filtered using a 0.22-µm PES low binding syringe-driven filter unit (Millex™ GP, Millipore, Ireland). Sodium phosphate, sodium sulfate, sodium azide, copper chloride, ascorbic acid, ethylenediaminetetraacetic acid (EDTA), hydrochloric acid (HCl), acetic acid, tris(hydroxymethyl)aminomethane (Tris), Tris-HCl, glycine, sodium dodecyl sulfate (SDS) and Tween 20 were purchased from Sigma-Aldrich, sodium hydroxide (NaOH) from Boom BV (Meppel, The Netherlands), methanol from Biosolve BV (Valkenswaard, the Netherlands) and the fluorescent dye 4,4'-dianilino-1,1'-binaphthyl-5,5'-disulfonic acid dipotassium salt (bis-ANS) from Fluka (Zwijndrecht, The Netherlands).

IgG stressing procedures

The IgG formulation (0.5 mg/ml) was stressed by five different accelerated stress methods to create aggregates. Freeze-thawing stress was performed by applying 10 cycles of incubation of 1 ml of IgG solution in 1.5-ml reaction tubes (Eppendorf, Hamburg, Germany) at -80°C for 20 minutes followed by incubation at room temperature (RT) for 20 minutes. The pH-shift stress consisted of changing 3 times the formulation buffer pH from pH 6 to pH 1 and back to pH 6 at RT. NaOH (5

M) and HCl (5 M) were alternatively added drop wise to induce the pH-shifts. Each cycle consisted in approximately 1 minute exposure to pH 1. The heat stress was performed by incubating 1 ml of IgG solution in 1.5-ml reaction tubes at 74°C for 15 minutes in an Eppendorf Thermomixer® R (Hamburg, Germany). The shake stress was done in an IKA KS 4000i control shaker (IKA WORKS, Wilmington, NC, USA) and consisted of placing 1 ml of IgG solution in 2-ml reaction tubes (Eppendorf) and shaking them with orbital agitation at 400 rpm for 16 hours at RT. The tubes were placed horizontally in the shaker to increase the turbulence inside. The metal-catalyzed oxidation was achieved by incubating IgG solution with 8 mM ascorbic acid and 0.08 mM $CuCl_2$ for 3 h at RT, according to Li *et al.* [28]. The reaction was stopped by adding EDTA (100 mM) to a final concentration of 1 mM. This sample was dialyzed extensively against formulation buffer with a 3.5 kDa MWCO Slide-A-Lyzer Cassette (Perbio Science, Etten-Leur, The Netherlands). The samples for injections were diluted 10 fold and stored at 4°C for 3 days, until being injected. The samples used for analysis are the physical mixture of 8 individually stressed samples (1 ml each) and stored at 4°C for 2-3 days, until being analyzed.

Visual inspection

Stressed samples were inspected visually, inside reaction tubes, for the presence of visible particles. Formulation buffer (transparent and uncolored) was used as a reference.

Size-exclusion chromatography (SEC)

SEC was performed on an Agilent 1200 (Agilent Technologies, Palo Alto, CA, USA) combined with a Wyatt Eclipse (Wyatt Technology Europe GmbH, Dernbach, Germany). A TSK Gel 4000 SW_{XL} column (300 mm × 7.8 mm) with a TSK Gel 4000 SW_{XL} precolumn (Tosoh Bioscience, Montgomeryville, PA, USA) was used. 100 µL of each formulation was injected and separation was performed at a flow rate of 0.5 ml/min. The elution buffer was composed of 100 mM sodium phosphate, 100 mM sodium sulfate, 0.05% (w/v) sodium azide at pH 7.1. UV detection was performed at 280 nm with the Agilent 1200 apparatus, whereas multiple angle laser light scattering (MALLS) detection was performed with an 18-angle DAWN HELEOS™ detector (Wyatt Technology Europe, Dernbach, Germany) operating with a 50-nW solid-state laser at 658 nm. The molecular weight of the IgG peaks was calculated with the

Astra software version 5.3.1.5 (Wyatt Technology Europe, Dernbach, Germany). An extinction coefficient of 1.69 (ml mg^{-1} cm^{-1}), a dn/dc of 0.185 (ml/g) and a second virial coefficient of 0 were used. The calculation of the molecular weight was based on the Zimm equation [29].

In order to calculate the percentage of fragments, monomers, oligomers, protein recovery and total aggregation, the area under the curve (AUC) of the UV signal was used. For the relative protein recovery, the total AUC of the stressed samples was compared with the total AUC of the unstressed sample, which was set to 100%. Total aggregation percentages take into account not only the AUC of the oligomers but also the percentage of protein not recovered, which normally comprises aggregates that are too big to enter the column.

Asymmetrical flow field flow fractionation (AF4)

AF4 was performed on an Agilent 1200 combined with a Wyatt Eclipse apparatus, UV detection (at 280 nm) and MALLS detection. For the separation, a small channel equipped with a 350 μm spacer of medium width and a regenerated cellulose membrane with a cut-off of 10 kDa was used. The channel flow was set to 0.9 ml/min and the injection flow was 0.2 ml/min. Four μl of each IgG formulation was injected. The total focusing period was 4 min at a focus flow of 1.5 ml/min. For the separation, an initial cross-flow of 1.5 ml/min was applied for 15 min, then the cross-flow was lowered to 0.3 ml/min within 5 min using a linear gradient and kept at this flow rate for 10 min, then lowered to 0.1 ml/min within 3 min using a linear gradient and kept at this flow rate for 10 min, then immediately lowered to 0.0 ml/min. The running buffer was composed of 100 mM sodium phosphate, 100 mM sodium sulfate and 0.05% sodium azide at pH 7.1. The AUC of the UV signal was used in order to calculate the percentages of fragments, monomers, oligomers, protein recovery and total aggregation, as described in the SEC section.

Nanoparticle tracking analysis (NTA)

NTA measurements were performed with a NanoSight LM20 (NanoSight, Amesbury, United Kingdom), equipped with a sample chamber with a 640-nm laser and a Viton fluoroelastomer O-ring, as described previously [13]. Briefly, the samples were injected in the sample chamber with sterile BD Discardit II syringes (Becton, Dickinson and Company, Franklin Lakes, NJ, USA) until the liquid reached

the tip of the nozzle and measurements were taken at 27 °C with a viscosity of 0.89 centipoise. The buffer viscosity was measured in an AR-G2 rheometer from TA Instruments (New Castle, DE, USA). The NTA 2.1 software was used for capturing and analyzing the data. The samples were measured for 40 seconds with manual shutter and gain adjustments. At least six measurements of each sample were performed and the mean was obtained. The heat stressed sample was diluted 20 times before measurements, whereas the pH-shift stressed sample was diluted 10 times and required the use of the *extended dynamic range* mode due to the high polydispersity observed. Final counts were adjusted based on the dilution factor.

Light obscuration (LO)

LO measurements were performed on a PAMAS SVSS system (PAMAS GmbH, Rutesheim, Germany) equipped with a HCB-LD-25/25 sensor and a 1-ml syringe. Each sample was measured three times, with each measurement consisting of a pre-run volume of 0.3 ml followed by three runs of 0.2 ml at a flow rate of 10 ml/min. The final results are a mean of the three runs and the error bars represent the standard deviation between them. The shake stressed sample was diluted 4 times before measurements and the final counts were adjusted.

Circular dichroism (CD)

CD was performed with a Jasco J-815 CD spectrometer in combination with a Jasco PTC- 423S temperature controller (Jasco International, Tokyo, Japan) at 25 °C. The samples were diluted to 0.1 mg/ml for far-UV CD and kept at 0.5 mg/ml for near-UV CD measurements. The shake stressed sample was centrifuged at 10 000 rpm for 1 minute and the supernatant was used undiluted for far-UV CD measurements. The samples were measured in quartz cuvettes (Hellma GmbH, Muellheim, Germany) with a path length of 1 mm for far-UV CD and 10 mm for near-UV CD. CD spectra were collected in a continuous scanning method from 200 to 250 nm for far-UV CD and from 250 to 320 nm for near-UV CD. The measurements were performed at a scanning speed of 50 nm/min, a response time of 2 s, a bandwidth of 1 nm, a sensitivity of 100 m°, steps of 0.5 nm and an accumulation of 10 scans. Using the Spectra Analysis Software (version 1.53.04, Jasco), the spectra were background-corrected by subtracting the spectrum of the buffer and smoothed with GraphPad Prism® 5 (GraphPad Software, San Diego CA, USA) with a 0^{th} order polynomial

smoothing and 4 neighbors on each value. Data were calculated as mean residue ellipticity according to Kelly *et al.* [30], using a mean amino acid residue weight of 113 suggested by Aghaie *et al.* [31] for IgG.

Steady-state fluorescence spectroscopy

Steady-state fluorescence was measured with a Tecan Infinite M1000 plate reader (Tecan Benelux, Giessen, Netherlands) with 96-well plates (Greiner Bio-One, Alphen a/d Rijn, The Netherlands), a sample volume of 200 µl per well (n = 3), a gain of 189 and a Z-position of 21500 µm. Bis-ANS was added to the wells to a final concentration of 1 µM. The samples were excited at 385 nm and the emission spectra were recorded from 400 nm to 600 nm. The spectra of the 3 wells were averaged and the average was then smoothed in the GraphPad Prism® 5 software with a 0^{th} order polynomial smoothing and 4 neighbors on each value.

Filtration with coomassie blue staining

A volume of 3 ml of ultrapure (milli-Q) water was filtered through 0.22-µm PES syringe-driven filter units of 13 mm from Millipore, to wash out any particulate matter that could have been present in the membrane. Then 1.5 ml of each IgG sample was filtered through these filters, with exception of the shake stress sample, from which only 150 µl were used, due to membrane blocking issues. The membranes were incubated with Coomassie Brilliant Blue R-250 (Biorad) in 45% (v/v) methanol (Biosolve BV) and 10% (v/v) acetic acid for 10 minutes. The membranes were then distained with a solution containing 10% (v/v) methanol and 10% (v/v) acetic acid for 3 hours. The membranes were analyzed with an Axioskop microscope (Carl Zeiss, Munich, Germany), using a 20x amplification objective. Images were collected randomly using the ProgRes CapturePro v2.8.8 software (Jenoptik AG, Jena, Germany).

Sodium dodecyl sulfate polyacrylamide gel electrophoresis (SDS-PAGE)

SDS-PAGE was performed with a Biorad Mini-Protean 3 module (Bio-Rad, Hercules, CA, USA), as described previously [21]. Briefly, 11 µg of protein were loaded in 4–20% linear gradient Tris-HCl Ready Gels from Bio-Rad and the gels were run under

non-reducing and reducing (sample buffer containing 5% (v/v) β-mercaptoethanol from Sigma Aldrich) conditions at 100 V and at RT. The bands were detected by Coomassie Brilliant Blue R-250 staining and the gels were scanned with a Bio-Rad GS-800 densitometer and Quantity One software.

Western blotting

SDS-PAGE gels run under non-reducing conditions were blotted onto a PVDF membrane (Biorad) with a Biorad Mini Trans-Blot electrophoretic transfer cell and a transfer buffer containing 25 mM Tris, 200 mM glycine, 10% (v/v) methanol and 0.1% SDS (w/v) at pH 8.3. The blots were blocked for 1 hour at RT with 5% (w/v) non-fat milk powder (ELK, Campina Melkunie, Eindhoven, the Netherlands) in TBS-$T_{0.05}$ (50 mM Tris-HCl, 150 mM sodium chloride and 0.05% (w/v) Tween 20, pH 7.4) with constant orbital shaking. After washing with TBS-T0.05, the blots were probed overnight at 4°C with primary antibodies in milk solution as follows: anti-human Ig κ light chain constant region antibody (rabbit monoclonal IgG, 1:1000, Abcam, Cambridge, United Kingdom) and anti-human IgG_1 heavy chain constant region antibody (mouse polyclonal IgG, 1:2000, Abcam). The blots were washed with TBS-$T_{0.05}$ and probed for 1 hour at RT with appropriate secondary antibodies in milk solution as follows: anti-rabbit IgG (goat polyclonal IgG, horse radish peroxidase (HRP) labeled, 1:2000, Jackson ImmunoResearch, West Grove, PA, USA) and anti-mouse IgG (goat polyclonal IgG, HRP labeled, 1:2000, Jackson ImmunoResearch). Afterwards, the blots were washed with TBS-$T_{0.05}$ and incubated with ECL Plus reagent (GE Healthcare, Buckinghamshire, United Kingdom) for 2 minutes and detected with a Typhoon 9400 fluorescence imager (GE Healthcare).

Dot blotting

For dot blotting analysis, different volumes of each IgG sample (0.5 mg/ml) were spotted two nitrocellulose membranes (VWR International, Amsterdam, the Netherlands) to make up a total protein amount of 10, 5, 2 and 1 μg per spot. The blots were treated and analyzed with the same conditions above described for Western blotting.

Mouse strain

Five feature mice developed at the Babraham Institute (United Kingdom) carry the human Ig heavy and both κ- and λ-light chain transloci in a background in which the endogenous heavy and κ-light loci have been inactivated. As a result they have basal expression of human IgM, Igκ and Igλ and are capable of forming a large human antibody repertoire involving translocus rearrangement and somatic hypermutation [27]. Originally these mice have been developed in order to produce therapeutic human MAbs of desired specificities. However, their endogenous expression of human antibodies may also render them a good model to study immunogenicity of human MAbs. Nontransgenic (NTG) mice were used as a control in our experiment. These mice are from the same breeding stock as five-feature translocus mice, but lost the human genes along the breeding process.

Breeding and genotyping

Frozen five feature embryos were transported from the Babraham Institute to the local animal housing facility at the Utrecht University, where they were implanted in pseudo pregnant females. Pups were genotyped for TG state (see appendix), and used to set up a stable TG mouse line. In order to obtain both TG mice and their NTG littermates for the experiments, breeding was performed by crossing a heterozygote TG male with a heterozygote TG female. This breeding scheme ensured transfer of all transgenes to the offspring, although still a significant number of NTG littermates were born. The TG state of the offspring was determined by isolating in chromosomal DNA isolated from ear tissue and subsequent PCR to determine the presence of the human heavy chain and human κ and λ light chains (see appendix for primers). Absence of mouse heavy and κ light chains was of less importance to the study and therefore not tested.

Animal experiment

A total of 78 TG mice and 78 NTG littermates (females and males, 10-14 weeks of age at the start of the experiment) were included in the study. All mice had free access to food (Hope Farms, Woerden, The Netherlands) and water (acidified).

TG mice and NTG littermates (n=13) were treated with unstressed IgG formulation, or 1 out of 5 stressed IgG formulations, once per week for 6 weeks (intraperitoneal

injections, 5 µg protein/injection). The interval between injections was 1 week. The formulations were mildly vortexed before injections in order to prevent aggregate deposition in the tubes. Blood was collected submandibularly from all mice before treatment was started (week 0), during the 6 week injection period (before injections on weeks 3 and 5), and during a 7 week washout phase (weeks 7, 9, 11 and 13). At 10 weeks after the last injection (week 16) blood was collected by heart puncture and mice were sacrificed. Blood was collected in Lithium-heparin gel tubes and spun down (3000 g, 10 minutes, 4 °C) in order to isolate the plasma. Plasma was stored at −80 °C until analysis. This experiment was approved by the Institutional Ethical Committee (Utrecht University).

ADA ASSAY

In order to test plasma samples for ADAs against the injected IgG, a bridging ELISA was used. In short, 96 well F-bottom ELISA-plates (Greiner Bio-One, Frickenhausen, Germany) were coated with 0.5 µg/ml of unstressed IgG in phosphate buffered saline (PBS) and stored overnight at 4 °C. Prior to use, the plates were washed five times with PBS containing 0.05% (w/v) of Tween-20 (PBS-$T_{0.05}$), and incubated for 1 hour at RT with plasma samples serially diluted (starting dilution 1:100) in high performance ELISA buffer (HPE, Business Unit Reagents, Sanquin, Amsterdam). Subsequent to washing with PBS-$T_{0.05}$, the plates were incubated for 1 hour at RT with 1 µg/ml of unstressed IgG biotinylated in HPE buffer (biotinylation of the drug was adapted from Van Schouwenburg *et al.* [32]). After washing with PBS-$T_{0.05}$, the plates were incubated for 20 minutes at RT with 1:10000 of Avidin-HRP (Invitrogen, Merelbeke, Belgium) in HPE buffer. The plates were then washed with PBS-$T_{0.05}$ and developed with TMB substrate (Invitrogen) for 15 minutes. The development was stopped by adding 0.18 M of H_2SO_4. Absorbance was measured at 405 nm (SpectroStar Nano, Isogen, De Meern, The Netherlands). The 100-fold diluted plasma samples were arbitrarily defined positive if their optical density (OD) was at least 0.5 higher than the negative control. ADA titers were determined by plotting the absorbance values of the dilution series against log dilution. The plots were fitted to a sigmoidal dose-response curve using GraphPad Prism® 4. The reciprocal of the dilution of the EC50 value was defined as the ADA titer. Plasma samples considered positive (OD > 0.5) but having too low OD for assessing titers via EC50 (OD ~ 1.45) were given an arbitrary titer of 75.

Statistics

Using the SPSS software v. 16 (Microsoft, Redmond, WA, USA), a non-parametric Mann-Whitney U test was used to assess statistical difference in titers between TG and NTG responders. Significant difference in the number of responders between groups was determined with the McNemar's test. A calculated probability (P value) equal or below 0.05 was considered to be statistically significant.

RESULTS

Characterization of stressed IgG formulations

Fragments, monomers and oligomers

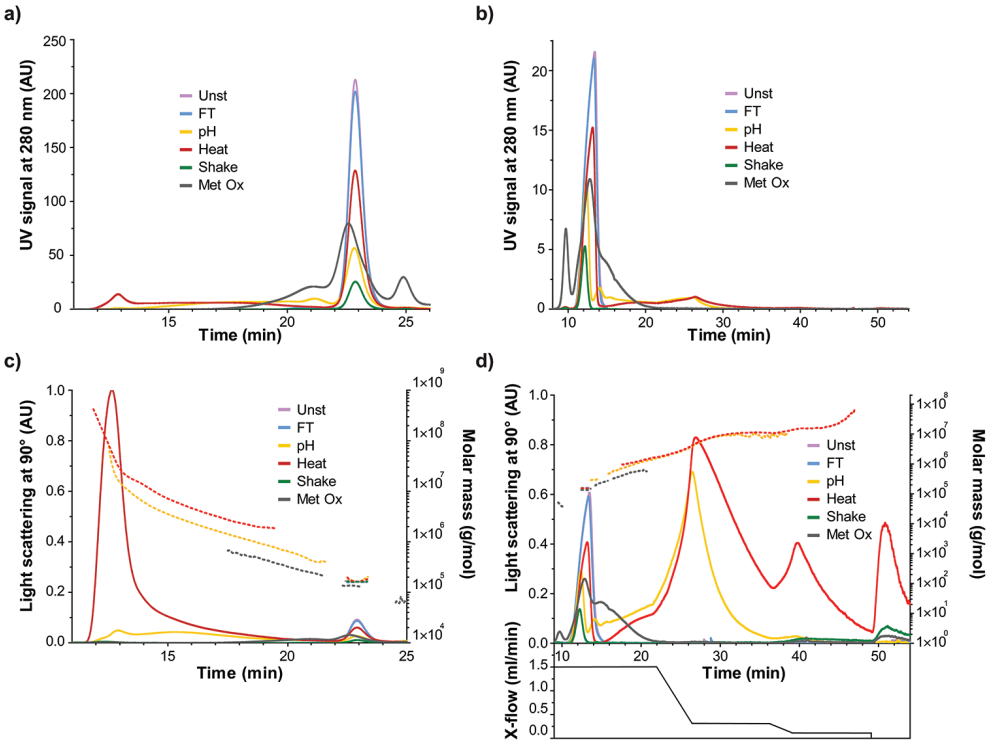

Figure 9.1: SEC and AF4 chromatograms of unstressed (Unst), freeze-thawed (FT), pH-shifted (pH), heated (Heat), shaken (Shake) and metal-catalyzed oxidized (Metal Ox) IgG formulations: (a) SEC with UV detection at 280 nm; (b) AF4 with UV detection at 280 nm; (c) SEC with MALLS detection and the estimated molar mass of each peak; (d) AF4 with MALLS detection, the estimated molar mass of each peak and the channel cross-flow rate (X-flow) over time.

SEC and AF4 were used as orthogonal techniques to separate and quantify monomers and small oligomers present in the unstressed and stressed formulations. The detection was made by UV and MALLS, and the molar mass of each peak was estimated (Fig. 9.1). The percentages based on the UV signal at 280 nm are summarized in Table 9.1.

Table 9.1: AUC percentages from SEC-UV280 and AF4-UV280 analysis of unstressed and stressed IgG formulations. Percentages of fragments, monomers and oligomers refer to the total AUC of each sample.

	SEC-UV (%)					AF4-UV (%)				
	Frag	Mon	Olig	Relative Recov	Total Agg	Frag	Mon	Olig	Relative Recov	Total Agg
Unst	0.7	98.0	1.2	100	1	0.1	99.9	0.0	100	0
FT	0.5	98.0	1.4	94	7	0.1	99.9	0.0	95	5
pH	1.7	49.8	48.5	63	67	0.0	45.3	54.7	65	71
Heat	1.0	64.2	34.8	94	39	0.1	64.7	35.2	93	40
Shake	2.0	96.6	1.4	12	88	0.0	96.4	3.6	12	88
Met Ox	35.8	46.6	17.6	N/A	N/A	13.0	56.7	30.3	N/A	N/A

Abreviations: Unst – unstressed; Mon – monomer; FT – freeze-thawed; Met Ox – metal-catalyzed oxidized; Olig – oligomers; Relative Recov – relative recovery (total AUC compared to total AUC of unstressed IgG); Total Agg – total aggregation (percentage not recovered + recovered oligomers); N/A – not available (see text).

All stressed IgG samples contained aggregates, detectable not only by the presence of oligomer peaks, but also by monomer peak loss when compared with the unstressed formulation. The overall AUC-based percentages obtained between the two techniques are quite comparable (Table 9.1).

The unstressed sample contained mostly monomers, 98.0% according to SEC-UV and 99.9% according to AF4-UV. Among the stress factors applied, freeze-thawing induced the smallest amount of IgG aggregates, since this sample only differs from the unstressed formulation by having a slightly smaller amount of monomer without direct evidence of aggregate formation (Fig. 9.1). The loss of monomer of about 5% observed for the freeze-thawed sample points to the formation of larger aggregates in a size range not covered by these two techniques.

The pH-shift stressed sample was the one with the highest percentage of oligomers (ca. 50%) and had the second highest total aggregation percentage (ca. 70%) according to both techniques. The heat stressed formulation also contained a considerably high percentage of oligomers (ca. 35%). The presence of larger oligomers can be clearly observed in the MALLS chromatograms of Fig. 9.1c and 9.1d. pH-shift stress induced the formation of a large amount of dimers, trimers

and other small oligomers, whereas heat stress induced mostly the formation of larger oligomers. The peaks of the AF4-MALLS signal of these two samples eluting after 20 minutes (Fig. 9.1d) are caused by changes in channel cross-flow. Every time the cross-flow decreased, more aggregates were released from the AF4 channel, presumably as a result of desorption from the membrane, which resulted in the appearance of a new peak [33].

The shake stressed sample had the highest total aggregation percentage (88%) according to both techniques. However, practically no oligomer peaks were detected for this sample, indicating that most of the aggregates were too large to be analyzed by these analytical methods.

Metal-catalyzed oxidation induced the formation of a large amount of fragments (35.8% according to SEC-UV) that have a distinct peak eluting at 25 minutes in SEC (Fig. 9.1a) and at 10 minutes in AF4 (Fig. 9.1b). This fragmentation seems to have been accompanied by oligomerization of fragments and/or intact monomers, which led to the broadening of the monomer peak. This broad peak had an AUC larger than the one of the unstressed formulation, which resulted in improbable relative recoveries (> 100%) for both techniques. It is possible that the oxidation process induced the formation of oxidized species and/or amino acids with higher extinction coefficients at 280 nm, which would have resulted in larger AUCs. In any case, the relative recovery and total aggregation percentages of oxidized samples could not be accurately calculated.

The estimated molar mass of the monomer peak of all but the oxidized sample was about 1.5×10^5 g/mol, which is consistent with the expected value for IgG. Monomers of the oxidized sample had an estimated molar mass of 1.3×10^5 g/mol. This may have to do with an eventual partially-unfolded state of the monomers and/or with the fragmentation state of the monomers. The oligomers of the oxidized sample also had a lower estimated molar mass than the ones of the pH-shift and heat stressed samples. This may have to do with a lower degree of unfolded state of oxidized oligomers and/or with a potentially higher extinction coefficient of these species (see above), as compared with the oligomers of pH-shift and heat stressed samples.

Subvisible aggregates

In order to analyze the size distribution and amount of aggregates that were too large to be analyzed by SEC or AF4, NTA and LO were used. NTA is an emerging

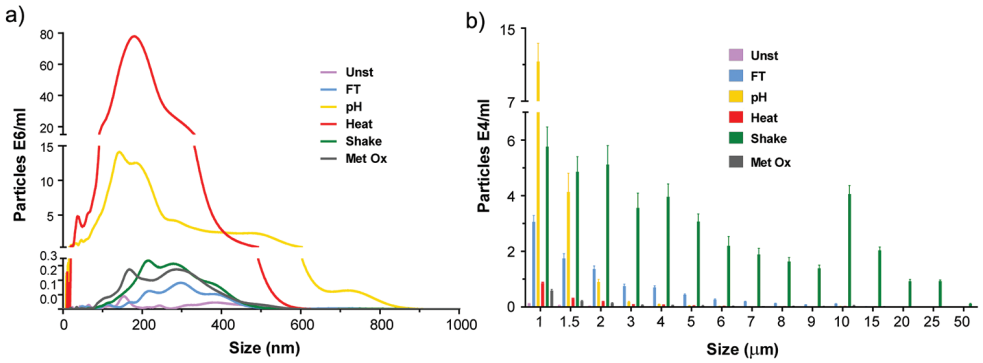

Figure 9.2: Size distribution of subvisible aggregates of unstressed (Unst), freeze-thawed (FT), pH-shifted (pH), heated (Heat), shaken (Shake) and metal-catalyzed oxidized (Metal Ox) IgG formulations: (a) submicron particles (determined by NTA), (b) micron-sized particles (determined by LO).

technique that enables the visualization, sizing and quantification of particles in the submicron range (ca. 40-1000 nm). LO particle counting is a technique that can count and measure the size of micron-sized particles (1-200 μm). NTA and LO size distribution graphs of the unstressed and stressed formulations are displayed in Fig. 9.2.

According to NTA results, the formulations with the highest amount of submicron aggregates were ranked as follows: heated (ca. 1×10^{10} agg./ml) > pH-shift stressed (ca. 3×10^{9} agg./ml) > oxidized and shaken (both with ca. 7×10^{7} agg./ml) > freeze-thawed (ca. 4×10^{7} agg./ml) > unstressed (1×10^{7} agg./ml). The size average of these submicron aggregates was fairly similar between the stressed samples (Fig. 9.1a), exception for the pH-shift stressed sample. This sample was very polydisperse and was the only one containing a fairly high amount of submicron aggregates larger than 600 nm. For this reason, this sample was the only one analyzed with the *extended dynamic range* mode, optimal for very polydisperse samples [13]. However, most aggregates larger than 600 nm contained multiple scattering centers, which added a rotational variable that cannot be analyzed correctly by the software. Thus, the amount of large submicron aggregates in the pH-shift sample was actually higher than the one obtained by NTA.

According to LO results, the formulations with the highest amount of micron-sized aggregates were ranked as follows: shaken (ca. 4.1×10^{5} agg./ml) > pH-shift stressed (ca. 1.7×10^{5} agg./ml) > freeze-thawed (ca. 8.9×10^{4} agg./ml) > heated (ca. 1.6×10^{4} agg./ml) > oxidized (ca. 1.3×10^{4} agg./ml) > unstressed (3.0×10^{3} agg./ml). The size bin with the highest amount of particles was between 1 and 1.5 μm for all samples.

All samples presented a skewed particle size distribution with most particles being in the lower size bins, except for the shaken sample, for which the distribution was broad and multimodal.

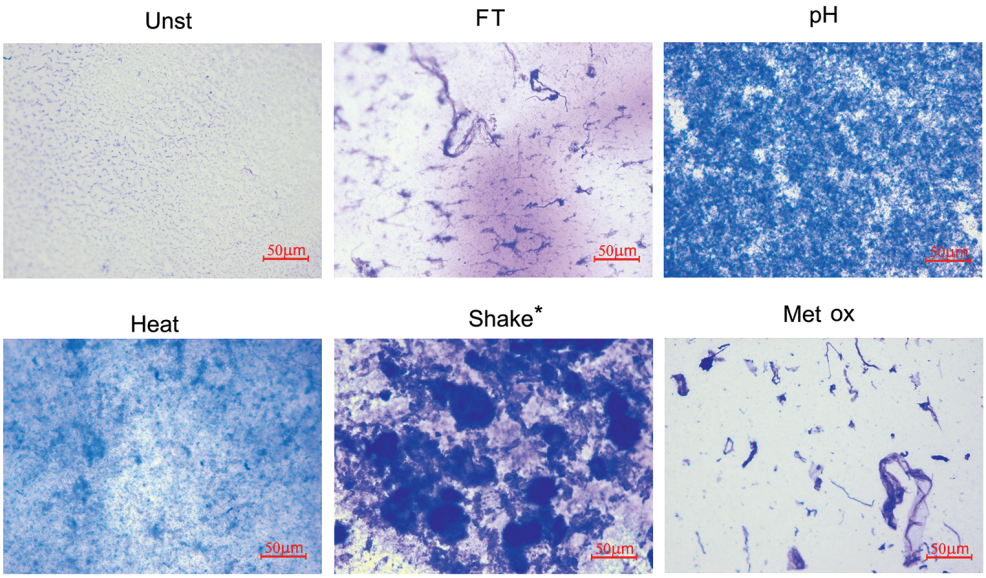

Figure 9.3: Representative microscopy images (20x amplification) of unstressed (Unst), freeze-thawed (FT), pH-shifted (pH), heated (Heat), shaken (Shake) and metal-catalyzed oxidized (Metal Ox) IgG formulations after filtration through a 0.22 µm filter, followed by staining with Coomassie Brilliant Blue.
* The filtered volume used for the shaken formulation was 10 times lower than that for the other formulations due to filter blockage.

In order to obtain some information about the morphology of the subvisible aggregates in each sample, the formulations were filtered through a 0.22 µm filter and the aggregates retained on the membrane were stained with Coomassie Brilliant Blue. The membranes were then analyzed with a light microscope and representative images of each sample are shown in Fig. 9.3.

As expected, the shaken sample contained the biggest aggregates of all stressed samples. These aggregates were fairly rounded and seem to be relatively dense. Freeze-thawed micron-sized aggregates resemble loose threads with random knots. The oxidized sample showed a mixture of thread-like structures, compact irregular shapes and dense smoke-like structures. pH-shift stress induced aggregates that are numerous and relatively small, in such a way that it is impossible to describe their morphology. Heat induced aggregates were so small, when analyzed by this

technique, that only a faint blue cloud with occasional dark spots can be observed. It is important to mention that this is not a quantitative technique, since a variable amount of aggregates may be removed from the membrane during staining and destaining incubation periods.

Visible aggregates

Visual inspection revealed that all stressed formulations remained free of visible particles during the whole time course of the experiment, except the shake stressed sample. In this sample very small visible particles were observed right after stress. Most of these precipitates remained adsorbed to the air bubbles caused by the stress, indicating a high degree of hydrophobicity of these aggregates. These air bubbles disappeared by the time of injection/analysis, when only a small white deposit was observable.

Structural changes

In order to obtain information about the overall structural changes induced by the different stresses, the formulations were analyzed by CD and bis-ANS fluorescence. From the far-UV CD region (200–250 nm), which corresponds to the peptide bond absorption, information on the secondary structure of a protein can be obtained [30]. The near-UV CD region (250–320 nm) reflects the environment of the aromatic amino acid side chains and therefore yields information about the tertiary structure of a protein [30]. Bis-ANS is a dye that fluoresces intensely only in hydrophobic microenvironments, such as exposed hydrophobic pockets of proteins, thus yielding information about the tertiary structure [34]. The CD and bis-ANS fluorescence results are shown in Fig. 9.3.

The far-UV CD spectrum (Fig. 9.4a) of the unstressed IgG formulation has a minimum at around 220 nm and a maximum at 204 nm, indicative of a high ß-sheet structure, which is typical for IgG [35, 36]. All stressed samples showed a clear reduction of the mean residue ellipticity ([θ]MR) at 204 nm, indicating that some changes in secondary structure occurred in all formulations. The spectrum of the heat stressed sample was the one that most changed, with a distinctly more negative [θ]MR at 220 nm, whereas the other samples showed only marginal spectral changes at this wavelength. The spectrum of the freeze-thawed sample is the one with fewer overall changes. It may be important to notice that most of the shake stress induced aggregates were not present in this sample for this measurement, so

the spectrum obtained for this sample represents mostly the remaining monomer. These aggregates severely interfered with far-UV CD measurements, mainly due to light scattering, and thus had to be spun down before these measurements.

The near-UV CD spectrum (Fig. 9.4b) of the unstressed formulation has a distinctive positive peak at 295 nm (tryptophan) and a negative band in the range between 250 and 290 nm (aromatic amino acid residues and cysteine), which is typical for IgG [35, 37]. The spectrum of the freeze-thawed formulation is shifted to more negative [θ]MR and has approximately the same shape as the unstressed sample. The spectrum of the heated sample is equally shifted but has some shape differences, particularly from 250 to 280 nm and from 300 to 320 nm. The oxidized sample showed clear spectral changes, with reduced [θ]MR between 290 and 320 nm and significantly increased [θ]MR between 250 and 290 nm, as compared with the unstressed sample. The spectrum of the pH-shifted not only has a different shape, but is also considerably shifted to lower [θ]MR. Such pronounced changes can be attributed to light scattering effects, which can cause artifacts due to: (i)

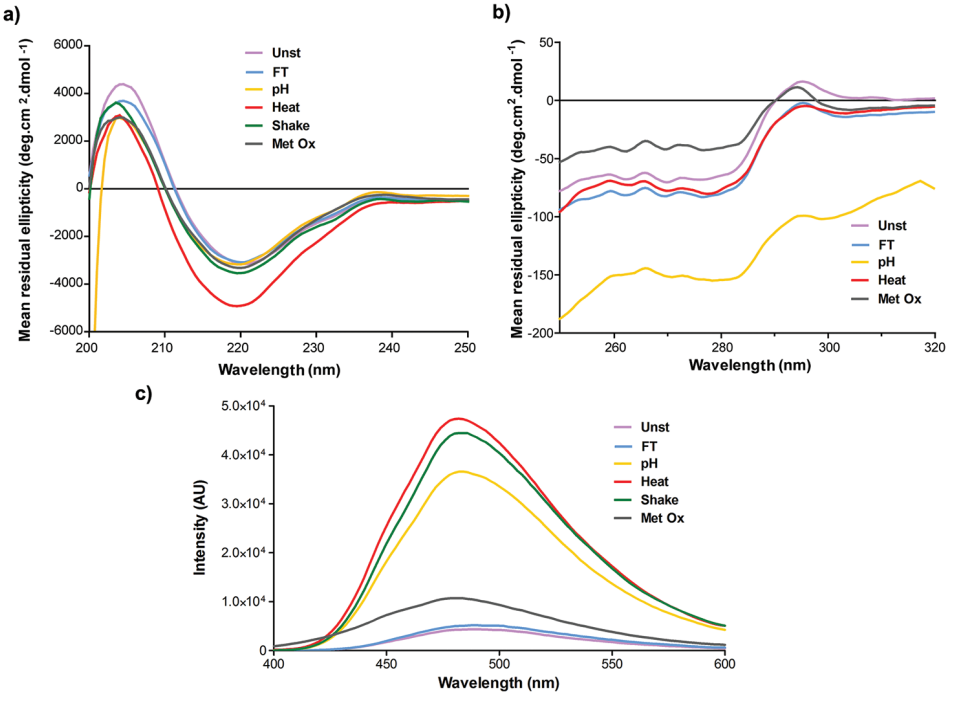

Figure 9.4: Structural characterization of unstressed (Unst), freeze-thawed (FT), pH-shifted (pH), heated (Heat), shaken (Shake) and metal-catalyzed oxidized (Metal Ox) IgG formulations by (a) far-UV CD, (b) near-UV CD and (c) Bis-ANS fluorescence.

differential light scattering, arising when light falls on chiral particles of dimensions comparable to or greater than its wavelength and (ii) absorption flattening due to the high protein concentration in aggregates [30]. In fact, such light scattering effects were so pronounced with the shake stressed formulation that the near-UV CD results of this sample had to be discarded.

In Fig. 9.4c it is possible to observe that all stressed samples exhibited increased bis-ANS fluorescence, as compared with the unstressed formulation. The fluorescence intensity of stressed samples followed the order: heated > shaken > pH-shifted > oxidized > freeze-thawed. These results indicate that the conformational changes, already observed by CD, lead to enhanced exposure of hydrophobic patches, especially in the heated, shaken and pH-shift stressed samples.

Intermolecular bonds

SDS-PAGE was performed to elucidate whether the aggregates of stressed formulations were composed of covalently or noncovalently linked monomers. Under non-reducing conditions (Fig. 9.5a) all formulations showed a major band at around 150 kDa, which corresponds to the monomeric IgG. All formulations also showed thin bands with molecular weights smaller than the monomer band, indicating some degree of fragmentation, even in the unstressed sample, which however could be due to sample treatment. The oxidized sample lane contained a considerable amount of fragments and the monomer band was considerably fainter than the ones from other samples. The lane of the oxidized sample had an overall darker tone than the ones of others samples for sizes below 250 kDa, suggesting the presence of fragments and small oligomers of monomers/fragments distributed throughout a wide range of molecular weights. Heated and shaken samples were the only ones containing a clear band on top of the gel. This indicates that these samples contained covalent aggregates that were too large to enter the gel.

Under reducing conditions (Fig. 9.5b) all formulations showed two main bands at about 50 and 25 kDa, deriving from the heavy and light chain. The unstressed, freeze-thawed, heated and shaken formulations showed also bands at 75, 125 and 150 kDa. These bands correspond to combinations of heavy and light chain fragments, meaning that not all the disulfide bridges were broken. Interestingly, the pH-shift stressed did not contain these resistant fragments and the overall tone of the oxidized sample lane remained darker for sizes below 150 kDa than the tone of other lanes. The aggregated bands on top of the lanes of heated and shaken

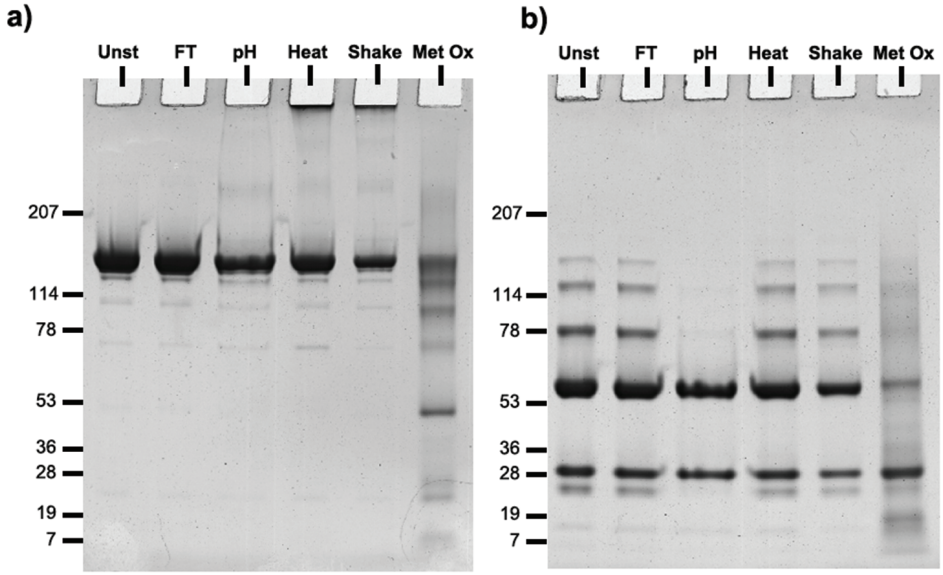

Figure 9.5: SDS-PAGE gels of unstressed (Unst), freeze-thawed (FT), pH-shifted (pH), heated (Heat), shaken (Shake) and metal-catalyzed oxidized (Metal Ox) IgG formulations stained with Coomassie Brilliant Blue under (a) non-reducing and (b) reducing conditions.

samples were no longer present under these conditions, indicating that they were covalently linked via disulfide bridges.

Integrity of native epitopes

Western blotting and dot blotting were used to verify the integrity of native epitopes in stressed formulations. Western blotting was used to obtain information about the epitopes of species separated by SDS-PAGE, whereas dot blotting enabled a more general overview of epitope integrity without separation of monomers and aggregates under denaturing conditions. The blots were probed with anti-heavy chain and anti-light chain antibodies (Fig 9.6).

Fig. 9.6a and 9.6b show that both antibodies were able to detect the monomers of all stressed formulations, except for the oxidized sample. According to these results, it seems that either (i) the metal-catalyzed oxidation damaged most of the native epitopes of this IgG or (ii) this protein was too spread through the gel lane to be clearly detected. The Western blot probed with the anti-light chain antibody (Fig. 9.6a) has fainter bands than the one probed with the anti-heavy chain antibody (Fig 9.6b). In fact, in the latter blot it is possible to observe that the oxidized sample

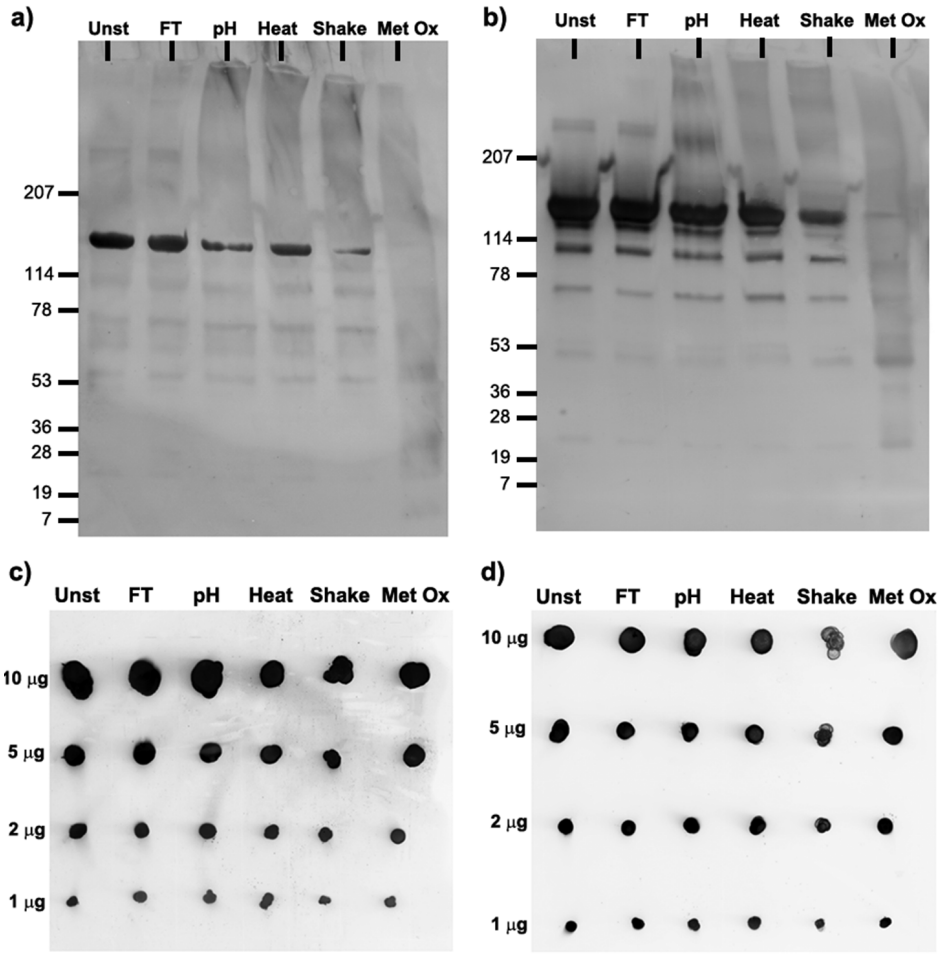

Figure 9.6: Western blots and dot blots of unstressed (Unst), freeze-thawed (FT), pH-shifted (pH), heated (Heat), shaken (Shake) and metal-catalyzed oxidized (Metal Ox) IgG formulations: Western blots detected with (a) monoclonal anti-human κ light chain antibody (b) polyclonal anti-human heavy chain antibody; Dot blots detected with (c) monoclonal anti-human κ light chain antibody (d) polyclonal anti-human heavy chain antibody. The numbers on the left side of the Western blots represent the band positions (in kDa) of the molecular weight markers.

lane has a darker tone from 50 to 150 kDa than all other samples. This supports the hypothesis that the epitopes of the oxidized formulation were still intact, but the protein in this sample was too sparsely distributed to originate a clear band.

The dot blots show that all IgG samples contained intact native epitopes after stress, even the oxidized sample, supporting the hypothesis mentioned above. No clear differences were observed between the dots of the unstressed sample and all stressed samples.

ADA TITERS

The immunogenicity of stressed formulations was tested by repeated injections in TG and NTG mice. These TG mice carry the human genes of Ig heavy and light chains, so they were expected to be more tolerant than the NTG mice to the human IgG administered in this study [25, 38]. ADA titers were obtained by bridging ELISA from plasma collected before and during the injection period (6 weeks) and during a washout period of 10 weeks (Fig. 9.7).

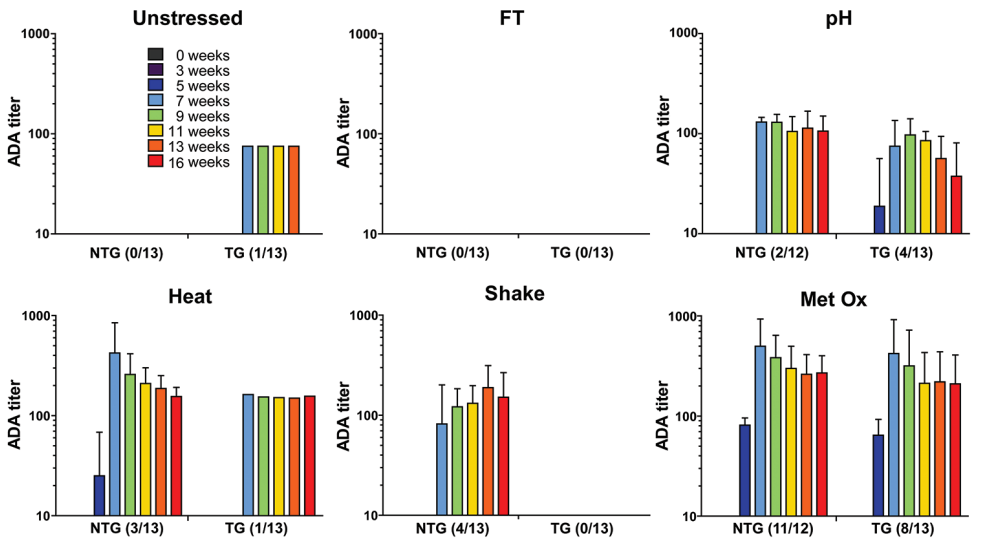

Figure 9.7: ADA titers of the sera of non-transgenic (NTG) and transgenic (TG) mice treated with unstressed (Unst), freeze-thawed (FT), pH-shifted (pH), heated (Heat), shaken (Shake) and metal-catalyzed oxidized (Metal Ox) human IgG formulations. Time points before the first injection (week 0), during the injection period (week 3 and 5) and after the last injection (week 7 to 16) are shown. The titers are from responders only and the error bars represent the standard deviation of the mean values.

Of all the mice administered with unstressed formulation, only one TG mouse responded by ADA formation (OD > 0.5). Because titers were too low to calculate, an arbitrary titer of 75 was given. This weak antibody response was transient and disappeared before the last week of the washout period, in contrast to the antibody responses to the stressed formulations, which were more persistent. Thus, the unstressed formulation was very poorly immunogenic and did not evoke a substantial antibody response in TG and NTG mice.

All stressed formulations induced an antibody response in at least 4 mice per total group (TG + NTG), with exception of the freeze-thawed formulation, which did not induce measurable ADAs in any mouse. Oxidized, heated and pH-shift stressed formulations were able to elicit an antibody response in both TG and NTG mice, whereas the shaken formulation only elicited the formation of ADAs in NTG mice. The groups administered with heated, shaken and pH-shift stressed formulations had a relatively small number of responders per total group (4-6 out of 26 mice). On the other hand, an antibody response was observed in 19 out of 25 mice treated with the oxidized formulation. The ADAs induced by stressed formulations appeared 1 week before/after the last injection and most responders still had relatively high ADA titers during the last week of the washout period.

According to Mann-Whitney's test, the overall titers observed in NTG responders are significantly higher than the ones observed in TG responders (P value = 0.003). Further analysis revealed that only the NTG and TG mice treated with the oxidized formulation show significant differences in titers (P value = 0.045). The small number of responders in the other groups (i.e., low statistical power) likely contributes to the absence of significant difference in titers between NTG and TG mice, since the group with the second largest number of responders (pH-shift) shows nearly significant difference between TG and NTG titers (p=0.079). In addition to statistical comparison of antibody titers, the McNemar's test was performed to assess a potential difference in number of responders between TG and NTG for all treatment groups together. Also here, no significant difference between the total number of TG and NTG responders was found (P value = 0.146).

DISCUSSION

The type of immune response that NTG mice develop against a human protein (classical immune response against a foreign protein) is expected to be different from the one developed by TG mice tolerant to this specific human protein (breaking/circumventing immune tolerance) [39]. In fact, immunogenicity studies, involving the injection of either recombinant human insulin or recombinant human IFN-α in NTG and immune tolerant TG mice, show that when practically aggregate-free formulations of these proteins were injected in NTG mice, most of them developed ADAs, whereas TG mice did not [6, 38, 40]. However, in our study, an immune reaction against unstressed human IgG in NTG mice was not observed. In fact, several studies have shown that the administration of aggregate-free foreign IgG can

be very well tolerated in different animal species and in human patients, sometimes even when formulated in incomplete Freund's adjuvant or with lipopolysaccharides as adjuvants [41-45].

The immunological mechanism of ADA induction to therapeutic proteins is not completely understood. Even though the presence of aggregates seems to play an important role on the development of ADAs, not all aggregates are equally immunogenic [5, 6, 38, 46, 47]. The stress methods used in this study induced different types of degraded IgG formulations. These contained different amounts of aggregates that varied in size distribution, type of intermolecular bounds, conformation, hydrophobicity and morphology. All formulations conserved intact epitopes after stress. Even though this was not clear for the monomers of the oxidized sample (Fig. 9.6a and 9.6b), a strong dot blot signal was observed for this sample (Fig. 9.6c and 9.6d).

Freeze-thawing induced the lowest percentage of total aggregation (Table 9.1) and the lowest level of conformational changes (Fig. 9.4), as compared with all other stressed methods. The aggregates of the freeze-thawed formulation were mostly micron-sized. In fact, this sample had the third highest amount of micron-sized aggregates of all stressed samples. The morphology of these aggregates was rather similar to the one of micron-sized aggregates of the oxidized formulation (Fig. 9.5). Even so, this sample was not able to induce a measurable antibody response in a single NTG or TG mouse. These results indicate that the micron-sized aggregates of this IgG, created by freeze-thawing cycles, are not immunogenic in these mice. They also suggest that the morphology of aggregates *per se* is not a good predictive feature for the immunogenicity of this IgG.

The pH-shift stressed formulation was heavily aggregated. This sample was characterized by having the most polydisperse set of aggregates, ranging from dimers to a few micrometers. This formulation induced rather low ADA titers in a relatively small amount of mice. Curiously, it elicited an immune response in more TG mice (31%) than in NTG mice (17%), even though this difference turned out to be statically not significant. These results indicate that aggregates induced by pH-shift stress increase the risk of immunogenicity of this IgG in these mice.

The heated formulation contained a large amount of oligomers and small submicron aggregates. This stress method induced pronounced structural changes and the formation of covalent aggregates. The antibody reaction to this sample was mild, with 23% of NTG and 8% of TG responders. Nevertheless, these results indicate that IgG aggregates induced by heat stress increase the risk of immunogenicity.

The shaken formulation exhibited the highest percentage of aggregates (88%) and contained mostly very large micron-sized aggregates. This sample was the only one containing visible precipitates. The micron-sized aggregates of this sample appeared to be fairly rounded and relatively dense under the microscope. At least some of these aggregates were covalently linked. The extent of structural changes caused by this stress method could not be properly determined due to the interference of large aggregates. However, these changes are expected to be substantial, since this formulation showed one of the highest levels of bis-ANS fluorescence. Despite the great extent of aggregation and the large size of these aggregates, this formulation was only able to induce a measurable immune response in 31% of NTG mice and no ADA formation was observed in TG mice. These results indicate that aggregates induced by shake stress may only slightly increase the risk of immunogenicity.

The oxidized formulation was the one that elicited the strongest ADA response in the highest percentage of mice: 92% of NTG and 61% of TG mice. This result is consistent with the findings of other immunogenicity studies performed in NTG and TG mice, in which recombinant human IFN-α and recombinant human IFN-β formulations stressed by metal-catalyzed oxidation revealed the highest immunogenic potential of a wide range of stressed formulations [38, 47]. In our study, the oxidized IgG formulation was characterized by the following features: no visible aggregates, a small amount of subvisible aggregates, a large amount of fragments and fragment-derived oligomers, low hydrophobicity, elongated micron-sized aggregates with various shapes and densities, pronounced conformational changes and several chemical changes. Even though these features may give a hint on what may be relevant for immunogenicity of this IgG, the extreme heterogeneity of the aggregates present in this formulation make it impossible to pinpoint one specific species as the immunodominant one. For example, assuming that subvisible aggregates are not relevant for the immunogenicity of this IgG, based on the low amount detected in this sample, may be wrong. There is no evidence that rules out the possibility that this small amount of (metal-catalyzed oxidized) subvisible aggregates, or any other aggregate fraction, is all it takes to trigger a strong antibody response.

Metal-catalyzed oxidation of proteins is known to induce, among other modifications, the formation of mixed-disulfide derivatives and carbonyl derivatives of some amino acid residues, such as glutamyl semialdehyde, 2-amino-adipylsemialdehyde, pyroglutamyl and methionyl sulfoxide [48]. Reactive oxidized protein species are involved in a wide range of biological pathways and, according to some immunological models, the presence of a significant amount of these oxidized

species in the blood stream is considered a major danger signal for the immune system [49]. According to an immunogenicity study performed by Hermeling *et al.*, involving the injection of degraded recombinant human IFN-α in TG mice, oxidation *per se* is unlikely to be responsible for the high immunogenicity observed for oxidized formulations [38]. In our study, the oxidized IgG formulation contained a fair amount of aggregates, most likely formed by oxidized species, which indeed induced a high antibody response.

There was no statistically significant difference between the overall number of TG and NTG responders. However, the difference between ADA titers produced by TG and NTG responders was statistically significant: TG responders showed lower ADA titers. This was mostly due to the contribution of the group treated with oxidized formulation, and to a lesser extent to the other stressed IgG treated groups. This difference is not perceptible from the "Met Ox" graph of Fig. 9.7, given that a logarithmic scale was used. However, ADA titers of NTG responders to the oxidized formulation were 24% higher than the ones produced by TG responders. This significant difference may indicate different immune reaction mechanisms between TG and NTG mice.

It is hard to draw a definite conclusion about the advantage of using this specific TG mouse strain for assessing immunogenicity of human IgG, as compared to their NTG counterpart. Nevertheless, this study was able to provide valuable information regarding the immunogenic potential of differently stressed IgG formulations.

CONCLUSIONS

In this study, differently stressed IgG formulations were administered to TG and NTG mice, with the purpose of correlating the type and amount of aggregates with their immunogenic potential. In general, stress-induced aggregation of IgG leads to enhanced immunogenicity, but not all aggregates seem to pose the same immunogenic risk. The metal-catalyzed oxidized IgG formulation was the most immunogenic. The presence of oxidized IgG species, probably incorporated in aggregates, has more impact on the immunogenicity of this IgG than any other aggregate feature investigated in this work: size, amount, structural conformation, hydrophobicity, morphology and type of intermolecular bonds. In any case, stressed formulations were ranked according to their immunogenic potential as follows: metal-catalyzed oxidized > heated ≈ pH-shift stressed ≈ shaken > freeze-thawed.

For the first time, the risk of different types and amounts of degraded IgG, in particular aggregates, on immunogenicity has been studied in transgenic mice

containing human Ig genes. This study provided useful insights on IgG aggregate-related immunogenicity, but clearly more research is needed to be able to determine the immunogenic potential of different types and amounts of IgG aggregates and other degradants.

AKNOWLEDGEMENTS

This research was supported by the Technology Foundation STW, the applied science division of NWO and technology program of the Dutch Ministry of Economic Affairs. We thank Stefan Romeijn for his technical support with AF4 measurements.

REFERENCES

[1] S. Lawrence, "Pipelines turn to biotech," Nature biotechnology, vol. 25, p. 1342, Dec 2007.
[2] G. M. Bartelds, C. L. Krieckaert, M. T. Nurmohamed, P. A. van Schouwenburg, W. F. Lems, J. W. Twisk, B. A. Dijkmans, L. Aarden, and G. J. Wolbink, "Development of antidrug antibodies against adalimumab and association with disease activity and treatment failure during long-term follow-up," JAMA : the journal of the American Medical Association, vol. 305, pp. 1460-8, Apr 13 2011.
[3] G. M. Bartelds, C. A. Wijbrandts, M. T. Nurmohamed, S. Stapel, W. F. Lems, L. Aarden, B. A. Dijkmans, P. P. Tak, and G. J. Wolbink, "Clinical response to adalimumab: relationship to anti-adalimumab antibodies and serum adalimumab concentrations in rheumatoid arthritis," Annals of the rheumatic diseases, vol. 66, pp. 921-6, Jul 2007.
[4] H. Schellekens, "Bioequivalence and the immunogenicity of biopharmaceuticals," Nat Rev Drug Discov, vol. 1, pp. 457-62, Jun 2002.
[5] A. S. Rosenberg, "Effects of protein aggregates: an immunologic perspective," The AAPS journal, vol. 8, pp. E501-7, 2006.
[6] A. Braun, L. Kwee, M. A. Labow, and J. Alsenz, "Protein aggregates seem to play a key role among the parameters influencing the antigenicity of interferon alpha (IFN-alpha) in normal and transgenic mice," Pharmaceutical research, vol. 14, pp. 1472-8, Oct 1997.
[7] C. N. Gamble, "The role of soluble aggregates in the primary immune response of mice to human gamma globulin," International archives of allergy and applied immunology, vol. 30, pp. 446-55, 1966.
[8] H. C. Mahler, W. Friess, U. Grauschopf, and S. Kiese, "Protein aggregation: pathways, induction factors and analysis," Journal of pharmaceutical sciences, vol. 98, pp. 2909-34, Sep 2009.
[9] J. den Engelsman, P. Garidel, R. Smulders, H. Koll, B. Smith, S. Bassarab, A. Seidl, O. Hainzl, and W. Jiskoot, "Strategies for the assessment of protein aggregates in pharmaceutical biotech product development," Pharmaceutical research, vol. 28, pp. 920-33, Apr 2011.
[10] J. F. Carpenter, T. W. Randolph, W. Jiskoot, D. J. Crommelin, C. R. Middaugh, G. Winter, Y. X. Fan, S. Kirshner, D. Verthelyi, S. Kozlowski, K. A. Clouse, P. G. Swann, A. Rosenberg, and B. Cherney, "Overlooking subvisible particles in therapeutic protein products: gaps that may compromise product quality," Journal of pharmaceutical sciences, vol. 98, pp. 1201-5, Apr 2009.
[11] S. K. Singh, N. Afonina, M. Awwad, K. Bechtold-Peters, J. T. Blue, D. Chou, M. Cromwell, H. J. Krause, H. C. Mahler, B. K. Meyer, L. Narhi, D. P. Nesta, and T. Spitznagel, "An industry perspective on the monitoring of subvisible particles as a quality attribute for protein therapeutics," Journal of pharmaceutical sciences, vol. 99, pp. 3302-21, Aug 2010.

[12] A. Hawe, W. L. Hulse, W. Jiskoot, and R. T. Forbes, "Taylor Dispersion Analysis Compared to Dynamic Light Scattering for the Size Analysis of Therapeutic Peptides and Proteins and Their Aggregates," Pharmaceutical research, May 11 2011.
[13] V. Filipe, A. Hawe, and W. Jiskoot, "Critical evaluation of Nanoparticle Tracking Analysis (NTA) by NanoSight for the measurement of nanoparticles and protein aggregates," Pharmaceutical research, vol. 27, pp. 796-810, May 2010.
[14] J. G. Barnard, S. Singh, T. W. Randolph, and J. F. Carpenter, "Subvisible particle counting provides a sensitive method of detecting and quantifying aggregation of monoclonal antibody caused by freeze-thawing: insights into the roles of particles in the protein aggregation pathway," Journal of pharmaceutical sciences, vol. 100, pp. 492-503, Feb 2011.
[15] K. Wuchner, J. Buchler, R. Spycher, P. Dalmonte, and D. B. Volkin, "Development of a microflow digital imaging assay to characterize protein particulates during storage of a high concentration IgG1 monoclonal antibody formulation," Journal of pharmaceutical sciences, vol. 99, pp. 3343-61, Aug 2010.
[16] J. G. Barnard, M. N. Rhyner, and J. F. Carpenter, "Critical evaluation and guidance for using the coulter method for counting subvisible particles in protein solutions," Journal of pharmaceutical sciences, vol. 101, pp. 140-53, Jan 2012.
[17] A. S. De Groot, J. McMurry, and L. Moise, "Prediction of immunogenicity: in silico paradigms, ex vivo and in vivo correlates," Current opinion in pharmacology, vol. 8, pp. 620-6, Oct 2008.
[18] D. Wullner, L. Zhou, E. Bramhall, A. Kuck, T. J. Goletz, S. Swanson, N. Chirmule, and V. Jawa, "Considerations for optimization and validation of an in vitro PBMC derived T cell assay for immunogenicity prediction of biotherapeutics," Clinical immunology, vol. 137, pp. 5-14, Oct 2010.
[19] V. Filipe, A. Hawe, H. Schellekens, and W. Jiskoot, "Aggregation and immunogenicity of therapeutic proteins," in Aggregation of therapeutic proteins, W. Wang and C. J. Roberts, Eds., ed New Jersey: John Wiley & Sons, 2010, pp. 403-433.
[20] S. Hermeling, H. Schellekens, C. Maas, M. F. Gebbink, D. J. Crommelin, and W. Jiskoot, "Antibody response to aggregated human interferon alpha2b in wild-type and transgenic immune tolerant mice depends on type and level of aggregation," J Pharm Sci, vol. 95, pp. 1084-96, May 2006.
[21] M. M. van Beers, M. Sauerborn, F. Gilli, V. Brinks, H. Schellekens, and W. Jiskoot, "Aggregated recombinant human interferon Beta induces antibodies but no memory in immune-tolerant transgenic mice," Pharmaceutical research, vol. 27, pp. 1812-24, Sep 2010.
[22] V. Brinks, W. Jiskoot, and H. Schellekens, "Immunogenicity of therapeutic proteins: the use of animal models," Pharmaceutical research, vol. 28, pp. 2379-85, Oct 2011.
[23] H. Schellekens, "How to predict and prevent the immunogenicity of therapeutic proteins," Biotechnol Annu Rev, vol. 14, pp. 191-202, 2008.
[24] M. M. van Beers, M. Sauerborn, F. Gilli, S. Hermeling, V. Brinks, H. Schellekens, and W. Jiskoot, "Hybrid transgenic immune tolerant mouse model for assessing the breaking of B cell tolerance by human interferon beta," Journal of immunological methods, vol. 352, pp. 32-7, Jan 31 2010.
[25] S. Hermeling, W. Jiskoot, D. Crommelin, C. Bornaes, and H. Schellekens, "Development of a transgenic mouse model immune tolerant for human interferon Beta," Pharmaceutical research, vol. 22, pp. 847-51, Jun 2005.
[26] S. Hermeling, H. Schellekens, C. Maas, M. F. Gebbink, D. J. Crommelin, and W. Jiskoot, "Antibody response to aggregated human interferon alpha2b in wild-type and transgenic immune tolerant mice depends on type and level of aggregation," Journal of pharmaceutical sciences, vol. 95, pp. 1084-96, May 2006.
[27] I. C. Nicholson, X. Zou, A. V. Popov, G. P. Cook, E. M. Corps, S. Humphries, C. Ayling, B. Goyenechea, J. Xian, M. J. Taussig, M. S. Neuberger, and M. Bruggemann, "Antibody repertoires of four- and five-feature translocus mice carrying human immunoglobulin heavy chain and kappa and

lambda light chain yeast artificial chromosomes," Journal of immunology, vol. 163, pp. 6898-906, Dec 15 1999.
[28] S. Li, T. H. Nguyen, C. Schoneich, and R. T. Borchardt, "Aggregation and precipitation of human relaxin induced by metal-catalyzed oxidation," Biochemistry, vol. 34, pp. 5762-72, May 2 1995.
[29] B. H. Zimm, "The dependence of the scattering of light on angle and concentration in linear polymer solutions," The Journal of physical and colloid chemistry, vol. 52, pp. 260-7, Jan 1948.
[30] S. M. Kelly, T. J. Jess, and N. C. Price, "How to study proteins by circular dichroism," Biochimica et biophysica acta, vol. 1751, pp. 119-39, Aug 10 2005.
[31] A. Aghaie, A. A. Pourfathollah, S. Z. Bathaie, S. M. Moazzeni, H. K. Pour, and S. Banazadeh, "Structural study on immunoglobulin G solution after pasteurization with and without stabilizer," Transfusion medicine, vol. 18, pp. 62-70, Feb 2008.
[32] P. A. van Schouwenburg, G. M. Bartelds, M. H. Hart, L. Aarden, G. J. Wolbink, and D. Wouters, "A novel method for the detection of antibodies to adalimumab in the presence of drug reveals "hidden" immunogenicity in rheumatoid arthritis patients," Journal of immunological methods, vol. 362, pp. 82-8, Oct 31 2010.
[33] S. Juna and A. Huber, "Effect of varying flow regimes upon elution behaviour, apparent molecular characteristics and hydrodynamic properties of amylopectin isolated from normal corn starch using asymmetrical flow field-flow fractionation," Journal of chromatography. A, Nov 19 2011.
[34] A. Hawe, M. Sutter, and W. Jiskoot, "Extrinsic fluorescent dyes as tools for protein characterization," Pharmaceutical research, vol. 25, pp. 1487-99, Jul 2008.
[35] B. Demeule, M. J. Lawrence, A. F. Drake, R. Gurny, and T. Arvinte, "Characterization of protein aggregation: the case of a therapeutic immunoglobulin," Biochimica et biophysica acta, vol. 1774, pp. 146-53, Jan 2007.
[36] J. T. Pelton and L. R. McLean, "Spectroscopic methods for analysis of protein secondary structure," Analytical biochemistry, vol. 277, pp. 167-76, Jan 15 2000.
[37] A. Imanishi and T. Isemura, "Circular dichroic spectra of L-cystine and its dihydrochloride crystals in KBr disc in relation to the circular dichroism of disulfide bonds in proteins," Journal of biochemistry, vol. 65, pp. 309-12, Feb 1969.
[38] S. Hermeling, L. Aranha, J. M. Damen, M. Slijper, H. Schellekens, D. J. Crommelin, and W. Jiskoot, "Structural characterization and immunogenicity in wild-type and immune tolerant mice of degraded recombinant human interferon alpha2b," Pharmaceutical research, vol. 22, pp. 1997-2006, Dec 2005.
[39] H. Schellekens, "Immunogenicity of therapeutic proteins," Nephrology, dialysis, transplantation : official publication of the European Dialysis and Transplant Association - European Renal Association, vol. 18, pp. 1257-9, Jul 2003.
[40] J. L. Ottesen, P. Nilsson, J. Jami, D. Weilguny, M. Duhrkop, D. Bucchini, S. Havelund, and J. M. Fogh, "The potential immunogenicity of human insulin and insulin analogues evaluated in a transgenic mouse model," Diabetologia, vol. 37, pp. 1178-85, Dec 1994.
[41] M. E. Weksler, G. Bull, G. H. Schwartz, K. H. Stenzel, and A. L. Rubin, "Immunologic responses of graft recipients to antilymphocyte globulin: effect of prior treatment with aggregate-free gamma globulin," The Journal of clinical investigation, vol. 49, pp. 1589-95, Aug 1970.
[42] J. C. Cerottini, P. H. Lambert, and F. J. Dixon, "Comparison of the immune responsiveness of NZB and NZB X NZW F1 hybrid mice with that of other strains of mice," The Journal of experimental medicine, vol. 130, pp. 1093-105, Nov 1 1969.
[43] C. E. Biro and G. Garcia, "The Antigenicity of Aggregated and Aggregate-Free Human Gamma-Globulin for Rabbits," Immunology, vol. 8, pp. 411-9, Apr 1965.
[44] E. S. Golub and W. O. Weigle, "Studies on the induction of immunologic unresponsiveness. 3. Antigen form and mouse strain variation," Journal of immunology, vol. 102, pp. 389-96, Feb 1969.
[45] M. Fujiwara, S. Fujiwara, C. Yoshizaki, and A. Awaya, "Strain differences in the immunogenicity of

aggregated human IgG and the adjuvant action of lipopolysaccharide on the low-responder strain of mice," Japanese journal of microbiology, vol. 20, pp. 141-6, Apr 1976.
[46] W. V. Moore and P. Leppert, "Role of aggregated human growth hormone (hGH) in development of antibodies to hGH," The Journal of clinical endocrinology and metabolism, vol. 51, pp. 691-7, Oct 1980.
[47] M. M. van Beers, M. Sauerborn, F. Gilli, V. Brinks, H. Schellekens, and W. Jiskoot, "Oxidized and aggregated recombinant human interferon beta is immunogenic in human interferon beta transgenic mice," Pharmaceutical research, vol. 28, pp. 2393-402, Oct 2011.
[48] E. R. Stadtman, "Metal ion-catalyzed oxidation of proteins: biochemical mechanism and biological consequences," Free radical biology & medicine, vol. 9, pp. 315-25, 1990.
[49] S. Gallucci and P. Matzinger, "Danger signals: SOS to the immune system," Current opinion in immunology, vol. 13, pp. 114-9, Feb 2001.

APPENDIX

Chromosomal DNA isolation

- Add 20 µl of ear punch buffer* to each tube of ear clips from individual mouse
- Add 2 µl of Proteinase K (Fermentas, 10 mg/ml)
- Incubate at 55°C for 15 minutes
- Vortex vigorously
- Continue incubation at 55°C for another 15 minutes (or longer)
- Add 200 µl of distilled water and for each tube pick a whole on the lid (with syringes)
- Incubate the tubes for 10 minutes at 55°C and then chill on ice for 5 minutes
- Vortex, and spin down for 5 min at 13,000 rpm
- The supernatant contained DNA that is ready to be used for PCR

*Ear punch buffer contains

- 50 mM Tris-HCl pH 8.0 (Trizma Base) – 0,303 g
- 20 mM NaCl – 0.0584 g
- 1 mM EDTA – 0.0146 g
- 1 % SDS – 2.5 ml (of 20% SDS solution)
- Add up to 50 ml with ddH_2O

Per PCR reaction tube contains:

- 0.3 µl DNA
- 3.5 µl dNTPs (Takara)
- 0.5 µl Primer forward
- 0.5 µl Primer reverse
- 2 µl Buffer 3 (ELT Roche)
- 0.3 µl ELT polymerase (ELT Roche)
- 12.9 µl distilled water

Name of primers	Primer sequence (5' – 3')
Heavy chain forward	ACT-GTG-TCC-CTG-TGT-GAT-GC
Heavy chain reverse	CCA-AGG-TCA-TTT-TGT-CCC-C
κ light chain forward	AGC-AAC-ACT-CTC-AGC-CAA-TG
κ light chain reverse	CTC-AGG-TTC-CAG-ATG-CGA-C
λ light chain forward	GGG-GCC-AAG-GCG-CAG-AGA-TCT-CAG-G
λ light chain reverse	CAC-TGG-GTT-CAG-GGT-TCT-TTC-CAC-C

Reaction	PCR program
Heavy & κ light chain	
1. Initial denaturation	95°C, 3 minutes
2. Denaturation	95°C, 30 seconds
Annealing	56°C, 1 minute
Elongation	72°C, 2 minutes
3. Denaturation	95°C, 1 minute
Annealing	56°C, 1 minute
Elongation	72°C, 2 minutes, repeat step3 for 30 cycles
4. Final Elongation	72°C, 10 minutes

λ light chain

The program for λ chain is similar to heavy and κ light chain, only the annealing temperature was increased to 60°C for 1 minute.

Chapter 10

Summary and perspectives

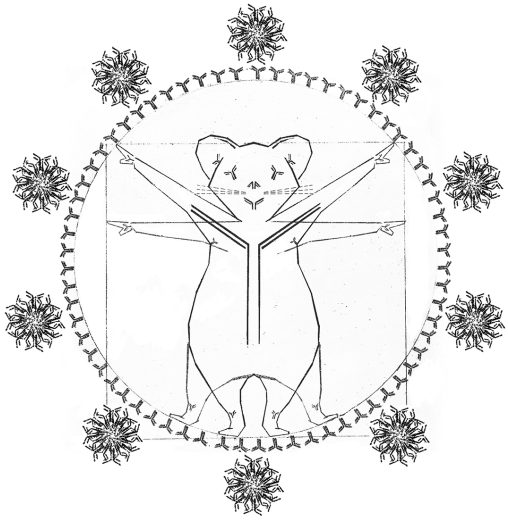

SUMMARY

Monoclonal antibodies (MAbs) are used to treat several chronic and severe diseases and are currently the fastest growing class of drugs (**Chapter 1**). However, a major concern associated with the use of MAbs, as for nearly all other therapeutic proteins, is that their repeated administration to patients often leads to the induction of undesirable anti-drug antibodies (ADAs), also known as immunogenicity. The development of ADAs in patients can lead to a wide range of clinical consequences, varying from none to life-threatening situations [1].

Immunogenicity has been a major issue ever since proteins were used as therapeutics. Even though advances have been made in understanding the mechanisms underlying immunogenicity of therapeutic proteins, opinions are often conflicting, and to a large extent based on assumptions rather than facts. Among the several factors playing a role in immunogenicity, the presence of protein aggregates in formulations has been put forward as a major concern [2]. However, despite the clear connection between protein aggregates and immunogenicity, little is known about the nature of the aggregate species responsible for immune reactions.

In **Chapter 2** the current knowledge about the correlation between immunogenicity and aggregates of therapeutic proteins is summarized. Repetitive epitope presentation has been pointed as the most likely cause of aggregate-related immunogenicity, since it might mimic well conserved microbial or viral patterns, to which the immune system has learned to vigorously react [3]. The risk caused by the presence of aggregates should be evaluated not only by the tendency of aggregates to trigger ADAs, but also by the clinical consequences that these ADAs may have. Given that therapeutic proteins may have different aggregation profiles and pose unique immunological risks, a case-by-case approach is needed. According to the type of immunogenic threat posed by protein aggregates, several immunological mechanisms have been proposed, which may or may not require T-cell help. The development of reliable models to predict the immunogenicity of protein aggregates is highly necessary, but is in some way dependent on the elucidation of these mechanisms.

In **Chapter 3** a new analytical method - nanoparticle tracking analysis (NTA) - was evaluated for the measurement of submicron protein aggregates and compared with dynamic light scattering (DLS). NTA enables the measurement of protein aggregates ranging in size from about 30 to 1000 nm. This technique can be more time-consuming

than DLS, but has some clear advantages. NTA enables the visualization of the sample, gives an approximate particle concentration and obtains size information based on the Brownian motion of individual particles. NTA is very accurate for sizing both monodisperse and polydisperse samples and has a substantially better peak resolution than DLS. NTA is very suitable for analyzing protein aggregates, but the monomers of most proteins cannot be detected, since they are under the lower detection limit. Care should be taken that sample preparation does not influence the aggregate distribution in the measurement cell. Altogether, these results show that NTA is a powerful characterization technique that complements DLS and is particularly valuable for analyzing polydisperse samples.

In **Chapter 4** the use of native electrospray ionization time-of-flight (ESI-TOF) mass spectrometry (MS) for the analysis of low-order oligomers of IgG was tested. IgG dimers, trimers, tetramers and other low-order oligomers were created by subjecting an IgG formulation to several pH-shifts. Proper sample preparation (dialysis against a MS-compatible volatile buffer) and chromatographic separation of monomer, dimer and trimer/tetramer fractions by size exclusion chromatography (SEC) resulted in improved MS analysis. Both the SEC protocol and the ESI-TOF MS technique were shown to leave the IgG oligomers largely intact. In conclusion, ESI-TOF MS is a useful method that adds to our current analytical arsenal to identify and characterize MAb oligomers.

The mechanism of IgG aggregation induced by pH-shift was investigated in **Chapter 5**. A short exposure of IgG to low pH results in the formation of a wide size range of non-native aggregates as well as a large amount of molten globules that seem to be the key element for the aggregation process. While some of these conformationally altered monomers fold back into the native state, others are converted into aggregates, presumably by a downhill polymerization mechanism. These results highlight the role of partially unfolded species in the aggregation of therapeutic proteins. Since the exposure of MAbs to low pH is often unavoidable during purification processes, it is important to ensure the structural integrity of the molecules during these processes, in order to avoid subsequent protein aggregation.

In **Chapter 6** the potential of a new analytical technique - fluorescence single particle tracking (fSPT) - for the characterization of submicron protein aggregates in human serum and plasma was evaluated. fSPT enables the measurement of protein aggregates in the size range from about 50 to 1000 nm. This technique provides comparable size distributions to the ones obtained with NTA for aggregates and nanoparticles in buffer and has the added advantage that it can also be applied

to look at samples in biological fluids. fSPT has also been shown to be suitable for selectively analyzing protein aggregates in complex formulations, such as those containing HSA. Using dual color fSPT, it was possible to verify that most of the aggregates created by heat stress, in an HSA-containing IgG formulation, were composed of a mixture of IgG and HSA.

The fate and behavior of subvisible IgG aggregates in biological fluids was investigated in **Chapter 7**. Whilst unstressed IgG remains apparently unchanged in serum (i.e. it did not spontaneously aggregate), certain aggregates of the same protein do. Aggregates formed by pH-shift were particularly susceptible, whereas the ones formed by heat stress seem to be stable. These results indicate that the aggregation profile may drastically change once the formulation is administered and emphasize the importance of analytical strategies for monitoring aggregation in undiluted biological fluids.

Chapter 8 described a pilot study performed to investigate the feasibility of *in vivo* fluorescent imaging of Alexa Fluor® 700 labeled protein (aggregates) in mice and to compare the localization of intraperitoneally injected non-aggregated and aggregated formulations of a human monoclonal antibody (IgG) and recombinant human interferon alpha 2a (IFN-α) over time. IFN-α aggregates induced by metal-catalyzed oxidation and IgG aggregates induced by shaking stress were injected and *in vivo* fluorescence images were captured over time. Results show that this setup is suitable to study biodistribution of labeled therapeutic proteins *in vivo*. Moreover, preliminary data suggests that aggregated IFN-α and IgG formulations have decreased elimination rates as compared with non-aggregated formulations. Protein present in aggregated formulations accumulated in the lower abdominal region, but it is impossible to know exactly in which organ/tissue and if it was due to previously formed protein aggregates or to accumulation of monomers.

In **chapter 9** the correlation between the type and amount of IgG aggregates and their immunogenic potential was investigated in transgenic (TG) mice (containing human Ig genes). In general, stress-induced aggregation of IgG led to enhanced immunogenicity, but not all aggregates to the same extent. The metal-catalyzed oxidized IgG formulation was the most immunogenic. From all the aggregate features investigated in this work (size, amount, structural conformation, hydrophobicity, morphology, type of intermolecular bonds, etc.) the presence of oxidized IgG species, most likely incorporated in aggregates, seemed to have the highest impact on the immunogenicity of this IgG. Stressed formulations were ranked according to their immunogenic potential as follows: metal-catalyzed oxidized > heated ≈ pH-shift

stressed ≈ shaken > freeze-thawed.

PERSPECTIVES

Characterization of protein aggregates in biopharmaceuticals

One of the main challenges of developing therapeutic proteins is their propensity to aggregate during manufacturing, storage and administration [4, 5]. Protein aggregates have been associated with adverse immune reactions and are a major concern for the pharmaceutical industry and regulatory agencies. Even though several analytical techniques are available for the characterization of protein aggregates, only a few are routinely used for quality control (QC) purposes by pharmaceutical companies (Table 10.1) [6].

The main challenges in analyzing protein aggregates lie in their fairly unstable nature and their wide size range of up to six orders of magnitude, from a few nm to a few mm. To properly characterize protein aggregates, a combination of several analytical techniques is necessary. Nevertheless, the available methods are often based on different physical measuring principles and, consequently, the results are not always congruent between complementary techniques.

Most analytical techniques used for QC of therapeutic protein products focus either on aggregates larger than 1 μm or smaller than 50 nm (Table 10.1), leaving a significant analytical gap in the subvisible size range. Recently, an article reflecting the opinion of a number of academic researchers and regulators of the U.S. Food and Drug Administration (FDA) warned the pharmaceutical industry that overlooking subvisible aggregates smaller than 10 μm during product QC could be compromising the safety and efficacy of therapeutic proteins [7]. One year later, an answer to this article came from major pharmaceutical and biotech companies stating that such aggregates constitute a much smaller fraction of protein as compared with currently monitored sizes (≥ 10 μm) and that the current limitations in analytical technologies make the measurement of these small subvisible aggregates unsuitable as specification for release, stability or comparability [8].

The United States Pharmacopeia (USP) states that particles > 10 μm should be controlled below 6000 particles/container and particles > 25 μm below 600 particles/container, although there are no studies reporting differences in immunogenicity between different sizes of aggregates [7]. In Chapter 9 of this thesis, all IgG stressed formulations administered in mice, with exception of the shake

Table 10.1: Typical analytical techniques used for protein aggregate characterization. The techniques evaluated in detail in this thesis are highlighted. Adapted from Engelsman *et al.* [6]

Method	Observable	Size range	Robust.[a]	Sens.[a]	Thrpt[a,b]	QC method
Visual inspection	Visible particles	>50 μm – mm	Medium	Medium	High	Yes
Turbidity	Optical density	N/A	High	Medium	Medium	Yes
Flow imaging	Concentration/size/ morphology	1–400 μm	Low	N/A	Medium	No
Light obscuration	Concentration/size	1–100 μm	Medium	Medium	Medium	Yes
Fluorescence microscopy	Particles/amyloid proteins	>1 μm – mm	Low	High	Low	No
Electron microscopy	Size/morphology	nm - μm	Low	N/A	Low	No
Optical microscopy	Size/morphology	>1 μm – mm	Medium	N/A	Low	No
DLS	Hydrodynamic size	1 nm – 5 μm	Medium	High	High	No
NTA	Concentration/size	30 nm – 1 μm	Medium	Medium	Medium	No
fSPT	Concentration/size	30 nm – 1 μm	Low	Medium	Low	No
AUC	Molecular weight/ shape	1 nm – 0.1 μm	Low	Medium	Low	No
SEC-UV	Hydrodynamic size	1–50 nm	High	Medium	High	Yes
AF4-UV	Hydrodynamic size	1 nm – few μm	Medium	Medium	High	No
Native MS	Mass/charge ratio	Atomic - MDa	Low	Medium	Low	No
Atomic force microscopy	Size/morphology	nm range	Medium	N/A	Low	No
SDS-PAGE	Molecular weight	kDa – MDa	Medium	Medium	High	Yes
Native PAGE	Electrophoretic mobility	kDa – MDa	Medium	Low	Medium	No
CE-SDS	Molecular weight/ Isoelectric point	kDa – MDa	Medium	Medium	High	Yes
UV-VIS spectroscopy	Optical density (presence of aggregates)/folding state shifts	N/A	Medium	Medium	High	No
Infrared spectroscopy	Secondary structure	N/A	Medium	N/A	Low	No
Raman spectroscopy	Secondary structure/ chemical characterization	N/A	Medium	N/A	Low	No
Fluorescence spectroscopy	Tertiary/quarternary structure	N/A	Medium	N/A	High	No
CD spectroscopy	Secondary/tertiary/ quaternary structure	N/A	Medium	N/A	Medium	No

[a]Scoring (low, medium, or high) was based on consensus of opinion of Engelsman *et al.* [6] or the opinion of the authors of chapters 3 and 4 of this thesis, for NTA and fSPT, respectively; [b]Low: <10; medium: 10–25, high: >25 per day and per operator; Sens.: sensitivity; Robust.: robustness; Thrpt: throughput; QC: quality

control; DLS: dynamic light scattering; NTA: nanoparticle tracking analysis; fSPT: fluorescence single particle tracking; AUC: analytical ultracentrifugation; SEC-UV: size exclusion chromatography with UV detection; AF4-UV: assymetrical flow-field flow fractionation with UV detection; MS: mass spectrometry; SDS-PAGE: sodium dodecyl sulfate polyacrylamide gel electrophoresis; CE-SDS: capillary sodium dodecyl sulfate electrophoresis; UV-VIS: UV visible; CD: circular dichroism; N/A = not applicable.

stressed formulation, would have passed USP standards and yet most of them had increased immunogenicity as compared with the unstressed formulation. These results support the concerns about only looking at aggregates ≥ 10 µm to ensure quality of therapeutic protein products.

Among the currently available techniques that cover the analytical size gap already mentioned, NTA (size range: 30 nm - 1 µm) and flow imaging (size-range: 1 - 400 µm) enable the visualization of aggregates in solution and provide accurate size distributions and approximate aggregate concentrations [9, 10], which is a combination of features not present in most other analytical techniques in this size range. Chapter 3 of this thesis describes the first study evaluating the use of NTA for measuring protein aggregates. This technique demonstrated great potential, but some drawbacks (discussed in chapter 3) are hindering an eventual implementation as a QC technique. Flow imaging seems to be more adapted and may even replace light obscuration as the standard validation technique for measuring micron-sized particles [11].

Monitoring protein aggregation in biological fluids

Analytical methods to investigate protein aggregates in biological fluids are scarce and very little is known about the fate of protein pharmaceuticals and their aggregates following administration. In theory, biological fluids should provide ideal conditions to prevent the aggregation of its components and the hypothesis of spontaneous aggregation of therapeutic proteins upon injection is usually not considered. However, the concentration of these therapeutic proteins at the site of administration is several fold normal concentration and this may lead to unexpected interactional scenarios. In chapter 7 of this thesis, different analytical techniques were used to monitor protein aggregation in serum. This rather unexplored research field may provide answers to aggregate-related immunogenicity questions, which may have pharmacokinetic/pharmacodynamic (PK/PD) implications.

In order to monitor therapeutic protein aggregation in biological media it is necessary to label the protein of interest. However a label may have an effect on

the aggregation profile of therapeutic proteins. [12]. Therefore, it is very important to ensure, on a case by case basis, that the label has a minor impact on the stability of the therapeutic protein before performing measurements in biological fluids. This may be a challenging and time-consuming process, but monitoring the fate of therapeutic proteins and their aggregates in biological media may provide crucial information for drug development phases and help to understand some of the adverse reactions observed for some of these drugs.

Biodistribution of therapeutic protein aggregates

Factors that may influence the biodistribution of therapeutic proteins include size, charge, target and off-target binding properties, route of administration, presence of aggregates in formulation and immunogenicity [13]. Biodistribution studies of therapeutic proteins are usually performed with radiolabeled compounds, with ^{125}I being the most commonly used isotope [14]. The typical parameters that are used to describe protein distribution include tissue concentrations, tissue-to-blood/plasma/serum concentration ratios, serum half-life and clearance. However, no studies have reported the aggregate biodistribution of therapeutic proteins.

In chapter 8 of this thesis, an innovative approach to investigate the localization/bioaccumulation of aggregated and monomeric IgG in mice is presented, showing differences in clearance and distribution profiles between aggregated and non-aggregated formulations. These preliminary results open the way for a new research approach on aggregate-related immunogenicity. Nowadays, *in vivo* imaging technologies enable unprecedented resolution, sensitivity and versatility. For example, using non-invasive fluorescence molecular tomography (FMT) [15] and the appropriate experimental conditions, it should be possible to detect and quantify in real time fluorescently labeled therapeutic proteins and their aggregates in all types of animal organs. One of the great advantages of using fluorescence for biodistribution studies is the ability to simultaneously track different fluorescent dyes emitting at different wavelengths, which considerably broadens experimental possibilities. This type of research could provide crucial information about the role of aggregates in immunogenicity of therapeutic proteins and should be further explored.

Aggregate-related immunogenicity

It is now clear that even highly pure formulations of fully human therapeutic

proteins may induce ADA formation in patients. The work described in chapter 9 strengthens the importance of protein aggregates for ADA formation to therapeutic MAbs. We have demonstrated that not all protein aggregates are equally immunogenic, but the heterogeneity of the aggregates makes it difficult to pinpoint the most/least immunogenic species. A possible follow-up study could be to fractionate the aggregates of stressed formulations and test the immunogenicity of the fractions separately. Nonetheless, given the inherent instability of aggregated systems, obtaining stable monomeric and aggregated fractionations from stressed formulations will be very challenging.

Understanding the mechanism by which aggregates trigger immune responses would be very helpful to be able to identify the aggregates that pose the highest risk for immunogenicity of therapeutic proteins. One of the most supported hypothesis states that protein aggregates presenting repetitive epitopes at a spacing of 5-10 nm are capable of cross-linking multiple B-cell receptors and trigger an antibody response without immunological memory [3, 16]. However, very few studies have directly addressed this subject and this hypothesis is mostly based on assumptions and sparse studies, mostly in the vaccine field. Thus, more research is needed to clarify the mechanisms of aggregate-related immunogenicity.

The number of therapeutic proteins in development phases will significantly increase during the next coming years and most of them will certainly induce immune responses in some patients. Humanization, T-cell epitope removal and PEGylation are some of the strategies used to circumvent immunogenicity of biopharmaceuticals. The future will teach us how successful these approaches really are. In any case, preventing aggregation during processing, formulation, transportation, storage and administration will remain an important approach to avoid adverse immune responses as much as possible.

REFERENCES

[1] H. Schellekens, “Bioequivalence and the immunogenicity of biopharmaceuticals,” Nat Rev Drug Discov, vol. 1, pp. 457-62, Jun 2002.

[2] A. S. Rosenberg, “Effects of protein aggregates: an immunologic perspective,” The AAPS journal, vol. 8, pp. E501-7, 2006.

[3] T. Fehr, M. F. Bachmann, E. Bucher, U. Kalinke, F. E. Di Padova, A. B. Lang, H. Hengartner, and R. M. Zinkernagel, “Role of repetitive antigen patterns for induction of antibodies against antibodies,” The Journal of experimental medicine, vol. 185, pp. 1785-92, May 19 1997.

[4] J. S. Bee, T. W. Randolph, J. F. Carpenter, S. M. Bishop, and M. N. Dimitrova, “Effects of surfaces and leachables on the stability of biopharmaceuticals,” Journal of pharmaceutical sciences, Apr 26 2011.

[5] M. E. Cromwell, E. Hilario, and F. Jacobson, “Protein aggregation and bioprocessing,” The AAPS journal, vol. 8, pp. E572-9, 2006.
[6] J. den Engelsman, P. Garidel, R. Smulders, H. Koll, B. Smith, S. Bassarab, A. Seidl, O. Hainzl, and W. Jiskoot, “Strategies for the assessment of protein aggregates in pharmaceutical biotech product development,” Pharmaceutical research, vol. 28, pp. 920-33, Apr 2011.
[7] J. F. Carpenter, T. W. Randolph, W. Jiskoot, D. J. Crommelin, C. R. Middaugh, G. Winter, Y. X. Fan, S. Kirshner, D. Verthelyi, S. Kozlowski, K. A. Clouse, P. G. Swann, A. Rosenberg, and B. Cherney, “Overlooking subvisible particles in therapeutic protein products: gaps that may compromise product quality,” Journal of pharmaceutical sciences, vol. 98, pp. 1201-5, Apr 2009.
[8] S. K. Singh, N. Afonina, M. Awwad, K. Bechtold-Peters, J. T. Blue, D. Chou, M. Cromwell, H. J. Krause, H. C. Mahler, B. K. Meyer, L. Narhi, D. P. Nesta, and T. Spitznagel, “An industry perspective on the monitoring of subvisible particles as a quality attribute for protein therapeutics,” Journal of pharmaceutical sciences, vol. 99, pp. 3302-21, Aug 2010.
[9] V. Filipe, A. Hawe, and W. Jiskoot, “Critical evaluation of Nanoparticle Tracking Analysis (NTA) by NanoSight for the measurement of nanoparticles and protein aggregates,” Pharmaceutical research, vol. 27, pp. 796-810, May 2010.
[10] J. G. Barnard, S. Singh, T. W. Randolph, and J. F. Carpenter, “Subvisible particle counting provides a sensitive method of detecting and quantifying aggregation of monoclonal antibody caused by freeze-thawing: insights into the roles of particles in the protein aggregation pathway,” Journal of pharmaceutical sciences, vol. 100, pp. 492-503, Feb 2011.
[11] D. K. Sharma, D. King, P. Oma, and C. Merchant, “Micro-flow imaging: flow microscopy applied to sub-visible particulate analysis in protein formulations,” The AAPS journal, vol. 12, pp. 455-64, Sep 2010.
[12] R. E. Crandall, J. Janatova, and J. D. Andrade, “The effects of radioiodination and fluorescent labelling on albumin,” Preparative biochemistry, vol. 11, pp. 111-38, 1981.
[13] B. L. Ferraiolo, M. A. Mohler, and C. A. Gloff, Protein pharmacokinetics and metabolism, 1st edition ed. New York: Plenum Press, 1992.
[14] Y. Vugmeyster, D. DeFranco, P. Szklut, Q. Wang, and X. Xu, “Biodistribution of [^{125}I]-labeled therapeutic proteins: application in protein drug development beyond oncology,” Journal of pharmaceutical sciences, vol. 99, pp. 1028-45, Feb 2010.
[15] K. O. Vasquez, C. Casavant, and J. D. Peterson, “Quantitative whole body biodistribution of fluorescent-labeled agents by non-invasive tomographic imaging,” PloS one, vol. 6, p. e20594, 2011.
[16] M. Sauerborn, V. Brinks, W. Jiskoot, and H. Schellekens, “Immunological mechanism underlying the immune response to recombinant human protein therapeutics,” Trends in pharmacological sciences, vol. 31, pp. 53-9, Feb 2010.

Nederlandse samenvatting

Monoklonale antilichamen (MAbs) worden gebruikt om verschillende chronische en ernstige ziekten te behandelen, en zijn op dit moment de snelst groeiende klasse van medicijnen (**Hoofstuk 1**). Een belangrijk aandachtspunt bij het gebruik van MAbs als geneesmiddel, zoals dat geldt voor bijna alle andere therapeutische eiwitten, is echter hun immunogeniciteit: herhaalde toediening aan patiënten leidt vaak tot het ontstaan van ongewenste anti-medicijn antilichamen (ADAs). De vorming van ADAs kan diverse klinische gevolgen hebben, zoals een verlies aan therapeutisch effect en soms zelfs levensbedreigende situaties.

Sinds eiwitten gebruikt worden als geneesmiddelen is immunogeniciteit altijd al een belangrijke kwestie geweest. Hoewel vooruitgang is geboekt in het begrijpen van de mechanismen die ten grondslag liggen aan de immunogeniciteit van therapeutische eiwitten, zijn de meningen vaak verdeeld en voor een groot deel gebaseerd op veronderstellingen in plaats van feiten. Onder de verschillende factoren die een rol spelen bij immunogeniciteit is de aanwezigheid van eiwitaggregaten in formuleringen altijd naar voren geschoven als een belangrijke risicofactor. Echter, ondanks de duidelijke samenhang tussen aggregaten en immunogeniciteit, is er nog steeds weinig bekend over welke aggregaten nu precies verantwoordelijk zijn voor immuunreacties.

In **Hoofdstuk 2** is de huidige kennis over de correlatie tussen immunogeniciteit en aggregatie van therapeutische eiwitten samengevat. De presentatie van repetitieve epitopen (aanwezig in eiwitaggregaten) aan B-cellen wordt gezien als de meest waarschijnlijke oorzaak van aggregaat-gerelateerde immunogeniciteit, aangezien het microbiële of virale patronen kan weerspiegelen, waarop het immuunsysteem krachtig reageert. Echter, ook andere immunologische mechanismen zijn denkbaar, waarbij T-cellen al dan niet een rol spelen. De ontwikkeling van betrouwbare modellen die de immunogeniciteit van eiwitaggregaten kunnen voorspellen is hoogst noodzakelijk. Ter ondersteuning daarvan is het van belang dat de immunologische mechanismen opgehelderd worden. Idealiter zouden zulke modellen niet alleen de incidentie en mate van ADA-vorming moeten voorspellen, maar ook de klinische gevolgen ervan.

In **Hoofdstuk 3** werd een nieuwe analytische methode –nanoparticle tracking analysis (NTA)– geëvalueerd voor de meting van sub-micron eiwitaggregaten, en vergeleken met dynamische lichtverstrooiing (DLS). NTA maakt de meting van eiwitaggregaten mogelijk die in grootte variëren van ongeveer 30 tot 1000 nm. Deze techniek kan meer tijd in beslag nemen dan DLS, maar heeft een aantal duidelijke voordelen. NTA maakt visualisatie van het monster mogelijk, geeft een

geschatte concentratie van de deeltjes en verschaft informatie over de grootte op basis van de Brownse beweging van individuele deeltjes. NTA kan de deeltjesgrootte voor zowel monodisperse als polydisperse monsters nauwkeurig bepalen en heeft een aanzienlijk betere resolutie dan DLS. NTA is zeer geschikt voor het analyseren van eiwitaggregaten, maar de monomeren van de meeste eiwitten kunnen niet worden gedetecteerd, omdat ze onder de ondergrens van detectie vallen. Voorzichtigheid is geboden dat de monstervoorbereiding niet van invloed is op de deeltjesgrootteverdeling van de aggregaten in de meetcel. Op grond van de resultaten kan geconcludeerd worden dat NTA een krachtige karakteriseringstechniek is die een welkome aanvulling is op DLS en bijzonder waardevol is voor het analyseren van polydisperse monsters.

In **Hoofdstuk 4** werd het gebruik van natieve electrospray ionisation time-of-flight (ESI-TOF) massaspectrometrie (MS) voor de analyse van MAb-oligomeren getest. Hiertoe werd, evenals in de hieropvolgende hoofdstukken, gebruikgemaakt van een model MAb, een monoklonaal IgG. IgG dimeren, trimeren, tetrameren en grotere oligomeren werden gemaakt door een IgG-formulering aan herhaalde pH-verschuivingen te onderwerpen. De juiste monstervoorbereiding (dialyse tegen een vluchtige, MS-compatibele buffer), alsmede de chromatografische scheiding van monomeer, dimeer- en trimeer-/tetrameerfracties door gelpermeatiechromatografie (SEC), resulteerde in verbeterde MS-analyse. Zowel het SEC-protocol als de ESI-TOF-MS techniek lieten zien dat de IgG oligomeren tijdens deze monstervoorbereiding grotendeels intact bleven. Concluderend, ESI-TOF-MS is een nuttige toevoeging aan ons huidige analytische arsenaal om IgG-oligomeren te identificeren en te karakteriseren.

Het mechanisme achter IgG-aggregatie die door pH-verschuiving wordt veroorzaakt werd onderzocht in **Hoofdstuk 5**. Aangezien MAbs tijdens de zuivering vaak blootgesteld worden aan een lage pH, is het belangrijk om de eiwitstructuur onder deze omstandigheden vast te stellen en aggregatie te voorkomen. Een korte blootstelling van IgG aan een lage pH resulteerde in de vorming van een groot scala aan aggregaten en een grote hoeveelheid aan van vorm veranderde monomeren, zogeheten molten globules, die de sleutel tot het aggregatieproces lijken te zijn. Terwijl sommige molten globules terugvouwen in de oorspronkelijke staat, klonteren andere samen tot aggregaten, vermoedelijk via een mechanisme dat in de literatuur wel aangeduid wordt met downhill polymerisatie. Deze resultaten wijzen op de rol van molten globules bij de aggregatie van therapeutische eiwitten na blootstelling aan een zure omgeving.

In **Hoofdstuk 6** werd een nieuwe analytische techniek – het volgen van enkelvoudige fluorescente deeltjes met fluorescence single particle tracking (fSPT)– geëvalueerd voor de karakterisering van sub-micron eiwitaggregaten in menselijk serum en plasma. De fSPT-techniek maakt de meting van fluorescente eiwitaggregaten met een grootte tussen ongeveer 50 en 1000 nm mogelijk. Deze techniek heeft een vergelijkbaar deeltjesgroottebereik als NTA, maar heeft als toegevoegde waarde dat er ook gekeken kan worden naar monsters in biologische vloeistoffen, zoals aangetoond werd voor geaggregeerd IgG. fSPT is ook geschikt gebleken voor het selectief analyseren van eiwitaggregaten in complexe formuleringen, welke bijvoorbeeld humaan serumalbumine (HSA) bevatten. Door IgG en HSA covalent te labelen met een verschillende fluorescerende kleurstof en door gebruikmaking van twee-kleuren fSPT, was het mogelijk om vast te stellen dat de meeste aggregaten, welke geïnduceerd waren door een HSA bevattende IgG-formulering kort te verhitten, uit een mengsel van IgG en HSA bestonden.

Het lot en gedrag van voor het blote oog onzichtbare, fluorescent gelabelde IgG-aggregaten in biologische vloeistoffen werd onderzocht in **Hoofdstuk 7**. Terwijl ongestresst IgG blijkbaar onveranderd blijft in serum (d.w.z. het aggregeerde niet spontaan), bleken bepaalde aggregaten van hetzelfde eiwit te veranderen van grootte. Met name aggregaten die gevormd waren door pH-verschuiving bleken gevoelig voor de invloed van serum, terwijl degenen die gevormd waren door een korte hittebehandeling stabiel leken te zijn. Deze resultaten wijzen erop dat het aggregatieprofiel drastisch kan veranderen wanneer een formulering wordt toegediend, en benadrukken het belang van analytische strategieën voor het meten van aggregaten in onverdunde biologische vloeistoffen.

In **Hoofdstuk 8** werd een voorstudie beschreven naar de haalbaarheid van fluorescente beeldvorming in-vivo voor het lokaliseren van fluorescent gelabelde eiwitaggregaten in muizen. Hiertoe werd Alexa Fluor® 700 covalent gekoppeld aan een humaan monoklonaal IgG en recombinant humaan interferon alfa-2a (INF-α). INF-α aggregaten (geïnduceerd door metaal-gekatalyseerde oxidatie) en IgG aggregaten (geïnduceerd door middel van schudden) werden intraperitoneaal geïnjecteerd, en in-vivo fluorescentiebeelden werden in de tijd vastgelegd. De resultaten laten zien dat deze methode geschikt is om de lotgevallen van therapeutische eiwitten en hun aggregaten in-vivo te bestuderen. Bovendien suggereren de voorlopige gegevens dat geaggregeerd INF-α en IgG een verlaagde eliminatiesnelheid hebben in vergelijking met de niet-geaggregeerde eiwitten. Geaggregeerd eiwit stapelde zich op in de lagere abdominale omgeving, maar het is met de huidige data onmogelijk om exact

vast te stellen in welk orgaan/weefsel dit plaatsvond.

In **Hoofdstuk 9** werd de correlatie tussen het type en de hoeveelheid IgG-aggregaten en hun immunogeniciteit onderzocht in transgene (TG) muizen (die menselijke Ig-genen bevatten). In het algemeen geldt dat door stress geïnduceerde aggregaten tot een verhoogde immunogeniciteit leidden, maar niet alle aggregaten in dezelfde mate. Van alle aggregaatkarakteristieken die in dit werk werden onderzocht (grootte, hoeveelheid, structurele conformatie, hydrofobiciteit, morfologie, type intermoleculaire bindingen, etc.) leek de aanwezigheid van geoxideerde IgG-moleculen, hoogstwaarschijnlijk opgenomen in aggregaten, de meeste invloed te hebben op de immunogeniciteit van dit IgG. Gestresste formuleringen werden als volgt gerangschikt volgens immunogeen potentieel: metaal-gekatalyseerde oxidatie > verwarmd ≈ pH verschuiving ≈ geschud > bevroren-ontdooid.

Abbreviations

ADAs	anti-drug antibodies
AF4	asymmetrical flow field-flow fractionation
APC	antigen presenting cell
AUC	area under the curve/analytical ultracentrifugation
BCR	B-cell receptor
BGG	bovine γ globulin
bis-ANS	4,4'-dianilino-1,1'-binaphthyl-5,5'-disulfonic acid dipotassium salt
CCD	charge coupled device
CD	circular dichroism
CDR	complementarity determining region
CLSM	confocal laser scanning microscopy
DC	dendritic cell
DDS	drug delivery system
DLS	dynamic light scattering
EDTA	ethylenediaminetetraacetic acid
ELISA	enzyme-linked immunosorbent assay
EPO	erythropoietin
ESI-TOF MS	electrospray ionization time-of-flight mass spectrometry
FCM	flow cytometry
FDA	U.S. food and drug administration
FOI	fluorescence optical imaging
fSPT	fluorescence single particle tracking
FT	freeze/thaw
HGG	human γ globulin
hGH	human growth hormone
HLA	human MHC II complex
HMW	high molecular weight
HRP	horse radish peroxidase
HSA	human serum albumin
i.m.	intramuscular
i.v.	intravenous
IFN-α	interferon-alpha
IgG	immunoglobulin
LO	light obscuration

MAb	monoclonal antibody
MALLS	multiple angle light scattering
MGDF	megakaryocyte growth and differentiation factor
MHC II	major histocompatibility complex class II
MW	molecular weight
NTA	nanoparticle tracking analysis
NTG	nontransgenic
OD	optical density
PAMP	pathogen-associated molecular pattern
PBS	phosphate buffered saline
PdI	polydispersity index
PK/PD	pharmacokinetic/pharmacodynamic
PLGA	poly (lactic-co-glycolic acid)
PMT	photomultiplier tube
PRCA	pure red cell aplasia
PRR	pattern recognition receptors
QC	quality control
s.c.	subcutaneous
SD	standard deviation
SDS-PAGE	sodium dodecyl sulfate/polyacrylamide gel electrophoresis
SEC	size exclusion chromatography
SEM	scanning electron microscopy
SSC	side scatter
Td	T-cell dependent
TG	transgenic
Ti	T-cell independent
TLR	toll-like receptors
TMC	N-trimethyl chitosan
TNF-α	tumor necrosis factor-alpha
USP	United States pharmacopeia
VLP	virus-like particles
Z-ave	Z-average diameter
[θ]MR	mean residue ellipticity

List of publications

Book chapters

Filipe V, Hawe A, Schellekens H and Jiskoot W. (2010) Aggregation and immunogenicity of therapeutic proteins, in Aggregation of therapeutic proteins (eds W. Wang and C. J. Roberts), John Wiley & Sons, Inc., Hoboken, NJ, USA. doi: 10.1002/9780470769829.ch10.

Papers

Filipe V, Hawe A, Jiskoot W. 2010. Critical evaluation of nanoparticle tracking analysis (NTA) by NanoSight for the measurement of nanoparticles and protein aggregates. Pharm Res 27(5):796-810.

Filipe V, Poole R, Kutscher M, Forier K, Braeckmans K, Jiskoot W. 2011. Fluorescence single particle tracking for the characterization of submicron protein aggregates in biological fluids and complex formulations. Pharm Res 28(5):1112-1120.

Hawe A, **Filipe V**, Jiskoot W. 2010. Fluorescent molecular rotors as dyes to characterize polysorbate-containing IgG formulations. Pharm Res 27(2):314-326.

Kukrer B, **Filipe V**, van Duijn E, Kasper PT, Vreeken RJ, Heck AJ, Jiskoot W. 2010. Mass spectrometric analysis of intact human monoclonal antibody aggregates fractionated by size-exclusion chromatography. Pharm Res 27(10):2197-2204.

Filipe V, Poole RA, Oladunjoye O, Braeckmans K, Jiskoot W. Detection and characterization of subvisible aggregates of monoclonal IgG in serum, accepted at Pharmaceutical Research

Filipe V[*], Kukrer B[*], Hawe A, Jiskoot W. Transient molten globules and metastable aggregates induced by brief exposure of a monoclonal IgG to low pH, accepted at Journal of Pharmaceutical Sciences

Filipe V, Basmeleh A, Jiskoot W, Brinks V. Immunogenicity of different stressed monoclonal IgG formulations in immune tolerant transgenic mice, manuscript in preparation

[*] contributed equally as first author

Curriculum vitae

Vasco Filipe was born on February 13th, 1982 in Kiev. In 2000 he finished his high school at Escola Secundária Anselmo de Andrade in Almada, Portugal. After graduating he started his Biological Engineering education at Instituto Superior Técnico in Lisbon, Portugal. During this period he did an internship at the Biological and Chemical Technology Institute in Oeiras, Portugal, where he worked on the production and stability of retroviral vectors for gene therapy. He graduated in 2005 and entered a Portuguese government program *Contacto*, in which he received a Fulbright grant to make an internship for 9 months at Élan Pharmaceuticals, in South San Francisco, California, USA. During this period he worked on Parkinson's disease studying Parkin interacting proteins, under the supervision of Dr. Jennifer Johnston.

In 2007 he started his PhD project under the supervision of Prof. Dr. Wim Jiskoot and Prof. Dr. Huub Schellekens. He was officially appointed at Utrecht University but performed all his work at Leiden University, Leiden, The Netherlands. The PhD project was entitled: "Monoclonal antibody aggregates: physicochemical characteristics, stability in biological fluids and immunogenicity". Vasco is currently working as a post-doc at the Division of Drug Delivery Technology at Leiden University.

Acknowledgements

When the revolutionary Cuban poet José Martí was asked what every man ought to do before he dies, he answered:

"Plant a tree, have a child and write a book."

Well, I can now say that I did them all! Planting trees and making babies are quite easy tasks, but the book... that's the tough one! Even though people tend to take this sentence literally (like I just did), these words have a much greater meaning: "Preserve the planet, ensure the survival of your species and contribute to society and generations to come." This thesis is the collection of my research and represents my small contribution to the scientific community (so far).

The completion of this thesis was only possible because I had the support from my coworkers, friends and family. Someone once said: "There comes a point in your life when you realize who really matters, who never did and who always will". I'm now starting to reach that point.

I will start by thanking Wim, my **super**visor. I don't want to sound obsequious, but I have nothing but good things to say from you. You possess a great scientific knowledge and you used it wisely to guide my research during these four years. All sprinkled with a great sense of humor. You managed to follow me closely (during our weekly meetings) and at the same time give me the space I needed to grow as an independent researcher. More than a supervisor, you became a friend and an example for me to follow in my coming scientific career.

I then thank Andrea, my teacher. When I arrived in this lab I had only a basic knowledge about protein characterization and didn't know how to use most of the analytical techniques. You taught me almost everything I know about this field and I really admire your efficiency, both at work and in your personal life. Thank you for your teachings, your patience and your friendship.

I also thank all the Utrecht team, who did all the *in vivo* work and the immunogenicity analysis of this research. Huub, who led this team with a great practical sense and

kept on posing me crucial questions. Vera, you were my reference point in Utrecht and made sure that everything went as it should. So many sample deliveries, meeting and discussions! I'm really glad that we had you on the project. You were the strong point of this all collaboration. Hafid: the assay-man. You were the "worker bee" behind all the immunogenicity tests. Melody, for all the discussions and tips. Grzegrorz, for the pilot study and Mies for helping me out with viscosity measurements. I must be one of the Utrecht University PhD students that spent less time in Utrecht, but every time I did, you guys made me feel at home. Thank you.

I also thank Robert Poole and Kevin, for joining me in the adventure of monitoring aggregates in biological fluids. Not an easy task, but it turned out to pay off at the end! Robert, you taught me a lot about fluorescent labeling and fluorescence in general. You were the perfect partner for the beer tasting trips to Gent, where we also measured some samples! Kevin, you opened up the doors for this entire section of my research and showed a great availability every time we had to make fSPT measurements. Thank you.

I'm also grateful to the two people that took care of the logistics in both ends: Connie in Leiden and Barbara in Utrecht. Thank you for your patience during the entire process. You are very good at what I'm terrible at: bureaucracy (a terrible but necessary evil).

In Leiden, I had the pleasure of working with a great group of people. The DDTeam suffered many changes over the years, but each member marked me in different ways. Some of these DDTeamers became really good friends and will always matter to me. *Diógenes, ficaste apenas um ano no nosso grupo, mas entraste directamente para a minha lista de melhores amigos. Nunca esquecerei as noitadas, as conversas, as risadas e a tua visita a Portugal (especialmente quando a Giulia me ligou com a notícia...). Hugo, com a tua boa disposição e amizade tornaste a minha integração em Leiden e no DDT bem mais fácil.* Christophe, when everybody kept coming and going, you were always there. Our friendship became stronger with time and I'm really glad to have shared my office and all my PhD time with you around. Miranda, as the senior PhD student in protein characterization, you shared a lot of your experience with me. It was a pleasure to have you and your great sense of humor as office mates. And talking about great office mates, Riccardo: *l'Italiano vero*. You always managed to bring the latin good vibe to the room. Ana Luísa, a tua vinda para o grupo foi

uma lufada de amizade que bem precisava, com tanta gente a ir-se embora. Não só pelo facto de partilharmos a mesma nação e cultura, mas porque partilhámos em grande parte a mesma forma de ver o mundo. Rapidamente te tornaste numa grande amiga e como sabes, eles não abundam no estrangeiro! Daniël Groen, my great Dutch friend. With your great sense of humor and love for beer and football, our friendship just grew naturally. With you I had the chance of knowing better the Dutch culture. Robert Rissmann, you were the only friend that truly understood the level of tiredness (and joy) that a PhD-baby can bring. I'm really glad to have you as a party/daddy mate. I also thank Varsha, Francisco (La Bomba), Tomo, Christian, Oliver, Bram, Ding, Başak, Suzanne, Jeroen, Romano, Andreas, Tue, Daniel Weinbuch, Anthippi and Nuch. Thank you so much for making my Leiden social life so great. I will never forget all the pub crawls, borrels, coffee breaks, laboutjes, late afternoon beers at sunny terraces, dinners, house parties and football matches. Da Dream Team was a great way to bound with the guys and we even won several tournaments. Ahhh... those were the glory days!

I'm also grateful to Joke, Gert, Elly, Michelle, Aat, Koen, Sun, Myrra, Maria Chiara, Dana, Enamul, Lolu and Eleni for their contribution to the great work environment of DTT and for helping me here and there every time I needed. This was a really special group. A special thank you goes to Stefan, who helped me a lot during these four years with technical issues. It would have taken me five years if it wasn't for him.

I would also like to thank all my students: Jonathan, Bukayo, Marika and Amar. All of them performed a really impressive work and some of it was included in my publications.

My stay in Leiden would not have been the same without my Tox and other non-work related friends. Jordi, my man! Always there, from the beggining till the end, you are the friend I could always count with. I was Turk and you were JD. *Pi, foste tu que me "lançaste" neste país e foste sempre o ombro amigo para os bons e maus momentos. Estar contigo faz-me sempre sentir de volta ao nosso Portugal... E por falar nisso, Miguelitos: a tua chegada fez-me sentir ainda mais em casa. Grande grande amigalhaço do passado, presente e futuro.* Nikos and Ana, you guys are a great couple and your good mood was always great to have around. Wies, always ready to party, to make a joke and to help whenever we needed a babysiter! Marc, your passage by Leiden was short, but enough to create strong bonds. I also thank

Sylvia, Lisa, Aude, Bram, Bas, Marja, Thijs, Sandra and Louise for their friendship, for their ocasional lab help and all the good times.

E já que estou numa de agradecer, agradeço também à minha família e amigos em Portugal, sem os quais a minha vida seria oca e insonsa. Não vou nomear todos um por um, mas vocês sabem quem são. Todas as minhas economias vão para viajar e poder estar com vocês, porque só assim consigo aguentar a dor de viver fora do meu querido Portugal.

Um especial obrigado aos meus pais, que sempre acreditaram em mim e me deram tudo o que podiam e não podiam, para que nunca me faltasse nada. Vocês são os melhores pais que podia desejar. Esta tese é o culminar de toda uma educação fantástica que me deram e, como disse no início, esta tese é dedicada a vocês. Outro obrigado especial vai para o meu irmão. Os nossos anos a viver sob o mesmo teto já lá vão, mas continuas sempre próximo. Acredita nas tuas capacidades e vais ver que irás muito longe. Agradeço também do fundo do coração aos meus tios Fernando e Isabel. Vocês foram os meus segundos pais e devo muito do meu fascínio pela ciência a ti (tio). Dedico também a vocês esta tese.

And last but not least, my wonderful Giulia. You are my inspiration and the basis of all my achievements since you entered my life. You always supported me enthusiastically and gave me the strength (and ideas) to solve my problems. With you by my side I felt like nothing could go wrong. In 2009 Matteo was born and we became proud and happy parents. Obrigado *Matteo pela alegria imensa que me deste todos os dias quando chegava a casa, tu fazias os problemas do trabalho parecerem realmente insignificantes.* Handling a baby and two PhDs abroad at the same time was not easy, but thanks to our great team work, we did it! You will always be my sweet November ☺ . *Merci pour tout* and see you later at home.

Obrigado a todos,

Vasco Filipe